



January 2013

Role Of The Alzheimer's Amyloid Precursor Protein In High Fat Diet Induced Obesity And Regulating Macrophage Phenotype

Kendra L. Puig

Follow this and additional works at: <https://commons.und.edu/theses>

Recommended Citation

Puig, Kendra L., "Role Of The Alzheimer's Amyloid Precursor Protein In High Fat Diet Induced Obesity And Regulating Macrophage Phenotype" (2013). *Theses and Dissertations*. 1469.
<https://commons.und.edu/theses/1469>

This Dissertation is brought to you for free and open access by the Theses, Dissertations, and Senior Projects at UND Scholarly Commons. It has been accepted for inclusion in Theses and Dissertations by an authorized administrator of UND Scholarly Commons. For more information, please contact zeinebyousif@library.und.edu.

ROLE OF THE ALZHEIMER'S AMYLOID PRECURSOR PROTEIN IN HIGH FAT
DIET INDUCED OBESITY AND REGULATING MACROPHAGE PHENOTYPE

by

Kendra Lynn Puig
Bachelor of Science, University of Wisconsin-Whitewater, 2009

A Dissertation
Submitted to the Graduate Faculty

of the
University of North Dakota

In partial fulfillment of the requirements

for the degree of
Doctor of Philosophy

Grand Forks, North Dakota
August
2013

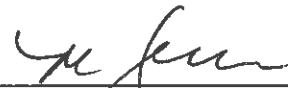
This dissertation, submitted by Kendra Puig in partial fulfillment of the requirements for the Degree of Doctor of Philosophy from the University of North Dakota, has been read by the Faculty Advisory Committee under whom the work has been done is hereby approved.



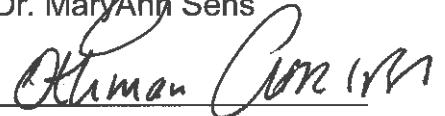
Dr. Colin Combs



Dr. Mikhail Golovko



Dr. MaryAnn Sens



Dr. Othman Ghribi



Dr. John Watt

This dissertation meets the standards for appearance, conforms to the style and format requirements of the Graduate School of the University of North Dakota, and is hereby approved.



Dr. Wayne Swisher
Dean of the Graduate School

June 10, 2013
Date

PERMISSION

Title Role of the Alzheimer's Amyloid Precursor Protein in High Fat Diet
Induced Obesity and Regulating Macrophage Phenotype

Department Pharmacology, Physiology, and Therapeutics

Degree Doctor of Philosophy

In presenting this dissertation in partial fulfillment of the requirements for a graduate degree from the University of North Dakota, I agree that the library of this University shall make it freely available for inspection. I further agree that permission for extensive copying for scholarly purposes may be granted by the professor who supervised my dissertation work or, in his absence, by the chairperson of the department or the dean of the Graduate School. It is understood that any copying or publication or other use of this dissertation or part thereof for financial gain shall not be allowed without my written permission. It is also understood that due recognition shall be given to me and to the University of North Dakota in any scholarly use which may be made of any material in my dissertation.

Kendra L Puig

Kendra L. Puig

6/4/13

Date

TABLE OF CONTENTS

LIST OF FIGURES.....	x
LIST OF TABLES.....	xiv
ACKNOWLEDGMENTS.....	xv
ABSTRACT.....	xix
CHAPTER	
I. INTRODUCTION.....	1
APP Expression, Processing, and Structure.....	1
APP Function in the CNS.....	2
APP Function and A β Pathology in Skin.....	4
APP Function and A β Pathology in Muscle.....	6
APP Function and A β Pathology in Adipose Tissue.....	8
APP Function and A β Pathology in Intestine.....	8
APP Function and Macrophage/Microglia.....	10
Amyloid Precursor Protein and Alzheimer's Disease.....	11
Obesity and Alzheimer's Disease.....	12
Amyloid Precursor Protein and Obesity.....	13
Adipose Tissue.....	15
Brain-Gut-Adipose-Tissue Communication Pathways.....	17
Enteric Nervous System.....	18
Macrophage and Microglia	19

Hypothesis.....	21
II. METHODS.....	22
Materials.....	22
Mice.....	23
High Fat vs. Control Diet Feeding	24
Western Blotting.....	24
Immunohistochemistry.....	26
Histological Stain.....	27
Glucose, Triglycerides, HDL and Total Cholesterol Measurements.....	28
Macrophage Isolation and Stimulation.....	28
Microglia Isolation and Stimulation.....	29
Intestinal Epithelial Cell Isolation and Stimulation.....	30
Enzyme-Linked Immunosorbent Assay (ELISA).....	31
Migration and Proliferation Assay.....	32
Prostaglandin Analysis.....	32
Uptake for Cell Cultures.....	33
Antibody-Based Cytokine Array.....	34
Adipocyte, Adipose Tissue Macrophage, and Fibroblast Isolation and Stimulation.....	34
Neuronal Isolation and Stimulation.....	36
Immunoprecipitation.....	37
Caco-2 Cells.....	37
Caco-2 and Microglia A β Uptake Assay.....	38

	Caco-2 Cell ELISA.....	38
	Caco-2 MTT Reduction Assay.....	39
	Blood Collection and LAL Assay.....	39
	Stool Weight.....	39
	Statistical Analysis.....	40
III.	AMYLOID PRECURSOR PROTEIN AND PROINFLAMMATORY CHANGES ARE REGULATED IN BRAIN AND ADIPOSE TISSUE IN A MURINE MODEL OF HIGH FAT DIET-INDUCED OBESITY....	41
	High fat diet feeding increased brain levels of APP and multiple pro-inflammatory proteins compared to control diet fed mice.....	41
	Proinflammatory protein immunoreactivity increased in neurons in brains from high fat diet versus control fed mice...	43
	High fat diet feeding increased APP and TNF- α protein levels compared to control diet fed mice in both subcutaneous and visceral fat depots.....	49
	Adipose tissue APP immunoreactivity from high fat diet fed animals localized to adipocytes and macrophage.....	50
	The APP agonist antibody, 22C11, increased macrophage cytokine production but had no effect on viability, lipid storage/accumulation, or TNF- α secretion in adipocytes.....	55
IV.	APP REGULATES BRAIN AND ADIPOSE CHANGES IN HIGH FAT DIET FED MICE.....	62
	APP ^{-/-} mice gained significantly less weight than wild type mice on high fat diet.....	62
	Measurement of fasting blood glucose, triglycerides, HDL and total cholesterol levels from wild type and APP ^{-/-} mice fed control and high fat diets.....	66
	Increased inflammatory response in the fat depots of APP ^{-/-} mice compared to wild type mice fed control and high fat diets.....	71

	Multiple protein markers of differentiation and activation differed in gonadal and perirenal fat depots of wild type and APP ^{-/-} mice fed high fat versus control diets.....	74
	Cytokine secretion differed from APP ^{-/-} and wild type peritoneal, intestinal, and adipose tissue macrophages isolated from mice fed control and high fat diets.....	81
	Differences in various protein marker levels characterized wild type vs. APP ^{-/-} macrophages.....	87
	Adipocytes from wild type and APP ^{-/-} cells demonstrated altered cytokine secretion and protein expression.....	89
	Protein quantitation, immunostaining, prostaglandin analysis, and fatty acid uptake quantitation in the neurons of APP ^{-/-} and wild type mice.....	98
	APP ^{-/-} microglia displayed an altered cytokine secretory profile, increased proliferation with decreased migration, and reduced phagocytic ability.....	107
V.	AMYLOID PRECURSOR PROTEIN EXPRESSION MODULATES INTESTINE IMMUNE PHENOTYPE.....	112
	Immunoreactivity differences between the ileum of APP ^{-/-} and C57BL6 control mice.....	112
	Quantitation of protein differences in the ileum of C57BL6 wild type and APP ^{-/-} mice.....	118
	In vitro migration, proliferation, and differentiation comparison of macrophages from APP ^{-/-} and C57BL6 wild type mice.....	119
	Profile of cytokine levels in ileum of APP ^{-/-} and C57BL6 wild type mice.....	124
	Differences in intestinal motility and absorption in APP ^{-/-} and C57BL6 mice.....	128
VI.	OVEREXPRESSION OF MUTANT AMYLOID PRECURSOR PROTIEN AND PRESENILLIN 1 MODULATES INTESTINE IMMUNE PHENOTYPE.....	131
	Histological differences were observed between the illeums of APP/PS1 and wild type mice.....	131

Significant differences in neuronal and inflammatory proteins were observed from ileum of APP/PS1 mice.....	133
No significant increase in quantitated A β levels were detected in the stool or intestinal lysate of APP/PS1 compared to wild type mice.....	134
Immunohistological differences were observed between the ileums of APP/PS1 and wild type control mice.....	134
No differences in intestinal motility but increased cytokine and IgA levels were observed in APP/PS1 versus wild type mice.....	142
Human intestinal epithelial cells secrete, take up, and respond to A β	146
VII. DISCUSSION.....	150
APPENDIX.....	175
LIST OF ABBREVIATIONS.....	176
REFERENCES.....	179

LIST OF FIGURES

Figure	Page
1. Average weight gain per week for mice fed a high fat versus control diet.....	42
2. APP and GFAP protein levels were increased in hippocampi of high fat versus control diet fed mice.....	44
3. Hippocampi of high fat diet fed mice demonstrated microglial (CD68), astrocytic (GFAP), and neuronal (Cox-2, APP and iNOS) immunoreactivity versus control diet mice.....	47
4. Microglia but not peritoneal macrophage demonstrated increased TNF- α secretion.....	48
5. APP and TNF- α levels increased in visceral and subcutaneous fat depots in high fat diet fed animals versus controls.....	51
6. APP, CD45, and CD68 immunoreactivity increased in the subcutaneous (abdominal) fat and visceral (pericardial) fat from high fat versus control diet fed mice with no robust change in A β immunoreactivity.....	53
7. APP and CD68 immunoreactivity co-localized in subcutaneous (abdominal) and visceral (heart) fat from high fat diet fed mice.....	54
8. Secreted levels of GM-CSF, IFN γ , and IL-13 increased in media from peritoneal macrophage stimulated with APP agonist antibody, 22C11, compared to IgG $_1$ isotype control.....	58
9. APP activation with agonist antibody did not alter cytokine secretion, viability, or Oil Red O staining of primary murine abdominal subcutaneous adipocytes.....	60
10. APP $^{-/-}$ mice gained significantly less weight than wild type mice fed either control or high fat diets.....	65
11. Measurement of fasting blood glucose and cholesterol levels in wild type and APP $^{-/-}$ mice on control and high fat diet.....	68

12. Liver from wild type mice fed high fat diet demonstrated increased lipid accumulation compared to APP ^{-/-} mice.....	70
13. Increased inflammatory protein levels in the fat depots of APP ^{-/-} mice compared to wild type mice.....	73
14. Protein marker levels differed in gonadal adipose tissue depots from wild type and APP ^{-/-} mice.....	76
15. Protein marker levels differed in perirenal adipose tissue depots from wild type and APP ^{-/-} mice.....	79
16. CD68 and APP immunoreactivity colocalized in adipose tissue and CD68 immunoreactivity increased in both gonadal and perirenal adipose tissue depots from wild type and APP ^{-/-} mice fed a high fat diet.....	80
17. Peritoneal macrophages cytokine secretion differed between wild type and APP ^{-/-} cells.....	84
18. Adipose tissue macrophages cytokine secretion differed between wild type and APP ^{-/-} cells.....	85
19. Intestinal macrophages cytokine secretion differed between wild type and APP ^{-/-} cells.....	86
20. Peritoneal macrophage PPAR γ , CD36, arginase-1 and CD86 levels and cytokine secretion differed between wild type and APP ^{-/-} cells.....	88
21. Quantification of protein levels, palmitic fatty acid uptake, and immunoprecipitation from wild type and APP ^{-/-} adipocytes.....	91
22. Quantitation of protein levels and cytokine secretion from APP ^{-/-} and wild type adipocytes.....	93
23. Adipocyte cytokine secretion was altered by A β 1-40 stimulation.....	96
24. Quantitation of select protein levels from APP ^{-/-} and wild type fibroblasts.....	97
25. Diverse protein differences and APP and IBA-1 immunoreactivity in the temporal cortex of wild type and APP ^{-/-} mice.....	99

26. Quantification of temporal cortex protein and prostaglandin levels, fatty acid uptake, and APP protein-protein interactions in neurons from wild type and APP ^{-/-} mice.....	102
27. Quantitation of cytokine levels in wild type and APP ^{-/-} temporal cortex.....	105
28. Quantitative comparison of protein levels in wild type and APP ^{-/-} cultured cortical neurons.....	106
29. Quantitation of cytokine secretory profile from wild type and APP ^{-/-} microglia stimulated with LPS and A β	109
30. APP ^{-/-} microglia had decreased proliferation, migration and phagocytic ability compared to wild type cells.....	111
31. Histology of the small intestine was similar in both APP ^{-/-} and wild type controls.....	113
32. Small intestine immunoreactivity for Cox-2 and MAP2 decreased in APP ^{-/-} mice compared to wild type controls with no change in occludin.....	116
33. Small intestine immunoreactivity for CD68 decreased in APP ^{-/-} mice compared to wild type controls with no change in GFAP or pTyr.....	117
34. Western blot analysis of Cox-2, CD68, CD40, CD11c and β III-tubulin demonstrated decreased protein levels in the small intestine of APP ^{-/-} compared to wild type mice.....	120
35. Peritoneal macrophages from APP ^{-/-} mice demonstrated significantly decreased migratory ability compared to wild type controls.....	122
36. APP ^{-/-} and wild type peritoneal macrophages demonstrated different cytokine secretory profiles compared to intestinal macrophages.....	125
37. Small intestine of APP ^{-/-} mice demonstrated altered levels of multiple cytokines compared wild type controls.....	127
38. APP ^{-/-} mice demonstrated intestinal motility and absorption differences compared to wild type mice.....	129
39. Histology of the small intestine was altered in APP/PS1 compared to wild type controls.....	132

40. Western blot analysis of APP, BACE, CD68, CD3, Cox-2, CD36, Synaptophysin, and PSD95 demonstrated increased protein levels in the small intestine of APP/PS1 compared to wild type mice.....	136
41. Small intestine immunoreactivity for APP, OC, and 4G8 increased in APP/PS1 mice compared to wild type controls with no change in A11..	138
42. Small intestine immunoreactivity for CD68, Cox-2 and CD36 increased in APP/PS1 mice compared to wild type controls with no change in occludin.....	139
43. Small intestine immunoreactivity for synaptophysin and MAP2 increased in APP/PS1 mice compared to wild type controls with no change in pTyr and pSrc.....	141
44. Small intestine of APP/PS1 mice demonstrated altered levels of multiple cytokines compared wild type controls.....	144
45. APP/PS1 mice demonstrated no difference in intestinal motility and absorption compared to wild type mice, but have increased IgA in intestinal lumen compared to wild type mice.....	145
46. Caco-2 cells produce and uptake A β , but A β and LPS and alter cytokine secretion profile with no effect on viability.....	148

LIST OF TABLES

Table	Page
1. Commercial diet formulations for control and high fat diet.....	24

ACKNOWLEDGMENTS

Apart from the efforts of myself, the success of any project depends largely on the encouragement and guidance of many others. I will take this opportunity to express my gratitude to the people who have been instrumental in the successful completion of this project.

I would like to thank Dr. Colin Combs for being the best graduate advisor I could have ever asked for; it has been and will continue to be a pleasure to work for you. Thank you for believing in my abilities, encouraging me to think creatively about a multitude of projects, and providing me advice not only as a graduate student, but in life in general to guide me in my career path.

I also wish to express my sincere appreciation to the other members of my advisory committee for their guidance and support during my time in the doctoral program at the University of North Dakota. Dr. Misha Golovko, thank you for allowing me to rotate through your lab to learn extraction methods and providing my project with the prostaglandin, fatty acid uptake, and olive oil analysis. Dr. John Watt, thank you for allowing me to use a tremendous amount of time on your cryostat. Thank you for assisting me in troubleshooting different tissue cutting issues as well as allowing me to learn paraffin embedding and cutting in your lab. Dr. MaryAnn Sens, thank you for allowing me to use your supplies and

get assistance from your staff for help on my projects. Dr. Othman Ghribi, thank you for your encouragement through my progression as a graduate student.

I would like to thank my past and current lab members for all their support and assistance with my projects. Angie Floden, thank you for making a remarkable first impression; you will and have always had a calming effect on me, making the world seem a little less stressful. I would like to thank Keiko Rausch for your patience in teaching me western blotting my first summer as a REU student. Thank you Susan Austin for getting me off to a great start on a few of my projects and providing me with your knowledge associated with these projects. Cindy Sondag, thank you for all your much appreciated graduate school advice and laboratory knowledge. Gunjan Dhawan Manocha, thank you for all your advice as a seasoned graduate student and for being my bosom buddy while you were here. Your friendship both inside the lab during regular and not so regular work hours as well as outside the lab going shopping and to movies is vastly cherished. Lalida "Joy" Rojanathammanee, thank you for understanding me, being a true friend both inside and outside the lab; going shopping and to movies is treasured tremendously. Allison Hendrickson, Jessie Gertken, and Andrew Rebel, thank you for all your technical expertise, making stock solutions, stocking lab supplies, and helping me to weigh my mice. All your efforts allowed me to use my time towards the greatest benefit to the lab. Siri Urquhart, thank you for being my rock this past year, assisting me with any project or task that was asked of you without complaint. Thank you to the many summer students for trying to teach me patience and testing my abilities to teach effectively.

Dr. Holly Brown-Borg and Dr. James Porter, thank you for allowing me to rotate through your lab and learn new techniques. Shar Rakoczy, thank you for having the patience to teach me new techniques when I was a rotating student as well as all your additional technical expertise these past years. Hongyan Wang and Xudong Zhou, thank you for your technical expertise in Alcian Blue, H&E, and Mason's Trichrome staining techniques. I would like to thank Dr. Mark Musch for his technical expertise on lysing intestinal tissue. I would also like to thank Dr. Gayle Callis and Dr. Mary Herman for their excellent advice on freezing and cutting adipose tissue.

Administrative Officers Julie Horn and Deb Kroese, thank you for all your assistance in filling out all the paperwork. Special thanks go to you Julie for being an excellent listener and my shoulder to vent to, especially this past year when things got a little too hectic. Thank you to all the graduate students for being remarkable classmates and believing in my abilities enough to ask me for my help.

I would like to acknowledge Dr. Van Doze for accepting me into the Research Experience for Undergraduates program in the summer of 2008, allowing me to have the opportunity to intern with Dr. Colin Combs and fall in love with the lab, without which I would have never come to UND to pursue my graduate degree. I would also like to acknowledge the funding sources that made this PhD work possible. I was funded through Dr. Colin Combs via the National Institutes of Health [P20RR017699, 1R01AG026330, 1R01AG045819, School of Medicine Research Grant, Research Development and Compliance Seed Grant],

the Department of Pharmacology, Physiology and Therapeutics, and the University of North Dakota Graduate School Summer Doctoral Fellowship. My work was also supported in part by travel grants: Doctoral Student Travel Support Program UND Graduate School, Intercollegiate Academic Fund Travel Award, and Biolegend Travel Award.

Extraordinary thanks go to my family both immediate and extended for understanding my commitments to school and accepting my absence at various events. I would like to thank my sister Kelley for her support in coming out to work and live with me this past year, providing me with assistance not only at work but also at home, making my life a little less hectic. I would like to thank my sister Kerri for all her support in my decisions to pursue higher education and her assistance in proofing my papers for classes. I would like to thank my mom for her assistance in proofing my papers through classes and providing me with motivation to go to college and pursue any career my heart desired. I would like to thank my dad for coming to the lab and fixing the door of the lab's -80 freezer and for providing me with the original technical knowledge that allows me to look at things from a unique technical perspective.

Thanks again to everyone who has provided me with the encouragement and guidance to complete this project.

ABSTRACT

Obesity is reportedly at epidemic proportions in the U.S. with a myriad of potential dietary, lifestyle, and genetic factors contributing to its rise in prevalence. In the U.S. 20-25% of adults suffer from obesity and its associated co-morbid conditions including cardiovascular disease, diabetes, metabolic syndrome and Alzheimer's disease (AD) making it a leading health care concern. AD affects nearly 5.4 million individuals in the U.S. with expected numbers nearly tripling over the next few decades and currently represents the sixth leading cause of death in the U.S. and fifth amongst individuals 65+. A form of autosomal dominant AD is associated with mutations in the gene coding for the ubiquitously expressed transmembrane protein, amyloid precursor protein (APP). Proteolytic processing of APP provides the beta amyloid (A β) peptide that is characteristic of AD plaque pathology. Amyloid precursor protein (APP) derived A β peptides have been extensively investigated in Alzheimer's disease pathology of the brain. However, the function of full length APP in the central nervous system remains unclear. Even less is known about the behavior of this ubiquitously expressed protein and its metabolites outside of the central nervous system. Therefore, we sought to broaden our understanding of the expression and function of APP and its proteolytic fragments in specific non-neuronal tissues. Although the majority of research effort is currently focused on neuronal A β production and its effects on

cells, prior work in our lab demonstrated a novel role for APP in regulating the phenotype of monocytic lineage cells. Therefore, we hypothesized that APP can behave as a proinflammatory receptor on these cells involved in modulating their tissue infiltration and differentiation. Based upon the fact that midlife obesity is a risk factor for Alzheimer's disease and both obese adipose tissue and Alzheimer's disease brains share a common presence of increased, reactive macrophage and microglia, respectively, we hypothesized that APP may have a common role in both diseases regulating the infiltration or proinflammatory activation of microglia and macrophage characterizing both diseases. Indeed, recent data has demonstrated that APP levels are increased in adipose tissue from obese versus control individuals. To test this idea we utilized a high fat diet feeding paradigm on both C57BL6 wild type and APP^{-/-} mice to examine any role for APP and high fat diet dependent changes in adipose tissue, brain, and intestine. In vivo changes were compared to those obtained using primary cells isolated from the murine models. Collectively, these data suggest that APP does regulate microglia and macrophage phenotype in a manner responsible for altering their behavior in tissue specific fashion. This suggests that immune-related functions of APP may be a common type of pathophysiology linking the complex diseases of obesity and Alzheimer's disease.

CHAPTER I

INTRODUCTION

APP Expression, Processing, and Structure

Amyloid precursor protein (APP) is a type I integral membrane protein with a large extracellular N-terminal domain, a hydrophobic transmembrane domain, and a short C-terminus intracellular domain (Kang et al., 1987a, Dyrks et al., 1988) (Figure 1). There are three major isoforms of the protein derived from alternative splicing, APP751, APP770, APP695, with APP695 demonstrating highest levels of expression in brain (Ponte et al., 1988, Tanaka et al., 1988, Tanaka et al., 1989). As previously reviewed (Zheng and Koo, 2011, Zhang et al., 2012), APP undergoes post-translational processing via two pathways, the non-amyloidogenic and the amyloidogenic. In the non-amyloidogenic pathway, APP is sequentially cleaved first by α -secretase (ADAMs) to generate an N-terminal sAPP- α fragment. The remaining C83 C-terminal fragment is further cleaved by γ -secretase (Presenilin1 or Presenilin2, Presenilin enhancer 2 (PEN2), Anterior pharynx-defective 1 (APH1) and Nicastrin) to release a P3 peptide and its C-terminal intracellular counterpart, the APP intracellular domain (AICD). In the amyloidogenic processing pathway, APP is again sequentially cleaved but first by the β -secretase (BACE1) to yield the N-terminal sAPP- β

fragment. The remaining C99 C-terminal fragment undergoes ϵ and γ cleavages by γ -secretase to release the amyloid beta ($A\beta$) 1-40/42 peptides and an AICD. A characteristic accumulation of $A\beta$ peptides in the brains of AD patients has helped to draw research focus to these particular peptide metabolites of APP. Finally, APP can also be processed by caspase 3 to release cytotoxic C31 and Jcasp fragments. Amyloid precursor protein and mRNA have been shown to be expressed in the brain, thymus, heart, muscle, lung, kidney, adipose tissue, liver, spleen, skin, and intestine (Selkoe et al., 1988, Joachim et al., 1989, Yamada et al., 1989, Sandbrink et al., 1994, Akaaboune et al., 2000, Herzog et al., 2004, Galloway et al., 2007, Lee et al., 2008b). Therefore, even though the function and processing of APP in neurons may appear particularly relevant to the study of AD, the wide-spread expression of the protein suggests it has a broader role in both normal and disease physiology.

APP Function in the CNS

Much of the study of amyloid precursor protein (APP) has focused on changes in the central nervous system during Alzheimer's disease (AD) pathology. APP is expressed in the brain primarily by neurons (LeBlanc et al., 1991) where it can be metabolized to $A\beta$ 1-40 and 1-42 peptides which aggregate to form amyloid plaques characteristic of AD (Kang et al., 1987b). Moreover, mutations in the gene coding for APP (Goate et al., 1991) or its protease presenilins (Schellenberg et al., 1992, Levy-Lahad et al., 1995, Sherrington et al., 1995) are responsible for a rare autosomal dominant form of disease.

As previously reviewed (Zheng and Koo, 2011, Zhang et al., 2012), in the central nervous system (CNS) full length APP has been suggested to function as a cell surface receptor contributing to cell adhesion and cell-cell interactions via its extracellular domain possibly through trans-dimerization. The C-terminus of APP contains a YENPTY sequence between residues 682 and 687 that is a consensus sequence for a phosphotyrosine binding domain interaction. The N-terminal fragment, sAPP- α , is neuro-protective, promotes neurite outgrowth and synaptogenesis, facilitates learning and memory, acts as a growth factor and regulates cell adhesion (Mattson et al., 1993, Furukawa et al., 1996a, Furukawa et al., 1996b, Mattson, 1997, Herzog et al., 2004, Siemes et al., 2006, Gakhar-Koppole et al., 2008, Ma et al., 2009). On the other hand, the N-terminal sAPP- β fragment can stimulate axonal pruning and neuronal cell death (Nikolaev et al., 2009). APP cleavage to generate the A β peptide can lead to peptide-mediated neurotoxicity, neurofibrillary tangle formation and synaptic loss (Selkoe et al., 1988, Shankar and Walsh, 2009). The APP intracellular domain (AICD) fragment that is often generated during proteolytic processing is capable of behaving as a transcription factor, controlling cell death and neprilysin-mediated A β degradation, altering calcium and ATP homeostasis, and regulating intracellular trafficking and cytoskeletal dynamics (Gandy et al., 1988, Suzuki et al., 1994, Iijima et al., 2000, Lu et al., 2000, Inomata et al., 2003, Pardossi-Piquard et al., 2005, Xu et al., 2007). However, considerably less work has been published describing the function and expression of full-length APP or its cleavage products

outside the central nervous system in spite of the well-recognized ubiquitous expression pattern.

APP Function and A β Pathology in Skin

APP expression in the mammalian epidermis is predominantly in basal keratinocytes, but can also be found in the melanocytes and in melanoma cells (Hoffmann et al., 2000, Herzog et al., 2004). APP is also expressed *in vitro* in the immortalized human keratinocyte cell line, HaCaT, as well as in proliferating primary keratinocytes (Herzog et al., 2004). A β deposits have been reported beneath the epidermal/dermal junction as well as near small blood vessels and glandular structures in human tissue (Joachim et al., 1989).

APP function has been previously reviewed (Herzog et al., 2004), in the epidermis where it appears that APP promotes cell adhesion to several components of the extracellular matrix based upon its *in vitro* interactions with perlecan, laminin, collagen type IV, and entactin (Narindrasorasak et al., 1991, Narindrasorasak et al., 1992, Narindrasorasak et al., 1995, Beher et al., 1996). Studies using wild type and APP^{-/-} mice demonstrate that APP may also function as a membrane receptor and regulate behavior of the axonal transport protein, kinesin-I, which mediates movement of membrane-bound compartments such as melanosomes along microtubules (Kamal et al., 2001). Interestingly, APP also appears to regulate copper homeostasis as suggested by its *in vitro* ability to reduce Cu(II) to Cu(I) leading to oxidative stress and apoptosis in the basal epidermis in human keratinocytes (Multhaup et al., 1996, Kagan et al., 2002).

In addition to these functions attributed to full length protein, the APP fragment, sAPP α , promotes human keratinocyte proliferation and migration and regulates melanocyte function *in vitro* (Lauffenburger and Horwitz, 1996, Hoffmann et al., 2000, Quast et al., 2003, Siemes et al., 2006). This is consistent with the fact that APP^{-/-} keratinocytes have reduced proliferative and cell substrate adhesion potential. These findings suggest that sAPP α belongs to a family of structurally similar cysteine-rich growth factors for epidermal keratinocytes involved in growth, differentiation and wound repair (Rossjohn et al., 1999).

APP or its metabolites may also play some role in epidermal pathology. For instance, APP levels are upregulated in keratinocytes in psoriasis, a very common chronic inflammatory human skin disease in which keratinocyte proliferation and differentiation are perturbed leading to alteration in epidermal thickness and composition (Romanowska et al., 2009). Processing of APP to A β *in vitro* in human psoriasis patient keratinocytes increases transcription of kynureninase, which can induce an inflammatory skin reaction (Romanowska et al., 2009). Increased APP expression also correlates with advanced melanoma progression in human tissues and downregulation by RNA interference *in vitro* in human melanoma cell lines results in terminal and irreversible differentiation (Botelho et al., 2010).

APP processing and A β release has also been shown to be regulated by PKC activity in cultured skin fibroblasts from familial Alzheimer's disease (FAD) patients, in which phorbol ester stimulation of PKC- α activity increases sAPP- α

and decreases A β secretion (Gasparini et al., 1998). A β secretion is basally elevated in cultured skin fibroblasts from FAD patients, suggesting that FAD has a deficit in PKC activity. FAD cultured fibroblasts also have increased total membrane bound calcium with attenuated calcium uptake as well as increased lactate production and altered glucose utilization compared to non-AD controls. This suggests that APP may be involved in regulating a disease phenotype in FAD epidermis (Gasparini et al., 1998).

Collectively, these findings from the skin indicate that APP and its metabolites have a role in regulating epidermal cell phenotypes with a significant ability to modulate proliferative and migratory behavior. Disease-associated changes in expression or processing of APP correlate with perturbations of these behaviors in a variety of diseases.

APP Function and A β Pathology in Muscle

APP is also present in the pre and post synaptic compartments of mouse skeletal muscle and in cultured murine myogenic cells (Akaaboune et al., 2000). APP is detected as early as murine embryonic day 16 (E16) in the cytoplasm of developing muscle fibers. By E18 APP distributes throughout the muscle fiber sarcoplasm and at birth (P0) APP immunoreactivity begins localizing to the neuromuscular junctions (NMJs). By postnatal day 5 (P5), APP immunoreactivity restricts to NMJs where it colocalizes with acetylcholine receptors (AChRs). In this NMJ localization, APP expression continually increases into adulthood (Akaaboune et al., 2000). Not surprisingly, APP expression is required for NMJ

synapse formation of murine motor neurons (Wang et al., 2005b). In the absence of APP, murine NMJs demonstrate aberrant localization of presynaptic proteins with postsynaptic AChR clusters and decreased synaptic vesicles at presynaptic terminals and a significant increase in synaptic dysfunction (Wang et al., 2005b).

These critical roles of APP in NMJ function suggest that altered expression or behavior of APP or its metabolites may be involved in disease. Muscle fibers of patients with the debilitating skeletal muscle disorder, inclusion-body myositis (IBM), have intrafiber “plaque-like” accumulation of intracellular A β which is preferentially greater for A β 42 than A β 40 (Askanas and Engel, 2006). Accordingly, APP and A β are suggested to accumulate in skeletal muscle of IBM patients where they are hypothesized to act through a variety of mechanisms to promote myofiber degeneration, atrophy, and death (Greenberg, 2010). In addition, A β 40 and A β 42 levels are elevated in the temporalis muscles of AD vs. nondemented individuals suggesting some perturbation of neuromuscular function (Kuo et al., 2000).

These data from muscle indicate that APP and its metabolites have not only a developmental role in NMJ formation but also may be critically involved in regulating normal transmission at this specialized form of synapse. Moreover, altered expression or accumulation of APP or its breakdown products in muscle, at least, correlates with diverse disease conditions but may also play a role in neuromuscular pathology.

APP Function and A β Pathology in Adipose Tissue

APP and its A β fragments are also expressed in human adipose tissue adipocytes and macrophages (Lee et al., 2008b). Obesity upregulates APP levels *in vivo* in human adipose tissue, which correlates with insulin resistance, hyperinsulinemia, and an increase in the expression profile of the proinflammatory genes, MCP-1, MIP-1 α , and IL-6, in human adipocytes *in vitro* (Lee et al., 2008b). Elevated human adipocyte APP gene expression *in vivo* also correlates with increased plasma A β 40 levels (Lee et al., 2009b). TNF α stimulation increases APP protein levels *in vitro* in 3T3-L1 adipocytes in a dose-dependent manner (Sommer et al., 2009). These data from human studies indicate that APP expression in adipose tissue appears to be up-regulated during pro-inflammatory conditions, such as obesity, and is positively regulated by direct proinflammatory stimulation of adipocytes. However, the function of APP or its metabolites basally or during proinflammatory upregulation in adipose tissue remains unclear.

APP Function and A β Pathology in Intestine

APP and A β levels are increased in absorptive columnar epithelial cells in mice fed a high fat diet that is enriched in saturated fat and cholesterol. However, A β levels are attenuated by fasting for 65hr suggesting that APP or its metabolites may regulate chylomicron biosynthesis (Galloway et al., 2007). A β immunoreactivity colocalizes with apo B in small intestine enterocytes along the lengths of the villi and A β levels are attenuated in mice fed a diet free of

saturated fat but supplemented with cholesterol, again supporting the idea that A β is involved in chylomicron biosynthesis (Galloway et al., 2009, Pallebage-Gamarallage et al., 2009). Enterocyte A β immunostaining localizes to perinuclear regions suggesting a location within the golgi apparatus or rough endoplasmic reticulum (Galloway et al., 2007). There may also be some contribution of APP or its metabolites to traditionally non-intestine related disease. For instance, A β immunoreactive plaques are detectable in the intestines of AD patients (Joachim et al., 1989). These findings indicate that APP expression and metabolite generation are not limited to a particular cell type in the digestive system with a myriad set of functions attributed to these proteins ranging from specific absorption and gut motility to immune response.

The mammalian intestines are not only characterized by a unique enteric nervous system (Harrington et al., 2010, Tomita et al., 2010) and APP isoform expression (Yamada et al., 1989, Arai et al., 1991) but also an abundance of resident immune cell types, including macrophages necessary for monitoring resident and foreign microbial exposure (Santaolalla et al., 2010). Although A β in the intestine and brain have been reported (Gravina et al., 1995, Johnson-Wood et al., 1997, Li et al., 2004, Galloway et al., 2007, Galloway et al., 2009, Hellstrom-Lindahl et al., 2009), the role of APP in the enteric nervous system is not clear. Our laboratory has demonstrated that APP on monocytes is critical for adhesion dependent activation, extravasation through the endothelium and acquisition of a reactive phenotype (Sondag and Combs, 2004a, 2006b, 2010a). Therefore, APP expression in immune cells in the brain and intestinal tissue likely

regulates the proinflammatory environment in these tissues. Indeed, it was not unreasonable to predict that the proinflammatory environment and microglia/macrophage numbers are to some degree dependent upon APP expression or metabolism.

APP Function and Macrophage/Microglia

Our prior studies (Sondag and Combs, 2004b, 2006a, 2010b) as well as others (Bauer et al., 1991, Bullido et al., 1996, Vehmas et al., 2004, Spitzer et al., 2010) have demonstrated that APP is also expressed on immune cells where it appears to play a role in regulating cellular phenotype. For example, expression on monocytic lineage cells appears to regulate the ability of these cells to interact with extracellular matrix and mediate various cell-cell interactions (Austin and Combs, 2010, Sondag and Combs, 2010b). In addition, APP expression increases in both macrophages and microglia in the presence of a reactive, stimulatory environment (Haass et al., 1991, Banati et al., 1994a, Monning et al., 1994, Banati et al., 1995a, Banati et al., 1995b, Gehrmann et al., 1995a, Gehrmann et al., 1995b, Monning et al., 1995, Itoh et al., 2009).

We have also observed that agonist antibody stimulation of APP leads to a diverse change in proinflammatory protein expression and cytokine secretion as well as release of A β peptides from monocytic cells (Sondag and Combs, 2004b, 2006a). Recently, others have suggested that secreted A β peptides are anti-microbial (Soscia et al., 2010) fitting well with the ability of immune cells to make the peptides upon activating ligand stimulations (Sondag and Combs,

2006a, Spitzer et al., 2010). Finally, a variety of studies have demonstrated that APP metabolites and A β peptides in both their fibrillar and oligomeric forms are potent activating stimuli for macrophages, monocytes, and microglia (Klegeris et al., 1994, Yan et al., 1998, Combs et al., 1999, Yates et al., 2000, Smits et al., 2001, Yazawa et al., 2001, Ikezu et al., 2003, Uryu et al., 2003, Xiong et al., 2004, Floden and Combs, 2006, Sondag et al., 2009, Maezawa et al., 2010). Collectively, these data suggest that APP and its proteolytic products may serve as regulators of proinflammatory phenotype in particular immune cells.

Amyloid Precursor Protein and Alzheimer's Disease

Alzheimer's disease is clinically described as loss of memory, progressive impairment of cognition and various behavioral and neuropsychiatric disturbances (Saijo and Glass, 2011). A hallmark of Alzheimer's disease (AD) brains is the accumulation of amyloid beta (A β) plaques and neurofibrillary tangles composed of hyperphosphorylated tau (Perry et al., 1989, Joachim et al., 1991, Paloneva et al., 2002, de Haas et al., 2008). A β is a peptide cleavage product of amyloid precursor protein (APP) which aggregates to form extracellular plaques within the AD brain (Kang et al., 1987b). A β serves as a potent proinflammatory stimulus for microglia lending support to the idea that the reactive microgliosis in AD brains is due to A β stimulation (Meda et al., 1995, Bitting et al., 1996, Lorton et al., 1996, Combs et al., 1999, Lorton et al., 2000, Lue et al., 2001, Wu et al., 2004, Sondag et al., 2009, Dhawan et al., 2012).

Obesity and Alzheimer's Disease

Alzheimer's disease (AD) affects nearly 5.3 million individuals in the U.S. with expected numbers nearly tripling over the next few decades and currently represents the seventh leading cause of death in the U.S. (Alzheimer Association Annual Report, 2010). Unfortunately, the severity of this disease pales in comparison to the number of adults in the U.S. suffering from obesity (20-25% of adults, CDC 2008 report) and its associated co-morbid conditions including cardiovascular disease (est. 81 million, American Heart Association 2010 update) and diabetes (est. 23.6 million, CDC, 2007 update). Deaths associated with obesity related cardiovascular disease and stroke are the number one cause of death in the U.S. Although they may appear initially as disparate conditions, the risk of developing Alzheimer's disease is increased by middle age obesity, type II diabetes, and cardiovascular/cerebrovascular disease (Despres, 2003, Craft, 2005, Kivipelto et al., 2005, Despres and Lemieux, 2006, Razay et al., 2006, Wolozin and Bednar, 2006, Gunstad et al., 2007, Luchsinger and Mayeux, 2007, Razay et al., 2007, Whitmer, 2007, Whitmer et al., 2007, Beydoun et al., 2008, Despres et al., 2008, Luchsinger, 2008, Profenno and Faraone, 2008, Despres, 2009, Fitzpatrick et al., 2009, Luchsinger and Gustafson, 2009b, a, Mattson, 2009, Ross and Despres, 2009, Sommer et al., 2009). This data offers the provocative idea that a common mechanism of pathophysiology is shared between all these conditions.

Obesity, particularly in mid-life, is an increased risk factor for AD independent of other conditions (Kivipelto et al., 2005, Whitmer, 2007, Whitmer

et al., 2007, Beydoun et al., 2008, Profenno and Faraone, 2008, Fitzpatrick et al., 2009, Profenno et al., 2010). Particular saturated versus unsaturated fat ingestion at midlife also increases the risk of developing AD (Laitinen et al., 2006, Eskelinen et al., 2008). In addition, metabolic syndrome and diabetes, often comorbid with obesity, are factors of increased risk for AD in some (Razay et al., 2006, 2007, Profenno and Faraone, 2008, Profenno et al., 2010) but not all studies (Raffaitin et al., 2009). Interestingly, late life obesity and metabolic syndrome are either not risk factors or actually decrease the risk of AD in several studies (Fitzpatrick et al., 2009, Hughes et al., 2009, Forti et al., 2010). Others have reported that obesity itself is associated with poorer cognitive performance in humans (Jeong et al., 2005, Gunstad et al., 2006, Gunstad et al., 2007) as well as decreased brain volumes (Gunstad et al., 2008) independent of age or disease. In spite of this abundance of correlational data, a particular mechanism linking the pathophysiology of obesity to the brain changes of AD remains unclear.

Amyloid Precursor Protein and Obesity

Obesity is reportedly at epidemic proportions in the U.S. with a myriad of potential dietary and lifestyle factors contributing to its rise in prevalence (Hill and Peters, 1998, Caterson and Gill, 2002, Brantley et al., 2005, Selassie and Sinha, 2011). However, genetic factors do also have a significant impact on this disorder (Farooqi and O'Rahilly, 2006, Frayling et al., 2007, Loos et al., 2008, Stoger, 2008, Lee, 2009, Lindgren et al., 2009, Choquet and Meyre, 2010, Beyerlein et

al., 2011, Farooqi, 2011, Herrera et al., 2011, Ramachandrappa and Farooqi, 2011). The fact that it is a risk factor for diabetes, heart disease, metabolic syndrome and Alzheimer's disease make it a leading health care concern (Despres, 2003, Craft, 2005, Kivipelto et al., 2005, Despres and Lemieux, 2006, Razay et al., 2006, Wozozin and Bednar, 2006, Gunstad et al., 2007, Luchsinger and Mayeux, 2007, Razay et al., 2007, Whitmer, 2007, Whitmer et al., 2007, Beydoun et al., 2008, Despres et al., 2008, Luchsinger, 2008, Profenno and Faraone, 2008, Despres, 2009, Fitzpatrick et al., 2009, Luchsinger and Gustafson, 2009a, b, Mattson, 2009, Ross and Despres, 2009, Sommer et al., 2009).

Recent data suggests that APP expression or function may also be involved in the pathophysiology of obesity. Obesity is characterized by inflammation, adipocyte hypertrophy and infiltration of immune cells, particularly macrophage. It is known that adipose tissue (Lee et al., 2008a, Lee et al., 2009a, Sommer et al., 2009) and adipocyte cell lines (Sommer et al., 2009) express APP. More importantly, adipose APP and A β 1-40 plasma levels increase in obese individuals (Lee et al., 2008a, Lee et al., 2009a) and plasma A β 1-42 and 1-40 levels correlate with increased body fat in humans (Balakrishnan et al., 2005, Leahey et al., 2007). Rodent studies have examined the brain in a variety of diet-induced obesity paradigms confirming that brain changes leading to increased A β levels occur in both AD transgenic (Levin-Allerhand et al., 2002, Kohjima et al., 2010) and wild type mice (Thirumangalakudi et al., 2008). These

findings indicate that changes in APP expression or function may be coordinated across diverse tissue types.

Adipose Tissue

Adipose tissue is considered an endocrine organ capable of secreting hormones and cytokines to mediate metabolic, hemodynamic, and hemostatic disturbances as well as inflammatory and immune responses. The primary cells of adipose tissue are adipocytes which are thought to arise from mesenchymal stem cells (MSCs) by a sequential differentiation pathway in which appropriate developmental triggers cause the MSCs to commit to the adipocyte lineage and become adipoblasts or preadipocytes (Cinti, 2012). These adipoblasts or preadipoblasts then transition through four phases: growth arrest, clonal expansion, early differentiation, and terminal differentiation (Cinti, 2012). The conversion from adipoblasts to adipocytes is stimulated by both PPAR γ and C/EBP to become either white or brown adipocytes, however the exact molecular events that govern white versus brown differentiation has yet to be elucidated (Gesta et al., 2007). Brown adipose tissue (BAT) is highly vascularized, innervated and consists of polygonal cells with a roundish nucleus and several cytoplasmic lipid droplets characterized by large mitochondria packed with cristae (Cinti, 2012). BAT is unique in its expression of uncoupling protein 1 (UCP1) which can uncouple oxidative phosphorylation from ATP synthesis and thereby resulting in the production of heat (thermogenesis) (Cannon and Nedergaard, 2004, Ricquier, 2005, Frontini et al., 2007). White adipose tissue

(WAT), on the otherhand, is five to six times less vascularized, is characterized by leptin and S100- β immunoreactive spherical cells with ~90% of their volume comprising of a single cytoplasmic lipid droplet and a 'squeezed' nucleus in order to store energy for the metabolic needs of the organ (Cinti, 2012).

To store energy, lipoprotein lipase (LPL) molecules on the endothelial surface of the capillary bind to a chylomicron and hydrolyze the triacylglycerol (Triglyceride) portion of the particle (Smith et al., 2006). This causes fatty acids (FAs) to be released into either the adipocyte where they are esterified into triacylglycerol or they bind to albumin within the capillary space to become part of the albumin-FA complex which can also enter the adipocyte or move into systemic circulation (Smith et al., 2006). Triacylglycerol within the adipocyte can then be hydrolyzed to FAs by hormone-sensitive lipase (HSL) or triacylglycerol lipase (Smith et al., 2006). When food intake exceeds energy expenditure, the adipose stores more triacylglycerol. Conversely when expenditure exceeds food intake, adipose releases more triacylglycerol. To meet this expansion of energy, the existing adipocytes increase in size. In addition, there is increased formation of new white adipocytes from pre-adipocytes or from a direct transformation of brown adipocytes to white adipocytes that occurs (Cinti et al., 1997, Hausman et al., 2001, Bachman et al., 2002). The excessive storage of triacylglycerol leads to obesity and associated conditions (Cinti, 2012).

Typically macrophage comprise 10-15% of the immune cells in lean adipose tissue, however in obese adipose tissue 45-60% of the cells are macrophage (Lumeng et al., 2007, Chawla et al., 2011). Macrophage can have

two distinct phenotypes M1 and M2. M1 is the classically activated, proinflammatory phenotype induced by LPS and IFN γ , typically found in “crown-like” structures around dying adipocytes in which they have enhanced cytokine production of TNF α , IL-6, IL-12 and generate reactive oxygen species to activate iNOS (Mantovani et al., 2004, Gordon and Taylor, 2005). M2 is the alternatively activated less inflammatory phenotype induced by IL-4 or IL-13. M2 macrophages are typically uniformly dispersed throughout the adipose tissue and have enhanced cytokine production of IL-10, IL-1 β and blocks iNOS activity (Gordon, 2003). Upon high fat feeding adipose tissue macrophages undergo a phenotypic switch from an anti-inflammatory M2 polarization to a proinflammatory M1 polarization state thereby losing their protective capacity (Lumeng et al., 2007). These findings, in conjunction with the previously described expression of APP on macrophages and adipocytes, suggest that APP may play a role in this phenotypic switching of macrophage polarization or fatty acid uptake in this tissue.

Brain-Gut-Adipose-Tissue Communication Pathways

The brain is responsible for controlling the metabolic inputs to maintain the peripheral energy state. To maintain energy expenditure, the brain generates neuronal and hormonal signals in response to the short-term signals produced by the gut and the long-term signals produced by the adipose tissue (Yi and Tschöp, 2012). In the hypothalamus located within the forebrain reside a number of nuclei, particularly the arcuate nucleus and the ventromedial hypothalamus,

which express adipokine receptors that can bind to adipokines such as leptin that are released from adipose tissue directing the brain to suppress appetite and stimulate energy expenditure (Gautron and Elmquist, 2011). In the nucleus tractus solitarius located within the hindbrain resides the dorsal motor nucleus of the vagus complex which receives signals from the gastrointestinal system via vagal afferents or the circulation delivering satiety hormones directing the brain to initiate or terminate feeding (Berthoud et al., 2006). Therefore communication between these organs is vital to controlling metabolic disorders.

Enteric Nervous System

Although APP processing has been described in the central nervous system, the process and consequences of APP and A β accumulation in the enteric nervous system have not been extensively studied. Elderly are often afflicted with debilitating intestinal disorders such as constipation, fecal incontinence, and evacuation (Camilleri et al., 2008, Roach and Christie, 2008, Everhart and Ruhl, 2009b, a) which could be due to a degenerating enteric nervous system. The enteric nervous system is homologous to the central nervous system sharing similar embryology, morphology and neurochemistry (von Boyen et al., 2002). It heavily innervates the small intestine and controls virtually all gastrointestinal (GI) functions, including motility, secretion, blood flow, mucosal growth and local immune system cell behavior (Goyal and Hirano, 1996). Indeed, the small intestine is host to multiple cells of the immune system which, through interactions with the enteric neurons, can also evoke alterations in

gut function (Goyal and Hirano, 1996). Therefore, these characteristics along with the knowledge that elderly, including AD patients (Johanson et al., 1992, Sonnenberg et al., 1994), experience GI dysfunction suggest that APP and A β may also accumulate in the enteric nervous system leading to immune cell activation and neuronal dysfunction in the digestive tract not unlike that observed in the diseased brain.

Macrophage and Microglia

Macrophage cells are of monocytic origin arising from bone marrow, from which they migrate into circulation, follow the general paradigm of leukocyte adhesion and trafficking, which involves rolling, adhesion and transmigration via integrins and other adhesion molecules into various tissues throughout the body (Ley et al., 2007). Based on their anatomical location and functional phenotype macrophages can be divided into subpopulations. For example, osteoclasts in bone, alveolar macrophages in the lungs, histiocytes in interstitial connective tissue, Kupffer cells in the liver, microglia in the brain, intestinal macrophage in the intestine, splenic macrophage in the spleen, adipocyte macrophage in adipose tissue, etc, are all forms of tissue specialized macrophage (Peranzoni et al., 2010, Murray and Wynn, 2011). Macrophages primary functions are to provide immune surveillance by: (1) ingesting and processing foreign materials, dead cells and debris; (2) recruiting additional macrophages in response to inflammatory signals; (3) antigen presenting; and (4) immune suppression (Murray and Wynn, 2011). Macrophages also work together to maintain tolerance

to the gut flora and food, by being bathed in IL-10 to mute any inflammatory response (Murray and Wynn, 2011).

Microglial cells are also of monocytic origin arising from bone marrow, from which they migrate and invade into the brain during early embryogenesis or via vessels or white matter tracts into the mature brain during homeostasis and inflammation (Kettenmann et al., 2011, Shi and Pamer, 2011). Once inside the brain they are transformed into the branched, ramified morphological phenotype or “resting microglia” until they are activated by a pathological event in which they undergo another transformation into an amoeboid morphology (Kettenmann et al., 2011). The “resting microglia” has a small soma with fine cellular processes which are used to scan the environment without disturbing the fragile neuronal circuitry. However, the “activated microglia” have reduced cellular processes in their amoeboid appearance in order to become more motile and actively move throughout the brain toward sites of pathological events (Kettenmann et al., 2011). In rodents, 5-20% of the total glial cells in the brain are microglia (Lawson et al., 1990, Perry and Gordon, 1991). Microglial cells are capable of migration, proliferation, and phagocytosis. Microglia can also: (1) induce and rearrange their surface molecules in order to communicate via cell-cell and cell-matrix interactions; (2) change expression of their intracellular enzymes; (3) release multiple factors or compounds that are proinflammatory, immunoregulatory, chemoattractive, or neurotrophic; (4) remove synapses from axotomized motoneurons, i.e. “synaptic stripping”, in order to remodel neuronal connectivity; and (5) participate in both innate and adaptive immune responses (Kettenmann

et al., 2011). The fact that these cells express APP, suggests that APP and its proteolytic products may serve as regulators in the multitude of functions or the proinflammatory phenotype of these particular immune cells.

Hypothesis

We predict that APP and its proteolytic fragments play a central role in the inflammatory pathophysiology of not only AD but also obesity. Although the proteolytic fragments are highly studied, the functions of the full length ubiquitously expressed APP protein have yet to be elucidated. The brain expresses high levels of neuronal APP, and recent data has demonstrated that APP levels are increased in adipose tissue from obese versus control individuals. As already mentioned, prior work in our lab has demonstrated a novel role for APP in regulating the phenotype of monocytic lineage cells. Therefore, we hypothesized that APP can behave as a proinflammatory receptor on these cells involved in modulating their tissue infiltration and differentiation. Based upon the fact that midlife obesity is a risk factor for Alzheimer's disease and both obese adipose tissue and Alzheimer's disease brains share a common presence of increased, reactive macrophage and microglia, respectively, we hypothesized that APP may have a common role in both diseases regulating the infiltration or proinflammatory activation of microglia and macrophage characterizing both diseases.

CHAPTER II

METHODS

Materials

Anti- β -Amyloid Precursor Protein (APP) and anti-occludin antibodies were purchased from Invitrogen (Carlsbad, CA, USA). Anti-mouse IgM (goat), anti-rabbit (goat), anti-goat (bovine), anti-rat (goat), and anti-mouse (bovine) horseradish peroxidase-conjugated secondary antibodies, Cox-2, CD40, CD14, TLR4, CD36, GAPDH, cSrc, PPAR γ , glut-4, arginase-1, Caveolin, VLDLR, CFABP, α -tubulin, and β actin antibodies were purchased from Santa Cruz Biotechnology (Santa Cruz, CA, USA). Elite Vectastain ABC Avidin and Biotin, Vector VIP, Vector DAB, biotinylated anti-rabbit, anti-mouse, and anti-rat antibodies were purchased from Vector Laboratories Inc (Burlingame, CA, USA). Synaptophysin and β III tubulin antibodies were purchased from Chemicon international, Inc (Temecula, CA, USA). CD45 antibody was purchased from BD Biosciences Pharmingen (San Jose, CA, USA). TNF- α , DLK, FABP4, APOE, FAS, adiponectin, leptin, Y188, and LPL antibodies were purchased from Abcam Inc (Cambridge, MA, USA). CD68 antibody was purchased from AbD Serotec (Oxford, UK). iNOS antibody was purchased from Alexis Biochemicals (San Diego, CA, USA). GFAP, BACE, pAKT, AKT, and PSD95 antibody was

purchased from Cell Signaling Technology Inc (Danvers, MA, USA). MAP2 antibody and MTT (3-(4,5-Dimethylthiazol-2-yl)-2,5-diphenyltetrazolium bromide) were purchased from Sigma-Aldrich (St. Louis, MO, USA). CD3, CD11c and FATP4 antibodies were purchased from Abcam Inc (Cambridge, MA, USA). TLR2 antibody was purchased from Imgenex (San Diego, CA, USA). pTyr antibody was purchased from Millipore (Billerica, MA, USA). PHF-1 antibody was a gift from Dr. Peter Davies (Albert Einstein College of Medicine, NY). Cox-2 and Prostaglandin (PG) E₂d₄ were purchased from Cayman Chemical (Ann Arbor, MI, USA). β -Amyloid (A β), rodent specific polyclonal antibody (SIG-39151) was purchased from Covance (Emeryville, CA, USA). Oligomer antibody (A11) was purchased from Invitrogen (Camarillo, CA, USA). A β clone 4G8 was purchased from Covance (Emeryville, CA, USA). Phosphotyrosine (4G10) antibody was purchased from Upstate (Temecula, CA, USA). IBA-1 antibody was purchased from Wako Chemicals (Richmond, VA, USA). Fibril antibody (OC) antibody was generously provided by Dr. Rakez Kayed (U. Texas, Galveston, USA) (Kayed et al., 2007). LRP (H4 clone) antibody was generously provided by Dr. Isa Hussaini (U. Virginia, Charlottesville, USA).

Mice

APP^{tm1Dbo}/J homozygous (APP^{-/-}) mice, APP/PS1 (APP^{swe},PSEN1dE9) mice, and wild type (C57BL6) mice were purchased from Jackson Laboratory. The APP/PS1 (APP^{swe},PSEN1dE9) transgenic animals express the human *APP*, amyloid beta (A4) precursor protein and the human *PSEN1*, presenilin 1.

Mice were provided food and water *ad libitum* and housed in a 12 hour light/dark cycle. Mice were maintained till appropriate age then euthanized via CO₂ asphyxiation followed by cervical dislocation and cardiac exsanguination. Animals were weighed prior to collection. The investigation conforms to the *Guide for the Care and Use of Laboratory Animals* (eighth edition, 2010). Animal use was approved by the University of North Dakota IACUC.

High Fat vs. Control Diet Feeding

At six weeks of age, 34 male weight matched C57BL6/J wild type mice were placed on either a 21.2% by weight high fat diet (Harlan Teklad TD.88137) or a 5.5% by weight regular fat diet (Harland Teklad 8640), *ad libitum* (Table1). 12 animals in each group were weighed each week for 22 weeks.

Table 1. Commercial diet formulations for control and high fat diet.

	Control Diet	High Fat Diet
protein (% by weight)	22	17.3
carbohydrate (% by weight)	40.6	48.5
fat (% by weight)	5.5	21.2
energy density (Kcal/g)	3	4.5

Western Blotting

Upon collection, the animals were perfused with PBS containing CaCl₂ and tissues (brain, hippocampus, visceral (pericardial or heart) fat, subcutaneous (abdominal or stomach) fat, and the ileum of small intestine were collected. Intestine was rinsed to remove lumen contents, flash frozen and pulverized.

Tissue samples were lysed using ice cold RIPA buffer (20mM Tris, pH 7.4, 150mM NaCl, 1mM Na₃VO₄, 10mM NaF, 1mM EDTA, 1mM EGTA, 0.2mM phenylmethylsulfonyl fluoride, 1% Triton, 0.1% SDS, and 0.5% deoxycholate) with protease inhibitors (AEBSF 1mM, Aprotinin 0.8μM, Leupeptin 21μM, Bestatin 36μM, Pepstatin A 15μM, E-64 14μM). For intestine tissue samples 50U/mL DNase1 (Amresco Inc, Solon, OH, USA) was also added to the RIPA buffer with protease inhibitors. To remove insoluble material cell lysates were sonicated and centrifuged (14,000 rpm, 4°C, 10 min). The Bradford method (Bradford, 1976a) was used to quantify protein concentrations. Proteins were resolved by 7%, 10% or 15% sodium dodecyl sulfate-polyacrylamide gel electrophoresis (SDS-PAGE) and transferred to polyvinylidene difluoride (PVDF) membranes for Western blotting using anti-APP, BACE, occludin, iNOS, Cox-2, synaptophysin, PSD95, MAP2, phospho-tau (PHF-1), TNF-α, GFAP, CD68, CD40, CD3, CD11c, TLR2, TLR4, CD36, FATP4, pTyr, pSrc, cSrc, glut-4, CD14, pAKT, AKT, FAS, PPARγ, FABP4, LRP, APOE, arginase-1,DLK, LPL, VLDLR, adiponectin, caveolin, leptin, βIII tubulin (loading control), α-tubulin (loading control), GAPDH (loading control). Antibody binding was detected with enhanced chemiluminescence (GE Healthcare, Piscataway, NJ, USA). In some instances, antibodies were stripped from blots with 0.2 NaOH, 10 min, 25°C, for antibody reprobing. Western blots were quantified using Adobe Photoshop software. In order to be able to compare all the samples per dietary condition for each antibody it was necessary to run two gels per antibody probe. To minimize any variability across gels, control and high fat diet samples were resolved and

transferred for individual antibody comparisons at the same time in the same gel running/transfer apparatus. The blots were incubated in the same antibody solution and visualized and quantified at the same time. This minimized the variability of across-gel comparisons. Optical density of bands were normalized against their respective loading controls and averaged (+/-SD).

Immunohistochemistry

Upon collection, the animals were perfused with PBS containing CaCl_2 and brain, hippocampus, visceral (pericardial/heart) fat, subcutaneous (abdominal/ stomach) fat, and/or intestine was collected and immersion fixed for 24 hrs in 4% paraformaldehyde, cryoprotected through two successive 30% sucrose changes. Brains were embedded in gelatin and serially sectioned (40 μm) via freezing microtome and immunostained using anti-APP, Y188, β -amyloid, CD68, iNOS, Cox-2, or GFAP antibodies or respective secondary only antibodies. Subcutaneous and visceral fat tissue samples were serially cryosectioned (10 μm) or paraffin embedded and sectioned (7 μm) for immunostaining with anti-APP, Y188, β -amyloid, CD45 or CD68 antibodies or respective secondary only antibodies. Ileum samples were serially cryosectioned (10 μm) for immunostaining with anti-APP, OC, A11, 4G8, CD68, Cox-2, occludin, MAP2, CD36, pTyr, pSrc, synaptophysin, and GFAP antibodies or respective secondary only antibodies. Antibody binding in brain or fat was visualized using Vector VIP or DAB as chromogens (Vector Laboratories, Burlingame, CA, USA). For double labeling, immunostained tissue was stripped of antibodies with 0.2N

HCl for 10 min prior to processing with the second primary antibody incubation and visualization steps. Images were taken using an upright Leica DM1000 microscope and Leica DF320 digital camera system. Figures were made using Adobe Photoshop 7.0 software.

Histological Stain

Upon collection, the animals were perfused PBS containing CaCl_2 and ileum of the small intestine and liver were collected and immersion fixed for 24hrs in 4% paraformaldehyde and cryoprotected through two successive 30% sucrose changes. A 1cm piece of ileum of small intestine was cut, then cut lengthwise and flattened for sectioning. Ileum samples were serially cryosectioned ($10\mu\text{m}$) for routine histology H & E (hematoxylin and eosin) and Alcian blue stains. Liver samples were paraffin embedded and sectioned ($7\mu\text{m}$) for H & E stain. For H & E stain, slides were rinsed in xylene three times for 1 min each, followed by rehydration in 2 changes of absolute alcohol for 2 min, then 95%, 80%, 70% alcohol for 1 min each, followed by a rinse in DH_2O for 1 min. Slides were then stained with Hematoxylin Regulars for 40 seconds followed by a rinse in running tap water for 10 dips, then differentiated with 3% acid alcohol for 2 dips, followed by rinse in running tap water for 10 dips. Slides were then blued in lithium carbonate (1% sodium bicarbonate) solution for 3-5 dips followed by rinsing again in running tap water before a 1 min rinse in 70% alcohol and then 5-10 seconds in Eosin. Slides were dehydrated two times each for 1 min in 95% alcohol, 100% alcohol and xylene followed by covering with Permount (Electron

Microscopy Sciences). For Alcian blue stain, slides were placed in 100% alcohol, 95% alcohol, 70% alcohol, and DH₂O for 1 min each then mordant in 3% aqueous acetic acid for 1 min, 1% Alcian blue in 3% acetic acid pH 2.5 for 10 min followed by rinse in running water for 5-6min and rinse in DH₂O. Slides were counterstained in Nuclear Fast Red 0.1% (kerechtrot) for 1.5 min then rinsed in running water for 10 min before dehydrating in 95% alcohol, 100% alcohol and xylene 2 times each for 1 minute before being covered with Permount.

Glucose, Triglycerides, HDL and Total Cholesterol Measurements

Prior to collection mice were fasted for 6hrs (water only) and then glucose, triglycerides, HDL and total cholesterol were measured using a CardioChek meter (Test Medical Symptoms @ Home, Inc, Maria Stein, OH, USA) and corresponding strips via tail lancet. After baseline measurements were recorded mice were injected intraperitoneally with 2g/kg glucose followed by 30, 60, 90, 120 min glucose measurements.

Macrophage Isolation and Stimulation

At collection non-elicited peritoneal macrophages were rinsed from the peritoneal cavity with sterile PBS, counted, plated and allowed to adhere to the tissue culture wells for 2-3 hours in DMEM/F12 plus PSN antibiotics (0.05mg/mL Penicillin, 0.05mg/mL Streptomycin, 0.1mg/mL Neomycin (Gibco, Carlsbad, CA, USA)). Ileum of the intestines were removed from the abdominal cavity and rinsed with sterile PBS inside and outside to remove residual contents.

Intestines were then rinse again with HBSS (8g NaCl, 0.4g KCl, 3.57g Hepes, 0.06g Na₂HPO₄ x 2 H₂O, 0.06 g KH₂PO₄ in 1 liter DH₂O) and then placed in sterile enzyme solution (5mM Glucose, 1.5% BSA, 5mg/mL Collagenase, 20% FBS in HBSS), minced and placed in 37°C incubator for 30 min to allow digestion to occur. Tissue was then triturated, filtered through a 70µm cell strainer, quenched with HBSS and spun for 4 min at full speed. The pellet was resuspended in HBSS, triturated and spun for another 4 min at full speed. The pellet was resuspended in DMEM/F12 plus PSN antibiotics and 400uL of suspended cells was plated in another 1mL of DMEM/F12 plus PSN antibiotics for 2-3 hours to allow adherence of macrophages. Nonadherent and non-macrophage cells were rinsed from the wells using ice-cold DMEM/F12. Macrophage were then plated in DMEMF12 containing isotype negative control 1µg/mL IgG₁ (Millipore, Billerica, Massachusetts USA), APP agonist antibody 1µg/mL 22C11 (Millipore, Billerica, Massachusetts USA), 25ng/mL LPS (Sigma) or 100nM Aβ1-40 or 100pM Aβ1-40 or media alone was added to the wells overnight for stimulation. Media was collected for ELISA and cytokine arrays.

Microglia Isolation and Stimulation

Acutely isolated microglia were collected at 22 weeks as previously described (Floden and Combs, 2006). Briefly, cortices were isolated, finely minced and filtered through 140 and 70 um filters then gently digested with DNase I and collagenase before being separated on a Percoll gradient. The

microglial layer was collected, counted and used for stimulations. Microglia were stimulated overnight with 25ng LPS, 10 μ M A β 1-40 or media alone.

Intestinal Epithelial Cell Isolation and Stimulation

Ileum of the intestines were removed from the abdominal cavity and rinsed with sterile PBS inside and outside to remove residual contents. Intestines were then rinse again with HBSS (8g NaCl, 0.4g KCl, 3.57g Hepes, 0.06g Na₂HPO₄ x 2 H₂O, 0.06 g KH₂PO₄ in 1 liter DH₂O) and then cut longitudinally to open and placed in 15nM dithiothreitol (Sigma-Aldrich, St. Louis, MO, USA) for 15 minutes at 37°C to remove mucus. Tissue was then further digested in HBSS + antibiotics (0.05mg/mL Penicillin, 0.05mg/mL Streptomycin, 0.1mg/mL Neomycin (Gibco, Carlsbad, CA, USA)) + 10% FBS + 1.5mg collagenase (Worthington, Lakewood NJ, USA) and 400U dispase (Sigma-Aldrich, St. Louis, MO, USA) for 45 minutes at room temperature then 45 minutes at 37°C on an agitator. Digestion was stopped by adding one volume of complete media (DMEMF12 + antibiotics + 10% DHS + 20% FBS). Cells were then spun, spent media was removed, and the pellet was resuspended in complete media + D-Sorbitol (Sigma-Aldrich, St. Louis, MO, USA) (buoyancy aid to help separate the crypts and single cells for the tissue pellet) and pipetted vigorously. Tissue was allowed to settle for 1 min and then supernatant was filtered through a 70 μ M cell strainer (BD Falcon, Franklin Lakes, NJ, USA). Filtered suspension was then spun and the pellet was suspended in complete media + 10mM L-glutamine (Sigma-Aldrich, St. Louis, MO, USA) and plated overnight. After 24 hours spent media was removed and

replaced with new media allowing the cells to culture for an additional 3 days prior to treatment. Epithelial cells were then stimulated overnight with 25ng/mL LPS, 10 μ M A β 1-40, or media alone.

Enzyme-Linked Immunosorbent Assay (ELISA)

Media was collected from overnight stimulation of macrophage or microglia was used to quantifying secreted TNF- α according to the manufacturer's protocol (R&D Systems, Minneapolis, MN, USA), secreted keratinocyte chemokine (KC), Regulated upon Activation, Normal T-cell Expressed, and Secreted (RANTES), Interleukin-6 (IL-6), Interleukin-1 beta (IL-1 β) according to the manufacturer's protocol (R&D Systems, Minneapolis, MN, USA), A β 1-40 and A β 1-42 Elisa (Invitrogen, Life Technologies, Grand Island, NY, USA). Stool washing samples were also diluted further by 1:5000 and 300 μ L of the dilute sample was added to the IgA Elisa plate according to manufacturer's protocol (Bethyl Laboratories Inc, Montgomery, TX, USA). Secretion was normalized to cell protein amount as determined by the Bradford method (Bradford, 1976b) after cells were lysed in ice cold RIPA buffer with protease inhibitors, sonicated, and spun to remove insoluble material. Data is the average (+/-SD). Tissue was weighed, lysed in RIPA buffer, sonicated, centrifuged, and then supernatant plated for quantifying levels of TNF- α , IL-6, IL-10, IL-4, MCP-1, IL-1 β , and adiponectin according to the manufacturer protocol (R&D Systems, Minneapolis, MN). Values were normalized by tissue weight.

Migration and Proliferation Assay

After rinses following the 2-3 hours of adherence, macrophages were removed with ice cold dissection media and gentle trituration. One set of macrophages (5,000 cells/well/96 well) had DMEM/F12 containing PSN antibiotics, 10% FBS and 5% horse serum added for 72hrs followed by an MTT (3-(4,5-Dimethylthiazol-2-yl)-2,5-diphenyltetrazolium bromide) reduction assay to indirectly measure cellular proliferation. The media was removed and replaced with 0.1mg/mL MTT for 4 hr. The precipitated formazan was dissolved in isopropanol and absorbance read at 560nm. Another set of macrophages (5,000 cells/well) were resuspended in DMEM/F12 and transferred to Transwell permeable support inserts (3µm, Corning Inc. Corning, NY, USA) in collagen coated 24 well dishes containing 25ng/mL LPS to measure transmigration by counting the number of migrated cells after 24 hours.

Prostaglandin Analysis

PG were analyzed as previously described (Golovko and Murphy, 2008). Brain samples (were homogenized in 1 mL of saline and extracted with 2 mL of acetone containing 0.005% butylated hydroxytoluene (BHT) following with 2 mL of chloroform with 0.005% BHT. PGE₂d₄ was used as internal standard. After extraction, the samples were dried under a stream of nitrogen and then redissolved in 30 µL of acetonitrile:water (1:2 by volume). Reverse-phase LC electrospray ionization mass spectrometry was used for PG analysis. The PG were separated on a Luna C-18(2) (3 µm column, 100 Å pore diameter, 150 x 2.0

mm) (Phenomenex, Torrance, CA, USA) with security guard cartridge system (Phenomenex, Torrance, CA, USA). The LC system consisted of an Agilent 1100 series LC pump with a wellplate autosampler (Agilent Technologies, Santa Clara, CA). The solvent system was composed of 0.1% formic acid in water (solvent A) and 0.1% formic acid in acetonitrile (solvent B). The flow rate was 0.2 mL/min. The separation program started with 10% of solvent B. At 2 min, the percentage of B was increased to 65% over 8 min, at 15 min the percentage of B was increased to 90% over 5 min, and at 35 min it was reduced to 10% over 2 min. Equilibration time between runs was 13 min. Mass spectrometry analysis was performed using a quadrupole mass spectrometer (API3000, Applied Biosystem, Foster City, CA, USA) equipped with a TurbolonSpray ionization source. Analyst software version 1.5.1 (Applied Biosystem, Foster City, CA, USA) was used for instrument control, data acquisition, and data analysis. The mass spectrometer was optimized in the multiple reaction-monitoring mode. The source was operated in negative ion electrospray mode at 450 °C, electrospray voltage was -4250 V, nebulizer gas was 8 L/min and curtain gas was 11 L/min. Declustering potential, focusing potential, and entrance potential were optimized individually for each analyte. The quadrupole mass spectrometer was operated at unit resolution.

Uptake for Cell Cultures

[1-¹⁴C]16:0, [1-¹⁴C]20:4 (*n*-6) and [1-¹⁴C]22:6 (*n*-3) were dissolved in ethanol and had a final specific activity of 55 nCi/nmol, 50 nCi/nmol and 51

nCi/nmol, respectively. Cells were incubated in serum free media containing fatty acid tracer (50 nCi/ml) for 5, 15 and 30 min at 37°C. Ethanol concentration in the medium was 0.2%. At the end of incubation, cells were washed twice with ice-cold phosphate-buffered saline and extracted with hexane:2-propanol (3:2) and an aliquot of lipid extract was assayed for radioactivity using liquid scintillation counter.

Antibody-Based Cytokine Array

The media from stimulated macrophage or microglia was removed, or tissue lysed in lysis buffer and quantitated by Bradford in which 1mg per sample, was used to probe a 40 cytokine antibody-based membrane array according to the manufacturer's protocol (Ray Biotech, Norcross, GA, USA). Optical density of dots were normalized against their respective positive controls and averaged (+/- SD).

Adipocyte, Adipose Tissue Macrophage, and Fibroblast Isolation and Stimulation

Adipocyte cultures were generated via a modification of a prior method (Fernyhough et al., 2004). Subcutaneous abdominal adipose tissue was removed from the mice, rinsed with sterile Hanks Balanced Salt Solution (HBSS), minced with scissors, placed in 35mm plates and incubated for 1hr @ 37C on a rocker in a sterile enzyme solution (5mM glucose, 1.5% BSA, 5mg collagenase in HBSS). Following incubation, adipocytes were spun at 186xg for 2 min and the two layers were separated into separate tubes. Both the upper and the lower layer was

resuspended in sterile HBSS to repeat the spin, rinse was repeated two times. The final lower layer (stromal vascular layer) was resuspended in DMEM/F12 + antibiotics (0.05mg penicillin/0.05mg streptomycin/0.01mg neomycin/mL) and plated on 24 well plates for 3 hours. Nonadherent and non-macrophage cells were rinsed from the wells using ice-cold DMEM/F12. Macrophages were then plated in DMEM/F12 containing 25ng LPS or 100nM A β 1-40 or 100pM A β 1-40 or media alone was added to the wells overnight for stimulation. Media was collected for ELISA and cytokine arrays. The final upper (adipocyte and fibroblast) layer was resuspended in DMEM/F12 + 10% FBS + 5% horse serum + antibiotics (0.05mg penicillin/0.05mg streptomycin/0.01mg neomycin/mL). The cells were added to 96 well plates, with DMEM/F12 +10% FBS +5% horse serum + antibiotics. The plates were then completely filled to the brim with media, covered with sterile parafilm, and inverted for 2 weeks to allow floating adipocytes to adhere to the tissue culture treated component of the plastic wells and the fibroblast could adhere to the opposite side of the flask. After 2 weeks, the media was removed, cells were lysed or the plates were placed right-side up so that adipocytes were now available for stimulation or left as is for fibroblast use. The cells were treated with serum free DMEM/F12 and unstimulated (control) or stimulated for 24hr with 1 μ g/mL IgG₁ (isotype negative control) or 1 μ g/mL 22C11 (APP agonist antibody) or 100nM A β 1-40. After 24 hours, secreted LDH was measured according to the manufacture protocol for both the media and the cell lysates using commercial reagents (Promega, Madison WI). Secreted media LDH values were normalized against cellular LDH values. Media

was also collected for ELISA analysis quantifying secreted TNF- α according to the manufacturer's protocol (R&D Systems, Minneapolis, MN). Cells were also fixed, stained with Oil Red O (Alfa Aesar, Ward Hill, MN, USA) and DAPI (4',6-diamidino-2-phenylindole) (Sigma Aldrich, St. Louis, MO, USA) counterstained and changes in Oil Red O absorbance (510nm) normalized to DAPI absorbance (358/461nm) were quantified via plate reader. Experiments were repeated three independent times.

Neuronal Isolation and Stimulation

Pregnant dams were sacrificed by CO₂ asphyxiation and cardiac exsanguination to isolated embryonic day 16 (E16) pups, Fetuses were removed from the uterus and the entire brain was removed. Using a dissecting microscope under the hood, both cortices were collected and meninges were removed. Cortices was minced into pieces and digested with 0.25% trypsin for 15-20min @ 37°C. Following digestion the trypsin was neutralized by adding the tissue to 10mL of FBS or DMEM/F12 with 5% horse serum, 10% FBS and antibiotics. The tissue was then removed from the serum or media and added to 10mL of Neurobasal media. Trituration was done to gently break up the tissue. Neurons were counted and plated accordingly for use. Neurons were stimulated overnight with 1 μ g/mL IgG₁ (isotype negative control), 1 μ g/mL 22C11 (APP agonist antibody), 1.2 μ M BACE inhibitor (β -secretase inhibitor II) (Calbiochem, Billerica, MA, USA), vehicle control DMSO, or media alone. Following overnight stimulation cells were lysed for Western blot analysis.

Immunoprecipitation

For co-immunoprecipitations, tissues or cells were collected and lysed in ice-cold triton lysis buffer (20mM Tris, pH 7.4, 150mM NaCl, 1mM Na₃VO₄, 10mM NaF, 1mM EDTA, 1mM EGTA, 0.2mM phenylmethylsulfonyl fluoride, and 1% Triton). Tissues or cells were homogenized using a teflon pestle. Homogenates were incubated on ice for 15 min, followed by centrifugation to remove insoluble material (14,000 rpm, 4 °C, 10 min). Homogenates were incubated with precipitating antibody (anti-APP or anti-CD36) (1 µg of antibody/mg protein lysate) for 2 h at 4 °C, followed by incubation with protein A/G agarose beads (Santa Cruz Biotech, Santa Cruz, CA) for 2 h at 4 °C. Resulting immunoprecipitates were washed three times in triton buffer and resolved by 10% SDS-PAGE and Western blotted as described.

Caco-2 Cells

Caco-2 cells were purchased from ATCC (Manassas, VA, USA). Caco-2 cells were maintained in DMEMF12 (Gibco, Life Technologies, Grand Island, NY, USA) supplemented with 10% FBS, 5% donor horse serum (Serum Source International, Charlotte, NC, USA) and antibiotics (0.05mg penicillin/0.05mg streptomycin/0.01mg neomycin/mL) (Sigma-Aldrich, St. Louis, MO, USA). Caco-2 cells were plated allowed to grow to confluence before removing supplemented media and replacing with serum free DMEMF12 with or without treatment. Following stimulation Caco-2 cells were used for A β uptake, MTT assays, ELISA, and Western blot analysis.

Caco-2 and Microglia A β Uptake Assay

FITC labeled A β 1-40 was prepared according to the manufacturer's protocol (rPeptide, Bogart, GA, USA). 500nM of the peptide was added to confluent cells in serum free DMEM/F12 for 4 hours in the absence or presence of 10ng/mL LPS. The media was then removed and extracellular peptide signal was quenched by rinsing cells with 0.25% trypan blue dissolved in PBS. A β uptake was quantified using a fluorescent plate reader (480 nm excitation and 520 nm emission).

Caco-2 Cell ELISA

Caco-2 cells were incubated overnight in serum free DMEM/F12 with or without 10ng/mL LPS, 100nM A β 1-40, 1 μ M A β 1-40, or 5 μ M A β 1-40. The media was collected for A β 1-40 and A β 1-42 (Invitrogen, Life Technologies, Grand Island, NY, USA), IL-8, MCP-1, MDC, IL-6, and TNF α ELISA (R&D systems, Minneapolis, MN, USA). The cells were lysed in using ice cold RIPA buffer with protease inhibitors and 50U/mL DNase1. To remove insoluble material cell lysates were sonicated and centrifuged (14,000 rpm, 4°C, 10 min). The Bradford method (Bradford, 1976b) was used to quantify protein concentrations for normalization of A β in the media and samples were used for Western blotting as previously described.

Caco-2 MTT Reduction Assay

The MTT assay was used to determine changes in cell viability using 3[4,5-dimethylthiazol-2-y1]-2,5-diphenyltetrazolium bromide (MTT, 100µg/mL) (M-2128) purchased from Sigma (St. Louis, MO) that we dissolved in DMEM/F12. Following the overnight stimulations, media was removed and the cells were incubated with MTT for 4 hours. The media was aspirated and the reduced formazan precipitate was dissolved in isopropanol. Absorbance values were read at 560/650nm via plate reader.

Blood Collection and LAL Assay

At the time of perfusion, blood was collected in heparinized tubes via heart puncture and spun at 190g~7400rpm for 10min at 4°C. Plasma was then transferred to sterile centrifuge tubes which were flash frozen to be analyzed the following day for lipopolysaccharide (LPS) quantitation according to the Genscript ToxinSensor™ Chromogenic LAL Endotoxin Assay Kit protocol (GenScript, Piscataway, NJ).

Stool Weight

Total stool weight was measured by placing the animals in a clean empty cage and collecting all stool produced over a 1hr time period. Stool was then desiccated at 80°C overnight to determine dry weight. Stool water was calculated as the difference between these two measurements.

Statistical Analysis

The data were analyzed by unpaired two-tailed t-test with or without Welch correction for unequal variance as required, by two-way repeated measures ANOVA with Holm-Sidak post hoc test, by two-way ANOVA with Holm-Sidak post hoc test, by one-way ANOVA with Holm-Sidak post hoc test or a Kruskal-Wallis nonparametric ANOVA with a Dunn's post hoc test were utilized for analysis.

CHAPTER III

AMYLOID PRECURSOR PROTEIN AND PROINFLAMMATORY CHANGES ARE REGULATED IN BRAIN AND ADIPOSE TISSUE IN A MURINE MODEL OF HIGH FAT DIET-INDUCED OBESITY

High fat diet feeding increased brain levels of APP and multiple pro-inflammatory proteins compared to control diet fed mice

In order to establish the system for comparing changes in adipose tissue to brain, a standard high fat diet feeding paradigm was used. 24 six week old weight-matched male C57BL6 mice were placed on either a 21.2% by weight high fat diet or a 5.5% by weight control diet, *ad libitum*, beginning at six weeks of age (Table 1). Twelve animals in each group were weighed weekly for 22 weeks and mean (+/-SD) weight gain per group was graphed versus time (Figure 1). By week five the high fat diet fed mice demonstrated a statistically significant increase in weight gain over the control diet fed mice (Figure 1). After 22 weeks, the high fat diet fed mice had on average a 217% total weight gain, whereas control diet fed mice had on average only a 158% total weight gain.

To examine whether proinflammatory or degenerative changes were occurring in the brains of high fat diet fed animals, Western blot analysis of hippocampi from both groups was performed. As expected, high fat diet fed mice demonstrated a significant increase in expression of APP when compared to

control diet fed mice (Figure 2). This did not correlate with any change in protein levels of the postsynaptic protein marker, PSD95, or the presynaptic marker, synaptophysin (Figure 2).

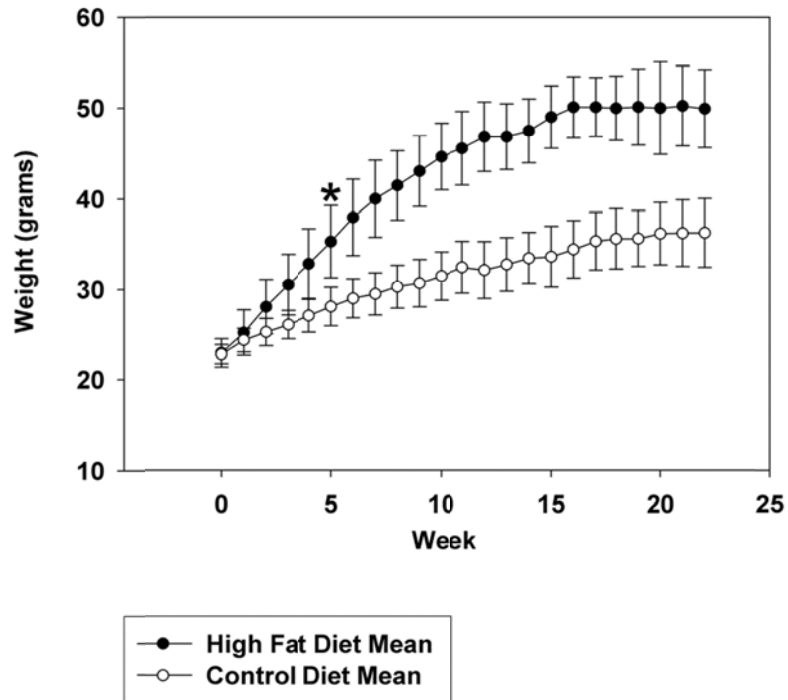


Figure 1. Average weight gain per week for mice fed a high fat versus control diet. C57BL6 mice at 6 weeks of age and weight matched were fed, *ad libitum*, a control (5.5% fat/weight) or high fat (21.2% fat/weight) diet for 22 weeks. 12 animals in each group were weighed weekly and mean (+/-SD) weight gain per group was graphed versus time. *P=0.001.

However, there was a significant increase in astrocyte GFAP protein levels, but no change in microglia CD68 protein levels associated with the high fat diet fed mice. Interestingly, two markers of inflammatory change, iNOS and Cox-2 were not altered in hippocampi of high fat diet versus control diet fed

animals (Figure 2). Although Cox-2 protein levels were not altered, we further examined enzyme activity and total brain prostaglandin (PG) levels (a sum of PGE₂, PGD₂, 6-*keto*PGF_{1α}, PGF_{2α}, and thromboxane B₂) were quantitated from animals in each diet group. Interestingly, high fat diet fed animals demonstrated a significant increase in brain prostaglandin levels compared to control fed animals indicating elevated arachidonic acid metabolism in spite of no significant change in protein levels of Cox-2 (Figure 2). Additionally, high fat diet feeding did not significantly alter phosphorylation levels of tau protein (Lang et al., 1992) as assessed using the PHF-1 antibody (Figure 2). These data demonstrate that high fat diet feeding stimulates an increase in APP protein levels in the brain which correlates with an increased level of gliosis and elevated prostaglandin levels. This supports the notion that the chronic inflammatory changes associated with peripheral tissue during diet-induced obesity extend into the brain. Moreover, these changes are consistent to some degree with those that are observed during Alzheimer's disease.

Proinflammatory protein immunoreactivity increased in neurons in brains from high fat diet versus control fed mice

Although the Western analysis demonstrated significant protein changes in high fat diet fed mice compared to controls, the cellular identity of those proteins was unknown. Understanding the cellular contribution was of particular interest since APP is expressed by several cells in the brain.

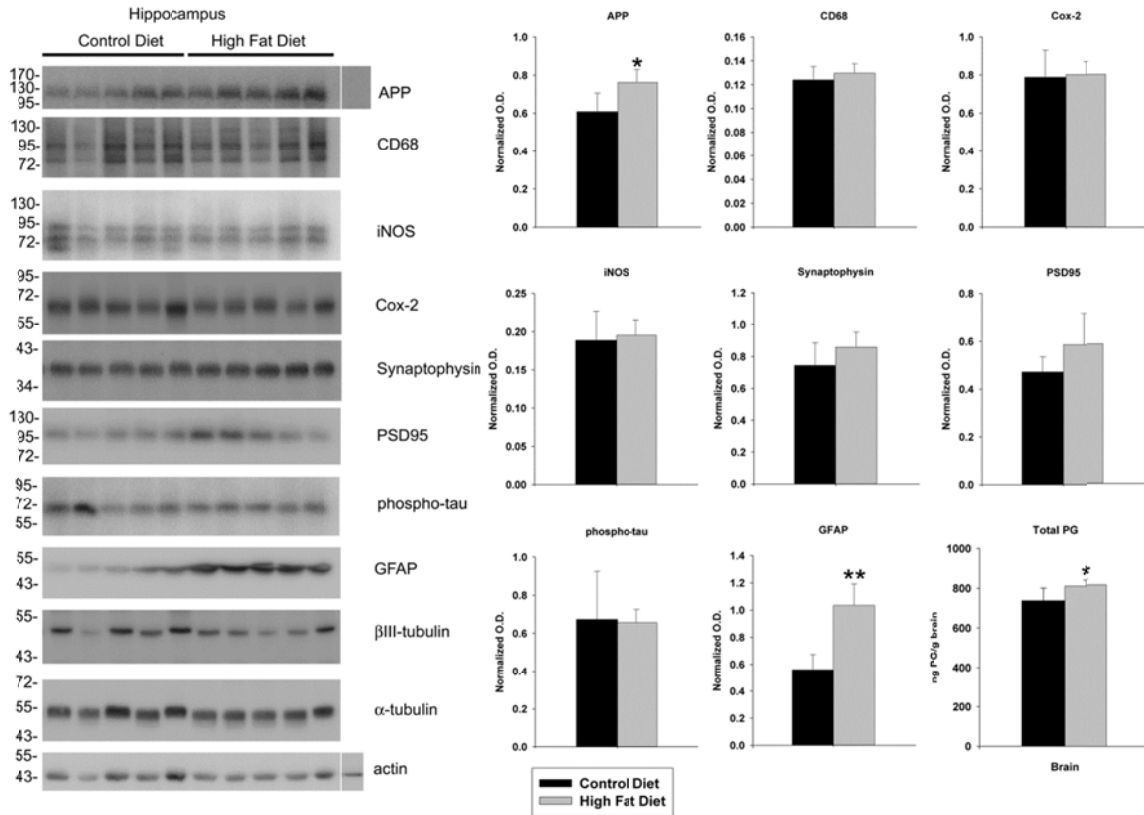


Figure 2. APP and GFAP protein levels were increased in hippocampi of high fat versus control diet fed mice. C57BL6 mice at 6 weeks of age and weight matched were fed, *ad libitum*, a control (5.5% fat/weight) or high fat (21.2% fat/weight) diet for 22 weeks. Hippocampus samples were collected from 5 animals for each diet. Comparable age hippocampi from APP^{-/-} mice were collected as negative controls for antibody specificity. The tissue was lysed, resolved by 10-15% SDS-PAGE and Western blotted using anti-synaptophysin, PSD95, APP, iNOS, Cox-2, GFAP, phospho-tau (PHF-1), CD68, β III tubulin (neuronal loading control), α -tubulin and actin (general loading control) antibodies. Arrowheads indicate bands of interest when nonspecific bands are present. Antibody binding was visualized by chemiluminescence. Blots from all

animals in each diet are shown. Optical densities of the Western blotted hippocampal proteins (APP, CD68, iNOS, Cox-2, GFAP, synaptophysin, PSD95, and phosphor-tau) from the control and high fat diet Western blots were normalized against their respective averaged O.D. values of combined α -tubulin+ β III tubulin+actin loading controls (+/- SD) from 5 animals for each diet. Total brain PG levels were quantitated as a sum of PGE₂, PGD₂, 6-ketoPGF_{1 α} , PGF_{2 α} , and thromboxane B₂ in each diet group. *P<0.05 and **P<0.01.

In order to determine which cells may be responsible for the changes in protein levels, immunohistochemistry was performed from the collected hippocampi. In agreement with the fact that the majority of APP is expressed by neurons in the brain (Bendotti et al., 1988) both high fat and control diet fed mice displayed neuronal immunoreactivity for APP with a diet-induced increase in immunoreactivity in the high fat diet fed mice (Figure 3). To examine whether APP was increasingly processed or deposited as the proteolytic fragment, beta amyloid (A β), brain sections were also immunostained using an anti-mouse A β antibody. However, there was no obvious change in intensity or distribution of A β immunoreactivity in the different diet fed animals (Figure 3). Cox-2, iNOS, and CD68 histologic analysis demonstrated what appeared to be elevated immunoreactivity for each (Figure 3) although this did not reach the level of statistical significance via Western blot analysis (Figure 2). Interestingly, the immunoreactivity for both Cox-2 and iNOS in high fat diet fed animals appeared within neurons as opposed to glia (Figure 3). Although, the difference in

immunoreactivity for reactive microglia (CD68) was modest, there was a clear increase in astrocyte GFAP immunoreactivity in the high fat diet fed animals compared to controls demonstrating that at least an astrogliosis was occurring (Figure 3). These data demonstrated that high fat diet feeding induced a reactive gliosis in the brain. However, since the Western blot analysis detected increased protein levels of APP within neurons, the proinflammatory changes were not limited to any particular cell type in the brain but instead appeared to include a multi-cellular response.

In spite of the fact that microglia and astrocytes demonstrated immunoreactivity for typical activation markers, CD68 and GFAP respectively, this was not necessarily a reflection of a contribution to any proinflammatory changes that were occurring. As a means of assessing this, microglia were further examined based upon our prior experience with isolating these cells from adult animals (Floden and Combs, 2006). For comparison, microglial secreted TNF- α levels were compared to values derived from resting peritoneal macrophage as a positive control. In general microglia isolated from the 22 week old control fed animals secreted far less TNF- α when compared to their peripheral cell counterparts (Figure 4). However, microglia from high fat diet fed mice secreted significantly more TNF- α than the control diet fed animals (Figure 4). This was entirely consistent with the subtle increase in CD68 immunoreactivity observed even though quantified Western blot analysis revealed no significant difference in CD68 protein levels in the brains of high fat diet fed mice compared to controls. Taken together, these data support the idea

that proinflammatory changes occur in brains of high fat diet fed animals. These involved not only neuronal upregulation of proteins but also increased cytokine secretion from reactive glia.

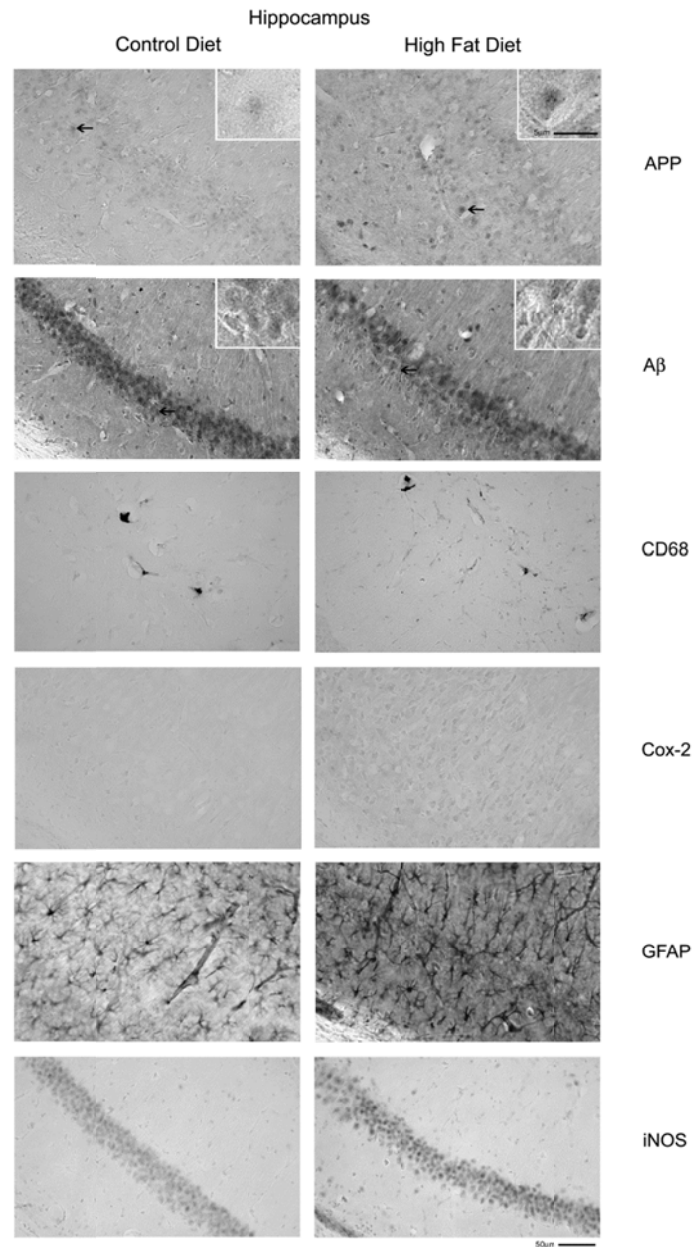


Figure 3. Hippocampi of high fat diet fed mice demonstrated microglial (CD68), astrocytic (GFAP), and neuronal (Cox-2, APP and iNOS) immunoreactivity versus control diet mice. C57BL6 mice at 6 weeks of age

and weight matched were fed, *ad libitum*, a control (5.5% fat/weight) or high fat (21.2% fat/weight) diet for 22 weeks. Tissue samples were collected, fixed in 4% paraformaldehyde, serially sectioned, and immunostained. Tissue sections were immunostained using anti-APP, A β , GFAP, CD68, Cox-2, and iNOS antibodies and antibody binding was visualized using Vector VIP as the chromagen. Arrows indicate the location of APP immunoreactivity shown as an enlarged inset in upper right corner of each panel. Representative images from 12 animals per condition are shown.

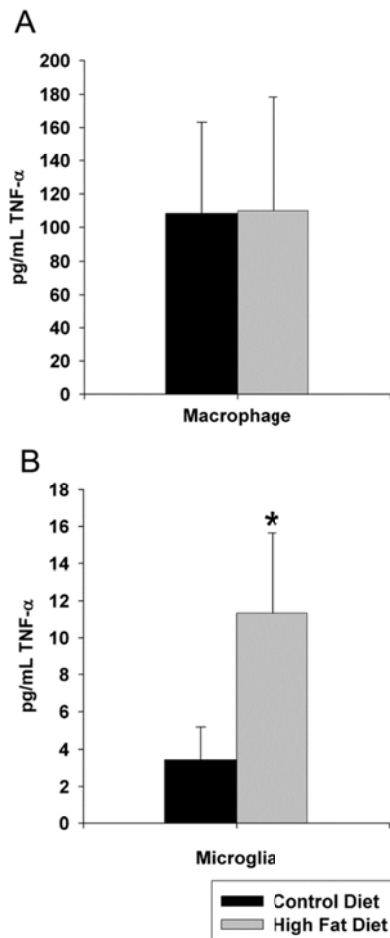


Figure 4. Microglia but not peritoneal macrophage demonstrated increased TNF- α secretion. C57BL6 mice at 6 weeks of age and weight matched were fed,

ad libitum, a control (5.5% fat/weight) or high fat (21.2% fat/weight) diet for 22 weeks. Microglia were isolated from brains for comparison to non-elicited peritoneal macrophage. Isolated microglia or macrophage from control and high fat diet fed mice were plated overnight in serum free DMEM/F12 media and secreted TNF- α levels were quantified by commercial ELISA. Data is the average (+/-SD) of 12 animals/condition. *P<0.05.

High fat diet feeding increased APP and TNF- α protein levels compared to control diet fed mice in both subcutaneous and visceral fat depots

Based upon the changes observed in the brain, adipose tissue was next examined to determine whether similar changes in proinflammatory protein expression occurred in the periphery. Because visceral and subcutaneous fat depots can have altered protein expression changes during diet-induced obesity (Borst and Conover, 2005, Poussin et al., 2008, Matsubara et al., 2009, Ibrahim, 2010) both types of adipose reservoirs were assessed. To begin comparing protein changes between brain and adipose tissue, Western blot analysis was again performed. Subcutaneous abdominal fat and visceral pericardial fat were examined as representative samples of two distinct fat depots. Precisely as observed in the brain, high fat diet fed mice demonstrated a significant increase in APP protein levels in both fat depots over control diet fed mice (Figure 5). To again assess if there was a proinflammatory change, the two proinflammatory protein markers quantified from brain, iNOS and Cox-2, were next examined in the fat depots. Consistently, the diets demonstrated no difference in either iNOS or Cox-2 protein levels in either type of adipose tissue (Figure 5). However,

based upon the fact that microglial-secreted TNF- α levels were increased in high fat diet fed mice and TNF- α elevations are a well characterized change in adipose tissue from obese individuals (Hotamisligil et al., 1995, Kern et al., 1995) or animals (Hotamisligil et al., 1993), we next quantified TNF- α protein levels. Similar to the changes observed from brain microglia, both visceral and subcutaneous fat depots demonstrated increased TNF- α levels compared to pair fed controls (Figure 5). These data demonstrate that although there were no significant differences between visceral and subcutaneous fat depots, the overall proinflammatory changes were consistent between adipose tissue and brain during high fat diet feeding. In particular, the proinflammatory proteins, Cox-2 and iNOS, were not significantly increased in either the brain or adipose tissue in spite of the observed elevation in TNF- α from both tissue types. Perhaps the most interesting observation was that APP levels increased in both brain and adipose tissue. This demonstrated that a coordinated, increased expression of APP occurred in the brain and adipose tissue upon diet-induced obesity along with acquisition of proinflammatory tissue phenotypes.

Adipose tissue APP immunoreactivity from high fat diet fed animals localized to adipocytes and macrophage

Although brain changes in APP were determined to be neuronally localized it was not likely that the increased APP levels in adipose tissue were also neuronal. Therefore, to identify the cellular origin of the increased APP levels in high fat diet fed adipose tissue immunohistochemistry was again performed. In both subcutaneous (Figure 6A) and visceral (Figure 6B) adipose

tissue increased APP immunoreactivity was observed in high fat diet fed versus control diet fed animals.

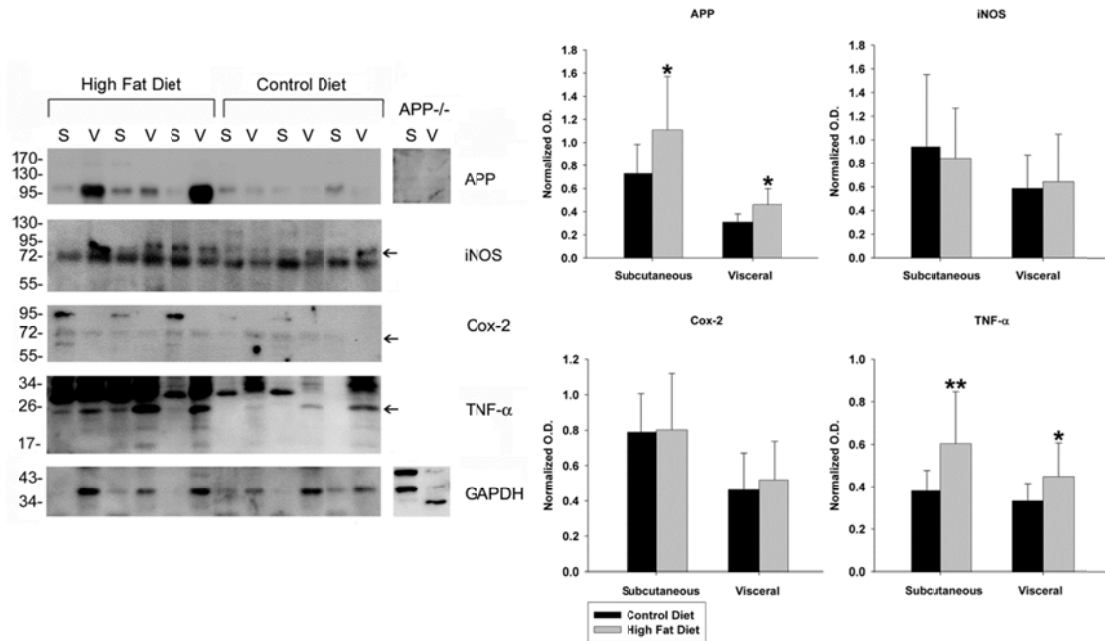


Figure 5. APP and TNF- α levels increased in visceral and subcutaneous fat depots in high fat diet fed animals versus controls. C57BL6 mice at 6 weeks of age and weight matched were fed, *ad libitum*, a control (5.5% fat/weight) or high fat (21.2% fat/weight) diet for 22 weeks. Pericardial visceral (v) and abdominal subcutaneous (s) fat were collected from 12 animals per group. The tissue was lysed, resolved by 10-15% SDS-PAGE and Western blotted using anti-APP, iNOS, Cox-2, TNF- α , and GAPDH (loading control) antibodies. Arrowheads indicate bands of interest when nonspecific bands are present. Antibody binding was visualized by chemiluminescence. A representative blot of three animals per condition from a total of 12/condition analyzed is shown. Optical densities of the adipose protein Western blots from the control and high fat diet subcutaneous and visceral samples were normalized against their

respective GAPDH loading controls and averaged (+/- SD) from 12 animals per each condition. *P<0.05, **P<0.01

Similar to the observations found during brain analysis, immunostaining of the two different adipose depots with anti-mouse A β antibody did not demonstrate a robust increase in immunoreactivity in high fat diet fed animals nor, any plaque-type patterns (Figure 6A). Although prior work has demonstrated increased adipocyte APP immunoreactivity in samples from obese humans, it was possible that the increased APP immunoreactivity observed in our animal paradigm was also localized to macrophage. Our prior work has shown that monocytic lineage cells express APP and levels increase upon differentiation and activation (Sondag and Combs, 2004a, 2006b, 2010a). Moreover, a variety of studies have demonstrated that increased macrophage infiltration into adipose tissue occurs during diet-induced obesity (Weisberg et al., 2003, Kanda et al., 2006, Coenen et al., 2007). Interestingly, both subcutaneous and visceral adipose tissue demonstrated increased immunoreactivity for CD68 to identify macrophage (Figure 6). Importantly, this increase in CD68 positive adipose tissue macrophage correlated precisely with the slight increase in CD68 positive microglia observed in the brains of high fat diet fed mice compared to controls (Figure 2).

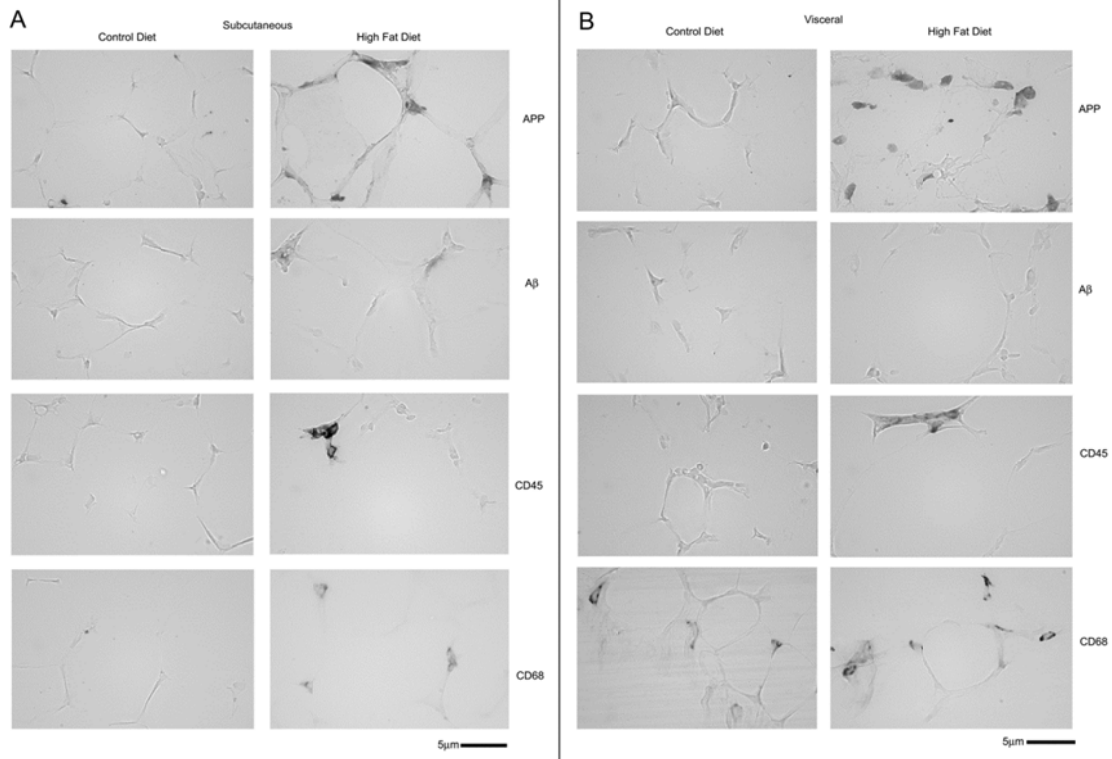


Figure 6. APP, CD45, and CD68 immunoreactivity increased in the subcutaneous (abdominal) fat and visceral (pericardial) fat from high fat versus control diet fed mice with no robust change in A β immunoreactivity.

C57BL6 mice at 6 weeks of age and weight matched were fed, *ad libitum*, a control (5.5% fat/weight) or high fat (21.2% fat/weight) diet for 22 weeks.

Subcutaneous abdominal and visceral pericardial adipose tissue was collected, immersion fixed in 4% paraformaldehyde, sectioned, and immunostained using anti-APP, A β , CD45 and CD68 antibodies and antibody binding visualized using Vector VIP as the chromogen. Representative images from 12 animals per condition are shown.

Double labeling immunohistochemistry was performed to determine whether a portion of the increased APP immunoreactivity observed was within adipose tissue infiltrated macrophage. In either type of adipose tissue a population of the APP immunoreactive cells also co-localized with CD68 immunoreactivity indicating that both adipocytes and macrophage may be responsible for the upregulation of APP observed in adipose tissue of high fat diet fed animals (Figure 7). Indeed, visceral adipose tissue demonstrated nearly complete co-localization of APP with CD68 immunoreactivity. These results confirm that increased APP levels observed in adipose tissue from high fat diet fed animals is multi-cellular with a significant portion likely from the increasing numbers of tissue infiltrating macrophage. This correlates with the increased levels of brain APP observed in high fat diet fed mice as well as the increased gliosis that occurs.

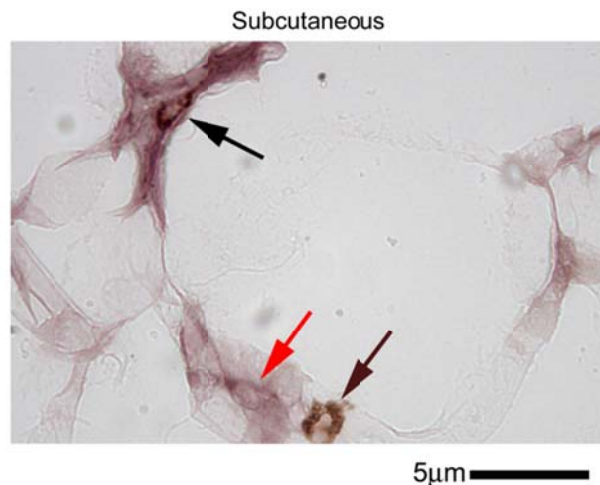


Figure 7. APP and CD68 immunoreactivity co-localized in subcutaneous (abdominal) and visceral (heart) fat from high fat diet fed mice. C57BL6 mice at 6 weeks of age and weight matched were fed, *ad libitum*, a control (5.5%

fat/weight) or high fat (21.2% fat/weight) diet for 22 weeks. Subcutaneous abdominal and visceral pericardial adipose tissue samples were collected, immersion fixed, serially sectioned and immunostained using anti-CD68 antibody and binding visualized using DAB as the chromogen. For double-labeling, tissue sections were stripped using 0.2N HCl and subsequently immunostained using anti-APP antibody and binding visualized using Vector VIP as the chromogen. A representative image from 12 animals per condition is shown. The brown arrow indicates CD68 immunoreactivity, the red arrow indicates APP immunoreactivity and the black arrow indicates double-label of CD68 and APP antibody binding.

The APP agonist antibody, 22C11, increased macrophage cytokine production but had no effect on viability, lipid storage/accumulation, or TNF- α secretion in adipocytes

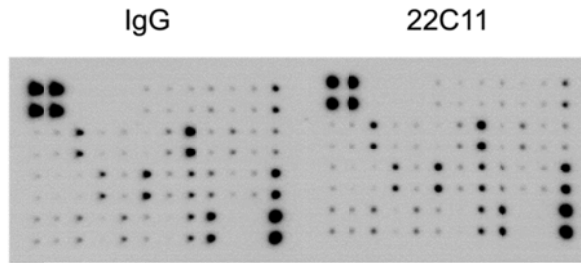
To begin examining whether increased expression of APP had any role in altering the phenotype of macrophage or adipocytes, primary murine cultures were generated from non-elicited peritoneal macrophage and subcutaneous adipocytes and then stimulated using an agonist antibody for APP (Sondag and Combs, 2006b). We first stimulated peritoneal macrophage with 1 μ g/mL IgG₁ (isotype control) or 22C11 (APP agonist antibody) and measured cytokine secretion (Figure 8). The APP agonist, 22C11, stimulated a significant increase in secretion of granulocyte-macrophage colony stimulating factor (GM-CSF) which reportedly increases the production of macrophages (Burgess et al., 1977). This was consistent with the increase in immunoreactivity for CD68 (macrophages) in both adipose tissue depots during high fat diet-induced

obesity. Stimulation with 22C11 also significantly increased secreted levels of IFN γ , a macrophage-activating factor, that plays a critical role in immunostimulatory and immunomodulatory effects (Wallet et al., Schroder et al., 2006). In contrast, 22C11 stimulation significantly increased secreted IL-13 levels which is reportedly responsible for down-regulation of macrophage activity and thereby inhibits the production of pro-inflammatory cytokines and chemokines (Doherty et al., 1993). Although these findings do not demonstrate precisely what secretory changes APP-overexpressing macrophage may be exhibiting *in situ* during diet-induced obesity, they do provide clear evidence that APP stimulated changes in macrophage phenotype are complex with alterations in both proinflammatory and anti-inflammatory secretion that will need to be further resolved *in vivo* in the diet-induced obesity model.

To assess any effect of APP on adipocyte phenotype, we next stimulated primary murine abdominal subcutaneous fat derived-adipocytes with 1 μ g/mL IgG $_1$ or 22C11 antibodies. Unlike the macrophage studies, agonist antibody stimulation of adipocytes did not produce any obvious change in phenotype. There was no significant toxicity of the 22C11 or IgG $_1$ stimulated adipocytes as assessed by LDH release (Figure 9A). Since TNF α levels were increased under diet-induced obesity conditions in both adipose tissue depots, TNF α secretion was measured from APP stimulated adipocytes (Figure 9B). However, the APP agonist, 22C11, did not stimulate a significant change in TNF α secretion. To assess a differentiative phenotype, stimulated adipocytes were stained and quantified using Oil Red O (Figure 9C and 9D) to examine lipid

storage/accumulation. APP stimulation with 22C11 produced no changes in Oil Red O staining. Although a minor subset of all the possible changes in adipocyte phenotype was examined, the data thus far indicates that viability, proinflammatory secretion, and differentiation state are not affected by APP signaling. This suggests that further investigation is needed to fully understand the role of APP in adipocyte biology both basally and during instances of increased APP expression such as that which occurs during diet-induced obesity.

This data demonstrates that both brains and adipose tissue from wild type mice had elevated APP levels localizing to neurons and macrophage/adipocytes, respectively. Adipose tissue and brain microglia from high fat diet fed wild type mice demonstrated increased TNF α and microglial/macrophage activation. Finally, APP agonist antibody stimulation of wild type macrophage cultures increased specific cytokine secretion with no obvious effects on adipocyte culture phenotype.



	IgG	22C11
BLC	0.89±0.12	1.25±0.48
CD30L	0.82±0.08	0.86±0.09
Ectaxin	0.88±0.09	0.90±0.1
Ectaxin-2	1.11±0.13	1.17±0.13
Fas Ligand	0.83±0.11	0.86±0.11
Fractalkine	0.92±0.12	0.91±0.1
GCSF	1.50±0.28	1.38±0.21
GM-CSF	0.78±0.05	0.88±0.06*
IFN γ	0.86±0.05	0.96±0.06*
IL-1 α	0.88±0.14	0.95±0.10
IL-1 β	0.80±0.08	0.87±0.09
IL-2	0.85±0.09	0.92±0.10
IL-3	0.73±0.09	0.79±0.08
IL-4	1.19±0.14	1.23±0.16
IL-6	0.97±0.28	0.74±0.08
IL-9	0.88±0.11	0.92±0.11
IL-10	1.04±0.31	1.02±0.25
IL-12p40p70	1.10±0.39	0.97±0.10
IL-12p70	1.19±0.18	1.15±0.08
IL-13	0.83±0.04	0.96±0.05**
IL-17	0.73±0.06	0.81±0.09
I-TAC	0.76±0.08	0.84±0.09
KC	1.10±0.27	1.03±0.18
Leptin	0.87±0.09	0.93±0.11
LIX	1.18±0.11	1.18±0.20
Lymphotactin	1.01±0.12	1.06±0.13
MCP-1 α	0.88±0.17	0.91±0.12
MCSF	1.45±0.16	1.50±0.22
MIG	0.85±0.08	0.89±0.11
MIP-1 α	0.96±0.09	0.98±0.10
MIP-1 γ	1.62±0.27	2.00±0.56
RANTES	0.76±0.06	0.85±0.08
SDF-1	0.97±0.11	1.09±0.09
TCA-3	1.49±0.11	1.64±0.15
TECK	0.76±0.06	0.82±0.08
TIMP-1	1.53±0.10	1.49±0.11
TIMP-2	0.95±0.08	1.01±0.09
TNF α	0.72±0.06	0.77±0.08
sTNFRI	1.53±0.15	1.66±0.15
sTNFRII	1.22±0.16	1.11±0.23

Figure 8. Secreted levels of GM-CSF, IFN γ , and IL-13 increased in media from peritoneal macrophage stimulated with APP agonist antibody, 22C11, compared to IgG₁ isotype control. Non-elicited peritoneal macrophage were

stimulated with 1µg/mL IgG₁ or 1µg/mL 22C11 APP agonist antibody overnight and the media was removed and used according in a commercial antibody-based 40 cytokine antibody array. A representative dot blot per each condition is shown. The optical densities of individual cytokine detection spots were normalized against their respective positive controls per blot and averaged (+/-SD) and graphed from 5 animals in each group. Data were analyzed via unpaired two-tailed t-test. *P<0.05, **P<0.01

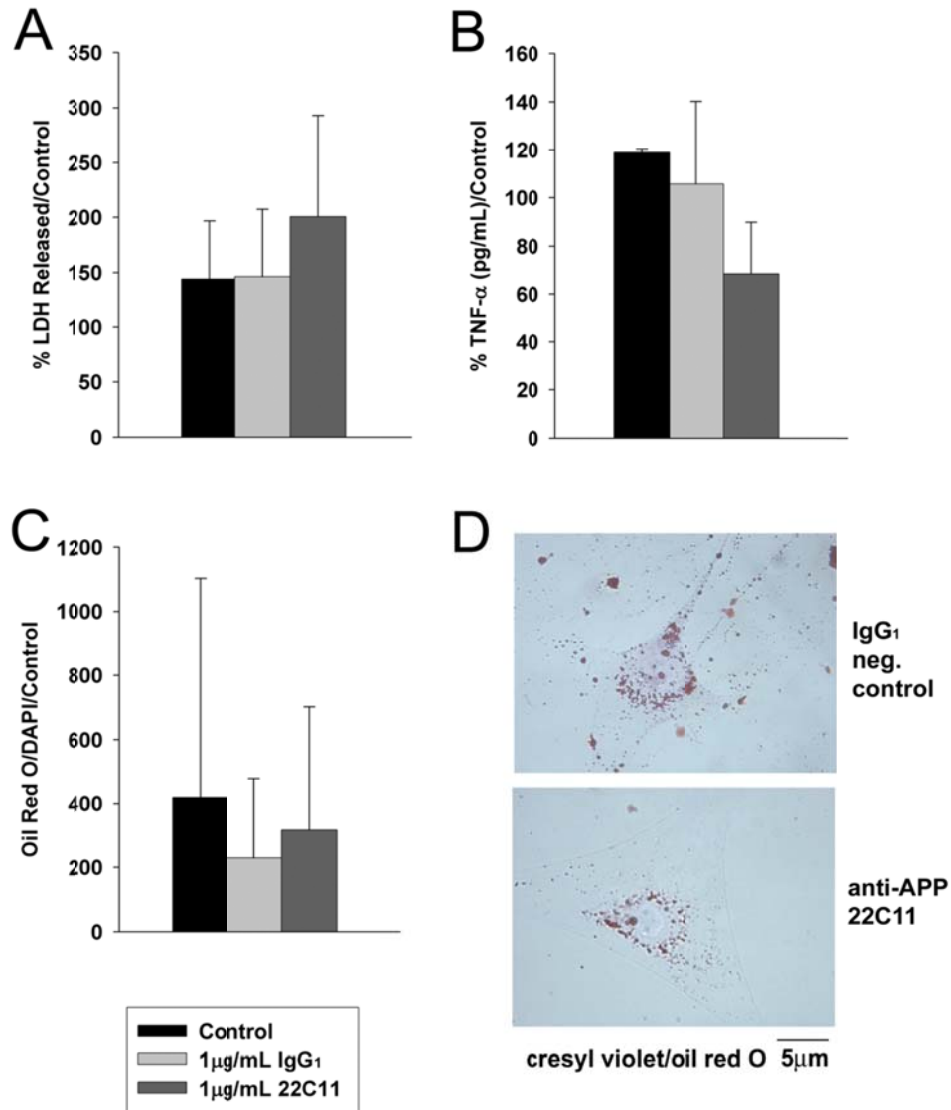


Figure 9. APP activation with agonist antibody did not alter cytokine secretion, viability, or Oil Red O staining of primary murine abdominal subcutaneous adipocytes. Adipocytes were harvested from subcutaneous abdominal fat from C57BL6 mice and cultured in DMEM/F12 with serum and antibiotics for one week. Cells were then placed into serum free DMEM/F12 and unstimulated (control) or stimulated for 24 hr with 1 μ g/mL IgG₁ (isotype control) or 1 μ g/mL 22C11 (APP agonist antibody). After 24 hours (**A**) Secreted LDH

released into the media normalized against cellular LDH was quantified to assess changes in cell viability upon APP stimulation. **(B)** Changes in secreted TNF α levels were also quantified from the media as a result of APP stimulation. **(C)** Cells were also fixed, stained with Oil Red O and DAPI counterstain and changes in Oil Red O absorbance (510nm) normalized to DAPI absorbance (358/461nm) were quantified via plate reader. **(D)** Representative images of Oil Red O and cresyl violet counterstained adipocytes are shown following 24 hr IgG₁ and 22C11 stimulation. Data are shown as mean (+/-SD) and are representative of three independent experiments. Data were analyzed via a one-way ANOVA.

CHAPTER IV

APP REGULATES BRAIN AND ADIPOSE CHANGES IN HIGH FAT DIET FED MICE

Based upon our observations that increased APP immunoreactivity occurred in both brains and adipose tissue with high fat diet feeding and APP modulated the phenotype of peritoneal macrophages, we predicted APP would have a role in the cellular differentiation and inflammatory changes that are produced in adipose tissue but also brain during high fat diet induced obesity. To examine this hypothesis we compared wild type and APP^{-/-} mice placed on control and high fat diets with the expectation that APP^{-/-} mice would have attenuated weight gain, cytokine production, and macrophage/microglial activation basally and on a high fat diet compared to wild type mice.

APP^{-/-} mice gained significantly less weight than wild type mice fed a high fat diet

Our first goal was to determine whether APP was required for weight gain due to high fat diet feeding. To assess comparative changes between wild type (C57BL6) and APP^{-/-} mice, we placed 10-11, 6 week old animals from each strain on a 5.5% by weight control diet or a 21.2% by weight high fat diet, *ad libitum*, for 22 weeks. Five to six animals in each group were weighed weekly and mean (+/-

SD) weight gain per group was graphed versus time (Figure 10A). There was a significant difference in mean starting weight between wild type and APP^{-/-} mice consistent with their smaller stature (Figure 10A). Therefore to accurately compare weight gain between groups we normalized weight per week to the initial starting weight of each respective mouse (Figure 10B). Wild type mice on high fat diet showed significantly increased weight gain vs. APP^{-/-} mice on control or high fat diets after 2 weeks. After 3 weeks of feeding, wild type mice on the high fat diet also demonstrated significantly increased weight gain over their wild type counterparts on control diet. On the other hand, after 18 weeks on a high fat diet, APP^{-/-} mice gained significantly more weight than the APP^{-/-} mice on control diet. To assess whether the differences in weight gain were due to food intake we weighed the food weight eaten by all groups during weeks 13-17. Since actual food weight eaten each week would not be an accurate measurement due to differences in animal weight, the food weight eaten by each animal was divided by its weight then averaged to determine the weight of food eaten, per animal body weight, per group (Figure 10C). Both genotypes ate significantly more control diet per body weight compared to high fat diet. In spite of the attenuated weight gain, APP^{-/-} mice ate significantly more food per body weight of either diet type compared to wild type mice.

In order to validate that the differences in weight gain were a result of changes in adipose tissue mass, total visceral (gonadal and perirenal) fat weight was measured between groups at the termination of the feeding paradigm following animal collection (Figure 10D & 10E). Two different visceral fat depots

were measured in these studies as visceral fat alone has been shown to be responsible for the metabolic consequences of obesity (Bjorntorp and Rosmond, 1999, Frayn, 2000, Wajchenberg, 2000, Thorne et al., 2002, Rodriguez et al., 2007). Both gonadal and perirenal fat depot weight of wild type mice on a high fat diet was increased compared to their control diet counterparts (Figure 10D & 10E). Gonadal but not perirenal fat depot weight of APP^{-/-} mice on the high fat diet was also significantly increased compared to their control diet counterparts (Figure 10E). This occurred in spite of the fact that both perirenal and perigonadal adipose tissue from APP^{-/-} mice on either diet were significantly less than their respective control diet wild type groups (Figure 10D & 10E). This overall decrease in adipose tissue mass was consistent with the attenuated weight gain displayed by the APP^{-/-} mice (Figure 10B).

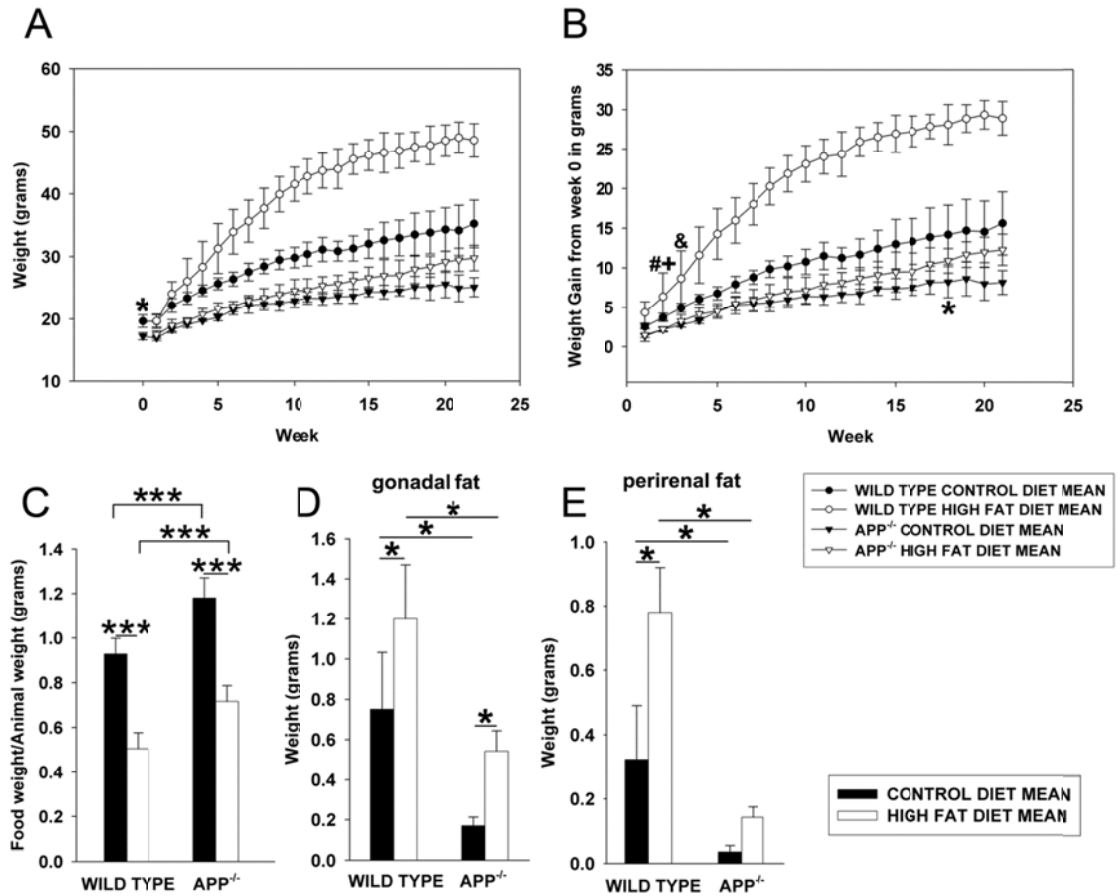


Figure 10. *APP*^{-/-} mice gained significantly less weight than wild type mice fed either control or high fat diets. High fat diet feeding in wild type and *APP*^{-/-} mice altered weight gain (A,B), regardless of the food intake (C) but altered fat depot weight (D,E). Data are expressed as mean +/- SD (n = 5 or 6). (B) Wild type mice on high fat diet vs. *APP*^{-/-} mice on control diet #P=0.006; vs. *APP*^{-/-} mice on high fat diet +P=0.007; vs. wild type mice on control diet &P=0.014. *APP*^{-/-} mice on high fat diet vs. *APP*^{-/-} mice on control diet *P=0.038. (C) ***P<0.001. (D,E) *P<0.05.

Measurement of fasting blood glucose, triglycerides, HDL and total cholesterol levels from wild type and APP^{-/-} mice fed control and high fat diets

Based upon the diminished weight gain of the high fat diet fed APP^{-/-} mice, we predicted that these animals would also have attenuated changes in plasma levels of total cholesterol, triglycerides, and HDL cholesterol as well as glucose tolerance compared to wild type mice on the high fat diet. Mice in both groups were fasted for 6 hours (water only) and levels of these metabolic parameters were measured (Figure 11). Glucose tolerance tests comparing the four groups demonstrated more efficient glucose uptake in control diet fed APP^{-/-} mice compared to their respective wild type controls with levels returning to baseline in the APP^{-/-} mice by 120 minutes post glucose injection (Figure 11A & 11B). However, both genotypes displayed impaired glucose clearance on high fat diet feeding demonstrating that changes in glucose sensitivity existed in the APP^{-/-} mice in spite of their attenuated weight gain (Figure 11B and 11D). As a further comparison, triglycerides, HDL and total cholesterol levels were also quantified from the animals. The APP^{-/-} mice on high fat diet did not display the increase in total cholesterol levels observed in the wild type mice fed high fat diet correlating again with the attenuated weight gain and adipose tissue mass in this group (Figure 11F).

Attenuated adipose tissue hypertrophy and attenuated total cholesterol levels in the APP^{-/-} mice fed the high fat diet suggested that, in addition to the inflammatory changes we predicted in these mice, there might also be differences in adipocyte behavior and fatty acid metabolism or uptake. In order to further examine the possibility that a problem with fatty acid metabolism, storage,

or uptake might exist in these mice we examined the liver of high fat fed mice since diet induced obesity is characterized by robust lipid accumulation in the liver. H & E staining of the livers from these mice revealed no histological differences between the two strains on control diet. However although high fat diet feeding resulted in a severe fatty change in the wild type mice, only a mild or moderate fatty change was observed in the APP^{-/-} mice (Figure 12). This provided further evidence that impairment of lipid metabolism, uptake, or storage may be occurring in these animals in a fashion that is dependent upon expression of APP and that is in addition to or linked with changes in immune cell behavior.

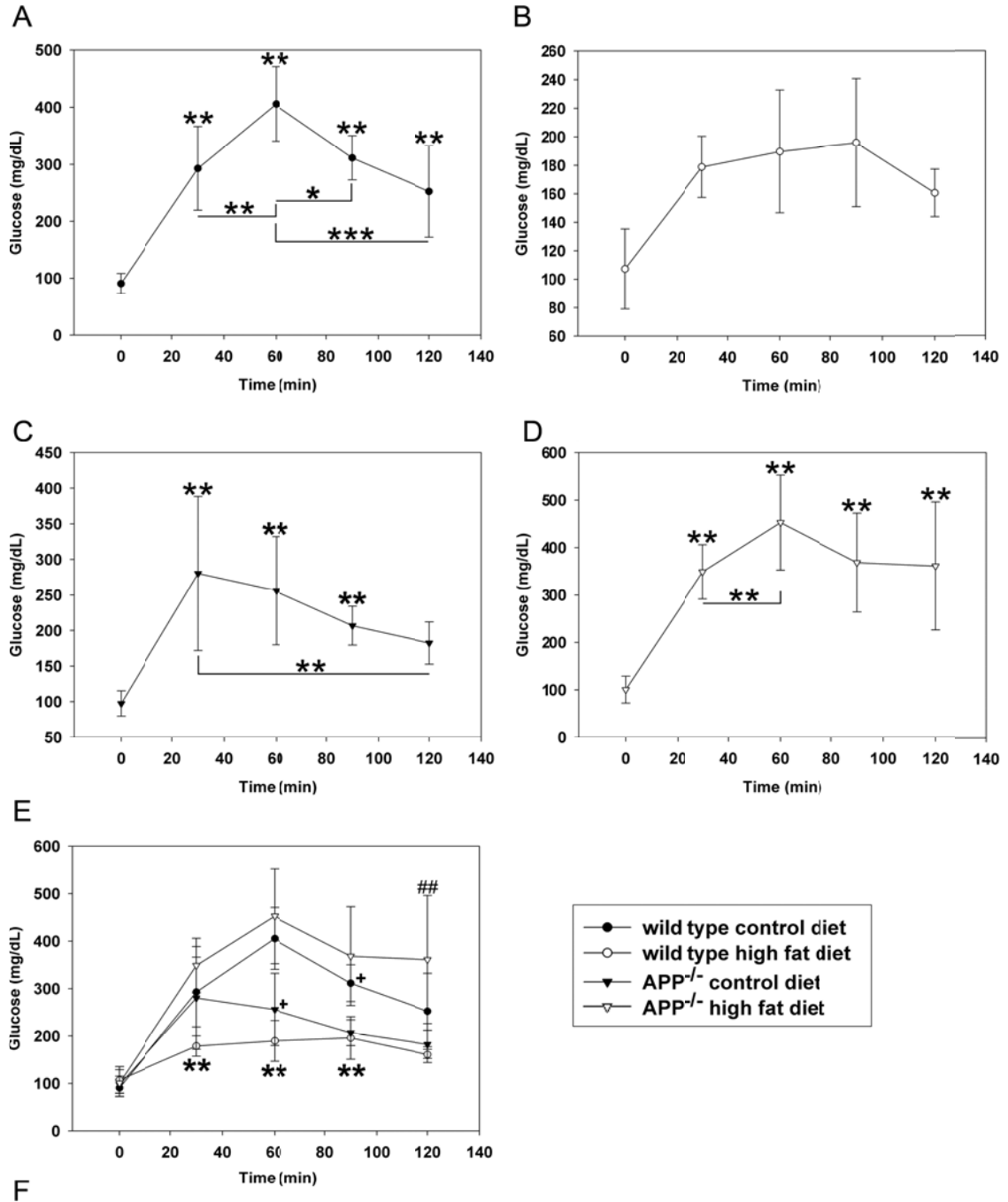


Figure 11. Measurement of fasting blood glucose and cholesterol levels in wild type and APP^{-/-} mice on control and high fat diet. After 22 weeks of diet feeding mice were fasted for 6hrs (water only) and then triglycerides, HDL

cholesterol, total cholesterol and glucose were measured using a CardioChek meter (Test Medical Symptoms @ Home, Inc, Maria Stein, OH, USA) and corresponding strips via tail lancet. After baseline measurements were recorded mice were injected intraperitoneally with 2g/kg glucose followed by 30, 60, 90, 120 min glucose measurements. Data are expressed as mean +/- SD (n = 5 or 6) *P<0.05, **P<0.01, ***P<0.001. (A) Wild type mice on high fat diet, (B) Wild type mice on control diet, (C) APP^{-/-} mice on high fat diet, (D) APP^{-/-} mice on control diet. (E) Combined four graphs (A-D). (E) 30 min **P<0.01 wild type on high fat diet vs. wild type on control diet and APP^{-/-} on both diets; 60 min and 90min **P<0.01 wild type high on fat diet vs. wild type on control diet and APP^{-/-} on high fat diet; 60min and 90 min ⁺P<0.05 APP^{-/-} mice on control diet vs APP^{-/-} mice on high fat diet and wild type mice on control diet; 120 min ^{##}P<0.01 APP^{-/-} mice on high fat diet vs APP^{-/-} mice on control diet and wild type mice on either diet. (F) triglycerides, HDL and total cholesterol measurements.

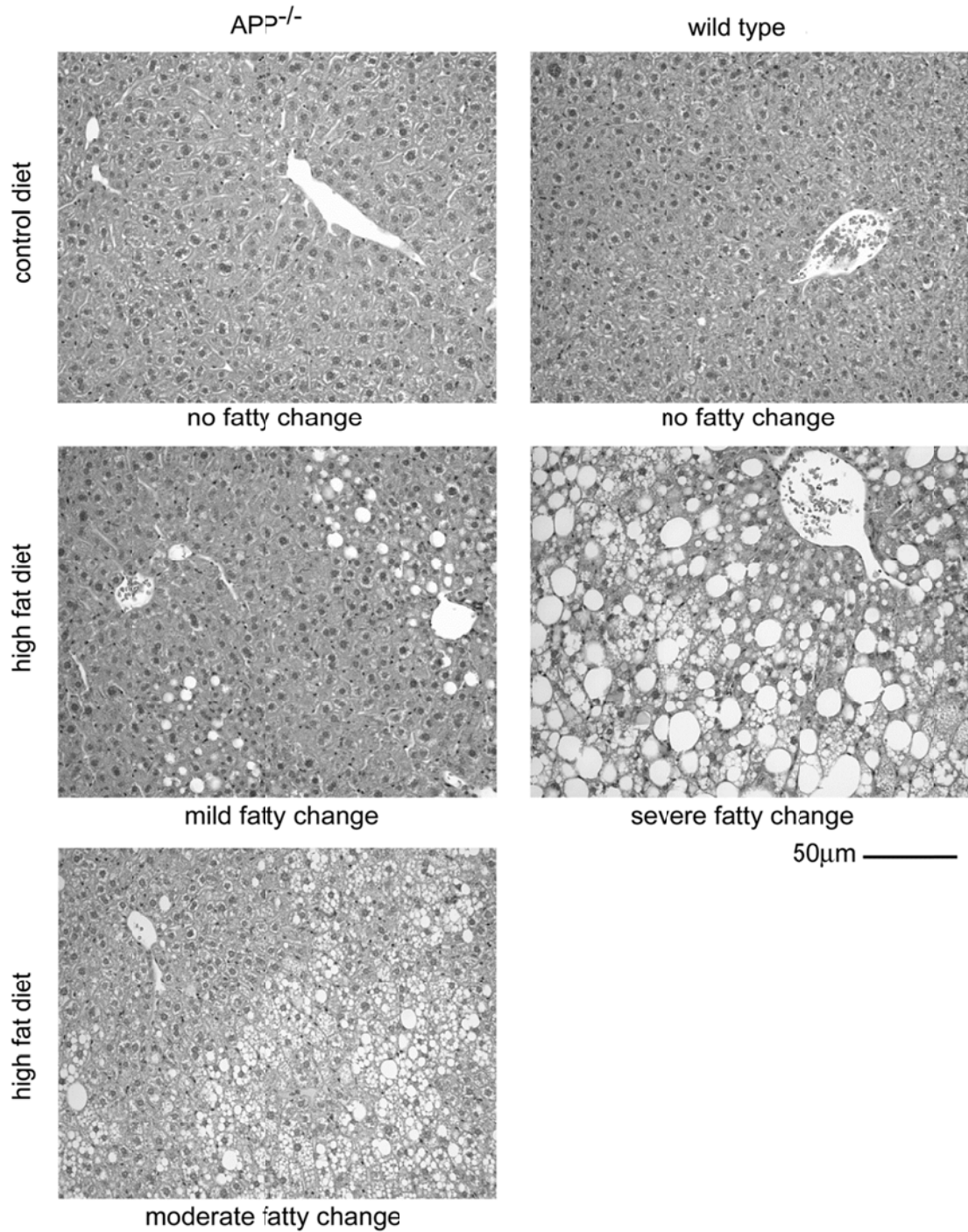


Figure 12. Liver from wild type mice fed high fat diet demonstrated increased lipid accumulation compared to APP^{-/-} mice. Male wild type and APP^{-/-} were fed control and high fat diet for 22 weeks and liver tissue was

collected, immersion fixed, sectioned, and stained using H&E. Representative images from 5-6 animals per condition are shown. The spectrum of lipid accumulation in APP^{-/-} livers from mild to moderate are both shown in contrast to the typical severe accumulation observed in wild type livers.

Increased inflammatory response in the fat depots of APP^{-/-} mice compared to wild type mice fed control and high fat diets

Several observations made from the high fat diet fed APP^{-/-} mice supported the possibility that some APP-dependent regulatory mechanism of lipid metabolism was impaired in these animals. However, we had not yet determined whether the predicted changes in macrophage activation or infiltration had occurred in these animals as well. In order to quantify changes in immune parameters, specific ELISAs were selected to broadly scan for changes in each group. Levels of proinflammatory markers, TNF- α , IL-1 β , IL-6, and monocyte chemotactic protein 1 (MCP-1) as well as anti-inflammatory markers, IL-10 and IL-4, and the glucose and fatty acid oxidation marker, adiponectin, were all quantified from perirenal, gonadal, and subcutaneous fat depots (Figure 13). Surprisingly, in spite of the smaller adipose tissue mass, APP^{-/-} mice fed a control diet demonstrated increased TNF- α , IL-10, IL-1, IL-1 β , and MCP-1 levels in perirenal and gonadal fat depots compared to wild type mice fed a control diet (Figure 13). APP^{-/-} mice fed a high fat diet had significantly higher levels of IL-6 and IL-4 but decreased MCP-1 only in gonadal fat compared to high fat diet fed wild type mice. Control diet fed APP^{-/-} mice compared to control diet fed wild type mice had increased levels of adiponectin in the perirenal fat with decreased levels in the

subcutaneous fat (Figure 13). This data demonstrated two critical observations. First, lack of APP clearly alters immune parameters in adipose tissue both on mice fed a regular or a high fat diet. Second, the role of APP in regulating any particular adipose tissue inflammatory phenotype appears quite complex with differences between the adipose tissue depots. These immune changes may or may not have been related to the attenuated weight gain observed from the APP^{-/-} mice.

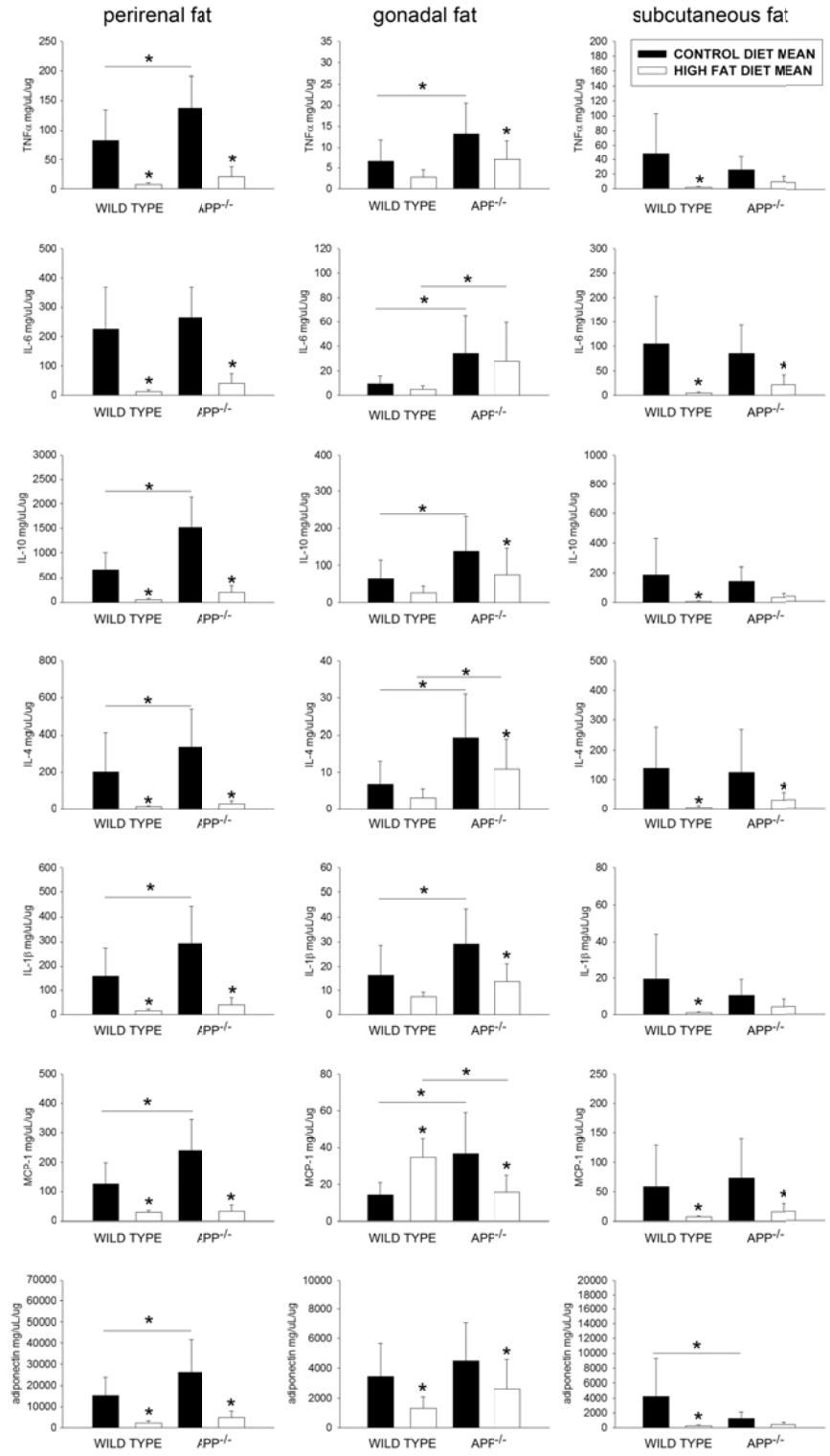


Figure 13. Increased inflammatory protein levels in the fat depots of $APP^{-/-}$ mice compared to wild type mice. Male wild type and $APP^{-/-}$ mice were fed

control and high fat diet for 22 weeks and perirenal, gonadal, and subcutaneous adipose tissue was collected to quantify IL-6, TNF α , IL-10, IL-4, IL-1 β , MCP-1, and adiponectin levels via ELISA. Data are expressed as mean \pm SD (n = 5 or 6), *P<0.05.

Multiple protein markers of differentiation and activation differed in gonadal and perirenal fat depots of wild type and APP^{-/-} mice fed high fat versus control diets

In order to better understand the differences in wild type and APP^{-/-} adipose tissue that were observed, protein differences in visceral depots were assessed for changes in markers of differentiation or activation for both adipocytes and macrophages. Western blot analysis of gonadal fat tissue following the 22 weeks of diet feeding demonstrated, as expected, elevated APP levels in wild type mice compared to their control diet counterparts (Figure 14). However, high fat diet feeding did not alter any protein marker level in gonadal adipose tissue from wild type mice. On the other hand, APP^{-/-} mice fed the high fat diet demonstrated significantly elevated gonadal adipose tissue levels of: an adipocyte differentiation marker, peroxisome proliferation activated receptor γ (PPAR γ); fatty acid synthase (FAS) which catalyzes the synthesis of palmitate; fatty acid binding protein 4 (FABP4) a fatty acid carrier protein; lipoprotein receptor protein (LRP) which is involved in lipid homeostasis and clearance of apoptotic cells; arginase-1, an M2 phenotype macrophage marker; and adiponectin, a protein responsible for glucose regulation and fatty acid breakdown; compared to control diet fed APP^{-/-} mice (Figure 14). In fact, it appeared that control diet APP^{-/-} gonadal adipose tissue was already significantly

different from wild type mice fed the control diet. Several protein levels were increased in the APP^{-/-} tissue. Specifically, APP^{-/-} gonadal fat had significantly higher levels of: cluster of differentiation 36 (CD36) which plays a role in fatty acid uptake and serves as a scavenger receptor; lipoprotein lipase (LPL) which hydrolyzes triglycerides in lipoproteins; delta like protein (DLK or Pref-1) is involved with differentiation of pre-adipocytes into adipocytes; toll like receptor 2 and 4 (TLR2 & TLR4) which are pattern recognition receptors involved in activating inflammatory signaling cascades; phospho-Akt (pAKT) which controls survival and apoptosis and is involved in insulin receptor signaling; caveolin which is involved in endocytosis; very-low-density-lipoprotein receptor (VLDLR) regulates cholesterol uptake and metabolism of triacylglycerol-rich lipoproteins; arginase-1; and adiponectin (Figure 14). Although the high fat feeding did not appear to alter the wild type gonadal adipose protein levels, The APP^{-/-} mice fed the high fat diet significantly increased several protein levels. These increases coupled with the existing basal elevations demonstrated a plethora of changes above the high fat diet fed wild type mice. Specifically, the following protein markers were all elevated in APP^{-/-} high fat diet fed gonadal adipose tissue: cluster of differentiation 14 (CD14) a co-receptor along with TLR4 for the detection of lipopolysaccharide; cluster of differentiation 68 (CD68) which is a M1 macrophage marker; glucose transporter type 4 (glut-4) which is the insulin-regulated glucose transporter; in addition to PPAR γ , FAS, DLK, FABP4, TLR2, TLR4, arginase-1, pAKT, caveolin, and adiponectin (Figure 14).

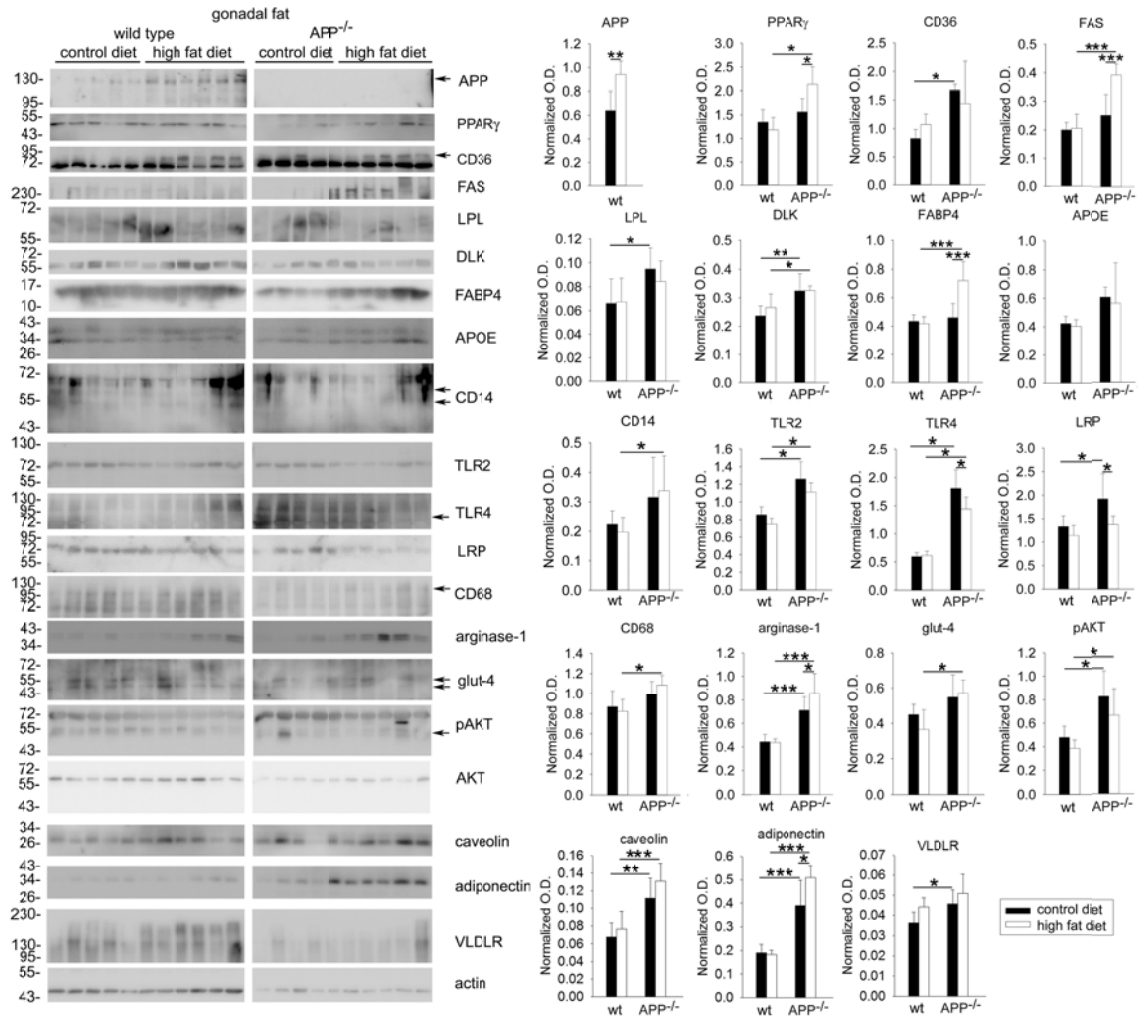


Figure 14. Protein marker levels differed in gonadal adipose tissue depots from wild type and $APP^{-/-}$ mice. Male wild type and $APP^{-/-}$ mice were fed a control or high fat diet for 22 weeks and gonadal adipose tissue was collected from 5-6 animals per group. The tissue was lysed, resolved by 10-15% SDS-PAGE and Western blotted using anti-APP, glut-4, CD14, TLR2, TLR4, CD68, pAKT, AKT, PPAR γ , CD36, FAS, LPL, DLK, FABP4, LRP, APOE, arginase-1, caveolin, adiponectin, VLDLR, and actin (loading control) antibodies.

Arrowheads indicate bands of interest when nonspecific bands are present.

Antibody binding was visualized by chemiluminescence. Optical densities were

quantified normalizing to actin as a loading control. Data are expressed as mean +/- SD (n= 5 or 6) *P<0.05, **P<0.01, ***P<0.001.

Although the differences on control and high fat diet were dramatic in gonadal fat, we appreciate that not all adipose tissue depots behave similarly. Therefore, we quantified protein changes in another visceral adipose tissue depot, perirenal fat. In contrast to the gonadal fat, wild type mice fed the high fat diet did show significant increases in several proteins. Wild type mice fed a high fat diet had elevated Apolipoprotein E (APOE) a component of chylomicron and intermediate-density lipoproteins that is essential for triglyceride catabolism; as well as APP, PPAR γ , CD36, FAS, LPL, DLK, CD14, TLR2, CD68, arginase-1, and adiponectin compared to the wild type mice fed control diet (Figure 15). Also unlike gonadal adipose tissue, the high fat diet fed APP^{-/-} perirenal adipose tissue did not display all of the increases. APP^{-/-} perirenal adipose tissue from mice fed high fat diet demonstrated only decreased LPL compared to APP^{-/-} mice fed the control diet (Figure 15). Nevertheless, similar to gonadal adipose tissue, perirenal adipose tissue from APP^{-/-} mice on control diet still demonstrated some significant increases compared to wild type mice fed control diet. APP^{-/-} perirenal adipose tissue demonstrated increased FAS, FABP4 and adiponectin protein levels compared to wild type mice fed control diet (Figure 15). The data demonstrate that not only APP but also diet regulates each depot discreetly.

Based upon our earlier work, we expected the increase in APP protein levels in wild type tissue to be localized primarily to macrophage and the changes in APP^{-/-} compared to wild type tissue to be a reflection of diminished

macrophage infiltration coupled with a particular activation phenotype. Therefore, immunostaining of the fat depots was performed using an anti-CD68 antibody to detect macrophage following the 22 weeks of high-fat diet feeding (Figure 16A & 16B). Unexpectedly, APP^{-/-} mice demonstrated robust reactive macrophage immunoreactivity even without high fat diet-feeding (Figure 16A & 16B) which was entirely consistent with the elevated proinflammatory cytokine levels in the APP^{-/-} adipose tissue (Figure 13). Even more interesting was the fact that APP^{-/-} adipocytes basally demonstrated a very obvious decrease in cell volume in animals fed a control diet (Figure 16A & 16B). As demonstrated previously, APP colocalized with immunoreactive macrophage (Figure 19C).

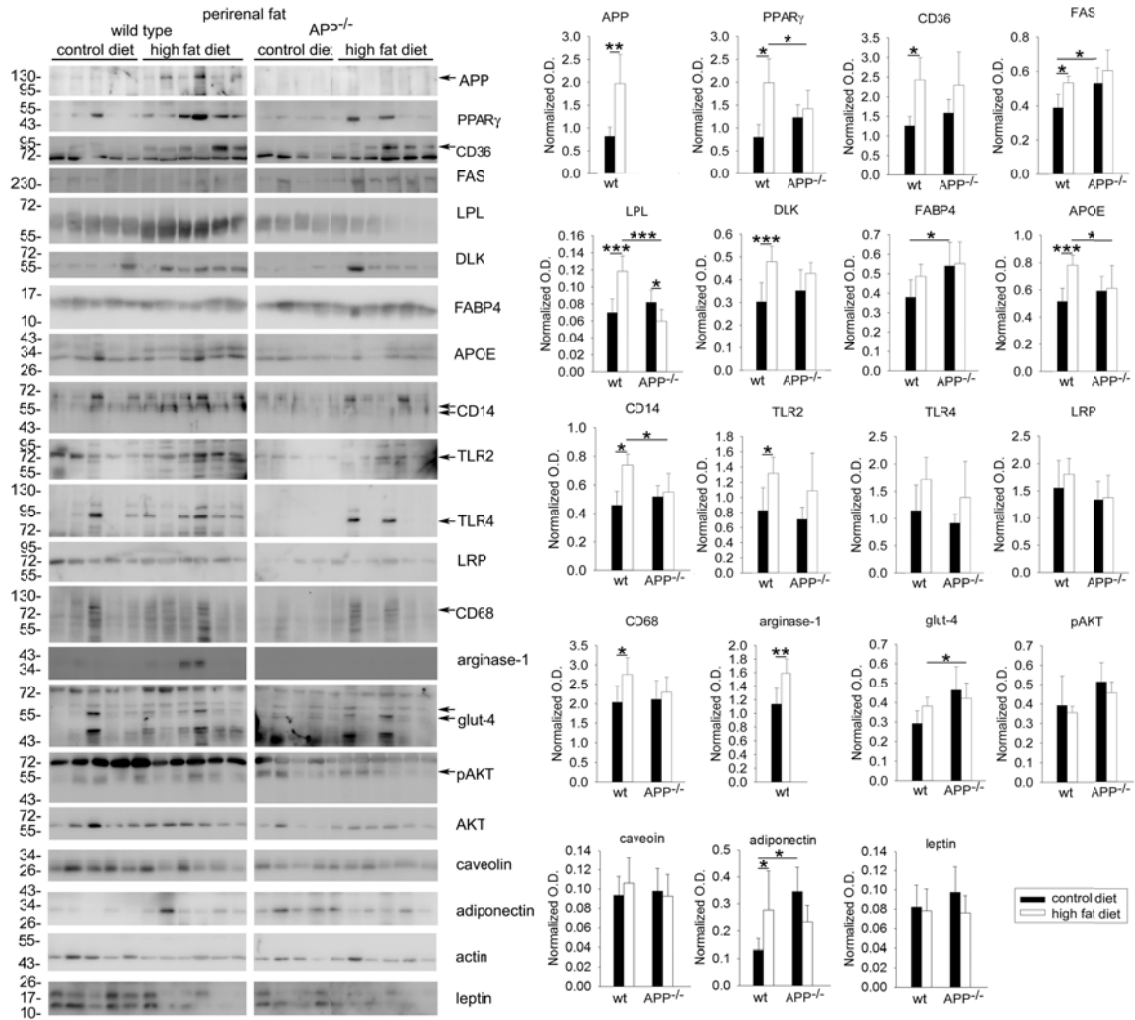


Figure 15. Protein marker levels differed in perirenal adipose tissue depots from wild type and $APP^{-/-}$ mice. Male wild type and $APP^{-/-}$ mice were fed a control or high fat diet for 22 weeks and perirenal adipose tissue was collected from 5-6 animals per group. The tissue was lysed, resolved by 10-15% SDS-PAGE and Western blotted using anti-APP, glut-4, CD14, TLR2, TLR4, CD68, pAKT, AKT, PPAR γ , CD36, FAS, LPL, DLK, FABP4, LRP, APOE, arginase-1, caveolin, adiponectin, leptin, and PPAR and actin (loading control) antibodies. Arrowheads indicate bands of interest when nonspecific bands are present. Antibody binding was visualized by chemiluminescence. Optical densities were quantified

normalizing to actin as a loading control. Data are expressed as mean \pm SD (n= 5 or 6) *P<0.05, **P<0.01, ***P<0.001.

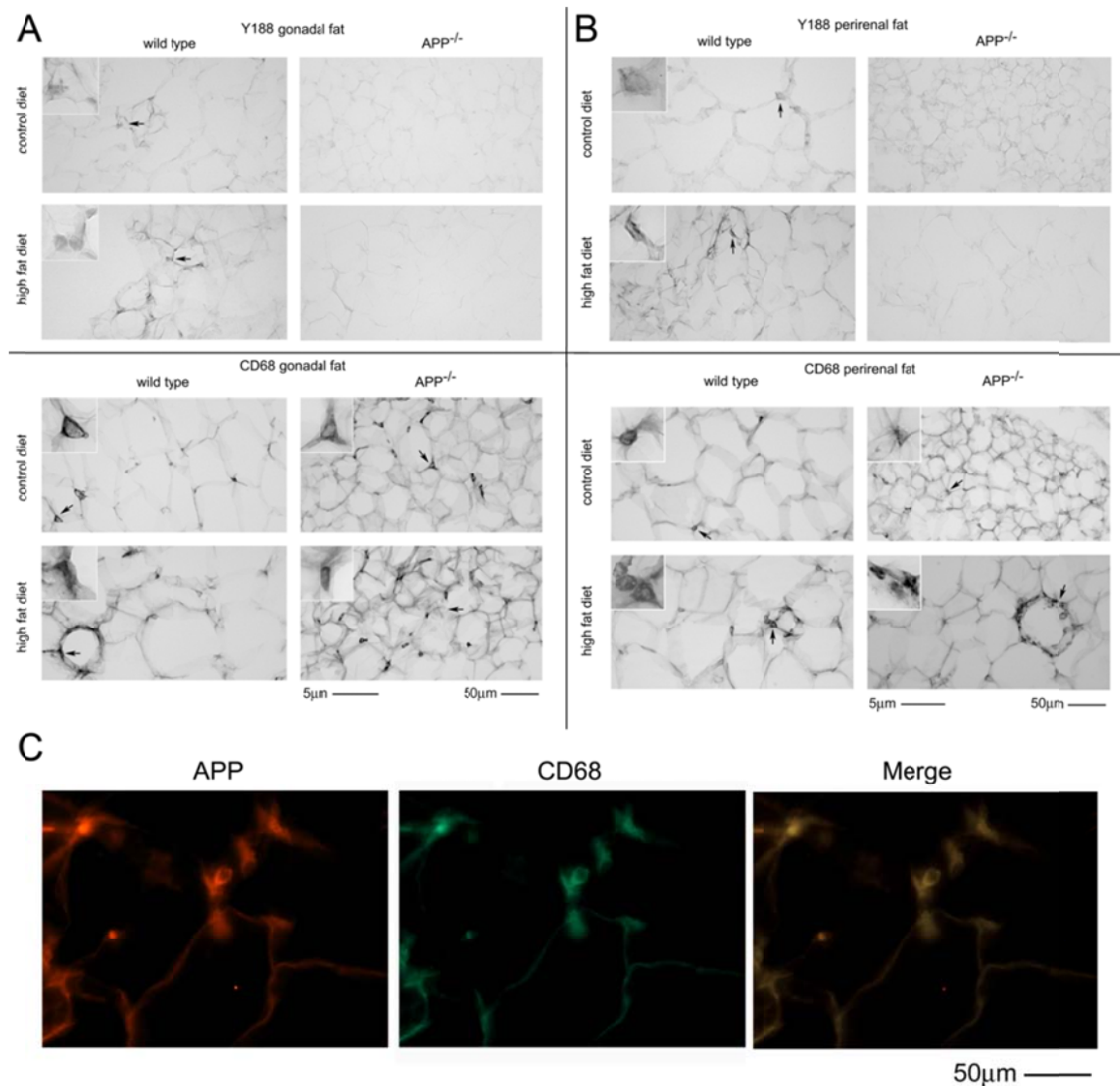


Figure 16. CD68 and APP immunoreactivity colocalized in adipose tissue and CD68 immunoreactivity increased in both gonadal and perirenal adipose tissue from wild type and $APP^{-/-}$ mice fed a high fat diet. (A) Gonadal and (B) perirenal adipose tissue was collected, immersion fixed, sectioned, and immunostained using anti-APP (Y188) and CD68 antibodies and antibody

binding visualized using Vector VIP as the chromogen. Representative images from 5-6 animals per condition are shown. (C) Gonadal and perirenal adipose tissue samples were immunostained using anti-CD68 antibody with FITC-conjugated secondary antibody and anti-APP antibody with texas red-conjugated secondary antibody. A representative gonadal fat image from 6 animals per condition is shown.

Cytokine secretion differed from APP^{-/-} and wild type peritoneal, intestinal, and adipose tissue macrophages isolated from mice fed control and high fat diets

Based upon the fact that the majority of APP immunoreactivity localized to macrophages in wild type adipose tissue, it was logical to assume that many of the changes observed thus far in APP^{-/-} mice and tissue were a consequence of loss of macrophage APP expression. In order to better define what role APP or its metabolites may have in regulating macrophage behavior, we isolated resting peritoneal macrophages from the control and high fat diet mice and stimulated them with or without a typical activating ligand, the endotoxin lipopolysaccharide (LPS), or an APP secreted metabolite, A β 1-40, to ask whether loss of APP or loss of stimulation from an APP metabolite induced a basal or activated phenotype change in wild type vs. APP^{-/-} cells (Figure 17). We again quantified levels of TNF- α , IL-6, IL-10, IL-4, IL-1 β , MCP-1, adiponectin as had been done in the adipose tissue depots. Unlike the findings made from adipose tissue, nonstimulated APP^{-/-} macrophages from control diet fed animals did not secrete higher levels of either molecule compared to wild type cells isolated from control diet fed mice. However, LPS stimulation of control diet fed APP^{-/-} macrophage did

demonstrate significantly increased secretion of IL-6, TNF α , IL-10 and IL-1 β compared to no changes in control diet wild type macrophages. This was entirely consistent with the low level of increased endotoxemia we had observed in the APP^{-/-} mice suggesting that the elevated cytokine levels in APP^{-/-} control diet fed mice may be due to macrophage hyperreactivity to LPS stimulation (Puig et al., 2012). Interestingly, control diet wild type and APP^{-/-} macrophages responded to A β stimulation with single cytokine level changes in typically described anti-inflammatory cytokines. Wild type cells demonstrated a significant increase in IL-4 levels while APP^{-/-} cells had elevated IL-10. Consistent with the fact that high fat diet feeding increases proinflammatory change, wild type cells isolated from high fat diet fed mice demonstrated increased secretion of multiple cytokines following LPS and A β stimulation. However, high fat fed APP^{-/-} macrophages only increased secretion of anti-inflammatory cytokines IL-4 and IL-10 upon LPS stimulation compared to their control diet cell counterparts.

Although peritoneal macrophages clearly differed between wild type and APP^{-/-} cells, their behavior did not completely mirror observations obtained from the tissue. One possibility is, of course, the fact that *in vitro* isolated cells can not accurately model all aspects of the complex environment or phenotype that occurs *in vivo*. However, another possibility is simply that peritoneal macrophages differ from other macrophages. Therefore, adipose tissue macrophages were isolated for comparison. Due to limitations in number and viability, only control diet fed macrophages from subcutaneous adipose tissue were compared with the expectation that their behavior would correlate best with

findings from subcutaneous adipose tissue. Cells from APP^{-/-} and wild type mice were again stimulated with or without LPS or A β 1-40 (Figure 18). Adipose tissue macrophages clearly differed from their peritoneal counterparts demonstrated by the fact that APP^{-/-} cells lacked the hyperresponsiveness to LPS stimulation. Indeed, the APP^{-/-} cells were not responsive to either LPS or A β and the wild type cells only responded to LPS with elevated TNF α levels. In addition, the secretory pattern from the adipose tissue macrophage did not correlate with the changes observed from subcutaneous control diet tissues. That is, there was no difference in adiponectin levels between APP^{-/-} and wild type adipose tissue macrophage. These data suggest, again, that wild type and APP^{-/-} macrophages have unique phenotypes that are dependent upon their tissue of origin. As an additional assessment of tissue specific differences in macrophages another distinct pool of cells, intestinal macrophage, were isolated from wild type and APP^{-/-} cells on control diet simply to compare basal and stimulated secretion for each of the proteins, IL-4, IL-6, IL-1 β , TNF α , IL-10, MCP-1, and adiponectin (Figure 19). Again, these cells displayed unique secretory profiles from either peritoneal or adipose macrophage. Neither genotype was responsive to either LPS or A β stimulation with APP^{-/-} cells having basally elevated levels for nearly all of the proteins. This elevation is again, however, consistent with the low level of endotoxemia demonstrated in APP^{-/-} mice.

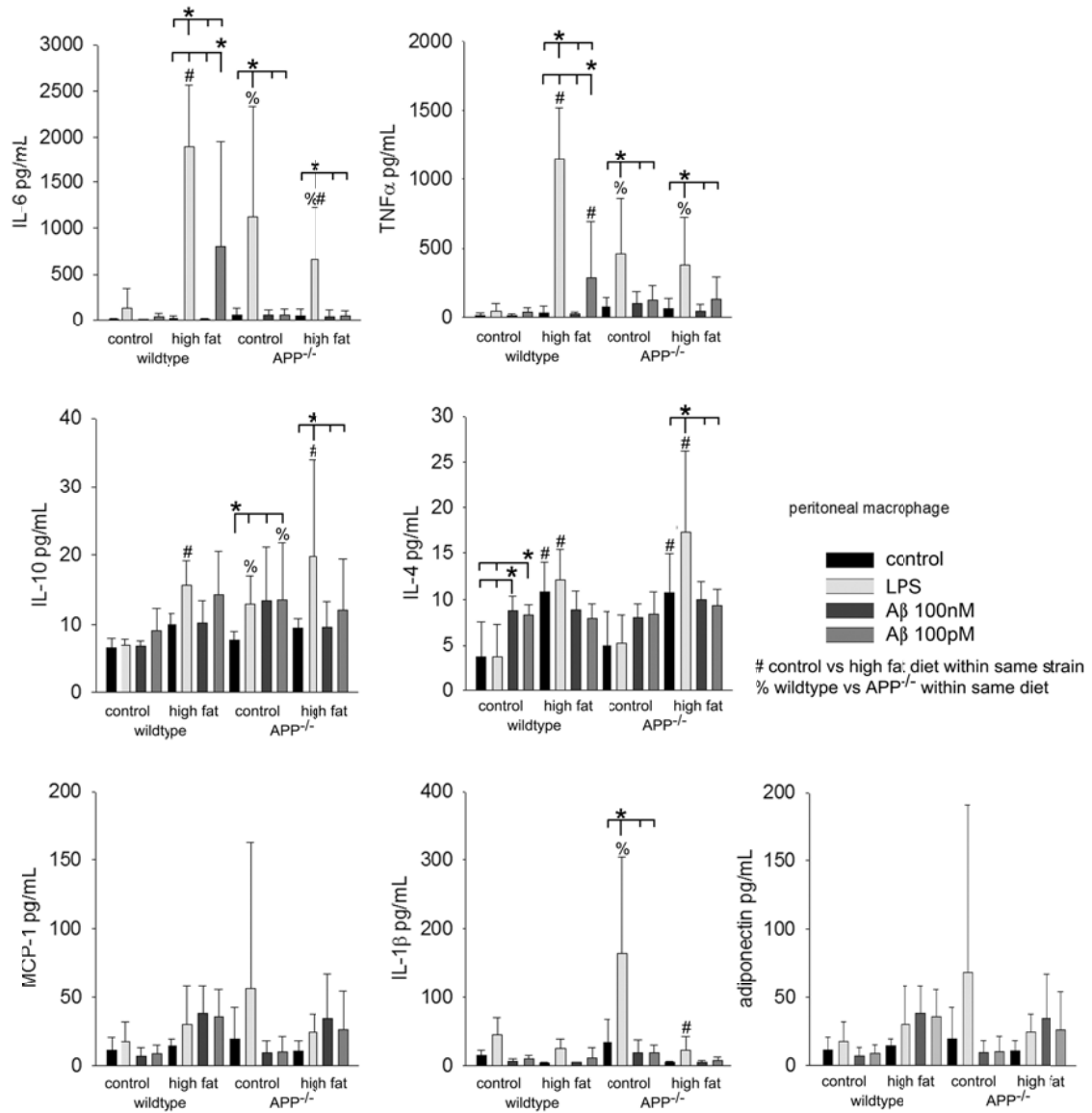


Figure 17. Peritoneal macrophage cytokine secretion differed between wild type and APP^{-/-} cells. Non-elicited, peritoneal macrophages from male wild type and APP^{-/-} mice fed both control and high fat diets for 22 weeks were isolated and stimulated with 10ng/mL LPS, 100nM Aβ 1-40, or 100pM Aβ 1-40 overnight and media was used to quantify IL-6, TNFα, IL-10, IL-4, IL-1β, MCP-1, and adiponectin secretion via ELISA. Data are expressed as mean +/- SD (n = 5), *P<0.05.

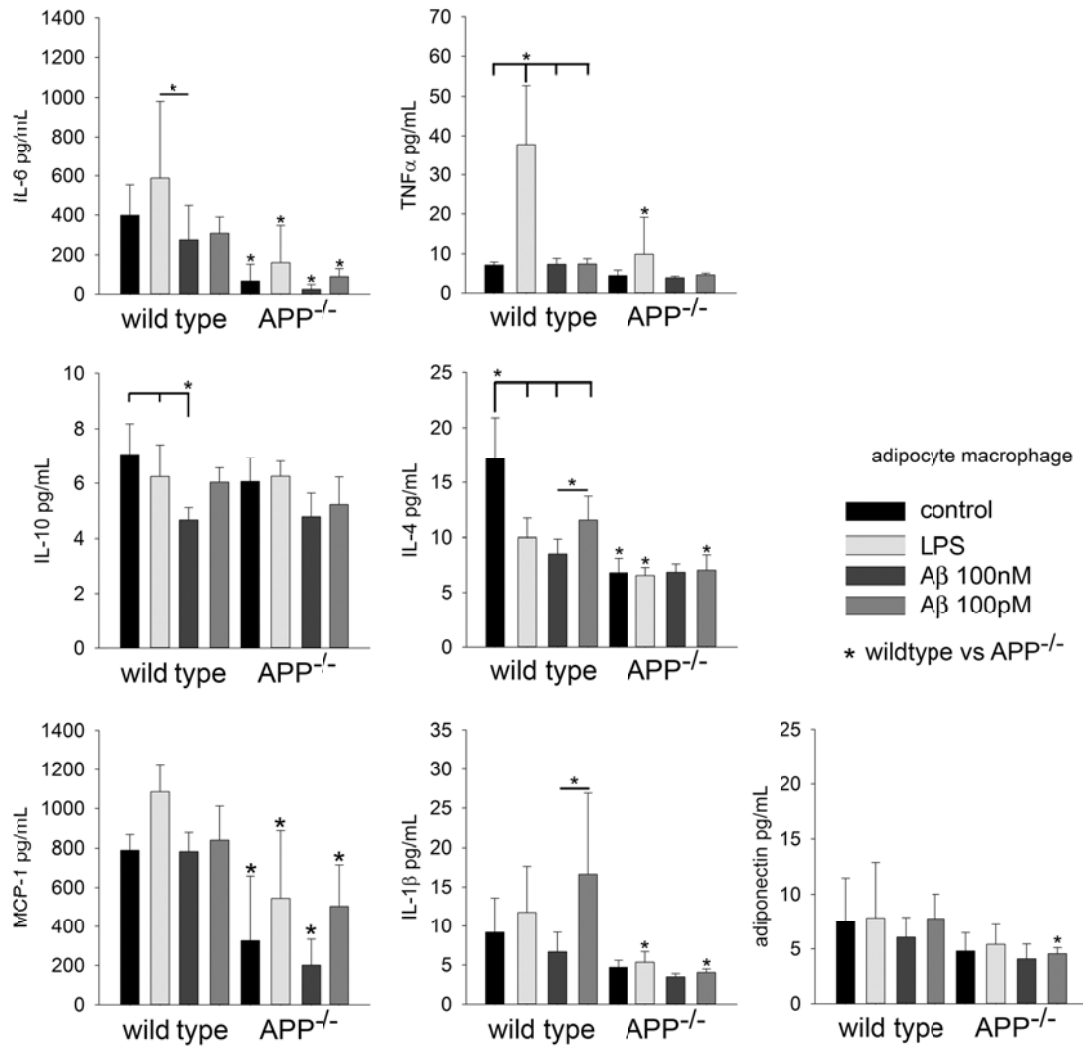


Figure 18. Adipose tissue macrophage cytokine secretion differed between wild type and APP^{-/-} cells. Adipose tissue macrophages from wild type and APP^{-/-} mice were isolated from subcutaneous adipose tissue and stimulated with 10ng/mL LPS, 100nM Aβ 1-40, or 100pM Aβ 1-40 overnight and media was collected to measure IL-6, TNFα, IL-10, IL-4, IL-1β, MCP-1, and adiponectin secretion via ELISA. Data are expressed as mean +/- SD (n = 5), *P<0.05.

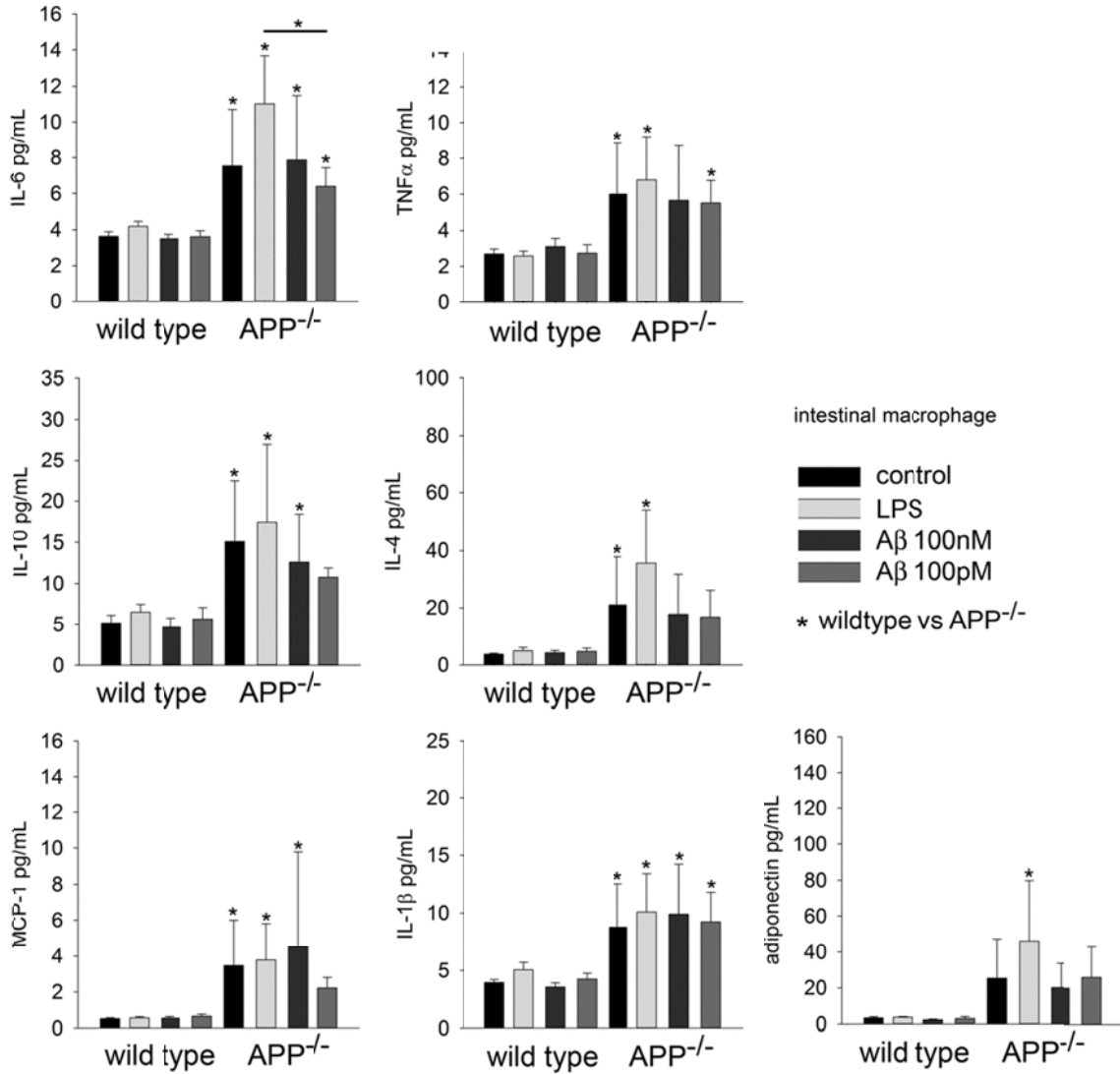


Figure 19. Intestinal macrophage cytokine secretion differed between wild type and APP^{-/-} cells. Intestinal macrophages from wild type and APP^{-/-} mice were isolated from small intestines and stimulated with 10ng/mL LPS, 100nM Aβ 1-40, or 100pM Aβ 1-40 overnight and media was collected to measure IL-6, TNFα, IL-10, IL-4, IL-1β, MCP-1, and adiponectin secretion via ELISA. Data are expressed as mean +/- SD (n = 5), *P<0.05

Differences in various protein marker levels characterized wild type vs. APP^{-/-} macrophages

Based upon the cytokine secretion differences between peritoneal, intestinal, and adipose macrophages, additional peritoneal macrophages from APP^{-/-} and wild type mice were again collected for *in vitro* stimulation with or without LPS to determine whether additional protein differences could be identified to better characterize the phenotypes between the cells types (Figure 20). With the caveat that the changes were likely unique to only this subtype of macrophage, peritoneal macrophages were used in these experiments as adipose tissue macrophage numbers were too limited for these types of analysis. Nonstimulated APP^{-/-} peritoneal macrophages demonstrated several differences from nonstimulated wild type cells. APP^{-/-} cells had decreased PPAR γ , CD36, arginase-1 and CD86 levels. Stimulation with LPS decreased PPAR γ , arginase-1 and CD86 levels in wild type cells compared to their unstimulated controls while APP^{-/-} cells increased CD36 levels compared to their controls. This again indicated fundamental differences basally and upon stimulation between the two genotypes. To more fully assess secretory profile differences in the macrophages media from stimulated macrophages was analyzed by an antibody anti-cytokine array (Figure 20C). Wild type macrophages stimulated with LPS had increased secretion of GCSF, IL-6, and KC with decreased secretion of GM-CSF, INF γ , and IL-13 (Figure 20C). Whereas APP^{-/-} macrophages stimulated with LPS also had increased GCSF, LPS stimulation in these cells also increased TIMP-1 secretion compared to basal levels of APP^{-/-} macrophages along with IL-1 α compared to LPS stimulated wild type macrophages (Figure 20C). Basally, APP^{-/-}

macrophages secreted less IL-13 compared to wild type macrophages (Figure 20C).

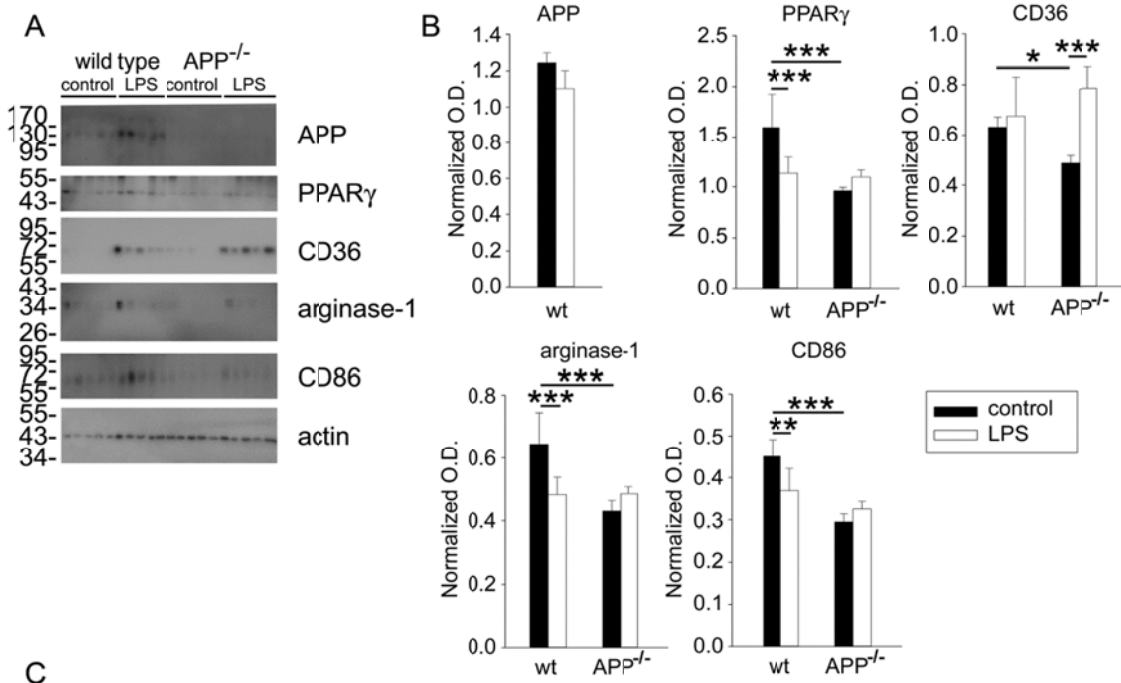


Figure 20. Peritoneal macrophage PPAR γ , CD36, arginase-1 and CD86 levels and cytokine secretion differed between wild type and APP^{-/-} cells. Non-elicited, peritoneal macrophages from male wild type and APP^{-/-} mice fed both control and high fat diets for 22 weeks were isolated and stimulated with 25ng/mL LPS overnight. Cells were lysed for Western blot analysis and media was used to quantify cytokine secretion via cytokine array. Data are expressed

as mean +/- SD (n = 5), *P<0.05, **P,0.01 to compare differences between strain. +P<0.05, ++P<0.01, +++P<0.001 to compare difference between stimulated with LPS and unstimulated.

Adipocytes from wild type and APP^{-/-} cells demonstrated altered cytokine secretion and protein expression

Although the macrophages had clear differences between phenotypes we appreciated that adipocytes also express APP and the differences in weight gain, and adipose tissue hypertrophy and lipid accumulation in the liver might be due to altered lipid uptake, storage, or metabolism as well. To begin addressing any changes in APP^{-/-} adipocytes that might help explain the tissue or animal phenotype differences subcutaneous adipocytes were isolated for comparison. Again, due to limitations in viability and numbers only subcutaneous cells were examined. APP^{-/-} adipocytes had increased levels of the differentiation marker (PPAR γ), fatty acid synthase (FAS) which catalyzes the synthesis of palmitate, the pre-adipocyte marker (Pref-1/Dlk), the cluster of differentiation 14 (CD14) a co-receptor along with TLR4 for the detection of lipopolysaccharide, and adiponectin the glucose regulation and fatty acid breakdown marker, as compared to wild type adipocytes (Figure 21). Since APP^{-/-} cells demonstrated an increase in fatty acid markers they were then used to determine whether this correlated with a difference in fatty acid uptake. To assess this, palmitic acid uptake was quantified in both genotype cells to find no significant difference in the ability of either genotype cell to take up this fatty acid (Figure 21C). This data indicate that although the APP^{-/-} and wild type adipocytes had similar abilities for

fatty acid uptake there were several differentiation markers that differed between the two. This indicated that changes in cellular phenotype were likely not limited to macrophage *in vivo* in adipose tissue in spite of the low level of adipocyte APP expression. Since a major adipocyte fatty acid uptake protein, CD36, was increased in the gonadal adipose tissue of APP^{-/-} mice, it was possible that APP was directly involved in regulating fatty acid uptake. To determine whether APP is part of a multi-protein complex with CD36, co-immunoprecipitation pull-down experiments from cultured adipocytes were performed. These demonstrated that APP and CD36 were not part of a multi-protein complex (Figure 21C) implying that loss of APP in the adipocytes does not alter the fatty acid uptake ability of CD36.

To answer the question of whether APP also served as a receptor on adipocytes, adipocytes cultures were stimulated with the APP agonist antibody, 22C11, as we had previously shown this antibody to directly stimulate the proinflammatory receptor actions of APP on monocyte/macrophage cells (Sondag 2004). Morphologically, cells from either genotype appeared similar (Figure 22C). Furthermore, stimulation with agonist antibody had no ability to alter levels of any protein marker compared to isotype matched negative control antibody stimulation (Figure 22A & 22B). However, quantitation of secreted cytokines from the media of the cultured adipocytes demonstrated that APP^{-/-} adipocytes basally released lower levels of IL-6, GCSF, and sTNFRI compared to wild type adipocytes indicating that their phenotype was different (Figure 22D). Surprisingly, negative control antibody stimulation significantly altered cytokine

levels from the untreated wild type cells values (Figure 22D). However, agonist antibody stimulation of wild type adipocytes did not alter values of any cytokine via array analysis from unstimulated control cells suggesting that although the phenotype of $APP^{-/-}$ and wild type adipocytes demonstrated subtle differences this was likely not due to loss of APP-mediated signaling.

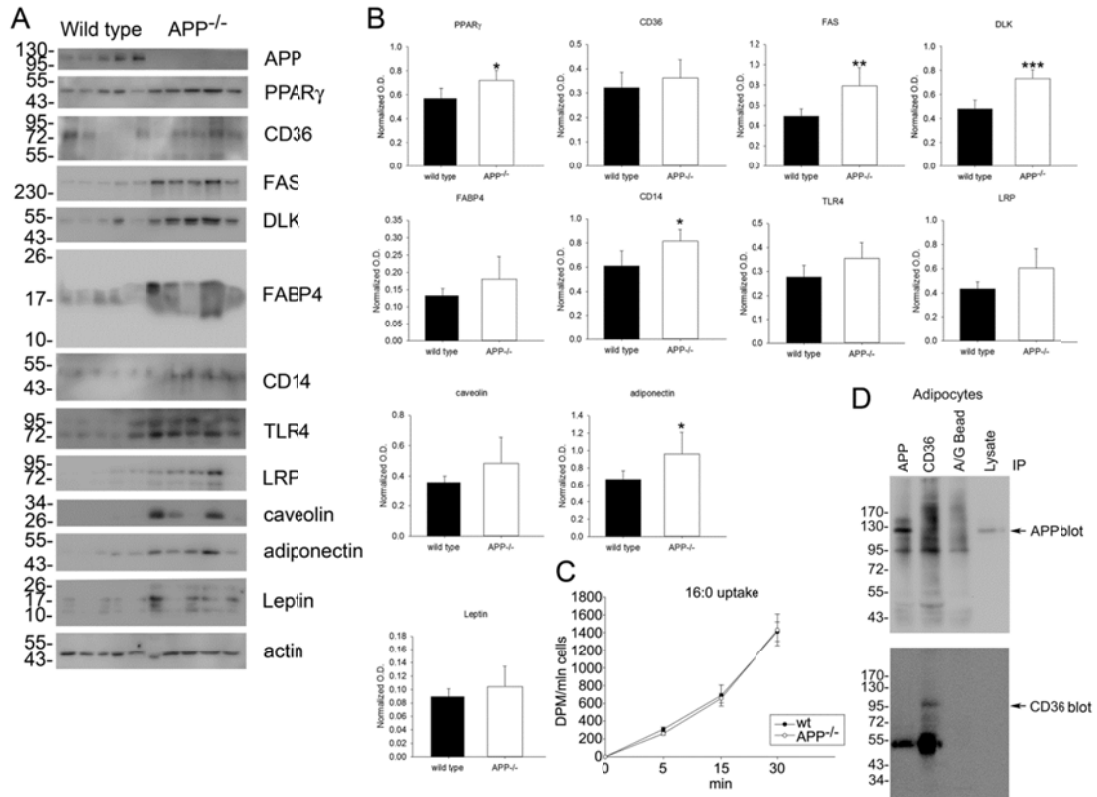


Figure 21. Quantitation of protein levels, palmitic fatty acid uptake, and immunoprecipitation from wild type and $APP^{-/-}$ adipocytes. Subcutaneous adipocytes from wild type and $APP^{-/-}$ mice were isolated and cultured for use. (A) Protein levels were examined via Western blot and (B) optical densities were quantified normalizing to actin as a loading control. (C) Radiolabeled palmitic fatty acid uptake was quantified from each cell type at 5 and 15 minutes. (D) To determine an association between APP and CD36, immunoprecipitations of

either APP or CD36 were performed from cultured wild type adipocytes followed by blotting with both antibodies. Data are expressed as mean +/- SD (b) (n = 10) *P<0.05, **P<0.01, ***P<0.001.

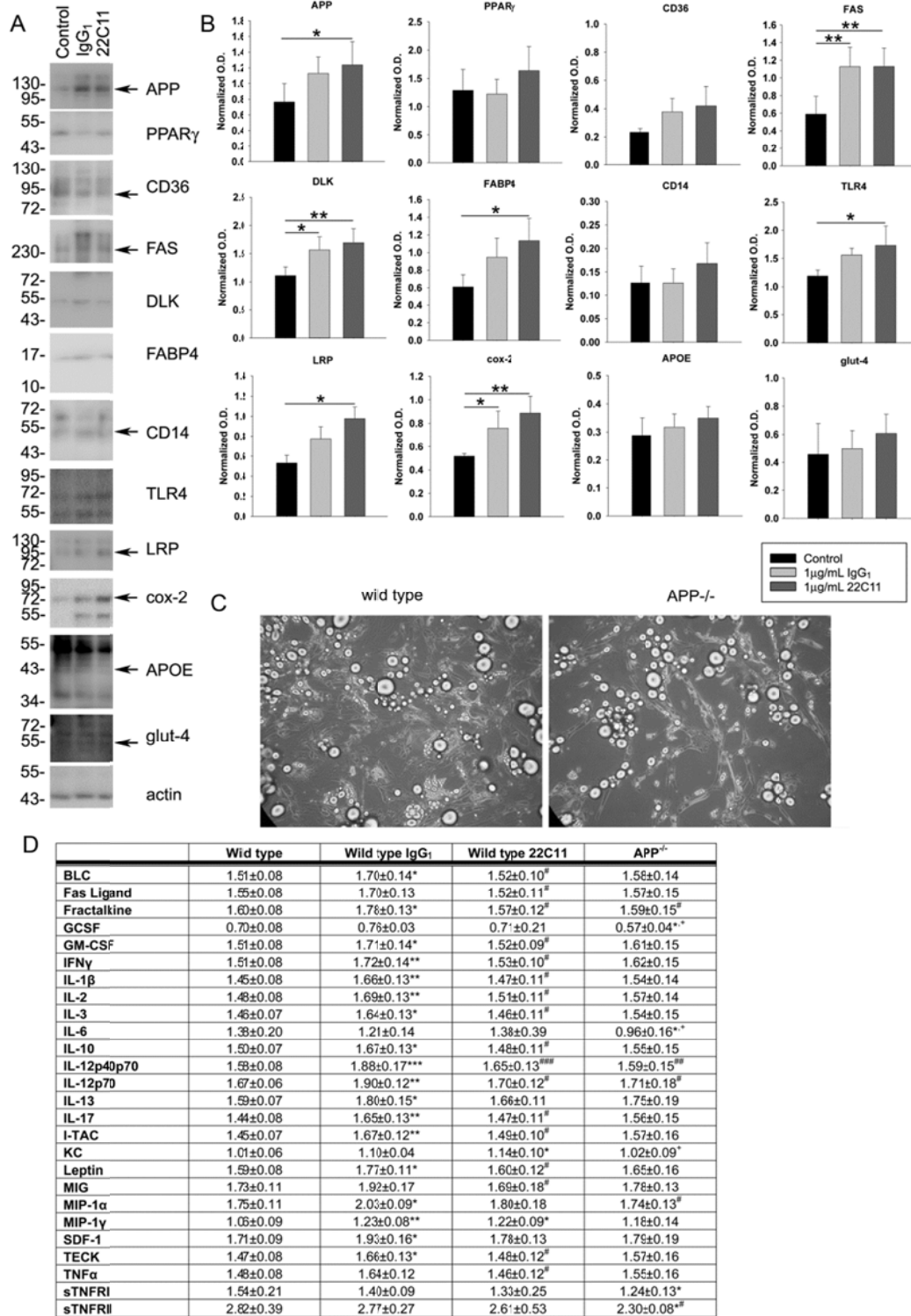


Figure 22. Quantitation of protein levels and cytokine secretion from APP^{-/-} and wild type adipocytes. Abdominal subcutaneous adipocytes were isolated

from wild type and APP^{-/-} mice, cultured and used for stimulations with or without 1 μg/mL of APP agonist antibody, 22C11, or isotype negative control IgG1. Western blots analysis was performed analyzing a variety of differentiation and activation markers and (B) values were quantified by normalizing by their respective actin loading controls. (C) Representative images from wild type and APP^{-/-} adipocytes are shown. (D) Media was collected from stimulated cells for cytokine array analysis. Data are expressed as mean ± SD (n = 6) *P<0.05, **P<0.01. (D) (n = 4) *P<0.05, **P<0.01, ***P<0.001 vs. Wild type; #P<0.05, ##P<0.01, ###P<0.001 vs. Wild type IgG₁; +P<0.05, ++P<0.01, +++P<0.001 vs. Wild type 22C11.

Although a receptor-type function of adipocyte APP was not a likely an explanation for genotype differences at the cellular or tissue level, it was reasonable to expect that the myriad altered cytokine secretions from APP^{-/-} macrophages, either basally or in response to stimuli, could be directly responsible for the altered adipocyte phenotype. However, another more tantalizing possibility was that loss of adipocyte stimulation with an APP metabolite such as Aβ, regardless of the cellular source of the peptide, could be the source of the adipocyte phenotype differences. In order to test this hypothesis, subcutaneous adipocytes were again grown and stimulated with Aβ₁₋₄₀ to simulate release from tissue macrophages or any other relevant cell. Adipocytes were stimulated with or without 100nM Aβ to again quantify their secretion of IL-6, TNFα, IL-10, IL-4, IL-1β, MCP-1, and adiponectin (Figure 23).

As expected, A β stimulation did affect wild type cells by specifically increasing cytokine secretion of only IL-10. Interestingly, A β also stimulated APP^{-/-} adipocytes to increase IL-10 secretion along with TNF α , IL-1 β , and IL-4. These data verified not only that adipocytes respond to A β stimulation but also that APP^{-/-} adipocytes have an altered secretory response to A β . This suggests, again, some fundamental activation or differentiation phenotype difference in adipocytes from APP^{-/-} mice that could involve altered stimuli from the extracellular milieu, including cytokines and A β .

As a negative control to validate whether or not the plethora of changes observed in adipose tissue, adipocytes, and macrophages were unique to these cells or could expand to any cell type that expressed APP, fibroblasts from wild type and APP^{-/-} mice were examined. Specifically, adipose tissue fibroblasts were compared. Western blot analysis of the fibroblasts demonstrated that, unlike macrophage and adipocytes, fibroblasts exhibited no difference in any of the protein levels measured (Figure 24). This supports the notion that changes in macrophage and, subsequently, adipocyte behavior resulting from loss of APP is the cause of the tissue and animal phenotype differences exhibited by APP^{-/-} mice fed control and high fat diets.

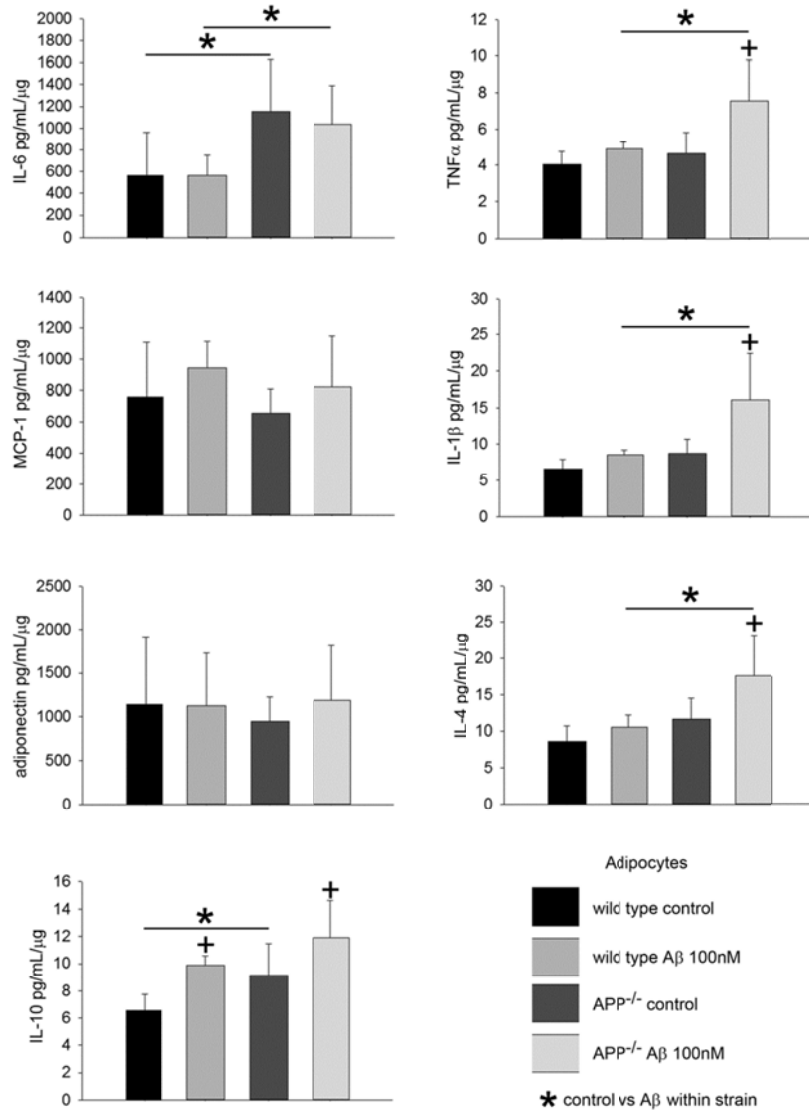


Figure 23. Adipocyte cytokine secretion was altered by Aβ 1-40 stimulation.

Adipocyte macrophages from wild type and APP^{-/-} mice were isolated from subcutaneous adipose tissue and stimulated with or without 100nM Aβ 1-40 overnight and media was collected to measure IL-6, TNFα, IL-10, IL-4, IL-1β, MCP-1, and adiponectin secretion via ELISA. Data are expressed as mean +/- SD (n = 5), *P<0.05 when comparing between strain, +P<0.05 when comparing within strain.

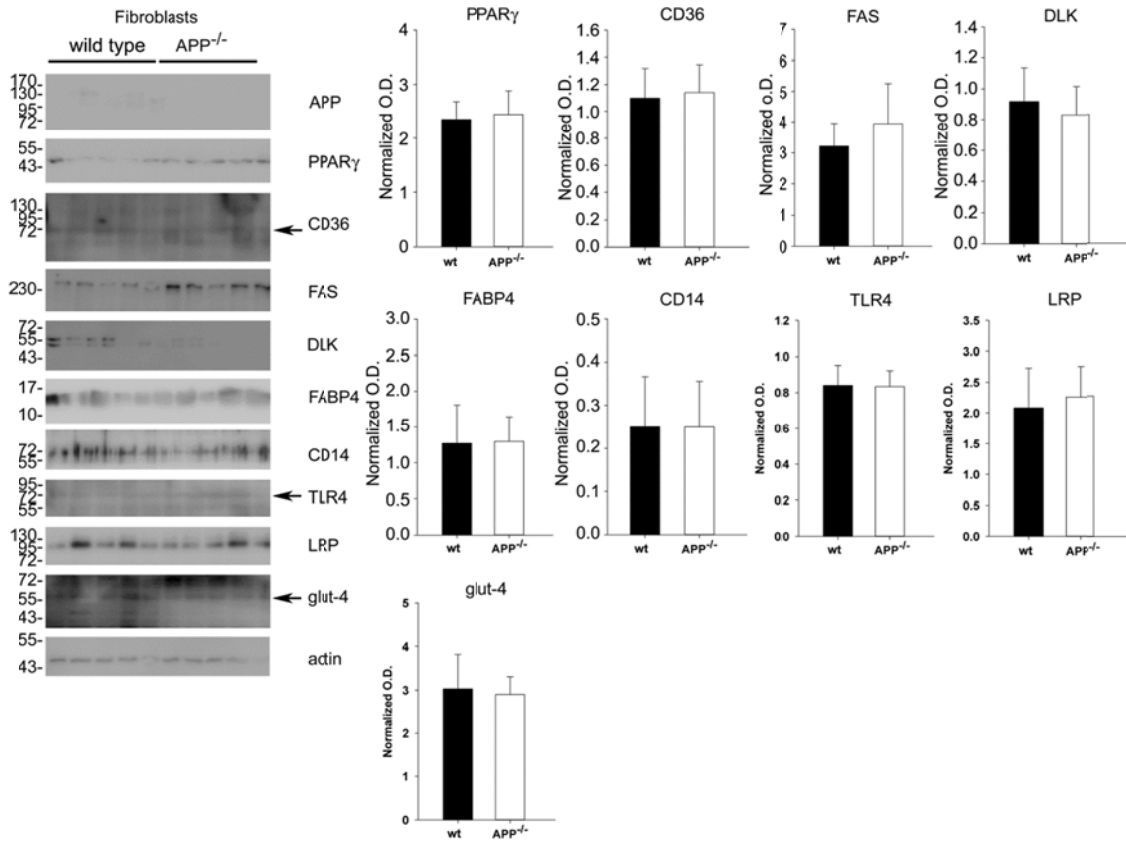


Figure 24. Quantitation of select protein levels from APP^{-/-} and wild type fibroblasts. Subcutaneous adipose tissue fibroblasts were isolated from wild type and APP^{-/-} mice and cultured for analysis. Protein levels of various markers of lipid metabolism or immune regulation were examined via Western blot and optical densities quantified by normalizing against actin loading controls. Data are expressed as mean \pm SD (B) (n = 6).

Protein quantitation, immunostaining, prostaglandin analysis, and fatty acid uptake quantitation in the neurons of APP^{-/-} and wild type mice

Based upon the differences observed in adipose tissue, particularly with regard to altered basal and stimulated macrophage phenotype, we assumed that similar alterations of brain microglia would occur in control and high fat diet fed APP^{-/-} mice. As we and others have reported (Blume 1989, Forloni 1992, Hung 1992, Ohyagi 1993, Smith 1993, Sola 1993, Willoughby 1992), neuronal APP and reactive microglia immunoreactivity did appear to have slight increases in the temporal cortex region of high fat diet fed wild type mice (Figure 25A & 25B). Similar to adipose tissue, APP^{-/-} brains exhibited reduced microglial immunoreactivity on a control diet but noticeably increased staining in high fat diet fed mouse brains (Figure 25B). However, unlike adipose tissue in which macrophage demonstrated robust APP immunoreactivity, IBA-1 positive microglia had no demonstrable co-localization with APP staining (Figure 25C). Several markers of inflammation, gliosis, fatty acid metabolism, and synaptic compartments were then compared via Western blot across diet and genotype (Figure 25D). Contrary to expectation, high fat diet feeding did not significantly increase APP protein levels in wild type mice as we have described in the hippocampus (Puig and Combs, 2012) (Figure 26). However, high fat diet fed brains had significantly increased levels of phosphorylated tau, CFABP, and APOE in wild type but not APP^{-/-} cortex (Figure 26). APP^{-/-} mice on high fat diet had reduced CD36, TLR2, TLR4, LRP, CD68, IBA-1, Cox-2, GFAP, CFABP, and APOE levels compared to wild type mice on high fat diet. Although there were differences in brain similar to adipose tissue in high fat diet dependent protein

changes across genotypes, the data similarly showed that loss of APP reflects in changes of both lipid and immune markers.

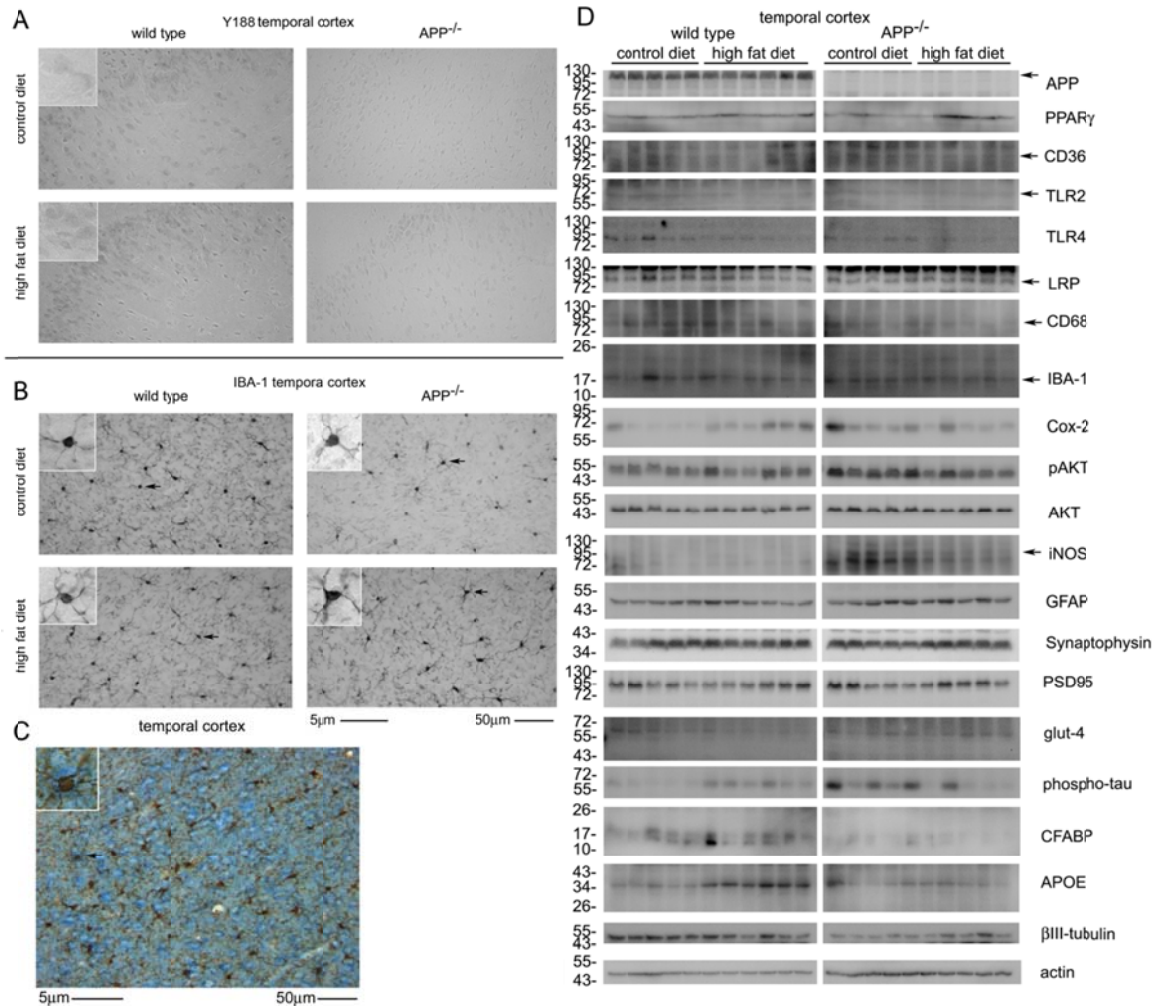


Figure 25. Diverse protein differences and APP and IBA-1 immunoreactivity in the temporal cortex of wild type and $APP^{-/-}$ mice. (A) APP (Y188) and (B) IBA-1 immunoreactivity and (C) APP(Y188) and IBA-1 double label immunoreactivity and (D) protein levels. Temporal cortex samples from wild type and $APP^{-/-}$ mouse brains were lysed, resolved by 10-15% SDS-PAGE and Western blotted using anti-synaptophysin, PSD95, APP, CD36, GFAP, TLR2, TLR4, iNOS, Cox-2, PPAR γ , phospho-tau (PHF-1), LRP, CD68, IBA-1, pAKT,

AKT, glut-4, CFABP, APOE, β III tubulin (neuronal loading control), or actin (general loading control) antibodies. Arrowheads indicate bands of interest when nonspecific bands are present. Antibody binding was visualized by chemiluminescence. Blots from all animals in each diet are shown. Brain tissue was collected, immersion fixed, serially sectioned, and immunostained using anti-IBA-1 antibody (microglial marker) or anti-APP antibody (Y188) and binding visualized using VIP or DAB as the chromogen. For double-labeling, CD68 stained tissue sections were stripped using 0.2N HCl and subsequently immunostained using anti-APP (Y188) antibody and binding visualized using Vector blue as the chromogen. Arrow indicates the location of immunoreactivity shown as an enlarged inset to the left of the panel. A representative image from 5-6 animals per condition is shown.

Also analogous to adipose tissue, several basal differences existed between wild type and APP^{-/-} brains fed control diets. APP^{-/-} mice on control diet had significantly lower protein levels of the inflammatory markers TLR2 and TLR4, the endocytic receptor (LRP), microglial markers CD68 and IBA-1, glucose transport receptor (glut4), and CFABP compared to wild type mice on control diet. Interestingly, APP^{-/-} mice on control diet demonstrated increased immune defense and proinflammatory marker (iNOS), pre-synaptic marker (synaptophysin), post synaptic marker (PSD95), and phospho-tau compared to wild type mice on control diet. This data again demonstrates a fundamental role for APP in regulating both immune and lipid-metabolism associated events. To

correlate the change in Cox-2 protein levels with decreased enzyme activity, brain levels of PGE₂, PGD₂, 6-*keto*PGF_{1α}, PGF_{2α} and thromboxane B₂ were quantitated from animals in each diet group (Figure 29B). Both basally and with diet, APP^{-/-} mice had significantly less PGE₂, PGD₂, thromboxane B₂ and 6-*keto*PGF_{1α} compared to their diet matched wild type mice. Interestingly wild type mice on high fat diet have elevated thromboxane B₂ and 6-*keto*PGF_{1α}. Since there was a decrease in fatty acid markers as well as prostaglandin levels in APP^{-/-} mice we checked to see if this corresponded to changes in fatty acid uptake. To assess this, palmitic acid uptake was quantified from cultured cortical neurons from wild type and APP^{-/-} brains. Consistent with the blots and prostaglandin analysis, APP^{-/-} neurons demonstrated attenuated 16:0 uptake ability at each time point examined (Figure 26C). These data directly supported the notion that APP regulates fatty acid uptake, at least in a cell type that abundantly expresses the protein, neurons. Since a major neuronal fatty acid uptake protein, CD36 (Le Foll et al., 2009, Martin et al., 2011, Le Foll et al., 2013), were decreased in brains of APP^{-/-} mice, it was possible that APP was directly involved in regulating fatty acid uptake. To determine whether APP is part of a multi-protein complex with CD36, co-immunoprecipitation pull-down experiments from cultured neurons were performed. These demonstrated that APP and CD36 were part of a multi-protein complex (Figure 26D) supporting the possibility that loss of APP alters the fatty acid uptake ability of CD36. Moreover, in contrast to adipocytes which express much lower levels of APP, APP appears to have a more definitive role in regulating fatty acid uptake in the brain.

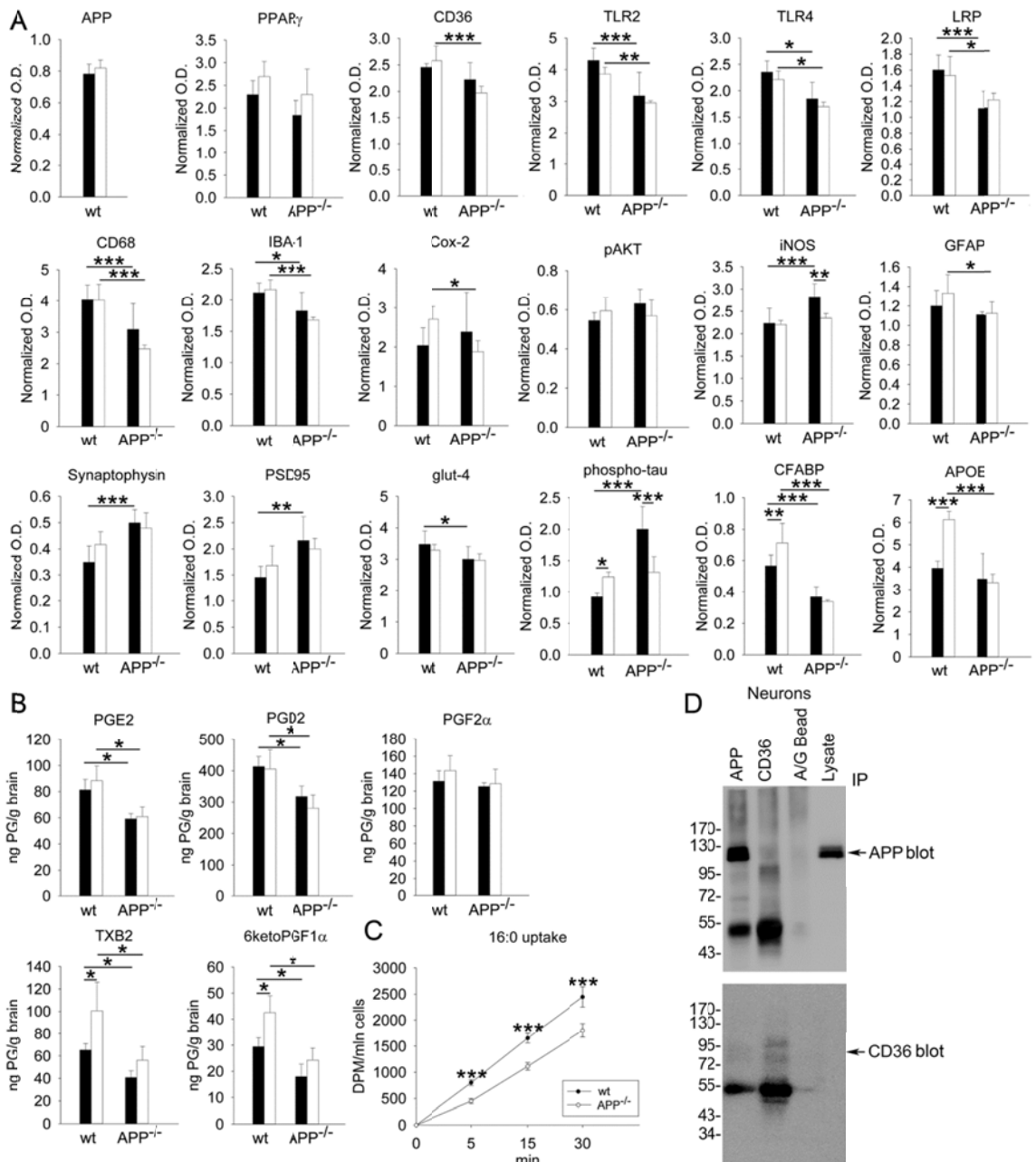


Figure 26. Quantitation of temporal cortex protein and prostaglandin levels, fatty acid uptake, and APP protein-protein interactions in neurons from wild type and APP^{-/-} mice. (A) Optical densities of the Western blotted temporal cortex tissue proteins from the control and high fat diet samples were normalized against their respective actin loading controls. (B) Brain samples were prepared

and analyzed on a quadrupole mass spectrometer to measure levels of PGE₂, PGD₂, 6-ketoPGF_{1α}, PGF_{2α}, and thromboxane B₂. (C) At 14 days *in vitro*, wild type and APP^{-/-} neurons were incubated with radiolabeled palmitic fatty acid to quantify time dependent uptake. (D) To determine an association between APP and CD36, immunoprecipitations of either APP or CD36 were performed from cultured wild type neurons followed by blotting with the both antibodies (D). Data are expressed as mean +/- SD (n = 5 or 6) *P<0.05, **P<0.01, ***P<0.001.

Since there were significant differences in microglial and inflammatory markers in the brains of APP^{-/-} mice versus wild types it was likely that, similar to macrophage, microglia would have altered secretory profiles across genotypes. To begin addressing this possibility of an altered immune milieu, a cytokine array analysis of the temporal cortex lysate was performed. This revealed a significant increase in eotaxin-2, fractalkine, IL-2, IL-13, IL-17, I-TAC, KC, MIP-1γ, RANTES, and TCA-3 in APP^{-/-} mouse brains supporting the idea once again that APP has a fundamental role in regulating both immune and lipid metabolism parameters (Figure 27). The fact that many cell types in the brain express APP complicated the interpretation of which cells were responsible for the protein differences observed by Western blot and cytokine array. However, based upon the immunostaining, the most dramatic increase in APP immunoreactivity was in neurons. Therefore, primary cortical neurons from wild type and APP^{-/-} mouse brains were grown to determine protein differences existed *in vitro* similar to observed from temporal cortex lysates. Surprisingly, wild type and APP^{-/-} neurons

did not differ for any of the same protein markers assessed from the tissue samples (Figure 28A & 28B). Since APP function can be stimulated in macrophage and microglia it was next determined whether stimulation of APP as a cell surface receptor could initiate changes in any of the protein markers. Neurons were stimulated with or without the APP agonist antibody, 22C11 to examine any subsequent changes in protein expression. However, unlike immune cells, antibody-mediated multimerization of APP did not result in any change in protein levels (Figure 28C & 28D). This suggested that the complex, multi-cell environment of the brain that resulted in robust changes in several markers was not replicated in the simplified single cell analysis of cultured neurons in spite of the fact that attenuated APP expression altered fatty acid uptake in these cells.

	wild type	APP ^{-/-}
BLC	0.12±0.02	0.23±0.13
CD30L	0.14±0.03	0.18±0.11
Eotaxin	0.12±0.04	0.17±0.10
Eotaxin-2	0.19±0.06	0.36±0.10**
Fas Ligand	0.09±0.05	0.20±0.09
Fractalkine	0.18±0.04	0.44±0.18*
GCSF	0.19±0.08	0.36±0.20
GM-CSF	0.13±0.04	0.17±0.10
IFN gamma	0.14±0.04	0.19±0.10
IL-1 alpha	0.28±0.07	0.35±0.11
IL-1 beta	0.05±0.03	0.13±0.06
IL-2	0.09±0.03	0.21±0.06**
IL-3	0.07±0.04	0.13±0.05
IL-4	0.25±0.09	0.30±0.08
IL-6	0.04±0.03	0.12±0.09
IL-9	0.19±0.06	0.28±0.10
IL-10	0.07±0.05	0.25±0.12
IL-12p40p70	0.06±0.03	0.27±0.17
IL-12p70	0.20±0.03	0.41±0.21
IL-13	0.13±0.03	0.27±0.15*
IL-17	0.04±0.01	0.35±0.14*
I-TAC	0.06±0.01	0.17±0.11*
KC	0.05±0.02	0.17±0.07**
Leptin	0.13±0.03	0.16±0.07
LIX	0.75±0.02	0.53±0.17
Lymphotactin	0.24±0.05	0.17±0.05
MCP-1	0.21±0.07	0.20±0.07
MCSF	0.33±0.05	0.36±0.07
MIG	0.14±0.04	0.23±0.08
MIP-1alpha	0.12±0.02	0.42±0.14
MIP-1gamma	0.28±0.06	0.81±0.24***
RANTES	0.09±0.03	0.65±0.21*
SDF-1	0.21±0.05	0.57±0.27
TCA-3	0.44±0.05	0.80±0.31*
TECK	0.08±0.02	0.24±0.10
TIMP-1	0.40±0.12	0.36±0.17
TIMP-2	0.18±0.03	0.21±0.11
TNF alpha	0.04±0.02	0.08±0.07
sTNFRI	0.15±0.04	0.25±0.16
sTNFRII	0.14±0.04	0.20±0.11

Figure 27. Quantitation of cytokine levels in wild type and APP^{-/-} temporal cortex. Temporal cortex was collected from wild type and APP^{-/-} mice, lysed, and

used for commercial cytokine arrays. Data are expressed as mean \pm SD (b) (n = 5) *P<0.05, **P<0.01.

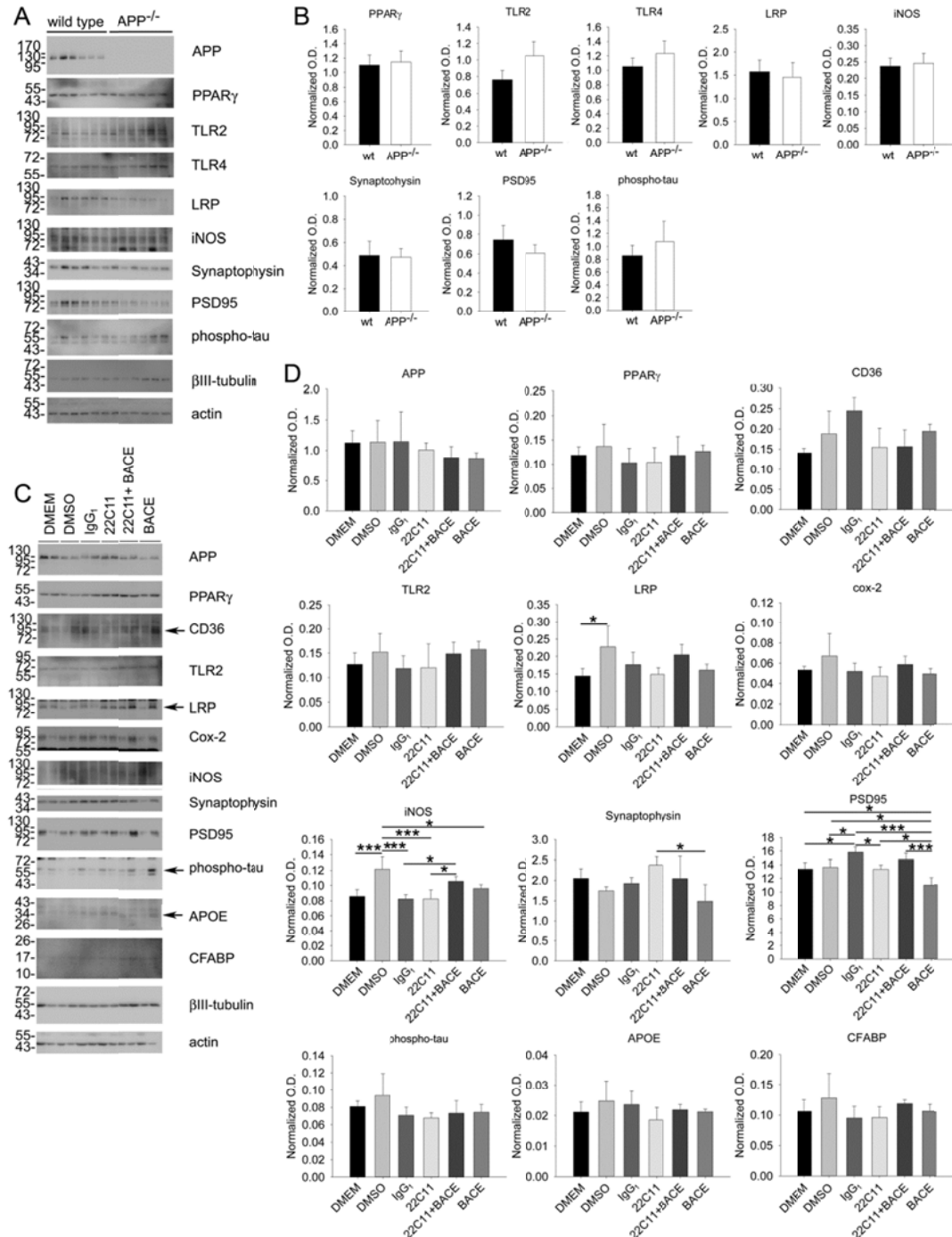


Figure 28. Quantitative comparison of protein levels in wild type and APP^{-/-} cultured cortical neurons. Primary cortical neurons were isolated from

embryonic day 16 wild type and APP^{-/-} mouse brains and cultured serum free for 14 days *in vitro* before use. (A) Western blot analysis of several proteins were examined and levels (B) quantified by normalizing against respective actin loading controls. Data are expressed as mean +/- SD (B) (n = 8) *P<0.05. Alternatively, wild type neuron cultures were stimulated with 1µg/mL isotype matched negative control antibody IgG₁, agonist antibody 1µg/mL 22C11, or 1.2µM BACE (β-secretase inhibitor II). (C) Protein levels were examined via Western blot and (D) optical densities quantified by normalizing against actin loading controls. Data are expressed as mean +/- SD (D) (n = 15).

APP^{-/-} microglia displayed an altered cytokine secretory profile, increased proliferation with decreased migration, and reduced phagocytic ability

Neuron culture analysis from wild type and APP^{-/-} mice did not identify any robust changes in several proteins examined either basally or with APP stimulation. However, other cell types express APP in the brain and the adipose tissue analysis suggested that macrophage, even when isolated *in vitro*, have dramatically altered phenotypes compared to wild type cells. To determine whether brain microglia also have an altered phenotype in APP^{-/-} mice perhaps contributing to the many changes observed in the brain, primary microglia cultures were grown from both genotypes. Microglia were stimulated with or without common stimulatory ligands, 25ng/mL LPS or 10µM Aβ 1-40 in order to quantify the cytokine secretory profiles (Figure 29). Stimulating wild type cells with LPS increased secretion of Eotaxin, Eotaxin-2, Fas Ligand, Fractalkine, GCSF, IL-3, IL-6, IL-9, IL-10, IL-12p40p70, IL12p70, IL-13, IL-17, I-TAC, KC,

MIG, MIP1 α , RANTES, SDF-1, TECK, TNF α , and sTNFR1 (Figure 32).

Stimulating wild type cells with A β 1-40 increased secretion of Eotaxin, Fas Ligand, Fractalkine, GCSF, GM-CSF, IL-1 β , IL-2, IL-3, IL-6, IL-9, IL-10, IL-12p40p70, IL12p70, IL-13, IL-17, I-TAC, KC, Leptin, MCP-1, MIG, MIP1 α , RANTES, SDF-1, TECK, TIMP-2, TNF α , and sTNFR1 (Figure 29). Stimulating APP^{-/-} cells with LPS increased secretion of only IL-1 α and IL-4 (Figure 29). On the other hand, stimulating APP^{-/-} cells with A β 1-40 increased secretion of BLC, Fas Ligand, GM-CSF, INF γ , IL-1 α , IL-1 β , IL-3, IL-4, IL-6, IL-10, IL-12p40p70, IL-13, IL-17, I-TAC, KC, Leptin, LIX, Lymphotactin, MCP-1, MCSF, MIG, MIP-1 α , RANTES, TECK, TIMP-1, TIMP-2, TNF α , and sTNFR1(Figure 29). Unstimulated APP^{-/-} microglia demonstrated increased GCSF secretion compared to unstimulated wild type microglia. In addition, LPS stimulated APP^{-/-} microglia had decreased secretion of IL-3, IL-6, IL-10, IL-12p40p70, IL-13, IL-17, RANTES, TNF α , and sTNFR1 compared to LPS stimulated wild type microglia (Figure 29). On the other hand, A β 1-40 stimulated APP^{-/-} microglia showed no difference in cytokine secretion compared to A β 1-40 stimulated wild type microglia. These data supported prior macrophage findings in that only this lineage of cells appeared to retain a robust difference in phenotype *in vitro*. Moreover, these secretory data suggest that in addition to observations from macrophage that APP appears to regulate each tissue specific macrophage uniquely, APP also regulates these cell responses in a stimuli specific manner (Figure 29).

MICROGLIA

STRAIN:	WILD TYPE			APP ^{-/-}		
	CONTROL	25ng LPS	10µM Aβ	CONTROL	25ng LPS	10µM Aβ
BLC	1.17±0.09	1.22±0.13	1.34±0.17	1.02±0.06	1.13±0.15	1.30±0.14 ^x
CD30L	1.17±0.12	1.31±0.16	1.33±0.18	1.12±0.07	1.13±0.19	1.33±0.19
Eotaxin	1.04±0.08	1.27±0.17 ⁺	1.33±0.16 ^x	1.06±0.06	1.11±0.18	1.28±0.11
Eotaxin-2	1.25±0.05	1.62±0.10 ⁺	1.57±0.15	1.29±0.09	1.48±0.35	1.57±0.18
Fas Ligand	0.96±0.11	1.24±0.13 ⁺	1.30±0.16 ^x	0.97±0.05	1.12±0.17	1.27±0.06 ^x
Fractalkine	1.07±0.12	1.35±0.08 ⁺	1.40±0.13 ^x	1.14±0.09	1.21±0.29	1.34±0.09
GCSF	1.03±0.09	1.55±0.15 ⁺⁺⁺	1.57±0.19 ^{xxx}	1.30±0.04 [*]	1.51±0.15	1.48±0.17
GM-CSF	1.10±0.03	1.25±0.12	1.32±0.19 ^x	1.06±0.03	1.19±0.16	1.33±0.06 ^x
IFNγ	1.09±0.04	1.28±0.16	1.31±0.19	1.07±0.04	1.29±0.18	1.39±0.08 ^x
IL-1α	1.22±0.14	1.36±0.10	1.29±0.12	1.08±0.14	1.32±0.11 ⁺	1.35±0.08 ^x
IL-1β	0.95±0.10	1.16±0.19	1.27±0.20 ^{xx}	0.99±0.04	1.05±0.13	1.22±0.06 ^x
IL-2	1.04±0.06	1.17±0.15	1.31±0.18 ^x	1.05±0.09	1.06±0.14	1.26±0.09
IL-3	0.92±0.11	1.26±0.09 ⁺⁺⁺	1.26±0.19 ^{xxx}	0.97±0.03	1.03±0.14 ^{**}	1.20±0.04 ^x
IL-4	1.25±0.18	1.33±0.08	1.37±0.11	1.07±0.04	1.39±0.16 ^{**}	1.37±0.20 ^x
IL-6	1.03±0.15	1.24±0.09 ⁺	1.26±0.16 ^x	0.97±0.06	1.07±0.13 [*]	1.22±0.06 ^x
IL-9	1.09±0.05	1.29±0.11 ⁺	1.33±0.15 ^x	1.08±0.04	1.21±0.15	1.26±0.09
IL-10	0.91±0.12	1.24±0.09 ⁺⁺⁺	1.29±0.20 ^{xxx}	0.97±0.05	1.01±0.12 ^{**}	1.23±0.07 ^{xx, #}
IL-12p40p70	0.95±0.11	1.26±0.09 ⁺⁺⁺	1.28±0.16 ^{xxx}	0.99±0.03	1.09±0.13 [*]	1.22±0.07 ^x
IL-12p70	1.26±0.07	1.54±0.17 ⁺	1.63±0.24 ^x	1.44±0.10	1.46±0.19	1.60±0.15
IL-13	1.08±0.04	1.29±0.17 ⁺	1.31±0.18 ^x	1.04±0.02	1.11±0.08 [*]	1.28±0.09 ^x
IL-17	0.92±0.11	1.30±0.13 ⁺⁺⁺	1.26±0.20 ^{xxx}	0.98±0.05	1.02±0.13 ^{**}	1.24±0.07 ^{x, #}
I-TAC	1.00±0.09	1.21±0.19 ⁺	1.33±0.15 ^{xx}	1.01±0.05	1.05±0.15	1.27±0.06 ^{x, #}
KC	0.94±0.11	1.24±0.11 ⁺⁺⁺	1.29±0.17 ^{xxx}	1.00±0.05	1.10±0.13	1.25±0.09 ^x
Leptin	1.04±0.11	1.22±0.22	1.38±0.18 ^{xx}	1.01±0.06	1.07±0.14	1.35±0.10 ^{xx, #}
LIX	1.40±0.19	1.51±0.14	1.58±0.11	1.34±0.12	1.52±0.15	1.64±0.17 ^x
Lymphotactin	1.41±0.21	1.66±0.36	1.68±0.24	1.28±0.08	1.33±0.07	1.78±0.26 ^{x, #}
MCP-1	1.21±0.19	1.35±0.22	1.59±0.22 ^x	1.22±0.10	1.38±0.25	1.57±0.10 ^x
MCSF	1.29±0.18	1.49±0.12	1.53±0.11	1.23±0.10	1.40±0.19	1.56±0.14 ^{xx}
MIG	0.99±0.13	1.26±0.19 ⁺	1.35±0.18 ^{xx}	1.03±0.02	1.09±0.12	1.32±0.08 ^x
MIP-1α	1.09±0.10	1.35±0.13 ⁺	1.42±0.16 ^{xx}	1.11±0.04	1.21±0.19	1.38±0.10 ^x
MIP-1γ	1.19±0.14	1.26±0.12	1.40±0.19	1.13±0.20	1.13±0.15	1.26±0.06
RANTES	0.94±0.13	1.37±0.15 ⁺⁺⁺	1.34±0.15 ^{xxx}	1.01±0.09	1.12±0.17 [*]	1.30±0.14 ^x
SDF-1	1.02±0.12	1.29±0.18 ⁺	1.42±0.12 ^{xxx}	1.19±0.12	1.26±0.16	1.44±0.14
TCA-3	1.25±0.23	1.38±0.05	1.47±0.18	1.30±0.12	1.33±0.19	1.54±0.17
TECK	1.04±0.08	1.21±0.13 ⁺	1.28±0.17 ^{xx}	0.98±0.04	1.07±0.10	1.22±0.04 ^{xx}
TIMP-1	1.39±0.16	1.45±0.15	1.64±0.14	1.35±0.13	1.39±0.11	1.67±0.14 ^{x, #}
TIMP-2	1.16±0.05	1.29±0.13	1.38±0.14 ^x	1.08±0.11	1.17±0.13	1.36±0.13 ^{xx}
TNFα	0.92±0.12	1.26±0.11 ⁺⁺⁺	1.26±0.19 ^{xxx}	0.99±0.06	1.00±0.11 ^{**}	1.22±0.06 ^{x, #}
sTNFR1	0.95±0.10	1.25±0.11 ⁺⁺⁺	1.30±0.17 ^{xxx}	0.98±0.04	1.05±0.09 [*]	1.26±0.07 ^{x, #}
sTNFR2	1.24±0.02	1.34±0.09	1.28±0.31	1.17±0.10	1.30±0.3	1.51±0.09

Figure 29. Quantitation of cytokine secretory profile from wild type and APP^{-/-} microglia stimulated with LPS or Aβ. Primary microglia cultures grown from postnatal day 1 wild type and APP^{-/-} microglia were grown and stimulated with 25ng/mL LPS or 10µM Aβ1-42. Media from overnight stimulation was used to probe a 40-cytokine antibody array. Comparison between conditions within

strain: A β vs Control ^xP<0.05, ^{xx}P<0.01, ^{xxx}P<0.001; LPS vs Control ⁺P<0.05, ⁺⁺P<0.01, ⁺⁺⁺P<0.001; A β vs LPS [#]P<0.05. Comparison between strains within condition: *P<0.05. **P<0.01, ***P<0.001.

As a way to further examine changes in microglial phenotype across genotypes we quantified their ability to proliferate, migrate through a collagen matrix as well as their ability to phagocytize A β as a typical ligand in the brain (Figure 33). APP^{-/-} microglia had increased proliferation in a 24 hour period compared to wild type cells possibly explaining why there was increased microglial immunoreactivity in the high fat diet fed brains of the APP^{-/-} compared to the APP^{-/-} control diet fed mice but similar to the wild type mice (Figure 28). However as expected, APP^{-/-} microglia were not able to migrate as well as wild type microglia nor were they able to phagocytize amyloid beta (Figure 33). These data support the basally lower levels of microglial immunoreactivity in APP^{-/-} brains suggesting that impaired brain infiltration occurs in these mice. Collectively, the microglial data indicates that APP plays a role in regulating many aspects of the fundamental phenotype of these cells including their secretory, proliferation, migration, and phagocytic abilities.

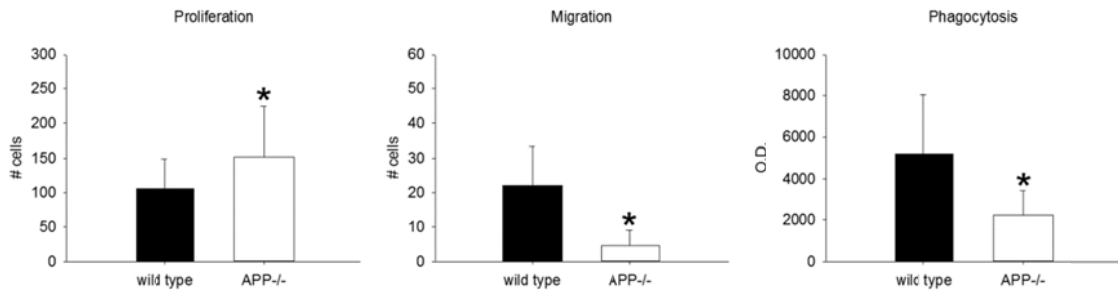


Figure 30. APP^{-/-} microglia had decreased proliferation, migration and phagocytic ability compare to wild type cells. Primary microglial cultures were grown from postnatal day 1 brains from wild type and APP^{-/-} microglia for use. Proliferation differences were quantified via MTT assay after a 24 hour incubation in serum containing media. Migration through a collagen matrix and FITC-conjugated 250nM A β 1-42 uptake were quantified after 6 hours. n=8 . *P>0.05.

CHAPTER V

AMYLOID PRECURSOR PROTEIN EXPRESSION MODULATES INTESTINE IMMUNE PHENOTYPE

Based upon prior work demonstrating that APP regulates the activation phenotype of monocytic lineage cells and since APP expression appeared to co-localize with macrophage in adipose tissue, we hypothesized that APP can regulate macrophage activation phenotype in tissues other than brain. In order to compare an environment in which neurons and macrophages are expected to abundantly express APP and a range of activating stimuli are continually being presented, we chose in this study to compare small intestine of wild type C57BL6 and APP^{-/-} mice. Based on our previously demonstrated role for APP in regulating monocytic lineage cell function, a lack of this protein in the dynamically activated immune environment of the intestine should result in significant alteration of immune parameters and perhaps neuronal and gut function in animals that lack the protein.

Immunoreactivity differences between the ileum of APP^{-/-} and C57BL6 control mice

In order to determine histological differences between APP^{-/-} and wild type C57BL6 mice, the ileum of small intestine was collected from adult (7 months of

age) mice and was fixed, sectioned and stained with hematoxylin and eosin and Alcian blue. Mice were collected at this age based upon prior observations that transgenic animals over-expressing mutant forms of APP demonstrate pathology in the gut at 6 months of age. This suggested that expression or function of endogenous APP, as was our study intent, may also be involved in regulating intestinal physiology at this age (Van Ginneken et al., 2011). There were no histological structural differences between the wild type C57BL6 and $APP^{-/-}$ mice (Figure 31).

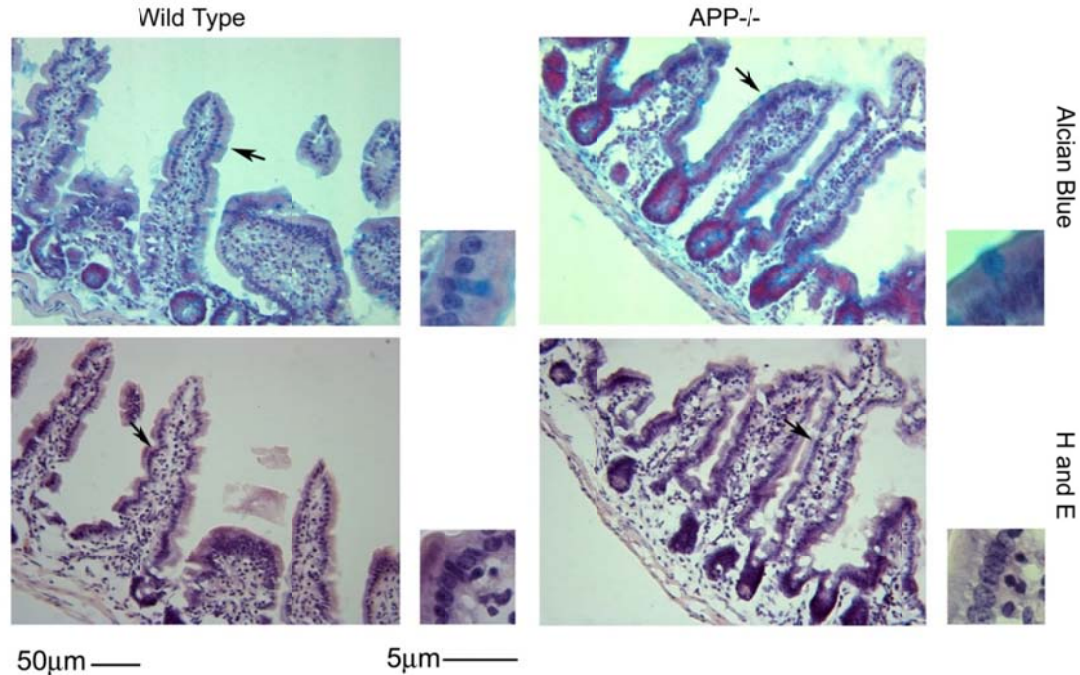


Figure 31. Histology of the small intestine was similar in both $APP^{-/-}$ and wild type controls. Ileum tissue samples were collected from C57BL6 wild type and $APP^{-/-}$ mice, fixed in 4% paraformaldehyde, serially sectioned, and stained using routine histology H & E (hematoxylin and eosin) and Alcian blue. Arrows indicate the location of the region of interest shown as an enlarged inset to the

right of each panel. Representative images from 5 animals per condition are shown.

In order to characterize APP immunoreactivity in the intestine, wild type C57BL6 and APP^{-/-} mice ileum of the small intestine was immunostained. Wild type mice demonstrated robust APP immunoreactivity within enterocytes and neurons and diffuse immunoreactivity within the smooth muscle of the muscularis externa (Figure 32). The tissue was then immunostained with a common intestine regulatory protein, cyclooxygenase-2 (Cox-2) as well as the tight junction protein, occludin, to gain an impression of intestinal phenotype. Both Cox-2 and occludin immunoreactivity again appeared primarily localized to the enterocyte layer with some areas of robust immunoreactivity for Cox-2 in the wild type intestines compared to APP^{-/-} mice (Figure 32). This supported the idea that APP expression regulates some aspects of intestinal immune cell behavior as well as that of enterocytes.

Based upon the fact that a portion of the APP immunoreactivity was clearly localized to neurons in wild type mice, the tissue was also stained with an anti-microtubule associated protein 2 (MAP2) antibody to visualize the integrity of the enteric plexi in the intestines. As expected, wild type mouse sections demonstrated robust immunoreactivity throughout the submucosa and lamina propria while the APP^{-/-} sections had visibly less immunoreactivity (Figure 32). This suggests that lack of APP expression also modulates neuronal integrity and likely enteric function in the small intestine. Since there was no obvious

immunoreactivity for APP observed within macrophages or other cell types throughout the intestinal layers (Figure 32) we then examined other cell types in the ileum of the small intestine. Wild type intestines demonstrated robust anti-CD68 immunoreactivity to identify macrophages while APP^{-/-} mice presented with a markedly decreased staining (Figure 33) suggesting either decreased activation or decreased numbers in the intestine. Because the phenotype of astrocyte-like enteric glia can contribute to maintenance of gut barrier integrity and inflammatory state (Savidge et al., 2007, Cirillo et al., 2011) we next assessed activation state of these cells.

Based upon the fact that a population of enteric glia are astrocytic in nature (Jessen and Mirsky, 1985) we immunostained the ileum of the small intestine with anti-GFAP antibodies (Figure 33). The GFAP immunoreactivity appeared to localize to the external portion of the muscularis externa. Unlike neuron and macrophage immunoreactivities there was no visible difference in astrocyte-like immunoreactivity between the wild type and APP^{-/-} intestine (Figure 33). To assess if APP expression resulted in tyrosine kinase activation in the ileum of the small intestine as another potential marker of immune cell macrophage activation, the ileum was stained with anti-pTyr antibodies. However, there was no obvious difference in pTyr immunoreactivity between wild type and APP^{-/-} intestines (Figure 33).

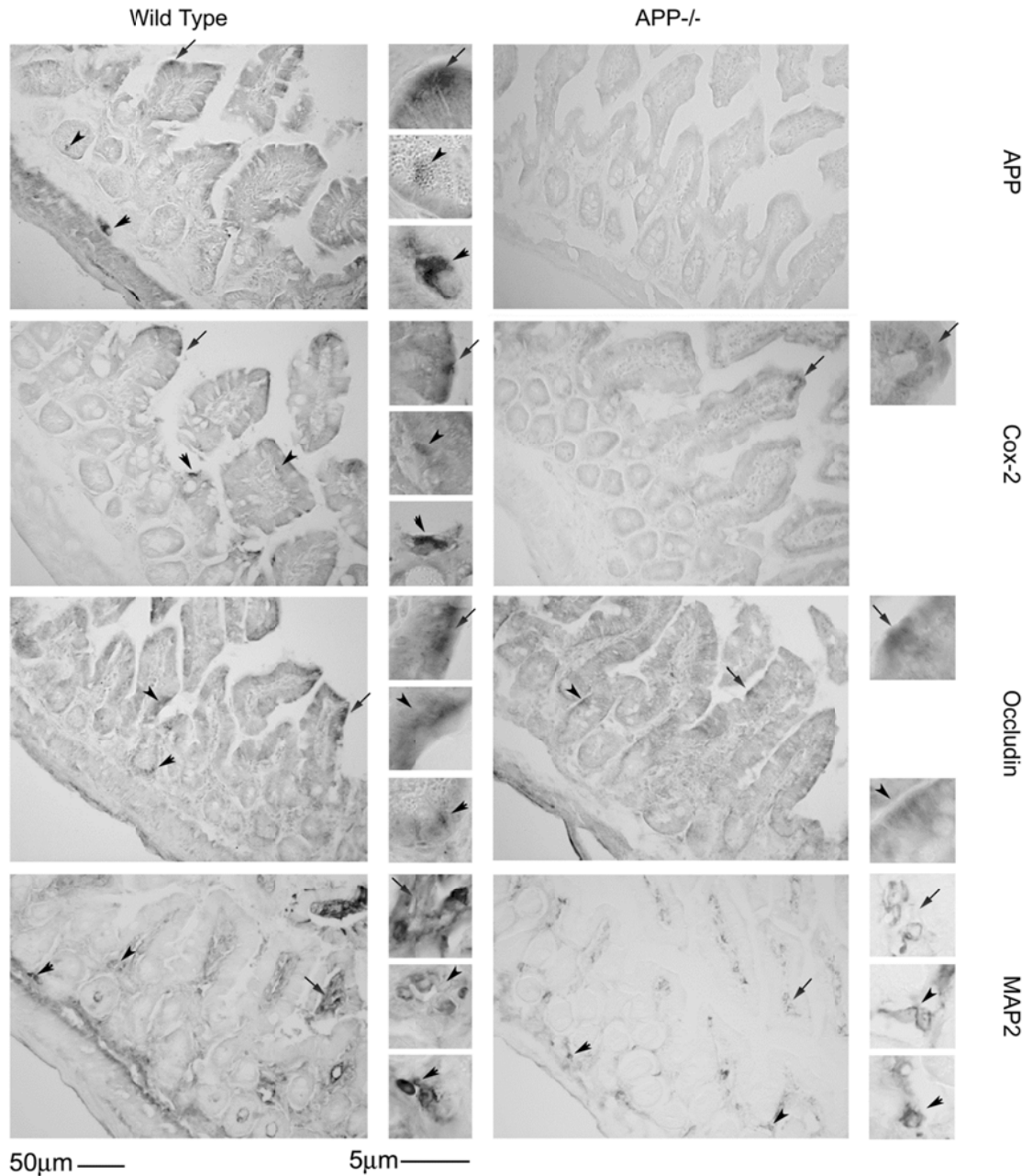


Figure 32. Small intestine immunoreactivity for Cox-2 and MAP2 decreased in APP^{-/-} mice compared to wild type controls with no change in occludin.

Ileum tissue samples were collected from C57BL6 wild type and APP^{-/-} mice, fixed in 4% paraformaldehyde, serially sectioned, and immunostained. Tissue sections were immunostained using anti-APP, Cox-2, occludin and MAP2

antibodies and antibody binding was visualized using Vector VIP as the chromagen. Arrows indicate the location of immunoreactivity shown as an enlarged inset to the right of each panel. Representative images from 5 animals per condition are shown.

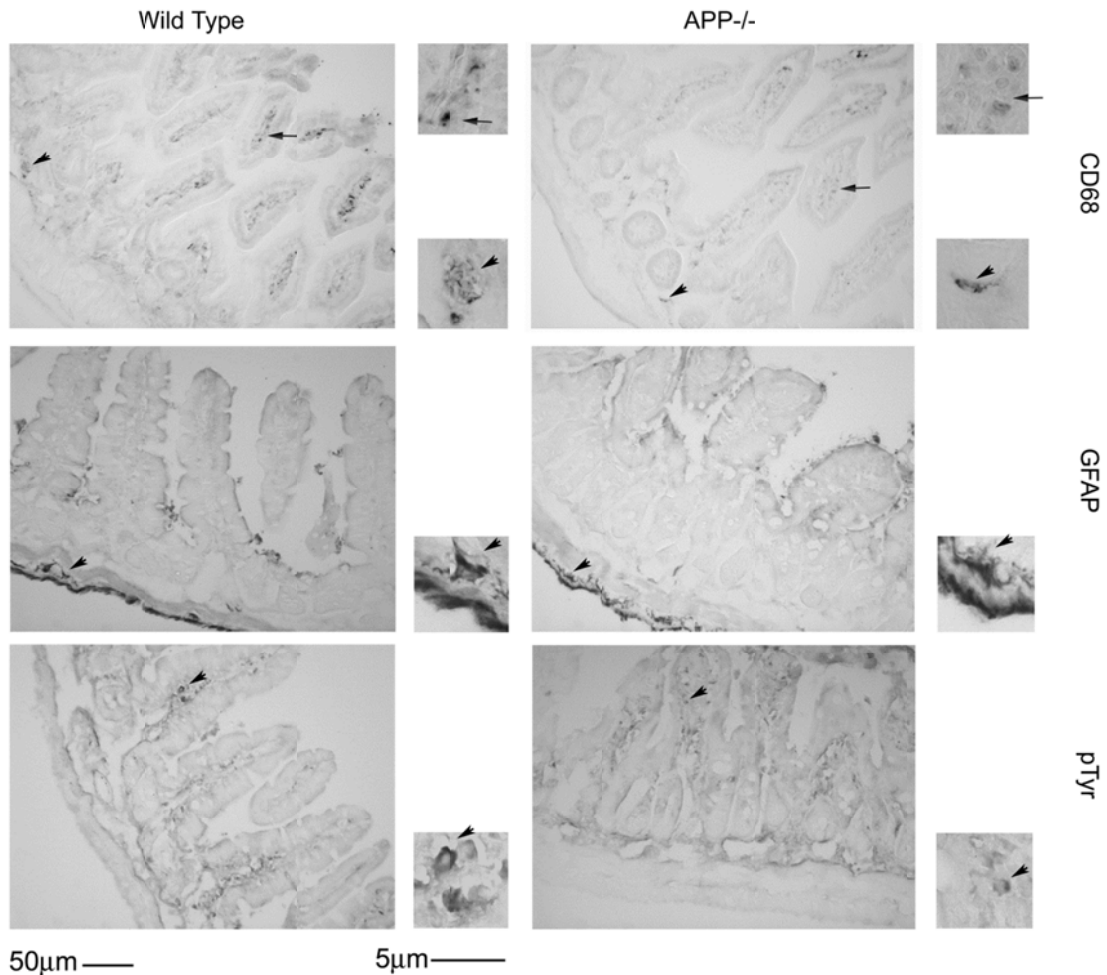


Figure 33. Small intestine immunoreactivity for CD68 decreased in APP^{-/-} mice compared to wild type controls with no change in GFAP or pTyr.

Ileum tissue samples were collected from C57BL6 wild type and APP^{-/-} mice, fixed in 4% paraformaldehyde, serially sectioned, and immunostained. Tissue sections were immunostained using anti-CD68, GFAP and pTyr antibodies and antibody binding was visualized using Vector VIP as the chromagen. Arrows

indicate the location of immunoreactivity shown as an enlarged inset to the right of each panel. Representative images from 5 animals per condition are shown.

Quantitation of protein differences in the ileum of C57BL6 wild type and APP^{-/-} mice

Based upon the qualitative changes in immunoreactivity patterns observed, it was necessary to quantify whether there were indeed protein level changes in wild type versus APP^{-/-} intestine. Ileum samples were analyzed to determine whether the changes observed by immunohistochemistry were significant. As expected, Western blot analysis demonstrated that Cox-2 and CD68 levels were significantly decreased in the APP^{-/-} mice compared to wild type controls with no difference in occludin, GFAP, and pTyr (Figure 34) consistent with the immunostaining observed (Figure 10). To assess whether other immune cell types present in the intestine besides macrophages were altered in APP^{-/-} mice, Western blots for markers of T-cells (CD3), B-cells (CD40), as well as dendritic cells (CD11c) were quantified. Although there was no change in CD3 levels there was a significant decrease in CD40 and CD11c protein levels in the APP^{-/-} compared to the wild type mice (Figure 12). As a measure of neuronal integrity, presynaptic and postsynaptic markers were also examined by Western blot. Interestingly, the total amount of neuronal β III-tubulin protein levels was decreased in APP^{-/-} as compared to wild type mice, with no difference in protein levels of the presynaptic (synaptophysin) or postsynaptic (PSD95) protein markers (Figure 34). This decrease in β III-tubulin levels was consistent with the observed decrease in dendritic marker, MAP2,

immunoreactivity in APP^{-/-} mice (Figure 32). A change in macrophage, B cell, and dendritic cell protein levels could correlate with altered expression of immunomodulatory receptors in the intestine. Therefore, critical pattern recognition receptor, TLR2 and TLR4, protein levels were examined as well. However there was no change in expression of either TLR between wild type and APP^{-/-} ileum of the small intestine (Figure 34). Finally, protein levels of necessary fatty acid transport proteins was assessed as an additional means of examining changes in intestinal barrier integrity. CD36 and FATP4 protein levels were analyzed, with again, no difference in expression between the wild type and APP^{-/-} ileum of the small intestine (Figure 34) suggesting again that epithelial function may be preserved in the APP^{-/-} intestines.

In vitro migration, proliferation, and differentiation comparison of macrophages from APP^{-/-} and C57BL6 wild type mice

Since Western blot analysis had validated that protein differences existed in neuronal proteins and enterocyte proteins in APP^{-/-} compared to wild type mice, we next sought to further examine the changes in CD68 positive macrophage immunoreactivity observed in the APP^{-/-} ileums. As intestinal macrophages have previously been shown to have very different responses to LPS (Grimm et al., 1995, Rogler et al., 1998), both peritoneal and intestinal macrophages have been included in our analysis as both contribute to the immunomodulatory behavior of the ileum of the intestine. One possibility for the decrease in CD68 immunoreactivity might simply be that APP^{-/-} cells were less able to migrate into the ileum.

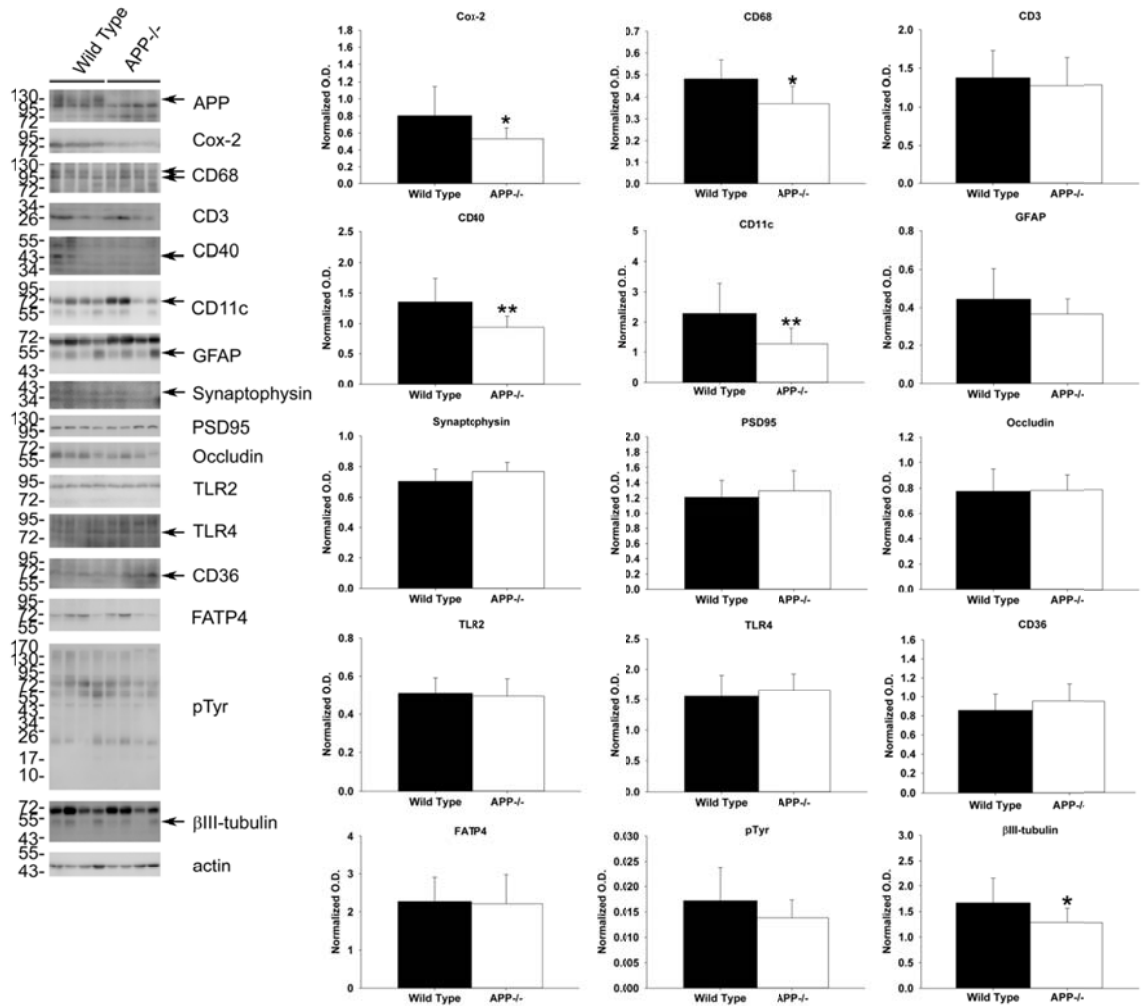


Figure 34. Western blot analysis of COX-2, CD68, CD40, CD11c and βIII-tubulin demonstrated decreased protein levels in the small intestine of APP^{-/-} compared to wild type mice. Ileum of the small intestine was collected from APP^{-/-} and C57BL6/J wild type mice. The tissue was lysed, resolved by 10-15% SDS-PAGE and Western blotted using anti-CD68, CD3, CD40, CD11c, GFAP, TLR2, TLR4, CD36, FATP4, pTyr, synaptophysin, PSD95, APP, Cox-2, occludin, βIII tubulin (neuronal loading control), or actin (general loading control) antibodies. Antibody binding was visualized by chemiluminescence. Blots from 4 of the animals for each strain are shown. Optical densities of the Western blotted

ileum proteins were normalized against their respective actin (Cox-2, CD68, CD3, CD40, CD11c, GFAP, TLR2, TLR4, CD36, FATP4, pTyr and occludin) or β III tubulin (synaptophysin and PSD95) loading controls and averaged (\pm SD) from 10 animals per each condition *P<0.05, **P<0.01.

As a means of testing this idea, we isolated non-elicited peritoneal macrophages and intestinal macrophages from wild type and APP^{-/-} mice at 2 months of age and compared the ability of these cells to migrate through a transwell culture insert *in vitro*. As expected, APP^{-/-} peritoneal macrophages demonstrated a significantly decreased ability to migrate through the insert into the LPS containing media below compared to wild type peritoneal cells. However, there was no significant difference in the migratory behavior of wild type and APP^{-/-} intestinal macrophages (Figure 35A and 35B). Another possibility for decreased CD68 immunoreactivity in the APP^{-/-} ileums could be due to an impaired differentiation or proliferation ability of APP^{-/-} cells. As a means of assessing proliferative ability of the cells, peritoneal and intestinal macrophages from wild type and APP^{-/-} animals were grown in the presence of serum for 72 hours. However, there was no significant difference in proliferative ability *in vitro* of either type of macrophage (Figure 35C and 35D). To examine differentiative or activation phenotype differences between the two genotypes, collected macrophages were stimulated 24 hr in the absence or presence of the potent bacterial endotoxin LPS and media were collected to assay secretion of select cytokines.

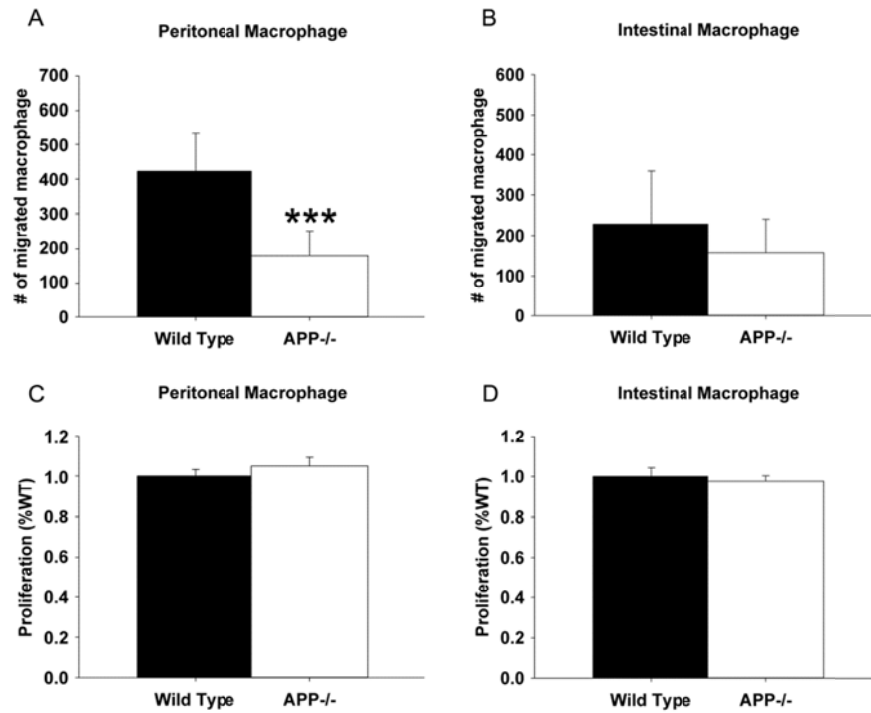


Figure 35. Peritoneal macrophages from $APP^{-/-}$ mice demonstrated significantly decreased migratory ability compared to wild type controls.

Non-elicited peritoneal macrophages and intestinal macrophages were isolated from $APP^{-/-}$ and C57BL6 control mice. (A) For migration assays, macrophages were grown in serum-free DMEM/F12. Cells were added to the top of transwell permeable support inserts placed into collagen coated dishes containing 25ng/mL LPS for 24hr in order to measure migration into the bottom well as assessed by the number of migrated cells. (B) For proliferation assays, macrophages were grown in DMEM/F12 with 10% FBS and 5% horse serum for 72 hours. MTT reduction assays were used as an indirect measure of cellular number to quantify proliferation. Results are mean (\pm -SD) from six animals per condition *** $P < 0.001$.

Based upon prior analysis of abundant peritoneal macrophages *in vitro* secretion, keratinocyte chemokine (KC), and interleukin-6 (IL-6) levels were quantified from the media as representative secretory factors from peritoneal and intestinal macrophages. Although there were no differences in LPS-stimulated levels between genotypes for KC cytokine secretion in the peritoneal macrophages, the APP^{-/-} peritoneal macrophages secreted significantly less KC compared to wild type cells during basal, unstimulated conditions (Figure 36A). LPS-stimulated wild type peritoneal macrophages had increased secretion of IL-6 compared to LPS-stimulated APP^{-/-} and untreated wild type peritoneal macrophages (Figure 36C). The LPS-stimulated intestinal macrophages had no change in secretion of KC or IL-6 compared to basal levels, suggesting that intestinal macrophages are unresponsive to LPS (Figure 36B and 36D). However, LPS stimulated APP^{-/-} intestinal macrophages had increased secretion of KC compared to LPS stimulated wild type intestinal macrophages. As well as, basally APP^{-/-} intestinal macrophages secreted more KC than wild type intestinal macrophages (Figure 36B).

As a follow up to the decreased migratory behavior of the APP^{-/-} peritoneal macrophages, Regulated upon Activation, Normal T-cell Expressed, and Secreted (RANTES) was measured from peritoneal macrophages stimulated with and without LPS (Figure 36E). As with the secretion of KC, LPS increased RANTES secretion with no significant difference between wild type and APP^{-/-} peritoneal macrophages (Figure 36E). To further compare phenotype differences particularly in intestinal macrophages, interleukin-1 beta (IL-1 β) was

next measured. Again as with KC and IL-6, LPS stimulation had no effect on wild type intestinal macrophages. However, LPS significantly increased secretion of IL-1 β from the APP^{-/-} intestinal macrophages as compared to the unstimulated APP^{-/-} intestinal macrophages as well as the LPS stimulated wild type intestinal macrophages (Figure 36F). Collectively, these findings suggest that peritoneal and intestinal macrophages of APP^{-/-} mice are phenotypically different with impaired migratory ability in peritoneal macrophages compared to their intestinal counterparts. More importantly, in spite of an apparent decrease in numbers of CD68 positive macrophages in the ileum of APP^{-/-} mice, these cells appear, to some degree, hyperreactive basally and in response to LPS stimulation when compared to wild type intestinal macrophages.

Profile of cytokine levels in ileum of APP^{-/-} and C57BL6 wild type mice

Based upon the *in vitro* macrophage secretory differences observed, the reduced CD68 ileum macrophage immunoreactivity, and the reduced protein levels of CD68, CD40, and CD11c it was reasonable to expect that levels of cytokines in the APP^{-/-} versus wild type ileums as a whole would also differ. To examine this possibility, ileums were collected from 7 month old animals and used to perform antibody-based cytokine arrays profiling 40 different cytokines. As expected, the APP^{-/-} ileums demonstrated significantly decreased levels of 12 different factors, CD30L, Eotaxin, Fas Ligand, Fractalkine, GCSF, IL-10, IL-12p40p70, IL-3, IL-9, MIG, MIP-1 γ , and sTNFR1, compared to wild type mice (Figure 37). Therefore, these findings were consistent with the

immunohistochemistry and further supported the notion that APP expression regulates immune cell phenotype in the intestine.

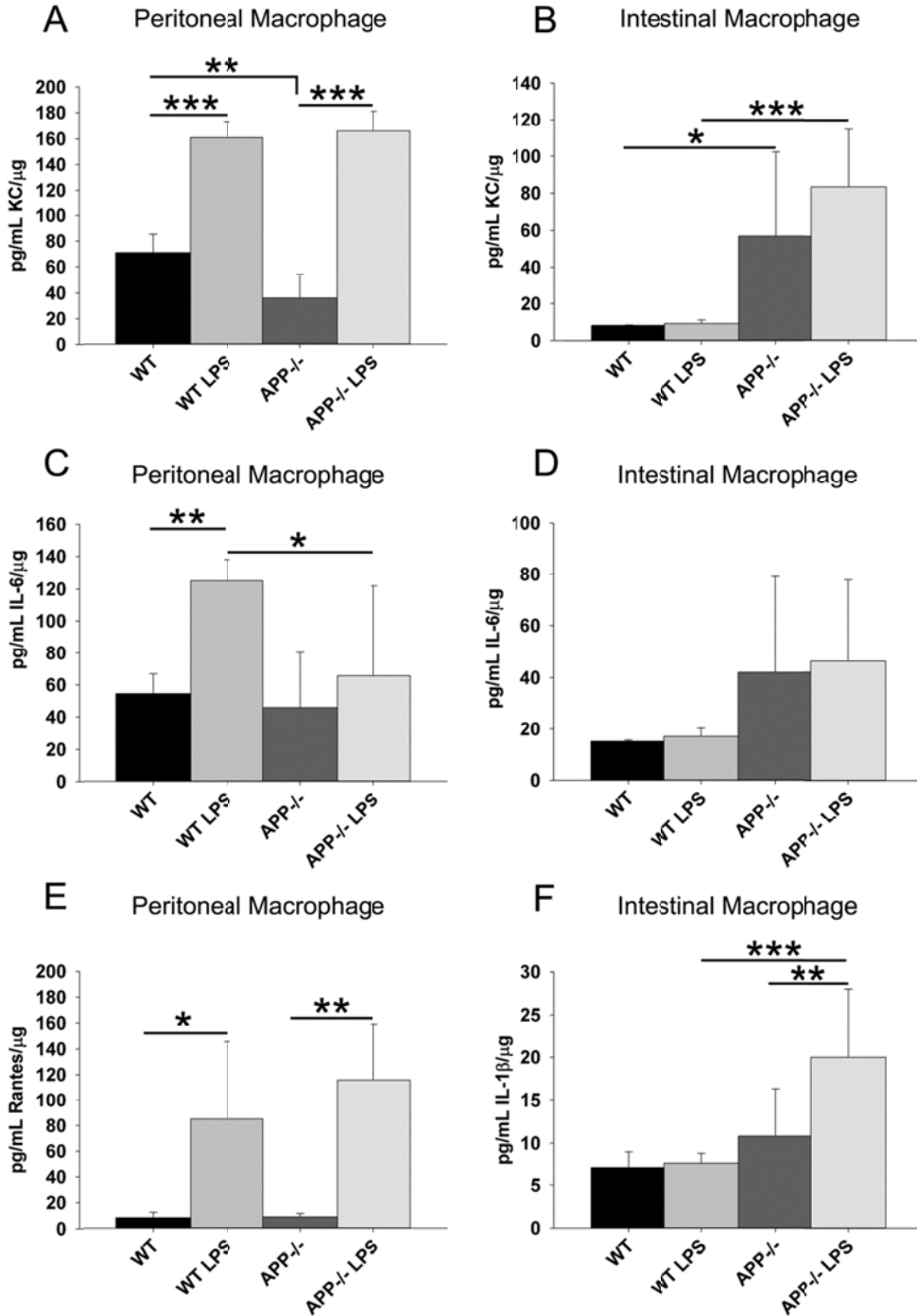
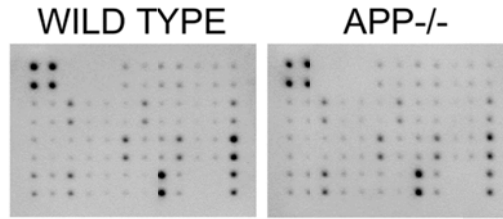


Figure 36. APP^{-/-} and wild type peritoneal macrophages demonstrated different cytokine secretory profiles compared to intestinal macrophages.

Non-elicited peritoneal macrophages and intestinal macrophages were isolated from C57BL6 wild type and APP^{-/-} mice. Macrophages were stimulated with or without 25ng/mL LPS, 24hr in serum-free DMEM/F12. Media was collected to quantify basal and stimulated secretion of KC, IL-6, RANTES and IL-1 β . The results are displayed as mean (+/-SD) from 6 animals in each group *P<0.05, **P<0.01, ***P<0.001.



	WT	APP ^{-/-}
BLC	0.98±0.06	0.94±0.04
CD30L	0.86±0.06	0.78±0.03*
Eotaxin	1.02±0.05	0.93±0.03*
Eotaxin-2	1.06±0.08	0.95±0.18
Fas Ligand	0.82±0.05	0.69±0.07*
Fractalkine	0.93±0.09	0.76±0.11*
GCSF	0.94±0.10	0.76±0.12*
GM-CSF	1.02±0.14	0.94±0.05
IFN gamma	0.93±0.09	0.85±0.03
IL-1 alpha	1.11±0.09	1.02±0.04
IL-1 beta	0.87±0.15	0.75±0.01
IL-2	0.84±0.10	0.78±0.01
IL-3	0.78±0.05	0.70±0.03*
IL-4	1.18±0.07	1.13±0.08
IL-6	0.80±0.05	0.73±0.08
IL-9	0.83±0.07	0.75±0.05*
IL-10	0.74±0.06	0.65±0.06*
IL-12p40p70	0.81±0.07	0.72±0.06*
IL-12p70	1.33±0.15	1.15±0.16
IL-13	0.99±0.12	0.96±0.02
IL-17	0.82±0.10	0.76±0.01
I-TAC	0.85±0.10	0.82±0.02
KC	0.84±0.09	0.83±0.05
Leptin	0.80±0.08	0.79±0.05
LIX	1.11±0.05	1.10±0.05
Lymphotactin	0.85±0.05	0.82±0.07
MCP-1	0.98±0.05	0.95±0.08
MCSF	1.43±0.07	1.32±0.13
MIG	0.82±0.07	0.73±0.05*
MIP-1alpha	0.90±0.10	0.84±0.03
MIP-1gamma	1.28±0.10	1.12±0.14*
RANTES	1.24±0.20	1.12±0.05
SDF-1	0.97±0.12	0.99±0.07
TCA-3	1.11±0.10	1.12±0.08
TECK	0.84±0.11	0.88±0.07
TIMP-1	0.75±0.07	0.77±0.07
TIMP-2	0.79±0.07	0.83±0.09
TNF alpha	0.75±0.08	0.70±0.07
sTNFRI	1.36±0.07	1.24±0.05*
sTNFRII	0.98±0.10	0.95±0.11

Figure 37. Small intestine of APP^{-/-} mice demonstrated altered levels of multiple cytokines compared wild type controls. Ileum from C57BL6 wild type

and APP^{-/-} mice were collected, lysed, and used in an antibody cytokine array. APP^{-/-} mice demonstrated decreased CD30L, Eotaxin, Fas Ligand, Fractalkine, GCSF, IL-10, IL-12p40p70, IL-3, IL-9, MIG, MIP-1 γ , and sTNFRI compared to wild type mice. A representative array for one animal from each genotype is shown. Optical densities of normalized dot intensities from 6 animals in each group are displayed as mean (+/-SD). *p<0.05

Differences in intestinal motility and absorption in APP^{-/-} and C57BL6 mice

A combined change in levels of multiple cytokines, proinflammatory and regulatory proteins, numbers of macrophages, and finally neuronal synaptic markers all suggest that the function of APP^{-/-} intestines would differ significantly compared to wild type control animals. In order to address intestinal function, mean stool production and water content were compared between the genotypes. Although this was not exclusively an assessment of small intestine behavior, APP^{-/-} animals generated significantly more stool per time period with increased water content (Figure 38A). This suggested increased motility and decreased absorption in the intestine of APP^{-/-} mice, which correlated with reduced body mass in these mice (Figure 38B). This suggests that APP^{-/-} may have reduced weight gain ability due to increased motility and reduced absorption. Moreover, the adverse consequence of decreased absorption in the smaller APP^{-/-} mice likely has a significant effect on overall physiology. As an additional means of assessing absorption, plasma levels of LPS were quantified from the blood of C57BL6 and wild type mice. Trace amounts of LPS are known

to be taken up into the blood from the intestines during normal absorption of fatty acids (Amar et al., 2008, Ghoshal et al., 2009). As now predicted, APP^{-/-} mice demonstrated significantly less LPS in their plasma compared to wild type mice again suggesting impaired intestinal absorptive function (Figure 38C).

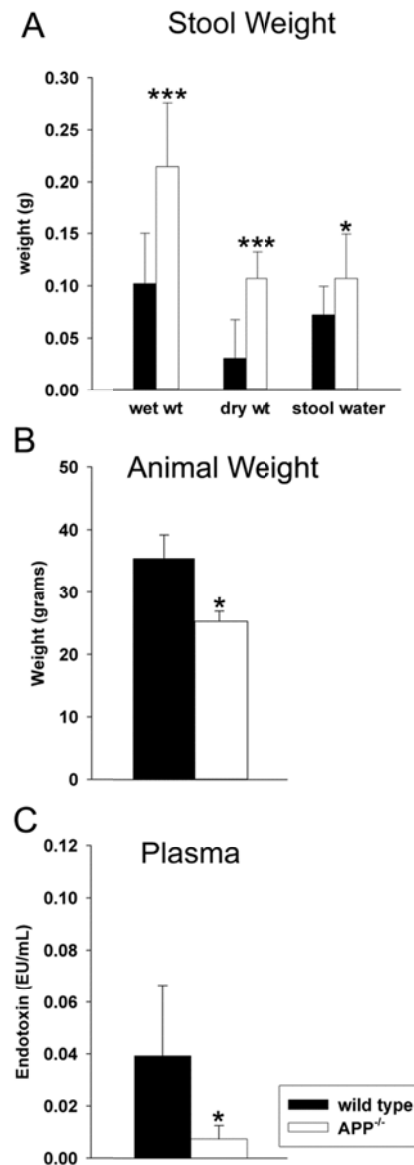


Figure 38. APP^{-/-} mice demonstrated intestinal motility and absorption differences compared to wild type mice. To compare overall intestinal absorption and motility, (A) water and stool production, (B) animal weight and (C)

uptake of LPS were quantified from C57BL6 wild type and APP^{-/-} mice. (A) To assess stool production and water absorption, wet and dry stool weights and the differences (water content) were collected over 1hr. Data from 13 animals in each group are displayed as mean (+/-SD). (B) To assess animal weight difference between strains, mice were weighed prior to collection. (C) To quantify uptake/transport of intestinal LPS into blood, whole blood was collected, plasma was separated and the LAL Endotoxin assay was performed according to manufacturer protocol. Data from 5 animals in each group are displayed as mean (+/-SD). *P<0.05, ***P<0.001.

CHAPTER VI

OVEREXPRESSION OF MUTANT AMYLOID PRECURSOR PROTEIN AND PRESENILLIN 1 MODULATES INTESTINE IMMUNE PHENOTYPE

Based upon the work in our previous chapter demonstrating that a lack of APP resulted in profound regulatory effects on protein expression in a range of small intestine cells including neurons, CD68 positive macrophages, and enterocyte epithelial cells which influenced the expression of multiple cytokine levels and intestinal motility changes, we hypothesized that overexpression of APP would also alter the intestinal phenotype. Therefore in this study we compare the small intestine of wild type C57BL6 and APP/PS1 mice to assess immune parameters and neuronal and gut function in response to increased APP and its metabolite A β .

Histological differences were observed between the ileums of APP/PS1 and wild type mice

Because our prior work had demonstrated dramatic plaque deposition and microgliosis in the brains of this particular strain of AD mouse model at 12-13 months of age, we elected to use 13 month old animals to examine any changes in intestines (Dhawan and Combs, 2012). As a representative section of the GI tract, we again focused our examination on the ileums (Puig and Combs, 2012). There appeared to be routine histological differences between the wild type and

APP/PS1 mice (Figure 39). H&E staining revealed an apparent increase in immune cells throughout the intestinal layers as well as an increase in Peyer's patch size in the APP/PS1 compared to the wild type (Figure 39). Surprisingly, Alcian Blue staining also revealed an increase in goblet cells (acid mucosubstances and acetic mucins) in the APP/PS1 compared to wild type mice.

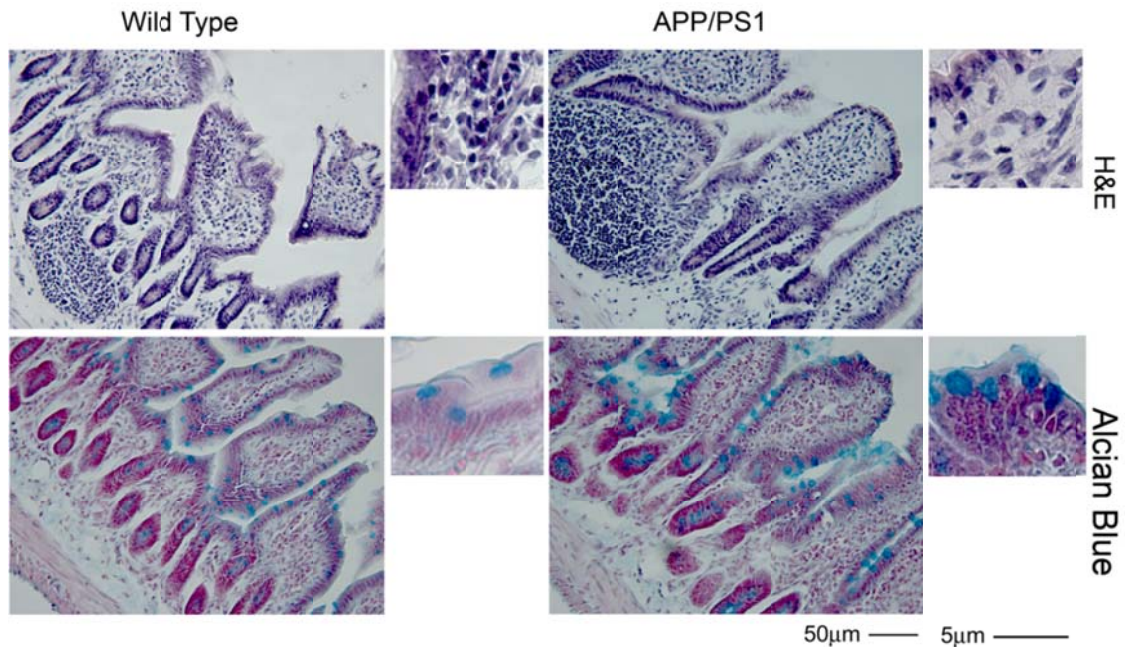


Figure 39. Histology of the small intestine was altered in APP/PS1 compared to wild type controls. Ileum tissue samples were collected from C57BL6 wild type and APP/PS1 mice, fixed in 4% paraformaldehyde, serially sectioned at 10µM, and stained using routine histology H&E (hematoxylin and eosin) and Alcian blue. Arrows indicate the location of the region of interest shown as an enlarged inset to the right of each panel. Representative images from 5 animals per condition are shown.

Significant differences in neuronal and inflammatory proteins were observed from ileum of APP/PS1 mice

The H&E staining prompted us to examine specific protein markers of immune cell change via Western blot to quantify any differences in wild type versus APP/PS1 ileums. Not only APP but also BACE levels were significantly increased in the APP/PS1 mice (Figure 40A and 40B). To delineate which immune cells were in fact increased as shown by the H&E staining, we quantified markers of macrophage (CD68), dendritic cells (CD11c), B-cells (CD40), and T-cells (CD3). Although there were no differences between strains in CD11c and CD40 levels, APP/PS1 mice demonstrated a significant increase in CD68 and CD3 protein levels compared to the wild type mice (Figure 40A and 40B). The increase in CD68 is similar to the increase we have prior observed in the brains of 12 month old APP/PS1 mice compared to wild type controls (Dhawan and Combs, 2012). To further characterize any inflammatory response in APP/PS1 mice, we quantified an increase in their Cox-2 protein levels compared to wild type mice. In order to examine whether any changes in intestinal barrier integrity or epithelial phenotype existed, we quantified CD36 (integral membrane protein) and occludin (tight junctional marker) levels. APP/PS1 mice had elevated CD36 but no occludin levels compared to the controls (Figure 40A and 40B). As a measure of neuronal integrity, presynaptic and postsynaptic markers were also examined by Western blot. Interestingly, APP/PS1 mice demonstrated increased protein levels of presynaptic (synaptophysin) and postsynaptic (PSD95) protein markers (Figure 40A and 40B). Because our prior work has demonstrated that APP and A β stimulation of immune cells is associated with tyrosine kinase-

mediated signaling (Sondag et al., 2009, Dhawan et al., 2012) we also determined whether any changes in overall protein phosphor-tyrosine (pTyr) or active phospho-Src (pSrc) levels existed in APP/PS1 mice compared to controls. However, APP/PS1 mice did not significantly differ in pTyr or pSrc levels compared to wild type control mice (Figure 40A and 40B).

No significant increase in quantitated A β levels were detected in the stool or intestinal lysate of APP/PS1 compared to wild type mice

In order to quantify A β levels in the ileums, intestinal lysates and stool washings were collected and used in A β 1-40 and A β 1-42 ELISAs. However, contrary to our expectations and the increased APP and BACE levels in the Western blot analysis (Figure 40A and 40B), no quantifiable increase in A β 1-40 or A β 1-42 was observed in the intestinal lysate or the stool washings (Figure 40C).

Immunohistological differences were observed between the ileums of APP/PS1 and wild type control mice

To provide qualitative cellular localization in support of the quantitative Western analysis, immunohistochemistry was performed. APP/PS1 and wild type mice demonstrated APP immunoreactivity within enterocytes and neurons and diffuse immunoreactivity within the smooth muscle of the muscularis externa with increased intensity in the APP/PS1 mice (Figure 41). Both strains demonstrated fibrillar A β (OC) immunoreactivity in the enterocytes, oligomeric A β (A11) and 4G8 immunoreactivity in the neurons and diffuse immunoreactivity within the smooth muscle of the muscularis externa (Figure 41). There appeared to be a

slight increase in fibrillar (OC) and 4G8 A β reactivity in the APP/PS1 compared to the wild type with no difference in oligomeric A β (A11) staining between the two strains (Figure 41).

To assess changes in particular cell types throughout the intestinal layers we further examined the ileum of the small intestine with a cell-selective antibodies marker. APP/PS1 intestines demonstrated robust increased anti-CD68 immunoreactivity to identify macrophages compared to the wild type ileums (Figure 42) suggesting either increased activation or increased numbers in the intestine, consistent with the increased CD68 levels observed via Western blot and the increased immune cell detection in the H&E stains. To further assess intestinal integrity, the tissue was then immunostained with a common intestine regulatory and proinflammatory protein, cyclooxygenase-2 (Cox-2), a tight junction protein, occludin, as well as, the integral membrane protein, CD36, to gain an impression of intestinal phenotype. Cox-2, CD36 and occludin immunoreactivity again appeared primarily localized to the enterocyte layer with some areas of robust immunoreactivity for Cox-2 and CD36 in the APP/PS1 intestines compared to the wild type mice (Figure 42). This collective staining supported the idea that mutant APP/PS1 expression regulates some aspects of intestinal immune cell behavior as well as that of enterocytes, suggesting that APP may play some role in not only immune changes but also digestion and absorption.

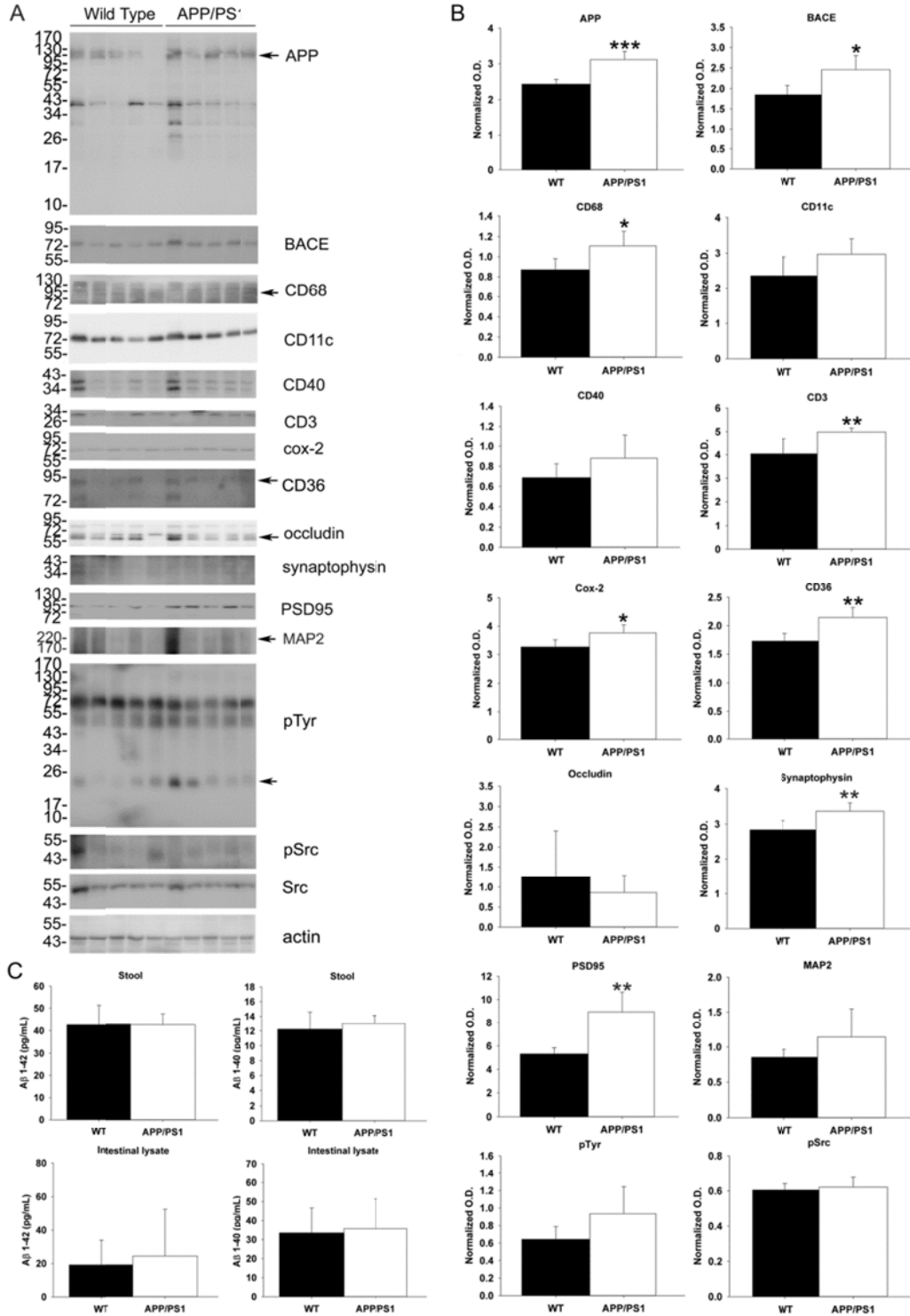


Figure 40. Western blot analysis of APP, BACE, CD68, CD3, Cox-2, CD36, Synaptophysin, and PSD95 demonstrated increased protein levels in the small intestine of APP/PS1 compared to wild type mice. Ileum of the small

intestine was collected from APP/PS1 and C57BL6 wild type mice. The tissue was lysed, resolved by 10-15% SDS-PAGE and Western blotted using anti-APP, BACE, CD68, CD11c, CD40, CD3, Cox-2, CD36, occludin, synaptophysin, PSD95, MAP2, pTyr, pSrc, cSrc (loading control), or actin (loading control) antibodies. Antibody binding was visualized by chemiluminescence. Blots from all animals are shown. Optical densities of the Western blotted ileum proteins were normalized against actin loading control and averaged (+/- SD) from 5 animals per each condition *P<0.05, **P<0.01, ***P<0.001

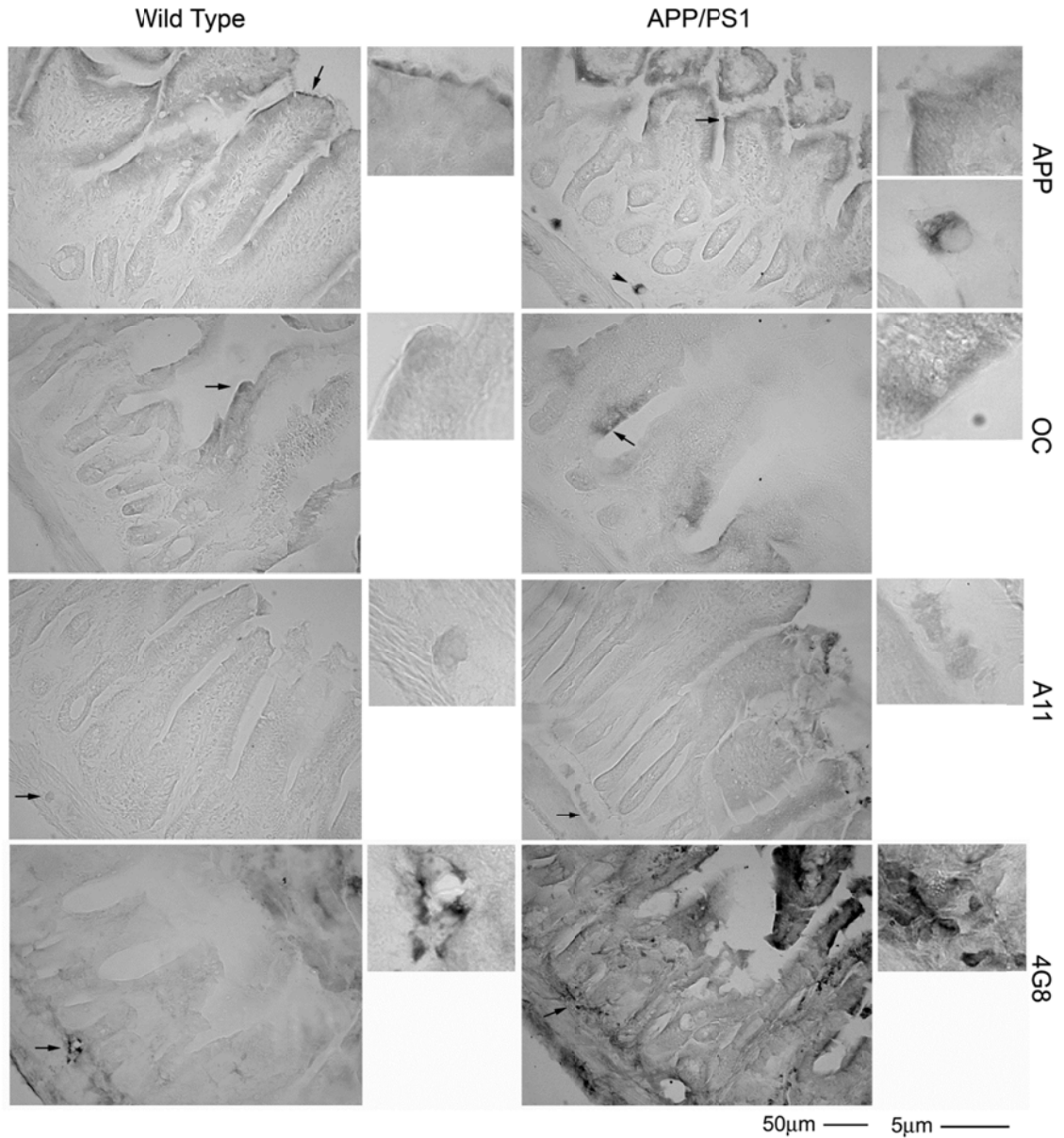


Figure 41. Small intestine immunoreactivity for APP, OC, and 4G8 increased in APP/PS1 mice compared to wild type controls with no change in A11. Ileum tissue samples were collected from C57BL6 wild type and APP/PS1 mice, fixed in 4% paraformaldehyde, serially sectioned, and immunostained. Tissue sections were immunostained using anti-APP, OC, A11, and 4G8 antibodies and antibody binding was visualized using Vector VIP as the chromagen. Arrows indicate the location of immunoreactivity shown as an

enlarged inset to the right of each panel. Representative images from 5 animals per condition are shown.

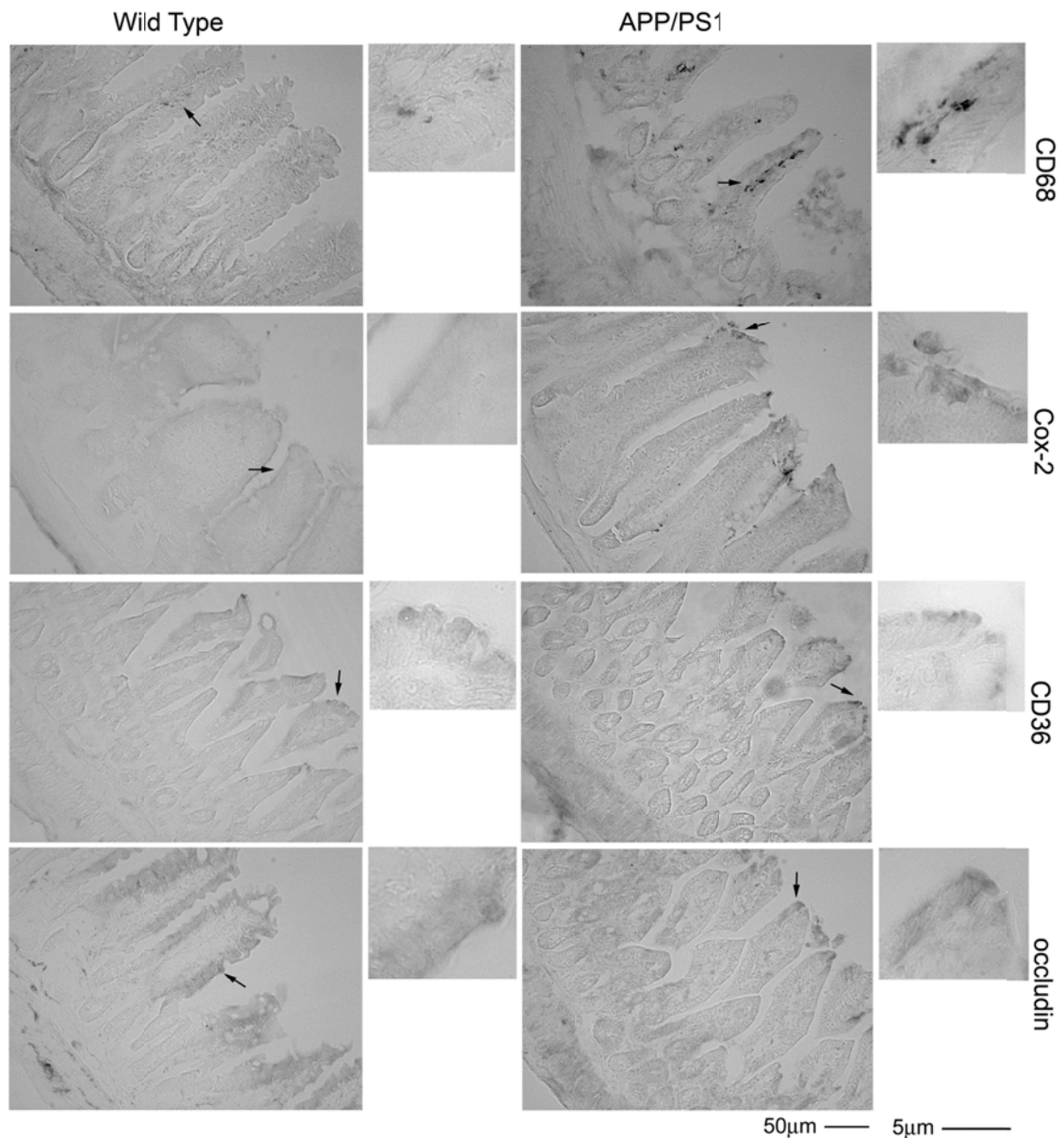


Figure 42. Small intestine immunoreactivity for CD68, Cox-2 and CD36 increased in APP/PS1 mice compared to wild type controls with no change in occludin. Ileum tissue samples were collected from C57BL6 wild type and APP/PS1 mice, fixed in 4% paraformaldehyde, serially sectioned, and

immunostained. Tissue sections were immunostained using anti-CD68, Cox-2, CD36 and occludin antibodies and antibody binding was visualized using Vector VIP as the chromagen. Arrows indicate the location of immunoreactivity shown as an enlarged inset to the right of each panel. Representative images from 5 animals per condition are shown.

Since a portion of the APP immunoreactivity was clearly localized to neurons in APP/PS1 and wild type mice and pre and post-synaptic markers were increased in the mutant animals by Western blot, the tissue was stained with an anti-synaptophysin and anti-microtubule associated protein 2 (MAP2) antibodies to better visualize the integrity of the enteric plexi in the intestines. However, wild type and APP/PS1 mouse sections demonstrated equally robust immunoreactivity throughout the submucosa and lamina propria (Figure 43). To determine whether cell-selective changes in tyrosine kinase-mediated signaling would localize to immune cells, the ileum was stained with anti-pTyr and pSrc antibodies. However, consistent with the Western blot analysis, there were no obvious differences in immunoreactivity intensity and staining appeared to localize primarily to enterocytes rather than immune cells (Figure 43).

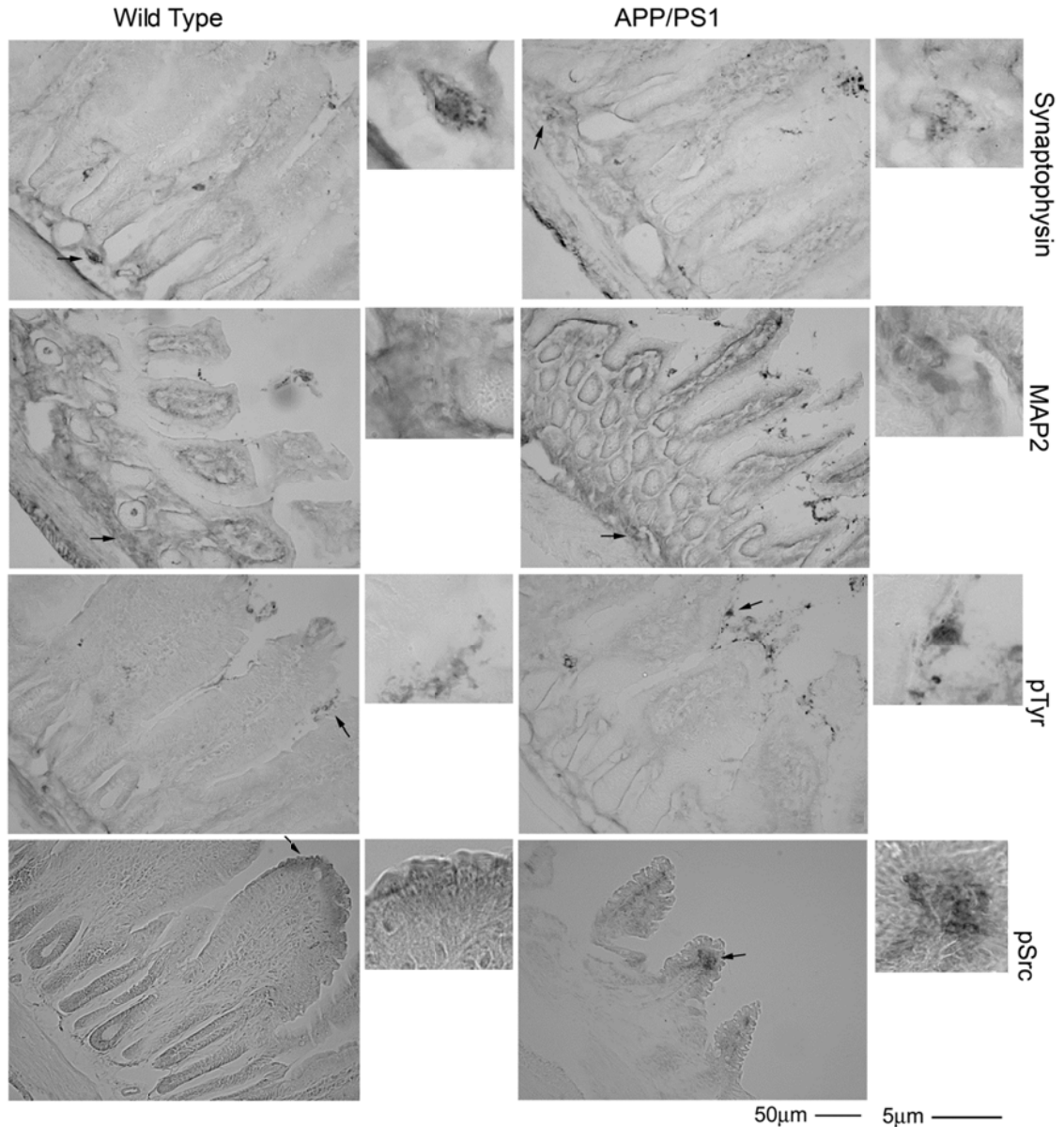


Figure 43. Small intestine immunoreactivity for synaptophysin and MAP2 increased in APP/PS1 mice compared to wild type controls with no change in pTyr and pSrc. Ileum tissue samples were collected from C57BL6 wild type and APP/PS1 mice, fixed in 4% paraformaldehyde, serially sectioned, and immunostained. Tissue sections were immunostained using anti-synaptophysin, MAP2, pTyr and pSrc antibodies and antibody binding was visualized using Vector VIP as the chromagen. Arrows indicate the location of immunoreactivity

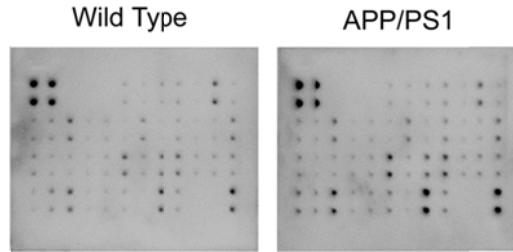
shown as an enlarged inset to the right of each panel. Representative images from 5 animals per condition are shown.

No differences in intestinal motility but increased cytokine and IgA levels were observed in APP/PS1 versus wild type mice

Based upon the increased Cox-2 and CD68 and CD3 levels as well as increased CD68 immunoreactive macrophage in the APP/PS1 ileums, it was reasonable to expect that levels of cytokines in the APP/PS1 versus wild type ileums would also differ. To examine this possibility, ileums were collected from 13 month old animals and used to perform antibody-based cytokine arrays profiling 40 different cytokines. As expected, the APP/PS1 ileums demonstrated significantly increased levels of 6 different factors, IL-12p70, LIX, MCP-1, MCSF, SDF-1, and TIMP-1 compared to wild type mice (Figure 44). These findings were consistent with the immunohistochemistry and protein expression changes suggesting proinflammatory and immune changes and further supported the notion that mutant APP/PS1 expression regulates immune cell phenotype in the intestine.

A combined change in levels of multiple cytokines, proinflammatory and regulatory proteins, and numbers of macrophages, suggested that the function of APP/PS1 intestines may differ significantly compared to wild type control animals. In order to address intestinal function, mean stool production and water content were compared between the genotypes. Although this was not exclusively an assessment of small intestine behavior, APP/PS1 animals did not generate any difference in stool or water content (Figure 45A).

Even though an overall difference in stool or water content was not seen in the APP/PS1 mice compared to controls, the changes observed thus far were actually more indicative of immune dysfunction. Therefore, luminal intestinal content was compared between genotypes using a commercially available IgA ELISA. There was increased IgA secretion in the APP/PS1 intestinal lumen compared to the wild type mice again supporting the notion that immune dysfunction characterized the mutant mice (Figure 45B).



	Wild Type	APP/PS1
BLC	1.00±0.12	1.08±0.15
CD30L	0.87±0.08	0.88±0.03
Eotaxin	0.98±0.12	1.01±0.07
Eotaxin-2	1.10±0.13	1.14±0.08
Fas Ligand	0.83±0.08	0.84±0.05
Fractalkine	0.92±0.09	0.94±0.11
GCSF	0.73±0.06	0.83±0.29
GM-CSF	1.02±0.08	1.01±0.05
IFN gamma	0.93±0.05	0.94±0.05
IL-1 alpha	1.23±0.27	1.35±0.07
IL-1 beta	0.92±0.19	0.82±0.05
IL-10	0.80±0.06	0.78±0.04
IL-12p40p70	0.87±0.11	0.94±0.15
IL-12p70	1.11±0.19	1.30±0.22*
IL-13	1.04±0.15	1.03±0.06
IL-17	0.86±0.08	0.85±0.04
IL-2	0.84±0.06	0.86±0.06
IL-3	0.79±0.03	0.81±0.04
IL-4	1.10±0.26	1.24±0.07
IL-6	0.77±0.13	0.87±0.27
IL-9	0.95±0.13	0.89±0.03
I-TAC	0.85±0.06	0.87±0.04
KC	0.80±0.21	0.83±0.19
Leptin	0.83±0.03	0.89±0.08
LIX	1.05±0.06	1.14±0.06*
Lymphotactin	0.87±0.08	0.94±0.06
MCP-1	0.78±0.06	0.91±0.17*
MCSF	1.30±0.16	1.49±0.07*
MIG	0.83±0.05	0.85±0.04
MIP-1alpha	0.92±0.07	0.94±0.09
MIP-1gamma	0.96±0.06	1.03±0.14
RANTES	0.90±0.17	0.94±0.07
SDF-1	0.99±0.04	1.12±0.09*
sTNFR1	1.09±0.13	1.10±0.14
sTNFR2	1.08±0.13	1.19±0.16
TCA-3	1.12±0.07	1.19±0.05
TECK	0.88±0.11	0.95±0.08
TIMP-1	0.80±0.04	0.87±0.05*
TIMP-2	0.85±0.05	0.89±0.06
TNF alpha	0.79±0.07	0.79±0.05

Figure 44. Small intestine of APP/PS1 mice demonstrated altered levels of multiple cytokines compared wild type controls. Ileum from C57BL6 wild type

and APP/PS1 mice were collected, lysed, and used in an antibody cytokine array. APP/PS1 mice demonstrated increased IL-12p70, LIX, MCP-1, MCSF, SDF-1, and TIMP-1 compared to wild type mice. A representative array for one animal from each genotype is shown. Optical densities of normalized dot intensities from 5 animals in each group are displayed as mean (\pm SD). * $P < 0.05$

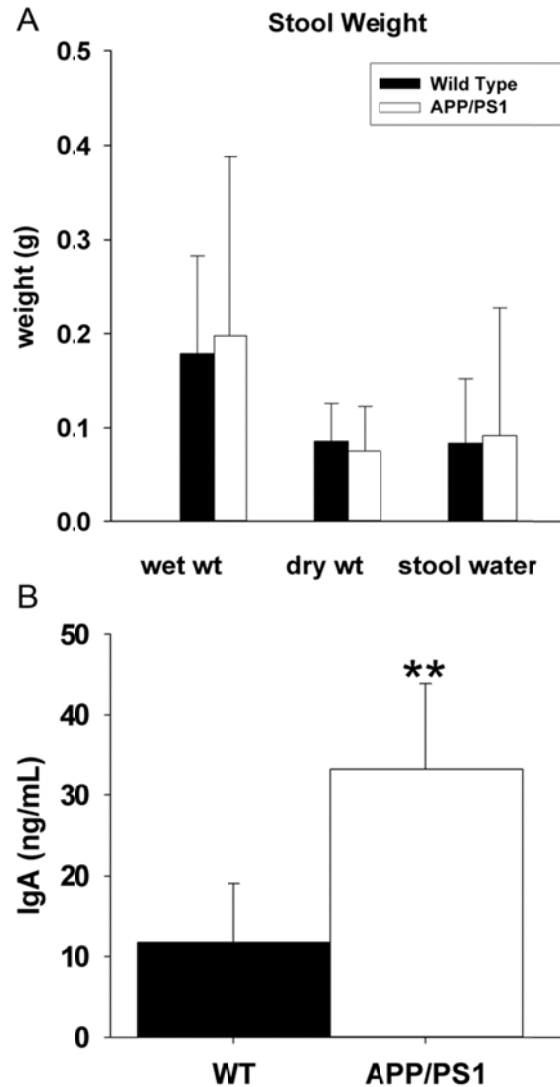


Figure 45. APP/PS1 mice demonstrated no difference in intestinal motility and absorption compared to wild type mice, but have increased IgA in intestinal lumen compared to wild type mice. To compare intestinal

absorption and motility, water and stool production were quantified from C57BL6 wild type and APP/PS1 mice. To assess stool production and water absorption, wet and dry stool weights and the differences (water content) were collected over 1hr. Data from 5 animals in each group are displayed as mean (+/-SD). Small intestine was washed with 7mL of HBSS to remove intestinal contents. Samples were diluted 1:5000 and 300uL of sample was added to the Elisa plate. Data from 7 animals in each condition are displayed as mean (+/-SD). **P<0.01

Human intestinal epithelial cells secrete, take up, and respond to A β

The 4G8 immunoreactivity observed in the APP/PS1 intestine suggested that cells were making and secreting A β perhaps as the source of macrophage activation and immune changes. Neuronal secretion of A β has been well described so we focused instead on the possibility that the enterocyte immunoreactivity for APP indicated that these cells could also be secreting A β peptide. To examine this possibility, we cultured the human enterocyte cell line, Caco-2, and stimulated them with and without a luminal relevant ligand, the bacterial endotoxin, lipopolysaccharide (LPS). Caco-2 cells secreted both A β 1-40 and A β 1-42, with higher quantifiable amounts of A β 1-40 compared to A β 1-42 upon stimulation with LPS (Figure 46A). Since A β 1-40 was the more abundantly secreted form of the peptide, we examined the possibility that enterocytes could be stimulated in an autocrine fashion in response to the peptide. To begin examining this, Caco-2 cells were incubated with fluorescently labeled A β 1-40 again in the absence or presence of the luminal ligand, LPS.

Caco-2 cells could, in fact, take up A β peptide although this was not affected by the presence of LPS (Figure 46B).

To determine whether the A β interaction altered Caco-2 phenotype in a fashion consistent with the immunohistochemistry and Western findings from mouse ileums, protein changes were examined in cells stimulated with increasing concentrations (100nM, 1 μ M, 5 μ M) of A β 1-40 or LPS. To confirm that our A β and LPS treatments were not causing cell death, cell viability was quantified via an MTT assay (Figure 46C). However, Western blot analysis of cell lysates indicated that neither A β nor LPS altered protein levels of APP, CD36, occluding or pSrc (Figure 46D and 46E). On the other hand, ELISA analysis from media collected from the stimulated cells showed that 1 μ M A β 1-40 increased IL-6 cytokine secretion by the Caco-2 cells (Figure 8F). These results indicate that enterocytes also have the potential to not only make A β but autocrine respond to secreted A β by proinflammatory change.

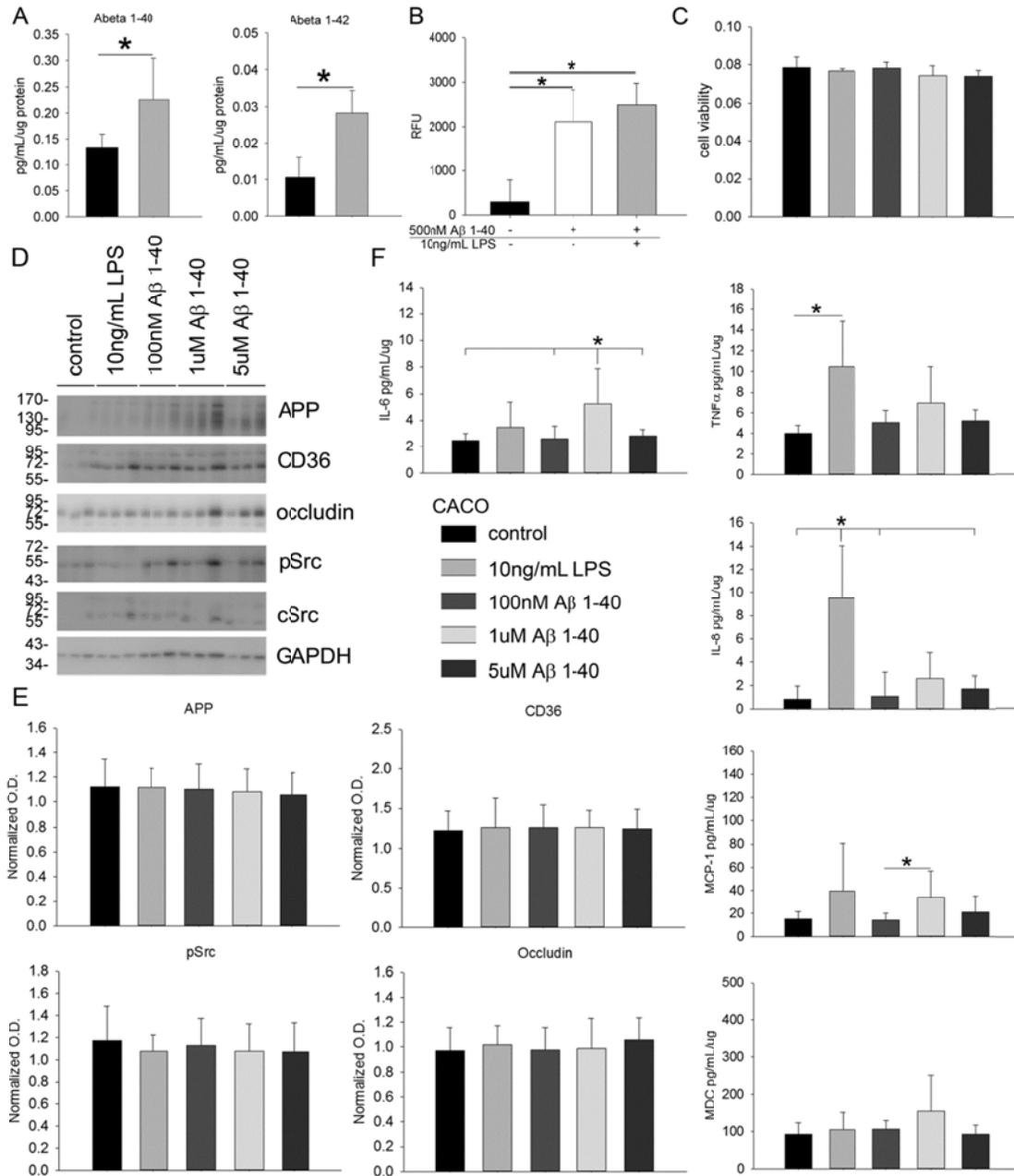


Figure 46. Caco-2 cells produce and uptake A β , but A β and LPS alter cytokine secretion profile with no effect on viability. To demonstrate Caco-2 cells ability to produce A β , Caco-2 cells were stimulated with 10ng/mL LPS and A β secretion was measured via A β 1-40 and A β 1-42 Elisa. To demonstrate Caco-2 cells ability to uptake A β , Caco-2 cells were incubated with or without 500nM A β 1-40 and with or without LPS and the fluorescence signal were

measured with a fluorescent plate reader (480 nm excitation and 520 nm emission). Caco-2 cells were treated overnight and then assessed via MTT assay to assess viability. Data are from 3 experiments in a replicate of 8 displayed as mean (+/-SD). *P<0.05. To assess protein expression Caco-2 cells were stimulated and then lysed for Western blotting. To demonstrate treatment effects on cytokine secretion cells were treated overnight and media was analyzed via IL-8, MCP-1, MDC, IL-6 and TNF α Elisas. Data are from 6 samples in each condition and are displayed as mean (+/-SD). *P<0.05.

CHAPTER VII

DISCUSSION

This work provides a novel data set demonstrating that APP expression has a dramatic regulatory effect on a variety of cell types beyond neurons. Our paradigm focused on high fat diet dependent changes in cells in the brains and adipose tissue primarily with a focus on macrophage and microglia. Consistent with our hypothesis, APP clearly regulates microglial and macrophage phenotype in a tissue specific fashion working directly as a receptor as well as providing a source of stimuli to these cells in the form of A β peptides. The myriad effects on these cells ranged from not only alteration of their secretory profile but also differences in their migratory ability, proliferation rate, and phagocytic ability. This is entirely consistent with our prior work and supports the idea that APP is a proinflammatory receptor that is involved in modulating tissue macrophage phenotypes in any number of conditions or diseases. Future work will determine in a cell-specific fashion precisely which conditions require a role for APP or A β effects on macrophage. This could lead to a role to a currently underappreciated role for APP in numerous immune dysfunction conditions providing a potential new target for intervention.

An additional and unexpected outcome from the study was the finding that numerous changes in lipid metabolism associated proteins were altered in not

only isolated cells but also tissue from APP^{-/-} animals both on control and high fat diets. This was supported by the fact that APP^{-/-} mice, unlike their wild type counterparts, were unable to increase APP levels in adipose tissue and brain and had attenuated adipocyte hypertrophy and weight gain when fed high fat diets. This data set not only demonstrated that high fat diet induced early Alzheimer's disease-like changes in the brain but also adipose tissue. This suggests that adipose tissue changes might parallel and serve as a surrogate tissue for monitoring brain changes with disease. Perhaps even more importantly, these data demonstrated that APP expression is required for high fat diet dependent weight gain and adipose tissue hypertrophy. This is the first demonstration, to our knowledge, of data clearly linking APP to high fat diet dependent obesity, a major risk factor for Alzheimer's disease. Although the precise mechanism linking loss of APP to the lipid-associated protein and adipose tissue changes is not entirely resolved, it is feasible that the altered inflammatory milieu produced by the APP deficient macrophage in each tissue, brain and adipose, contributes to the changes observed. Alternatively, it may be that APP has a direct and currently unknown role in regulating cellular fatty acid uptake. Although this was not supported by fatty acid uptake and oil red O analysis from APP^{-/-} adipocytes, neurons grown from APP^{-/-} mice clearly had attenuated fatty acid uptake. This was supported by the fact that neurons and not adipocytes had APP associated with the fatty acid uptake protein, CD36. One explanation is simply that cells which express high levels of APP, like neurons, utilize APP as a fatty acid uptake regulatory protein while other cells, like adipocytes, have their altered phenotype

due to loss of stimuli from cytokines or A β in an APP^{-/-} environment. Again, future work will need to determine, apparently in a cell-specific fashion, precisely how, and if, APP regulates fatty acid uptake, storage, or turnover. This also suggests the exciting possibility that APP or stimulation with its metabolites directly regulates lipid metabolism. Again, this supports the abundant data linking midlife obesity with increased risk of Alzheimer's disease. At the very least, the APP changes observed may serve as one of the growing list of bio-markers that identify obesity-related changes.

Our results provide a crucial data set of comparison changes in brain versus adipose tissue that was lacking from earlier studies which have focused on a particular organ. Prior work from human subjects has demonstrated increased adipose tissue APP and plasma A β levels in obese subjects (Balakrishnan et al., 2005, Lee and Pratley, 2007, Lee et al., 2008a, Lee et al., 2009a, Sommer et al., 2009) although comparable brain data was not reported. Similarly, brain but not adipose data from Alzheimer's disease transgenic rodent studies using diet-induced obesity paradigms have indicated that obesity correlates with increased levels of brain A β (Levin-Allerhand et al., 2002, Ho et al., 2004, Kohjima et al., 2010) although not necessarily an increase in full length APP as we observed. Our findings are in greater agreement with those of Thirumanagalakudi and colleagues who found using wild type C57BL6/J mice that a high fat/high cholesterol diet induced increased brain changes in APP, A β , and diverse proinflammatory proteins (Thirumangalakudi et al., 2008) although a related study in C57BL6/J mice reported no change in brain APP or A β levels

(Moroz et al., 2008). To link these diverse data sets we suggest, that based upon our findings, a high fat feeding paradigm producing a diet-induced obesity in animals expressing APP under the control of its endogenous promoter is sufficient to increase APP expression in both adipose and brain tissue simultaneous with similar proinflammatory changes that occur in each tissue.

It is not clear what the exact stimulus is to increase APP levels in the cell types in our paradigm although we speculate that proinflammatory stimuli are responsible. It is well established that obesity correlates with a host of increased circulating proinflammatory molecules (van Dielen et al., 2001, Poitou et al., 2006, Antuna-Puente et al., 2008, Fain, 2010) released by both adipocytes and adipose macrophage (Fain, 2006, 2010, Fain et al., 2010). Prior work from the 3T3-L1 adipocyte cell line has demonstrated that stimulation with TNF- α is sufficient to increase APP expression (Sommer et al., 2009). We (Sondag and Combs, 2004a, 2006b, 2010a) as well as others (Schmechel et al., 1988, Bauer et al., 1991, Haass et al., 1991, Banati et al., 1993, Banati et al., 1994a, Banati et al., 1994b, Monning et al., 1994, Banati et al., 1995a, Banati et al., 1995b, Gehrmann et al., 1995a, Gehrmann et al., 1995b, Monning et al., 1995) have demonstrated that APP expression and plasmalemmal localization in monocytic lineage cells, including macrophage and microglia, increases during proinflammatory or degenerative conditions. Finally, neurons themselves have a well-established ability to increase APP expression during diverse degenerative and inflammatory stimulations (Blume and Vitek, 1989, Forloni et al., 1992, Hung

et al., 1992, Willoughby et al., 1992, Ohyagi and Tabira, 1993, Smith et al., 1993, Sola et al., 1993).

It is important to point out that the focus of this work was on the particular cellular changes in full-length APP rather than assessment of APP processing to A β . However, we did assess potential A β generation and deposition in both brain and visceral and subcutaneous adipose tissue via immunostaining. Although the mouse A β -specific antibody detected no robust changes in either tissue from control or high-fat diet fed mice it is possible that A β production was increased in parallel with the increased APP protein levels observed in high fat diet-fed mice but was simply not detectable via immunostaining. We have not ruled out the possibility that a longer feeding paradigm and more sensitive detection method such as an A β ELISA might demonstrate a significant difference in APP processing to increased levels of A β between diets.

Indeed, prior work has already demonstrated that high fat/cholesterol feeding increases A β levels in the murine brain (Thirumangalakudi et al., 2008). This indicates, perhaps not surprisingly, that although APP levels were increased in brain and adipose tissue, its processing and perhaps function(s) is unique based upon cell type expression and requires future study. Regardless of what cell type is potentially producing the A β in brain and adipose tissue, the peptide in either its oligomeric or fibrillar form has been shown in numerous studies to be a potent stimulus for activating microglia and monocyte/macrophage cells to acquire a reactive phenotype (Meda et al., 1995, Bitting et al., 1996, Lorton et al., 1996, Combs et al., 1999, Lorton et al., 2000, Lue et al., 2001, Wu et al., 2004,

Sondag et al., 2009). Again, although processing of APP to A β was not the focus of this work, it is intriguing to consider that in addition to proinflammatory stimuli potentially driving increased APP expression, increased A β production may act in a feed-forward fashion to increase proinflammatory secretions in brain and adipose tissue by directly stimulating microglia and macrophage/adipocytes, respectively. Indeed, our data demonstrated that A β was a potent activating stimulus to these cells. These data support the idea that limiting inflammatory changes during diet induced weight gain may not only attenuate pathologic events in peripheral organs but also those in the brain. In fact, the use of non-steroidal anti-inflammatory drugs during mid-life, in particular, may offer some protective benefit against developing AD (Hayden et al., 2007).

Although our study has focused specifically on changes related to diet induced obesity it is difficult not to speculate that the changes observed may be directly relevant to the mechanism of Alzheimer's disease. As already mentioned, mid-life obesity is a well-recognized increased risk factor for developing AD (Kivipelto et al., 2005, Whitmer, 2007, Beydoun et al., 2008, Profenno and Faraone, 2008, Fitzpatrick et al., 2009, Profenno et al., 2010) and several rodent studies using transgenic mouse models of AD have demonstrated that diet-induced obesity paradigms increase A β levels in the brain (Levin-Allerhand et al., 2002, Ho et al., 2004, Kohjima et al., 2010). More importantly, caloric restriction of these transgenic models is sufficient to decrease brain A β levels and plaque load (Wang et al., 2005a). It was particularly interesting that microglia isolated from high fat diet fed mice basally secreted elevated levels of TNF α compared to

microglia from control diet fed mice. The ability to isolate these cells acutely from adult mouse brains without the confound of prolonged *in vitro* culturing in serum containing conditions allows us to quantify with confidence the basal microglial secretory phenotype in the brain during either diet paradigm. The elevated proinflammatory state suggested by the glia was supported by elevated levels of total prostaglandins in the high-fat diet fed mice. Although we did observe dramatic effects of APP stimulation on neuronal phenotype in this study it is interesting to speculate that APP-dependent stimulation of neurons may lead directly to increased neuronal prostaglandin production as well as generation of A β that may be direct stimuli for the increased microglial TNF α secretion that occurred in high-fat diet fed brains. This APP-dependent mechanism linking generation of these proinflammatory mediators with gliosis would certainly be reasonable to consider during similar degeneration events in AD.

Perhaps even more interesting is the possibility that APP dependent proinflammatory events contribute to the classic inflammatory changes commonly observed in peripheral adipose tissue during diet-induced obesity. For instance, based upon the increased APP levels observed in macrophage and adipocytes, we examined a role for APP in regulating the phenotype of these cells. Although we were unable to determine any phenotype change in adipocyte downstream of APP stimulation, they were stimulated by A β . In addition, macrophage exhibited a significant increase in secretion of three particular cytokines out of the 40 analyzed that may be relevant to adipose changes observed during high fat diet feeding. APP stimulation increased macrophage

secretion of GM-CSF, IFN γ , and IL-13. GM-CSF has a well characterized role in regulating infiltration of macrophage into adipose tissue (Kim et al., 2008). An APP-dependent increase in GM-CSF secretion would certainly help to explain some of the observed increased in reactive macrophage in the high fat diet adipose tissue. IFN γ has an increasingly apparent role in regulating not only adipocyte cytokine secretion including TNF α but also insulin resistance and infiltration of T cells into obese adipose tissue (Rocha et al., 2008, McGillicuddy et al., 2009, O'Rourke et al., 2009). Elevated IL-13 expression is a hallmark of recently defined alternative M2 phenotype macrophage in obese adipose tissue (Shaul et al.). Although APP stimulation did not alter adipocyte phenotype in our hands, A β stimulation did, and a more extensive assessment would likely identify APP and A β dependent changes in adipocytes relevant to obesity.

One interesting possibility is that an APP-APP dependent interaction between adipocytes and macrophage is involved in activating both cell types. That is, APP on macrophage may interact with APP on adipocytes in a complex trans APP-APP interaction as APP can act as a receptor for monocytic lineage cells (Sondag and Combs, 2004a). It is known that although adipocytes are quite capable of secreting a range of inflammatory molecules (Meijer et al.) that macrophage-adipocyte interaction can potentiate inflammatory changes that can occur during obesity and metabolic disorder (Nakarai et al.). Determination of specific roles for APP in macrophage and adipocyte changes during high fat diet feeding might be addressed in future work through the use of cell selective APP

knockout mice or cells selective expression of mutant forms of APP such as those associated with AD.

As already suggested, an interesting speculation is that if APP and/or A β levels increase in adipose tissue during obesity and AD and coordinated expression is tightly regulated between brain and fat then it is not unreasonable to predict that monitoring APP expression and metabolism in adipose tissue could serve as a surrogate for brain with regard to assessing efficacy of particular drug interventions or monitoring disease pathophysiology of obesity or AD. For instance, it is possible that a portion of any generated A β in adipose tissue could accumulate as amyloid deposits in either obese or AD individuals. It is well established that adipose tissue can accumulate amyloid proteins, for example, in individuals with rheumatoid arthritis which is often assessed via needle biopsy (Barile et al., 1993, Gomez-Casanovas et al., 2001).

Our study of intestines was an effort to address another tissue type in which fatty acid uptake and immune cell activation were a critical part of normal or pathological change during many conditions. As expected, lack of APP again resulted in numerous changes in the behavior of macrophages in the small intestine resulting in specific cellular dysfunction in the form of altered cytokine profiles, motility, and absorption.

Consistent with the idea that APP broadly regulates macrophage lineage cell phenotypes, our findings demonstrated that APP expression has profound regulatory effects on protein expression in a range of small intestine cells including neurons, CD68 positive macrophages, and enterocyte epithelial cells.

This represents, to the best of our knowledge, the first demonstration of a function for this protein in this manner.. Based upon the quantified differences in multiple cytokine expression levels as well as changes in intestinal motility and absorption it appears that APP has a role in gastrointestinal function as well.

It is important to point out, just like in the adipose tissue, that it is not clear whether lack of APP on one or multiple cell types is responsible for the changes in cytokine profile, enterocyte protein expression or motility and absorption observed. Also, in spite of the robust changes in macrophage behavior and cytokine levels in APP^{-/-} versus wild type mice, little detectable APP immunoreactivity was observed in macrophage-like cells in ileums of wild type mice. Based upon prior evidence of clear APP expression in monocytic lineage cells (Bauer et al., 1991, Bullido et al., 1996, Sondag and Combs, 2004b, Vehmas et al., 2004, Sondag and Combs, 2006a, 2010b, Spitzer et al., 2010) it is likely that the level of expression of APP in macrophages was simply not high enough to be detectable by the immunostaining procedure employed. Indeed, prior work from others has demonstrated in microglia that APP expression is upregulated when the cells are provided the appropriate stimulatory environment (Haass et al., 1991, Banati et al., 1994a, Monning et al., 1994, Banati et al., 1995a, Banati et al., 1995b, Gehrman et al., 1995a, Gehrman et al., 1995b, Monning et al., 1995, Bullido et al., 1996, Vehmas et al., 2004, Itoh et al., 2009). In this fashion, it is likely that APP expression still directly regulates macrophage phenotype in the intestine in spite of the limitations in detection using the visible light chromagen method. One intriguing hypothesis is simply that macrophage

numbers are limited due to impaired ability of APP^{-/-} cells to migrate into the submucosa and lamina propria. For instance, our prior work demonstrated that APP expression is required on both monocytes and endothelial cells for cell-cell interaction to occur necessary for monocytic adhesion required for activities such as diapedesis through the vasculature (Austin et al., 2009, Austin and Combs, 2010). It is possible that APP^{-/-} macrophages are limited in the intestine due to decreased influx through the vasculature. The impaired migratory ability of APP^{-/-} macrophages supports this notion.

On the other hand, it is also quite possible that APP and its proteolytic metabolites expressed on other cells, such as neurons or enterocytes are normally responsible for some level of CD68 positive macrophage numbers in the intestine. The robust detection of APP immunoreactivity that localized to enterocytes and neurons is entirely consistent with the fact that neurons particularly in the brain express large amounts of APP compared to other tissue types (Schmechel et al., 1988, Yamada et al., 1989, LeBlanc et al., 1991) and prior expression of at least the A β peptide, has been detected in rodent enterocytes (Galloway et al., 2007, Galloway et al., 2008, Galloway et al., 2009, Pallegage-Gamarallage et al., 2009). This suggests that lack of APP metabolites from neurons or enterocytes may lead to diminished stimulation of intestinal macrophages. Indeed, we as well as others have demonstrated in a plethora of studies that different multimeric forms of A β peptide or other APP fragments can directly stimulate immune cells such as monocytes, macrophages, and microglia to alter their phenotype (Klegeris et al., 1994, Yan et al., 1998, Combs et al.,

1999, Yates et al., 2000, Smits et al., 2001, Yazawa et al., 2001, Ikezu et al., 2003, Uryu et al., 2003, Xiong et al., 2004, Floden and Combs, 2006, Sondag et al., 2009, Maezawa et al., 2010). In this scenario, limited CD68 immunoreactivity in the APP^{-/-} intestine could be a consequence of not only loss of macrophage APP function but also loss of APP metabolite-stimulated signaling of macrophages by neurons or enterocytes.

Indeed, a lack of APP-dependent activation of immune cells or a lack of A β -dependent stimulation of immune cells in the ileum could possibly explain not only the decrease in CD68 protein levels but also other immune cells as well as the dramatic decrease in multiple cytokines in APP^{-/-} intestines. This scenario suggests that perhaps APP or its metabolites offer some sort of basal or inducible stimulatory signal to help regulate gut function. However, as the premise of the current study was to first document a novel change in intestinal immune phenotype in APP^{-/-} animals, further mechanistic dissection of the precise reason for changes in immune cell numbers or activation states remains a future goal. In fact, assessing changes in intestinal immune cell behavior as a consequence of APP expression and metabolism might be best addressed in the context of including animals that over-express human mutant APP characteristic of AD as we have done with the APP/PS1 data in this study. Provided that expression of the transgene occurs in the relevant cell types in the intestine, models such as these might offer insight into consequences of over-expression of APP or elevated A β levels on gut function and immune phenotype. More importantly, this might offer insight into consequences of mutant APP expression

in the gut as it relates to AD. It has already been demonstrated that A β immunoreactive plaques accumulate in the intestines of AD patients (Joachim et al., 1989) although evidence of enteric neuron loss is not established (Shankle et al., 1993, Van Ginneken et al., 2010). A role for APP or its proteolytic products in intestine function would provide not only insight into the immunoregulatory role of APP and its metabolites but also begin characterization of disease-relevant changes in a tissue other than the brain.

Although the most straightforward clinical application of our data set is to extrapolate to conditions of AD as we have done in which mutant APP has a known role in the biology of disease, it is interesting to speculate that APP may ultimately have a role in modulating immune cell behavior in conditions other than AD. For instance, the changes in CD68 immunoreactivity observed in APP^{-/-} mice combined with the cytokine profile changes suggests that systemic immune changes exist in these animals. We have only examined peritoneal macrophages and intestinal macrophages from the ileum in this study since our prior work has demonstrated a role for APP in monocytic lineage cell behavior (Sondag and Combs, 2004b, 2006a, 2010b). However, unlike the brain, the gut is home to a diverse population of dynamically changing and regulated immune cells that will likely be affected by any alteration of macrophage behavior. Indeed the decreased protein levels of CD40 and CD11c in the ileum suggest that levels or activation state of other immune cells such as B cells and dendritic cells are also altered in the in APP^{-/-} mice.

Furthermore, for simplicity and proof-of-concept we have limited this assessment to the ileum of the small intestine based upon the fact that it contains immune cell infiltrates and a robust enteric nervous system. However, future efforts to generate a comprehensive profile of all immune cell changes not only in the ileum but throughout the digestive tract particularly the large intestine would offer cell and region specific information that could be correlated with plasma and other organ changes in cytokine and immune cell differences in APP^{-/-} versus wild type mice.

The change in Cox-2 protein levels in APP^{-/-} mice certainly supports the idea that APP expression regulates gut function. A host of studies have documented a role for Cox-2 and its prostaglandin products in negatively regulating intestinal motility (Cong et al., 2007, Takechi et al., 2009, Fairbrother et al., 2011, Nylander, 2011, Shi et al., 2011). In addition, Cox-2 activity positively regulates intestine macrophage infiltration in a rodent model of sepsis (Osterberg et al., 2006) perhaps offering an additional mechanism explaining why APP^{-/-} mouse CD68 positive macrophage immunoreactivity was attenuated compared to wild type mice. Therefore the decrease in Cox-2 protein levels observed in the APP^{-/-} mice is entirely consistent with the increased motility and decreased water absorption observed in the collected stool samples. A change in absorptive capacity was further demonstrated by the significantly decreased levels of absorbed LPS in the APP^{-/-} mice. The uptake of bacterial flora-derived LPS into plasma of rodents and humans as a consequence of lipid absorption is a well-characterized phenomenon (Amar et al., 2008, Ghoshal et al., 2009). Although

this is not necessarily the only source for plasma LPS uptake, it correlates well with prior work and suggests that APP^{-/-} intestines may also have impaired lipid absorption. In addition, although we did not detect significant differences in occludin protein levels between genotypes it is quite feasible that the integrity of the gut epithelial barrier is impaired in the APP^{-/-} mice. Further work to provide additional measures of gut motility, barrier integrity, and absorption will better resolve the differences in gut function dependent upon expression of APP.

Another interesting difference between APP^{-/-} and wild type ileums was the decreased staining for MAP2 and the decrease in β III-tubulin protein levels in the APP^{-/-} mice. Based upon the role of the enteric nervous system in regulating absorption, secretion, and motility in the intestine it is feasible that the decrease in β III-tubulin levels reflects a dysfunction of the enteric nervous control of the intestine. Future work examining more refined assessment of intestinal function will offer insight into this question. This may have nothing to do with enterocyte or immune cell function but instead be the consequence of loss of neuronal APP expression. Certainly, prior work examining the brains of APP^{-/-} mice has demonstrated a similar decrease in MAP2 immunoreactivity (Seabrook et al., 1999).

It is important to point out that we compared intestinal and peritoneal macrophages in isolation when examining cytokine secretory phenotypes. Although this analysis clearly demonstrated differences not only between peritoneal and intestinal macrophages, it also verified that intestinal macrophages from APP^{-/-} mice are unique from their wild-type counterparts.

Perhaps the more physiologically relevant comparison was derived from the cytokine array comparison of wild type and APP^{-/-} ileums. This offered a broad screen of multiple cytokine changes that are a reflection of the more physiologically relevant multi-cell environment *in vivo*. Taking into account that the decreased levels of multiple cytokines in APP^{-/-} ileums are still only a snapshot into the dynamic immune changes among multiple cell types that regulate the gut, the array nevertheless does offer an interesting speculative opportunity for hypothesizing how APP may have a role in diverse intestinal conditions. For instance, it has been previously shown that CD30L plays a critical role in controlling inflammatory bowel syndrome in mice by increasing production of T-cells (Sun et al., 2008). Eotaxin mediates colonic eosinophilic inflammation (Waddell et al., 2011) and Fas Ligand has been shown to sequester double negative T cells in the gut epithelium (Hamad, 2010). Fractalkine can regulate increased IL-6 and TNF α release in the intestine (Niess and Adler, 2010) and IL-12 production is increased by T-cells in irritable bowel disease (Uza et al., 2011).

Therefore, since APP^{-/-} mice have decreased levels of these multiple cytokines they may have decreased risk for inflammatory gut disease such as irritable bowel disease which could be investigated further. The decrease in GCSF could explain why APP^{-/-} mice also have decreased dendritic cell marker protein, CD11c, as GCSF is the key factor in differentiating monocytes into dendritic cells (Metcalf, 1985). IL-10, an anti-inflammatory cytokine, may be decreased due to the decrease in T-cell and macrophage expression as IL-10

has been shown to be a potent suppressor of macrophages and T-cells functions *in vitro* (Kuhn et al., 1993). MIP-1 γ may also be decreased due to the decrease in macrophage and dendritic cell numbers or activation as it is constitutively expressed in these cells (Mohamadzadeh et al., 1996, Haddad and Belosevic, 2009). IL-9 has been shown to promote IL-13 up-regulation of innate immune receptors (Steenwinckel et al., 2009). Therefore the decrease in both IL-9 and IL-13 observed is probably protective in these APP^{-/-} mice as IL-13 has been shown to exert detrimental effects on epithelial barrier function by increasing epithelial cell apoptosis, derangement of tight junction integrity and acts as a key effector cytokine in ulcerative colitis (Heller et al., 2005). MIG has also been shown to be concomitantly expressed in ulcerative colitis (Egesten et al., 2007). TNF α has been implicated in the pathogenesis of Crohn's disease, and by selectively blocking TNFR1 the severity of TNBS-induced colitis in rats is ameliorated (Yin et al., 2011). Again, the collective decrease in the multiple cytokines suggests that absence of APP attenuates gut inflammatory response perhaps influencing the susceptibility of these mice to gut inflammatory disease.

We have taken some steps to determine consequences of AD mutant APP expression on intestinal function. As this is well described in brain already we intended, as already mentioned, to determine whether similar changes occurred in the intestines. With the understood caveat that APP/PS1 mice are not cell specific expression in any particular intestinal cell, the model provided an initial means of assessing whether the mutant represented a gain, loss, or no effect mutation in the intestine by comparison to the APP^{-/-} mice. Based upon the

dramatic differences in APP^{-/-} vs APP/PS1 intestines observed, we can tentatively conclude that the mutant expression behaves as a gain of function in the digestive tract. We demonstrated that overexpression of APP and possible metabolic cleavage in APP/PS1 mice increases immune cell deposition and regulates the protein expression of intestinal cells. Based upon the quantified increase in multiple cytokine expression levels as well as IgA secretion it again demonstrates that APP has a role in diverse tissue types including the intestine. In addition the expressed cytokine profile from the stimulated Caco-2 cells suggests that A β and LPS alter inflammation in the gut. Our results suggest that mutations in the gene coding for APP or altered processing of APP has effects in other tissues, such as the intestine, in addition or uniquely from any observed in the brain or adipose tissue.

However, contrary to the results seen in our APP^{-/-} mice, our APP/PS1 mice have increased expression of APP as well as BACE in the intestine which is similar to the increase A β expression seen in the temporal cortex of our twelve month old APP/PS1 mice in previous studies of ours as well as others (Aso et al., 2011, Dhawan and Combs, 2012). This is also consistent with that seen in the brain of several sporadic AD studies (Holsinger et al., 2002, Yang et al., 2003, Fukumoto et al., 2004, Cai et al., 2010, Miners et al., 2011), suggesting that BACE expression levels correlate to increased β -amyloid production in the brain (Li et al., 2004). The deposition of A β in the intestines of these APP/PS1 mice is also consistent with the A β immunoreactive plaques reported to accumulate in the intestines of AD patients (Joachim et al., 1989). Once again, this suggests

that APP and its metabolites have disease relevance in tissues other than the brain. Therefore, this increased A β in the intestine may contribute to the increased A β in the brain via β -amyloid's ability to regulate apolipoprotein in the plasma. A β has been shown to colocalizes with chylomicron-apoB in enterocytes (Galloway et al., 2009) as well as in cerebral amyloid plaques (Takechi et al., 2009) which has been correlated to increased plasma A β levels (Takechi et al., 2009).

The prominent inflammatory changes in AD brain (Akiyama, 1994, Eikelenboom et al., 1994, Aisen, 1997, Akiyama et al., 2000, Rogers, 2008) are also evident in our APP/PS1 ileums evidenced by the increase in the inflammatory marker Cox-2, macrophage marker CD68, and the T cell marker CD3. This increase in CD68 immunoreactivity and levels are consistent with the increased reactive microglia numbers that are associated with A β plaque pathology in the AD brain (McGeer et al., 1987, Akiyama and McGeer, 1990, Cras et al., 1990, Styren et al., 1990, Wood and Zinsmeister, 1991, Frautschy et al., 1998, Stalder et al., 1999, Wegiel et al., 2001, Sasaki et al., 2002, Dhawan and Combs, 2012). Increased CD68 positive macrophage could be due to the increase in cox-2. As previously stated, Cox-2 activity positively regulates intestinal macrophage infiltration in a rodent model of sepsis (Osterberg et al., 2006). The increase in T cells seen in the intestine is also consistent with reports from a number of AD patient studies that have shown more T-cells activated in AD patients than age-matched controls both in the periphery and brain (Togo et al., 2002, Town et al., 2005, Li et al., 2009). These data suggest that peripheral

accumulation of immune cells may possibly contribute to the increased immune cells population seen in the AD brain.

Along with Cox-2 there was a significant increase in CD36 levels in spite of no difference in occludin levels which were used as additional markers for assessing intestinal integrity. Active transport (Schulzke et al., 2005) and intestinal barrier integrity (Al-Sadi et al., 2011) have been shown to be regulated by occludin in mice both in knockout and *in vivo* siRNA studies, respectively. However, CD36 is also a critical fatty acid uptake regulatory protein suggesting that these APP/PS1 mice have increased dietary fatty acid and cholesterol uptake necessary for chylomicron formation (Nassir et al., 2007). The possibility of increased chylomicron formation fits very nicely with the increase in A β immunoreactivity we observed. As stated before, A β colocalizes with chylomicron-apoB in enterocytes (Galloway et al., 2009) and may lead to an increase in plasma A β levels.

Another interesting difference between APP/PS1 and wild type ileums was the equally robust staining for MAP2 and synaptophysin, consistent with the significant increase in protein levels of both the pre-synaptic marker, synaptophysin and the post-synaptic marker, PSD95, in the APP/PS1 mice. This is consistent with previous studies that have implicated a role for APP expression in regulating both pre-synaptic and post-synaptic integrity in the central and peripheral nervous system (Seabrook et al., 1999, Yang et al., 2005, Priller et al., 2006, Hoe et al., 2009, Wang et al., 2009, Lee et al., 2010, Weyer et al., 2011). Although differences in synaptic markers could indicate changes in neuron

numbers, hypertrophy, or sprouting responses in the APP/PS1 mice, we have not yet determined whether this occurs. Indeed, prior work in humans and AD mouse models has also not established whether neuron loss occurs in the enteric nervous system (Shankle et al., 1993, Van Ginneken et al., 2010). Since the enteric nervous system regulates absorption, secretion and motility in the intestine and we did not observe dramatic changes in motility or water absorption, it appears that the enteric system of the mice is not compromised at this age by overexpression of mutant APP or its metabolites.

As with lack of APP expression in the intestine (Puig et al., 2012), it is still not clear whether overexpression of APP in one or multiple cell types is responsible for the changes in immune cell number, cytokine profile, enterocytes protein expression, or mucosal secretion observed. Robust immunoreactivity of APP was observed in both enterocytes and neurons and both are clearly capable of metabolizing APP to A β . This suggested that mutant APP in either cell type might be responsible for all the changes observed. Because little detectable APP immunoreactivity was observed in macrophage in ileums of APP/PS1 and wild type mice, intestinal macrophage may be increased in the APP/PS1 mice due to increased migratory ability of peripheral macrophage. Our prior work demonstrated that monocytic adhesion and diapedesis through the vasculature requires APP expression on both monocytes and endothelial cells (Austin et al., 2009, Austin and Combs, 2010). Therefore, although we have not examined it, elevated APP expression on endothelial cells may facilitate increased recruitment of macrophage into the intestine. On the other hand, the numbers of overall

macrophage in the intestine may not be increased in the APP/PS1 mice but instead simply have increased reactivity. We, as well as numerous other groups, have demonstrated that different multimeric forms of A β peptide or other APP fragments can directly stimulate immune cells and alter their phenotype (Klegeris et al., 1994, Yan et al., 1998, Combs et al., 1999, Yates et al., 2000, Smits et al., 2001, Yazawa et al., 2001, Ikezu et al., 2003, Uryu et al., 2003, Xiong et al., 2004, Sondag et al., 2009, Maezawa et al., 2010). In addition, we have observed that A β can be taken up by, secreted by, and stimulates enterocyte Caco-2 cells. This APP metabolite-stimulated signaling of macrophages leading to elevated CD68 and even CD3 immunoreactivity could result from neuron or enterocyte secreted products and explain the increase in multiple cytokines in the APP/PS1 intestine.

Indeed, the diverse cytokine changes observed in the APP/PS1 intestine provides insight into the dynamic immune changes that occur in regulating the gut due to the presence of multiple cell types. For instance, in irritable bowel disease IL-12 production is increased by T-cells (Uza et al., 2011). LIX, also known as epithelial-derived neutrophil-activating peptide 78 (ENA-78), expression is increased in mice with dextran sodium sulfate induced colitis (Kwon et al., 2005) and also has been shown to play an important role in neutrophil recruitment from the lamina propria into the epithelial layer of the intestine (Keates et al., 1997). In general, monocyte chemoattractant protein-1 (MCP-1) plays an important role in recruitment of monocytes and macrophages to inflamed tissues (Yoshimura and Leonard, 1992). Macrophage-colony stimulating

factor (MCSF) influences monocyte/macrophage proliferation, differentiation, activation and is increased in inflammatory bowel disease (IBD) (Klebl et al., 2001). Both the increase in MCP-1 and MCSF are consistent with the increased CD68 immunoreactivity in these APP/PS1 mice. Stromal cell-derived factor-1 (SDF-1) also known as CXCL12 is also increased in IBD (Dotan et al., 2010), and tissue inhibitor of metalloproteinases 1 (TIMP-1) is increased in IBD (Naito and Yoshikawa, 2005), especially in ulcerative colitis (Wiercinska-Drapalo et al., 2003, Wang and Yan, 2006). The collective increase in cytokines associated with IBD suggests that the increase in APP, and its metabolite A β , may increase the susceptibility of these mice to gut inflammatory disease and once again supports our hypothesis that APP has a key role in modulating immune cell behavior in conditions other than AD.

We ultimately expect that a number of conditions involving immune cell behavior in the gut, such as irritable bowel syndrome and Crohn's disease, may well be altered in the absence of APP expression. Moreover, a role for APP in regulating immune responses may extend well beyond the gut to include conditions of immune dysfunction as varied as asthma and respiratory allergies since immune cells within the gastrointestinal system are not confined to this organ system but are free to migrate throughout the body. Future work to identify the extent of various immune cell phenotype changes dependent upon specific functions of APP or its metabolites will validate the role of this protein not only during normal physiology but a variety of diseases.

The structure and processing of APP is well described even though the function of the full length protein and its many metabolites remains unclear. This is compounded by the fact that the biology of this protein may be different depending upon the cell type or tissue involved. Indeed the bulk of our findings in this study as well as our prior work demonstrating that microglia and not neurons or astrocytes initiate a tyrosine kinase-dependent signaling response downstream of APP activation support this idea. Defining the function of APP and its proteolytic fragments in a cell-by-cell fashion will likely provide insight into not only Alzheimer's disease but myriad disease conditions such as psoriasis, obesity, gut inflammatory disease, inclusion-body myositis and other diseases of peripheral tissues. In fact, determining the behavior of APP and its products in peripheral cells may, by comparison, better define their normal and disease actions in neurons or within the brain since even this behavior remains unclear. For instance, appreciating the peripheral distribution and processing of APP may define mechanisms for increases in circulating A β levels which could cross the blood-brain-barrier and contribute to brain parenchymal A β load during AD (Mackic et al., 2002). More importantly, there exists the tantalizing possibility that targeting generation or function of APP and its breakdown products might be therapeutically applicable to conditions beyond AD. Perhaps even more intriguing is the fact that mutations in the gene coding for APP are responsible for the autosomal dominant forms of Alzheimer's disease (Goate et al., 1991). Therefore, it is likely not by coincidence then, that obesity is a risk factor for this

Alzheimer's disease (Razay and Vreugdenhil, 2005, Razay et al., 2006, 2007, Profenno and Faraone, 2008, Profenno et al., 2010).

APPENDIX

LIST OF ABBREVIATIONS

22C11	APP Agonist Antibody
4G8	Amyloid Beta Antibody
A11	Oligomer Antibody
AChRs	Acetylcholine Receptors
AD	Alzheimer's Disease
ADAMA	Disintegrin And Metalloprotease
AICD	APP Intracellular Domain
AKT	Protein Kinase B
ANOVA	Analysis of Variance
APH1	Anterior Pharynx-defective 1
apoB	Apolipoprotein B
APOE	Apolipoprotein E
APP	Amyloid Precursor Protein
A β	Amyloid Beta
BACE	Beta-Secretase
BAT	Brown Adipose Tissue
C/EBP	CCAAT-Enhancer-Binding-Protein
CD11c	Integrin, alpha X
CD14	Cluster of Differentiation 14
CD3	Cluster of Differentiation 3
CD36	Cluster of Differentiation 36
CD40	Cluster of Differentiation 40
CD45	Cluster of Differentiation 45
CD68	Cluster of Differentiation 68
CDC	Center for Disease Control
CFABP	Cardiac Fatty Acid-Binding Protein
CNS	Central Nervous System
Cox-2	Cyclooxygenase-2
cSrc	c-Src Tyrosine Kinase
DAPI	4',6-diamidino-2-phenylindole
DHS	Donor Horse Serum
DLK	Preadipocyte factor 1
ELISA	Enzyme-linked Immunosorbent Assay
FABP4	Fatty Acid Binding Protein 4
FAD	Familial Alzheimer's Disease
FAS	<i>Fatty acid synthetase</i>
FAs	Fatty Acids
FATP4	Fatty Acid Transport Protein 4

FBS	Fetal Bovine Serum
GAPDH	Glyceraldehyde 3-Phosphate Dehydrogenase
GFAP	Glial Fibrillary Acidic Protein
GLUT-4	Glucose Transporter Type 4
GM-CSF	Granulocyte-Macrophage Colony Stimulating Factor
H & E	Hemotaxilin and Eosin
HBSS	Hanks Balanced Salt Solution
HDL	High-density lipoprotein
HSL	Hormone-Sensitive Lipase
IBA-1	Ionized Calcium-Binding Adapter Molecule 1
IBM	Inclusion-Body Myositis
IgG ₁	Isotype Control
IL-1	Interleukin-1
IL-10	Interleukin-10
IL-12	Interleukin-12
IL-13	Interleukin-13
IL-1 β	Interleukin-1 β
IL-4	Interleukin-4
IL-6	Interleukin-6
IL-8	Interleukin-8
INF γ	Interferon-gamma
iNOS	inducible Nitric Oxide Synthase
KC	Keratinocyte Chemokine
LDH	Lactate Dehydrogenase
LPL	Lipoprotein Lipase
LPL	Lipoprotein Lipase
LPS	lipopolysaccharide
LRP	Lipoprotein receptor-related proteins
M1	Classically Activated Macrophage
M2	Alternatively Activated Macrophage
MAP2	Microtubule Associated Protein 2
MCP-1	Monocyte Chemoattractant Protein-1
MDC	Macrophage-derived chemokine
MIP-1 α	Macrophage Inflammatory Protein-1alpha
MSCs	Mesenchymal Stem Cells
MTT	3-(4,5-Dimethylthiazol-2-yl)-2,5-diphenyltetrazolium bromide
NMJ	Neuromuscular Junction
OC	Fibril Antibody
pAKT	phospho-Protein Kinase B
PEN2	Presenilin Enhancer 2
PG	Prostaglandin
PHF-1	PHD Finger Protein-1(phospho-tau)
PPAR γ	Peroxisome Proliferator-Activated Receptor Gamma
PSD95	Postsynaptic Density Protein 95
PSEN1	Presenilin 1
PSN	Penicilin Streptomycin Neomycin

pTyr	Phospho-Tyrosine
PVDF	Polyvinylidene Difluoride
RANTES	Regulated upon Activation, Normal T-cell Expressed, and Secreted
SDS-PAGE	Sodium Dodecyl Sulfate-Polyacrylamide Gel Electrophoresis
TLR2	Toll-Like Receptor
TLR4	Toll-Like Receptor 4
TNF α	Tumor Necrosis Factor-alpha
UCP1	Uncoupling Protein 1
VLDLR	Very-Low-Density-Lipoprotein Receptor
WAT	White Adipose Tissue

REFERENCES

- Aisen PS (1997) Inflammation and Alzheimer's disease: mechanisms and therapeutic strategies. *Gerontology* 43:143-149.
- Akaaboune M, Allinquant B, Farza H, Roy K, Magoul R, Fiszman M, Festoff BW, Hantai D (2000) Developmental regulation of amyloid precursor protein at the neuromuscular junction in mouse skeletal muscle. *Mol Cell Neurosci* 15:355-367.
- Akiyama H (1994) Inflammatory response in Alzheimer's disease. *Tohoku J Exp Med* 174:295-303.
- Akiyama H, Barger S, Barnum S, Bradt B, Bauer J, Cole GM, Cooper NR, Eikelenboom P, Emmerling M, Fiebich BL, Finch CE, Frautschy S, Griffin WS, Hampel H, Hull M, Landreth G, Lue L, Mrak R, Mackenzie IR, McGeer PL, O'Banion MK, Pachter J, Pasinetti G, Plata-Salaman C, Rogers J, Rydel R, Shen Y, Streit W, Strommeyer R, Tooyoma I, Van Muiswinkel FL, Veerhuis R, Walker D, Webster S, Wegrzyniak B, Wenk G, Wyss-Coray T (2000) Inflammation and Alzheimer's disease. *Neurobiol Aging* 21:383-421.
- Akiyama H, McGeer PL (1990) Brain microglia constitutively express beta-2 integrins. *J Neuroimmunol* 30:81-93.
- Al-Sadi R, Khatib K, Guo S, Ye D, Youssef M, Ma T (2011) Occludin regulates macromolecule flux across the intestinal epithelial tight junction barrier. *Am J Physiol Gastrointest Liver Physiol* 300:G1054-1064.
- Amar J, Burcelin R, Ruidavets JB, Cani PD, Fauvel J, Alessi MC, Chamontin B, Ferrieres J (2008) Energy intake is associated with endotoxemia in apparently healthy men. *Am J Clin Nutr* 87:1219-1223.
- Antuna-Puente B, Fève B, Fellahi S, Bastard JP (2008) Adipokines: the missing link between insulin resistance and obesity. *Diabetes Metab* 34:2-11.
- Arai H, Lee VM, Messinger ML, Greenberg BD, Lowery DE, Trojanowski JQ (1991) Expression patterns of beta-amyloid precursor protein (beta-APP) in neural and nonneural human tissues from Alzheimer's disease and control subjects. *Ann Neurol* 30:686-693.

- Askanas V, Engel WK (2006) Inclusion-body myositis: a myodegenerative conformational disorder associated with Abeta, protein misfolding, and proteasome inhibition. *Neurology* 66:S39-48.
- Aso E, Lomoio S, Lopez-Gonzalez I, Joda L, Carmona M, Fernandez-Yague N, Moreno J, Juves S, Pujol A, Pamplona R, Portero-Otin M, Martin V, Diaz M, Ferrer I (2011) Amyloid generation and dysfunctional immunoproteasome activation with disease progression in animal model of familial Alzheimer disease. *Brain Pathol.*
- Austin SA, Combs CK (2010) Amyloid precursor protein mediates monocyte adhesion in AD tissue and apoE(-)/(-) mice. *Neurobiol Aging* 31:1854-1866.
- Austin SA, Sens MA, Combs CK (2009) Amyloid precursor protein mediates a tyrosine kinase-dependent activation response in endothelial cells. *J Neurosci* 29:14451-14462.
- Bachman ES, Dhillon H, Zhang CY, Cinti S, Bianco AC, Kobilka BK, Lowell BB (2002) betaAR signaling required for diet-induced thermogenesis and obesity resistance. *Science* 297:843-845.
- Balakrishnan K, Verdile G, Mehta PD, Beilby J, Nolan D, Galvao DA, Newton R, Gandy SE, Martins RN (2005) Plasma Abeta42 correlates positively with increased body fat in healthy individuals. *J Alzheimers Dis* 8:269-282.
- Banati RB, Gehrman J, Czech C, Monning U, Jones LL, Konig G, Beyreuther K, Kreutzberg GW (1993) Early and rapid de novo synthesis of Alzheimer beta A4-amyloid precursor protein (APP) in activated microglia. *Glia* 9:199-210.
- Banati RB, Gehrman J, Kreutzberg GW (1994a) Glial beta-amyloid precursor protein: expression in the dentate gyrus after entorhinal cortex lesion. *Neuroreport* 5:1359-1361.
- Banati RB, Gehrman J, Lannes-Vieira J, Wekerle H, Kreutzberg GW (1995a) Inflammatory reaction in experimental autoimmune encephalomyelitis (EAE) is accompanied by a microglial expression of the beta A4-amyloid precursor protein (APP). *Glia* 14:209-215.
- Banati RB, Gehrman J, Monning U, Czech C, Beyreuther K, Kreutzberg GW (1994b) Amyloid precursor protein (APP) as a microglial acute phase protein. *Neuropathol Appl Neurobiol* 20:194-195.

- Banati RB, Gehrmann J, Wiessner C, Hossmann KA, Kreutzberg GW (1995b) Glial expression of the beta-amyloid precursor protein (APP) in global ischemia. *J Cereb Blood Flow Metab* 15:647-654.
- Barile L, Ariza R, Muci H, Pizarro S, Fraga A, Lavalle C, Garcia R, Lescano D, Barrios R, Frati A (1993) Tru-cut needle biopsy of subcutaneous fat in the diagnosis of secondary amyloidosis in rheumatoid arthritis. *Arch Med Res* 24:189-192.
- Bauer J, Konig G, Strauss S, Jonas U, Ganter U, Weidemann A, Monning U, Masters CL, Volk B, Berger M, et al. (1991) In-vitro matured human macrophages express Alzheimer's beta A4-amyloid precursor protein indicating synthesis in microglial cells. *FEBS Lett* 282:335-340.
- Behr D, Hesse L, Masters CL, Multhaup G (1996) Regulation of amyloid protein precursor (APP) binding to collagen and mapping of the binding sites on APP and collagen type I. *J Biol Chem* 271:1613-1620.
- Bendotti C, Forloni GL, Morgan RA, O'Hara BF, Oster-Granite ML, Reeves RH, Gearhart JD, Coyle JT (1988) Neuroanatomical localization and quantification of amyloid precursor protein mRNA by in situ hybridization in the brains of normal, aneuploid, and lesioned mice. *Proceedings of the National Academy of Sciences of the United States of America* 85:3628-3632.
- Berthoud HR, Sutton GM, Townsend RL, Patterson LM, Zheng H (2006) Brainstem mechanisms integrating gut-derived satiety signals and descending forebrain information in the control of meal size. *Physiology & behavior* 89:517-524.
- Beydoun MA, Beydoun HA, Wang Y (2008) Obesity and central obesity as risk factors for incident dementia and its subtypes: a systematic review and meta-analysis. *Obesity Reviews* 9:204-218.
- Beyerlein A, von Kries R, Ness AR, Ong KK (2011) Genetic markers of obesity risk: stronger associations with body composition in overweight compared to normal-weight children. *PLoS One* 6:e19057.
- Bitting L, Naidu A, Cordell B, Murphy GM, Jr. (1996) Beta-amyloid peptide secretion by a microglial cell line is induced by beta-amyloid-(25-35) and lipopolysaccharide. *J Biol Chem* 271:16084-16089.
- Bjorntorp P, Rosmond R (1999) Visceral obesity and diabetes. *Drugs* 58 Suppl 1:13-18; discussion 75-82.

- Blume AJ, Vitek MP (1989) Focusing on IL-1-promotion of beta-amyloid precursor protein synthesis as an early event in Alzheimer's disease. *Neurobiol Aging* 10:406-408; discussion 412-404.
- Borst SE, Conover CF (2005) High-fat diet induces increased tissue expression of TNF-alpha. *Life Sci* 77:2156-2165.
- Botelho MG, Wang X, Arndt-Jovin DJ, Becker D, Jovin TM (2010) Induction of terminal differentiation in melanoma cells on downregulation of beta-amyloid precursor protein. *J Invest Dermatol* 130:1400-1410.
- Bradford MM (1976a) A rapid and sensitive method for the quantitation of microgram quantities of protein utilizing the principle of protein-dye binding. *Analytical Biochemistry* 72:248-254.
- Bradford MM (1976b) A rapid and sensitive method for the quantitation of microgram quantities of protein utilizing the principle of protein-dye binding. *Anal Biochem* 72:248-254.
- Brantley PJ, Myers VH, Roy HJ (2005) Environmental and lifestyle influences on obesity. *J La State Med Soc* 157 Spec No 1:S19-27.
- Bullido MJ, Munoz-Fernandez MA, Recuero M, Fresno M, Valdivieso F (1996) Alzheimer's amyloid precursor protein is expressed on the surface of hematopoietic cells upon activation. *Biochim Biophys Acta* 1313:54-62.
- Burgess AW, Camakaris J, Metcalf D (1977) Purification and properties of colony-stimulating factor from mouse lung-conditioned medium. *J Biol Chem* 252:1998-2003.
- Cai Y, Xiong K, Zhang XM, Cai H, Luo XG, Feng JC, Clough RW, Struble RG, Patrylo PR, Chu Y, Kordower JH, Yan XX (2010) beta-Secretase-1 elevation in aged monkey and Alzheimer's disease human cerebral cortex occurs around the vasculature in partnership with multisystem axon terminal pathogenesis and beta-amyloid accumulation. *Eur J Neurosci* 32:1223-1238.
- Camilleri M, Cowen T, Koch TR (2008) Enteric neurodegeneration in ageing. *Neurogastroenterol Motil* 20:418-429.
- Cannon B, Nedergaard J (2004) Brown adipose tissue: function and physiological significance. *Physiological reviews* 84:277-359.
- Caterson ID, Gill TP (2002) Obesity: epidemiology and possible prevention. *Best Pract Res Clin Endocrinol Metab* 16:595-610.

- Chawla A, Nguyen KD, Goh YP (2011) Macrophage-mediated inflammation in metabolic disease. *Nature reviews Immunology* 11:738-749.
- Choquet H, Meyre D (2010) Genomic insights into early-onset obesity. *Genome Med* 2:36.
- Cinti S (2012) The adipose organ at a glance. *Dis Model Mech* 5:588-594.
- Cinti S, Frederich RC, Zingaretti MC, De Matteis R, Flier JS, Lowell BB (1997) Immunohistochemical localization of leptin and uncoupling protein in white and brown adipose tissue. *Endocrinology* 138:797-804.
- Cirillo C, Sarnelli G, Esposito G, Turco F, Steardo L, Cuomo R (2011) S100B protein in the gut: the evidence for enteroglia-sustained intestinal inflammation. *World J Gastroenterol* 17:1261-1266.
- Coenen KR, Gruen ML, Chait A, Hasty AH (2007) Diet-induced increases in adiposity, but not plasma lipids, promote macrophage infiltration into white adipose tissue. *Diabetes* 56:564-573.
- Combs CK, Johnson DE, Cannady SB, Lehman TM, Landreth GE (1999) Identification of microglial signal transduction pathways mediating a neurotoxic response to amyloidogenic fragments of beta-amyloid and prion proteins. *J Neurosci* 19:928-939.
- Cong P, Pricolo V, Biancani P, Behar J (2007) Abnormalities of prostaglandins and cyclooxygenase enzymes in female patients with slow-transit constipation. *Gastroenterology* 133:445-453.
- Craft S (2005) Insulin resistance syndrome and Alzheimer's disease: age- and obesity-related effects on memory, amyloid, and inflammation. *Neurobiol Aging* 26 Suppl 1:65-69.
- Cras P, Kawai M, Siedlak S, Mulvihill P, Gambetti P, Lowery D, Gonzalez-DeWhitt P, Greenberg B, Perry G (1990) Neuronal and microglial involvement in beta-amyloid protein deposition in Alzheimer's disease. *Am J Pathol* 137:241-246.
- de Haas AH, Boddeke HW, Biber K (2008) Region-specific expression of immunoregulatory proteins on microglia in the healthy CNS. *Glia* 56:888-894.
- Despres JP (2003) Potential contribution of metformin to the management of cardiovascular disease risk in patients with abdominal obesity, the metabolic syndrome and type 2 diabetes. *Diabetes Metab* 29:6S53-61.

- Despres JP (2009) Targeting abdominal obesity and the metabolic syndrome to manage cardiovascular disease risk. *Heart* 95:1118-1124.
- Despres JP, Lemieux I (2006) Abdominal obesity and metabolic syndrome. *Nature* 444:881-887.
- Despres JP, Lemieux I, Bergeron J, Pibarot P, Mathieu P, Larose E, Rodes-Cabau J, Bertrand OF, Poirier P (2008) Abdominal obesity and the metabolic syndrome: contribution to global cardiometabolic risk. *Arterioscler Thromb Vasc Biol* 28:1039-1049.
- Dhawan G, Combs CK (2012) Inhibition of Src kinase activity attenuates amyloid associated microgliosis in a murine model of Alzheimer's disease. *J Neuroinflammation* 9:117.
- Dhawan G, Floden AM, Combs CK (2012) Amyloid-beta oligomers stimulate microglia through a tyrosine kinase dependent mechanism. *Neurobiol Aging* 33:2247-2261.
- Doherty TM, Kastelein R, Menon S, Andrade S, Coffman RL (1993) Modulation of murine macrophage function by IL-13. *J Immunol* 151:7151-7160.
- Dotan I, Werner L, Vigodman S, Weiss S, Brazowski E, Maharshak N, Chen O, Tulchinsky H, Halpern Z, Guzner-Gur H (2010) CXCL12 is a constitutive and inflammatory chemokine in the intestinal immune system. *Inflamm Bowel Dis* 16:583-592.
- Dyrks T, Weidemann A, Multhaup G, Salbaum JM, Lemaire HG, Kang J, Muller-Hill B, Masters CL, Beyreuther K (1988) Identification, transmembrane orientation and biogenesis of the amyloid A4 precursor of Alzheimer's disease. *Embo J* 7:949-957.
- Egesten A, Eliasson M, Olin AI, Erjefalt JS, Bjartell A, Sangfelt P, Carlson M (2007) The proinflammatory CXC-chemokines GRO-alpha/CXCL1 and MIG/CXCL9 are concomitantly expressed in ulcerative colitis and decrease during treatment with topical corticosteroids. *Int J Colorectal Dis* 22:1421-1427.
- Eikelenboom P, Zhan SS, van Gool WA, Allsop D (1994) Inflammatory mechanisms in Alzheimer's disease. *Trends Pharmacol Sci* 15:447-450.
- Eskelinen MH, Ngandu T, Helkala EL, Tuomilehto J, Nissinen A, Soininen H, Kivipelto M (2008) Fat intake at midlife and cognitive impairment later in life: a population-based CAIDE study. *Int J Geriatr Psychiatry* 23:741-747.

- Everhart JE, Ruhl CE (2009a) Burden of digestive diseases in the United States part I: overall and upper gastrointestinal diseases. *Gastroenterology* 136:376-386.
- Everhart JE, Ruhl CE (2009b) Burden of digestive diseases in the United States part II: lower gastrointestinal diseases. *Gastroenterology* 136:741-754.
- Fain JN (2006) Release of interleukins and other inflammatory cytokines by human adipose tissue is enhanced in obesity and primarily due to the nonfat cells. *Vitam Horm* 74:443-477.
- Fain JN (2010) Release of inflammatory mediators by human adipose tissue is enhanced in obesity and primarily by the nonfat cells: a review. *Mediators Inflamm* 2010:513948.
- Fain JN, Tagele BM, Cheema P, Madan AK, Tichansky DS (2010) Release of 12 adipokines by adipose tissue, nonfat cells, and fat cells from obese women. *Obesity (Silver Spring)* 18:890-896.
- Fairbrother SE, Smith JE, Borman RA, Cox HM (2011) Characterization of the EP receptor types that mediate longitudinal smooth muscle contraction of human colon, mouse colon and mouse ileum. *Neurogastroenterol Motil.*
- Farooqi IS (2011) Genetic, molecular and physiological insights into human obesity. *Eur J Clin Invest* 41:451-455.
- Farooqi S, O'Rahilly S (2006) Genetics of obesity in humans. *Endocrine reviews* 27:710-718.
- Fernyhough ME, Vierck JL, Hausman GJ, Mir PS, Okine EK, Dodson MV (2004) Primary adipocyte culture: adipocyte purification methods may lead to a new understanding of adipose tissue growth and development. *Cytotechnology* 46:163-172.
- Fitzpatrick AL, Kuller LH, Lopez OL, Diehr P, O'Meara ES, Longstreth WT, Jr, Luchsinger JA (2009) Midlife and late-life obesity and the risk of dementia: cardiovascular health study. *ArchNeurol* 66:336-342.
- Floden AM, Combs CK (2006) Beta-amyloid stimulates murine postnatal and adult microglia cultures in a unique manner. *J Neurosci* 26:4644-4648.
- Forloni G, Demicheli F, Giorgi S, Bendotti C, Angeretti N (1992) Expression of amyloid precursor protein mRNAs in endothelial, neuronal and glial cells: modulation by interleukin-1. *Brain Res Mol Brain Res* 16:128-134.

- Forti P, Pisacane N, Rietti E, Lucicesare A, Olivelli V, Mariani E, Mecocci P, Ravaglia G (2010) Metabolic syndrome and risk of dementia in older adults. *J Am Geriatr Soc* 58:487-492.
- Frautschy SA, Yang F, Irizarry M, Hyman B, Saido TC, Hsiao K, Cole GM (1998) Microglial response to amyloid plaques in APPsw transgenic mice. *Am J Pathol* 152:307-317.
- Frayling TM, Timpson NJ, Weedon MN, Zeggini E, Freathy RM, Lindgren CM, Perry JR, Elliott KS, Lango H, Rayner NW, Shields B, Harries LW, Barrett JC, Ellard S, Groves CJ, Knight B, Patch AM, Ness AR, Ebrahim S, Lawlor DA, Ring SM, Ben-Shlomo Y, Jarvelin MR, Sovio U, Bennett AJ, Melzer D, Ferrucci L, Loos RJ, Barroso I, Wareham NJ, Karpe F, Owen KR, Cardon LR, Walker M, Hitman GA, Palmer CN, Doney AS, Morris AD, Smith GD, Hattersley AT, McCarthy MI (2007) A common variant in the FTO gene is associated with body mass index and predisposes to childhood and adult obesity. *Science* 316:889-894.
- Frayn KN (2000) Visceral fat and insulin resistance--causative or correlative? *Br J Nutr* 83 Suppl 1:S71-77.
- Frontini A, Rousset S, Cassard-Doulcier AM, Zingaretti C, Ricquier D, Cinti S (2007) Thymus uncoupling protein 1 is exclusive to typical brown adipocytes and is not found in thymocytes. *J Histochem Cytochem* 55:183-189.
- Fukumoto H, Rosene DL, Moss MB, Raju S, Hyman BT, Irizarry MC (2004) Beta-secretase activity increases with aging in human, monkey, and mouse brain. *Am J Pathol* 164:719-725.
- Furukawa K, Barger SW, Blalock EM, Mattson MP (1996a) Activation of K⁺ channels and suppression of neuronal activity by secreted beta-amyloid-precursor protein. *Nature* 379:74-78.
- Furukawa K, Sopher BL, Rydel RE, Begley JG, Pham DG, Martin GM, Fox M, Mattson MP (1996b) Increased activity-regulating and neuroprotective efficacy of alpha-secretase-derived secreted amyloid precursor protein conferred by a C-terminal heparin-binding domain. *J Neurochem* 67:1882-1896.
- Gakhar-Koppole N, Hundeshagen P, Mandl C, Weyer SW, Allinquant B, Muller U, Ciccolini F (2008) Activity requires soluble amyloid precursor protein alpha to promote neurite outgrowth in neural stem cell-derived neurons via activation of the MAPK pathway. *Eur J Neurosci* 28:871-882.

- Galloway S, Jian L, Johnsen R, Chew S, Mamo JC (2007) beta-amyloid or its precursor protein is found in epithelial cells of the small intestine and is stimulated by high-fat feeding. *J Nutr Biochem* 18:279-284.
- Galloway S, Pallegage-Gamarallage MM, Takechi R, Jian L, Johnsen RD, Dhaliwal SS, Mamo JC (2008) Synergistic effects of high fat feeding and apolipoprotein E deletion on enterocytic amyloid-beta abundance. *Lipids Health Dis* 7:15.
- Galloway S, Takechi R, Pallegage-Gamarallage MM, Dhaliwal SS, Mamo JC (2009) Amyloid-beta colocalizes with apolipoprotein B in absorptive cells of the small intestine. *Lipids Health Dis* 8:46.
- Gandy S, Czernik AJ, Greengard P (1988) Phosphorylation of Alzheimer disease amyloid precursor peptide by protein kinase C and Ca²⁺/calmodulin-dependent protein kinase II. *Proceedings of the National Academy of Sciences of the United States of America* 85:6218-6221.
- Gasparini L, Racchi M, Binetti G, Trabucchi M, Solerte SB, Alkon D, Etcheberrigaray R, Gibson G, Blass J, Paoletti R, Govoni S (1998) Peripheral markers in testing pathophysiological hypotheses and diagnosing Alzheimer's disease. *Faseb J* 12:17-34.
- Gautron L, Elmquist JK (2011) Sixteen years and counting: an update on leptin in energy balance. *The Journal of clinical investigation* 121:2087-2093.
- Gehrmann J, Banati RB, Cuzner ML, Kreutzberg GW, Newcombe J (1995a) Amyloid precursor protein (APP) expression in multiple sclerosis lesions. *Glia* 15:141-151.
- Gehrmann J, Banati RB, Wiessner C, Hossmann KA, Kreutzberg GW (1995b) Reactive microglia in cerebral ischaemia: an early mediator of tissue damage? *Neuropathol Appl Neurobiol* 21:277-289.
- Gesta S, Tseng YH, Kahn CR (2007) Developmental origin of fat: tracking obesity to its source. *Cell* 131:242-256.
- Ghoshal S, Witta J, Zhong J, de Villiers W, Eckhardt E (2009) Chylomicrons promote intestinal absorption of lipopolysaccharides. *J Lipid Res* 50:90-97.
- Goate A, Chartier-Harlin MC, Mullan M, Brown J, Crawford F, Fidani L, Giuffra L, Haynes A, Irving N, James L (1991) Segregation of a missense mutation in the amyloid precursor protein gene with familial Alzheimer's disease. *Nature* 349:704-706.

- Golovko MY, Murphy EJ (2008) An improved LC-MS/MS procedure for brain prostanoid analysis using brain fixation with head-focused microwave irradiation and liquid-liquid extraction. *J Lipid Res* 49:893-902.
- Gomez-Casanovas E, Sanmarti R, Sole M, Canete JD, Munoz-Gomez J (2001) The clinical significance of amyloid fat deposits in rheumatoid arthritis: a systematic long-term followup study using abdominal fat aspiration. *Arthritis Rheum* 44:66-72.
- Gordon S (2003) Alternative activation of macrophages. *Nature reviews Immunology* 3:23-35.
- Gordon S, Taylor PR (2005) Monocyte and macrophage heterogeneity. *Nature reviews Immunology* 5:953-964.
- Goyal RK, Hirano I (1996) The enteric nervous system. *N Engl J Med* 334:1106-1115.
- Gravina SA, Ho L, Eckman CB, Long KE, Otvos L, Jr., Younkin LH, Suzuki N, Younkin SG (1995) Amyloid beta protein (A beta) in Alzheimer's disease brain. Biochemical and immunocytochemical analysis with antibodies specific for forms ending at A beta 40 or A beta 42(43). *J Biol Chem* 270:7013-7016.
- Greenberg SA (2010) Theories of the pathogenesis of inclusion body myositis. *Curr Rheumatol Rep* 12:221-228.
- Grimm MC, Pullman WE, Bennett GM, Sullivan PJ, Pavli P, Doe WF (1995) Direct evidence of monocyte recruitment to inflammatory bowel disease mucosa. *J Gastroenterol Hepatol* 10:387-395.
- Gunstad J, Paul RH, Brickman AM, Cohen RA, Arns M, Roe D, Lawrence JJ, Gordon E (2006) Patterns of cognitive performance in middle-aged and older adults: A cluster analytic examination. *J Geriatr Psychiatry Neurol* 19:59-64.
- Gunstad J, Paul RH, Cohen RA, Tate DF, Spitznagel MB, Gordon E (2007) Elevated body mass index is associated with executive dysfunction in otherwise healthy adults. *Compr Psychiatry* 48:57-61.
- Gunstad J, Paul RH, Cohen RA, Tate DF, Spitznagel MB, Grieve S, Gordon E (2008) Relationship between body mass index and brain volume in healthy adults. *Int J Neurosci* 118:1582-1593.

- Haass C, Hung AY, Selkoe DJ (1991) Processing of beta-amyloid precursor protein in microglia and astrocytes favors an internal localization over constitutive secretion. *J Neurosci* 11:3783-3793.
- Haddad G, Belosevic M (2009) Transferrin-derived synthetic peptide induces highly conserved pro-inflammatory responses of macrophages. *Mol Immunol* 46:576-586.
- Hamad AR (2010) Analysis of gene profile, steady state proliferation and apoptosis of double-negative T cells in the periphery and gut epithelium provides new insights into the biological functions of the Fas pathway. *Immunol Res* 47:134-142.
- Harrington AM, Hutson JM, Southwell BR (2010) Cholinergic neurotransmission and muscarinic receptors in the enteric nervous system. *Prog Histochem Cytochem* 44:173-202.
- Hausman DB, DiGirolamo M, Bartness TJ, Hausman GJ, Martin RJ (2001) The biology of white adipocyte proliferation. *Obesity reviews : an official journal of the International Association for the Study of Obesity* 2:239-254.
- Hayden KM, Zandi PP, Khachaturian AS, Szekely CA, Fotuhi M, Norton MC, Tschanz JT, Pieper CF, Corcoran C, Lyketsos CG, Breitner JC, Welsh-Bohmer KA (2007) Does NSAID use modify cognitive trajectories in the elderly? The Cache County study. *Neurology* 69:275-282.
- Heller F, Florian P, Bojarski C, Richter J, Christ M, Hillenbrand B, Mankertz J, Gitter AH, Burgel N, Fromm M, Zeitz M, Fuss I, Strober W, Schulzke JD (2005) Interleukin-13 is the key effector Th2 cytokine in ulcerative colitis that affects epithelial tight junctions, apoptosis, and cell restitution. *Gastroenterology* 129:550-564.
- Hellstrom-Lindahl E, Viitanen M, Marutle A (2009) Comparison of Abeta levels in the brain of familial and sporadic Alzheimer's disease. *Neurochem Int* 55:243-252.
- Herrera BM, Keildson S, Lindgren CM (2011) Genetics and epigenetics of obesity. *Maturitas* 69:41-49.
- Herzog V, Kirfel G, Siemes C, Schmitz A (2004) Biological roles of APP in the epidermis. *Eur J Cell Biol* 83:613-624.
- Hill JO, Peters JC (1998) Environmental contributions to the obesity epidemic. *Science* 280:1371-1374.

- Ho L, Qin W, Pompl PN, Xiang Z, Wang J, Zhao Z, Peng Y, Cambareri G, Rocher A, Mobbs CV, Hof PR, Pasinetti GM (2004) Diet-induced insulin resistance promotes amyloidosis in a transgenic mouse model of Alzheimer's disease. *Faseb J* 18:902-904.
- Hoe HS, Fu Z, Makarova A, Lee JY, Lu C, Feng L, Pajoohesh-Ganji A, Matsuoka Y, Hyman BT, Ehlers MD, Vicini S, Pak DT, Rebeck GW (2009) The effects of amyloid precursor protein on postsynaptic composition and activity. *J Biol Chem* 284:8495-8506.
- Hoffmann J, Twiesselmann C, Kummer MP, Romagnoli P, Herzog V (2000) A possible role for the Alzheimer amyloid precursor protein in the regulation of epidermal basal cell proliferation. *Eur J Cell Biol* 79:905-914.
- Holsinger RM, McLean CA, Beyreuther K, Masters CL, Evin G (2002) Increased expression of the amyloid precursor beta-secretase in Alzheimer's disease. *Ann Neurol* 51:783-786.
- Hotamisligil GS, Arner P, Caro JF, Atkinson RL, Spiegelman BM (1995) Increased adipose tissue expression of tumor necrosis factor- α in human obesity and insulin resistance. *The Journal of clinical investigation* 95:2409-2415.
- Hotamisligil GS, Shargill NS, Spiegelman BM (1993) Adipose expression of tumor necrosis factor- α : direct role in obesity-linked insulin resistance. *Science (New York, NY)* 259:87-91.
- Hughes TF, Borenstein AR, Schofield E, Wu Y, Larson EB (2009) Association between late-life body mass index and dementia: The Kame Project. *Neurology* 72:1741-1746.
- Hung AY, Koo EH, Haass C, Selkoe DJ (1992) Increased expression of beta-amyloid precursor protein during neuronal differentiation is not accompanied by secretory cleavage. *Proceedings of the National Academy of Sciences of the United States of America* 89:9439-9443.
- Ibrahim MM (2010) Subcutaneous and visceral adipose tissue: structural and functional differences. *Obesity reviews : an official journal of the International Association for the Study of Obesity* 11:11-18.
- Iijima K, Ando K, Takeda S, Satoh Y, Seki T, Itohara S, Greengard P, Kirino Y, Nairn AC, Suzuki T (2000) Neuron-specific phosphorylation of Alzheimer's beta-amyloid precursor protein by cyclin-dependent kinase 5. *J Neurochem* 75:1085-1091.

- Ikezu T, Luo X, Weber GA, Zhao J, McCabe L, Buescher JL, Ghorpade A, Zheng J, Xiong H (2003) Amyloid precursor protein-processing products affect mononuclear phagocyte activation: pathways for sAPP- and Abeta-mediated neurotoxicity. *J Neurochem* 85:925-934.
- Inomata H, Nakamura Y, Hayakawa A, Takata H, Suzuki T, Miyazawa K, Kitamura N (2003) A scaffold protein JIP-1b enhances amyloid precursor protein phosphorylation by JNK and its association with kinesin light chain 1. *J Biol Chem* 278:22946-22955.
- Itoh T, Satou T, Nishida S, Tsubaki M, Hashimoto S, Ito H (2009) Expression of amyloid precursor protein after rat traumatic brain injury. *Neurol Res* 31:103-109.
- Jeong SK, Nam HS, Son MH, Son EJ, Cho KH (2005) Interactive effect of obesity indexes on cognition. *Dement Geriatr Cogn Disord* 19:91-96.
- Jessen KR, Mirsky R (1985) Glial fibrillary acidic polypeptides in peripheral glia. Molecular weight, heterogeneity and distribution. *J Neuroimmunol* 8:377-393.
- Joachim C, Games D, Morris J, Ward P, Frenkel D, Selkoe D (1991) Antibodies to non-beta regions of the beta-amyloid precursor protein detect a subset of senile plaques. *Am J Pathol* 138:373-384.
- Joachim CL, Mori H, Selkoe DJ (1989) Amyloid beta-protein deposition in tissues other than brain in Alzheimer's disease. *Nature* 341:226-230.
- Johanson JF, Sonnenberg A, Koch TR, McCarty DJ (1992) Association of constipation with neurologic diseases. *Dig Dis Sci* 37:179-186.
- Johnson-Wood K, Lee M, Motter R, Hu K, Gordon G, Barbour R, Khan K, Gordon M, Tan H, Games D, Lieberburg I, Schenk D, Seubert P, McConlogue L (1997) Amyloid precursor protein processing and A beta42 deposition in a transgenic mouse model of Alzheimer disease. *Proceedings of the National Academy of Sciences of the United States of America* 94:1550-1555.
- Kagan VE, Kisin ER, Kawai K, Serinkan BF, Osipov AN, Serbinova EA, Wolinsky I, Shvedova AA (2002) Toward mechanism-based antioxidant interventions: lessons from natural antioxidants. *Annals of the New York Academy of Sciences* 959:188-198.

- Kamal A, Almenar-Queralt A, LeBlanc JF, Roberts EA, Goldstein LS (2001) Kinesin-mediated axonal transport of a membrane compartment containing beta-secretase and presenilin-1 requires APP. *Nature* 414:643-648.
- Kanda H, Tateya S, Tamori Y, Kotani K, Hiasa K, Kitazawa R, Kitazawa S, Miyachi H, Maeda S, Egashira K, Kasuga M (2006) MCP-1 contributes to macrophage infiltration into adipose tissue, insulin resistance, and hepatic steatosis in obesity. *The Journal of clinical investigation* 116:1494-1505.
- Kang J, Lemaire HG, Unterbeck A, Salbaum JM, Masters CL, Grzeschik KH, Multhaup G, Beyreuther K, Muller-Hill B (1987a) The precursor of Alzheimer's disease amyloid A4 protein resembles a cell-surface receptor. *Nature* 325:733-736.
- Kang J, Lemaire HG, Unterbeck A, Salbaum JM, Masters CL, Grzeschik KH, Multhaup G, Beyreuther K, Muller-Hill B (1987b) The precursor of Alzheimer's disease amyloid A4 protein resembles a cell-surface receptor. *Nature* 325:733-736.
- Kayed R, Head E, Sarsoza F, Saing T, Cotman CW, Necula M, Margol L, Wu J, Breydo L, Thompson JL, Rasool S, Gurlo T, Butler P, Glabe CG (2007) Fibril specific, conformation dependent antibodies recognize a generic epitope common to amyloid fibrils and fibrillar oligomers that is absent in prefibrillar oligomers. *Mol Neurodegener* 2:18.
- Keates S, Keates AC, Mizoguchi E, Bhan A, Kelly CP (1997) Enterocytes are the primary source of the chemokine ENA-78 in normal colon and ulcerative colitis. *Am J Physiol* 273:G75-82.
- Kern PA, Saghizadeh M, Ong JM, Bosch RJ, Deem R, Simsolo RB (1995) The expression of tumor necrosis factor in human adipose tissue. Regulation by obesity, weight loss, and relationship to lipoprotein lipase. *The Journal of clinical investigation* 95:2111-2119.
- Kettenmann H, Hanisch UK, Noda M, Verkhratsky A (2011) Physiology of microglia. *Physiological reviews* 91:461-553.
- Kim DH, Sandoval D, Reed JA, Matter EK, Tolod EG, Woods SC, Seeley RJ (2008) The role of GM-CSF in adipose tissue inflammation. *Am J Physiol Endocrinol Metab* 295:E1038-1046.
- Kivipelto M, Ngandu T, Fratiglioni L, Viitanen M, Kareholt I, Winblad B, Helkala EL, Tuomilehto J, Soininen H, Nissinen A (2005) Obesity and vascular risk factors at midlife and the risk of dementia and Alzheimer disease. *ArchNeurol* 62:1556-1560.

- Klebl FH, Olsen JE, Jain S, Doe WF (2001) Expression of macrophage-colony stimulating factor in normal and inflammatory bowel disease intestine. *J Pathol* 195:609-615.
- Klegeris A, Walker DG, McGeer PL (1994) Activation of macrophages by Alzheimer beta amyloid peptide. *Biochem Biophys Res Commun* 199:984-991.
- Kohjima M, Sun Y, Chan L (2010) Increased food intake leads to obesity and insulin resistance in the tg2576 Alzheimer's disease mouse model. *Endocrinology* 151:1532-1540.
- Kuhn R, Lohler J, Rennick D, Rajewsky K, Muller W (1993) Interleukin-10-deficient mice develop chronic enterocolitis. *Cell* 75:263-274.
- Kuo YM, Kokjohn TA, Watson MD, Woods AS, Cotter RJ, Sue LI, Kalback WM, Emmerling MR, Beach TG, Roher AE (2000) Elevated abeta42 in skeletal muscle of Alzheimer disease patients suggests peripheral alterations of AbetaPP metabolism. *Am J Pathol* 156:797-805.
- Kwon JH, Keates AC, Anton PM, Botero M, Goldsmith JD, Kelly CP (2005) Topical antisense oligonucleotide therapy against LIX, an enterocyte-expressed CXC chemokine, reduces murine colitis. *Am J Physiol Gastrointest Liver Physiol* 289:G1075-1083.
- Laitinen MH, Ngandu T, Rovio S, Helkala EL, Uusitalo U, Viitanen M, Nissinen A, Tuomilehto J, Soininen H, Kivipelto M (2006) Fat intake at midlife and risk of dementia and Alzheimer's disease: a population-based study. *Dement Geriatr Cogn Disord* 22:99-107.
- Lang E, Szendrei GI, Lee VM, Otvos L, Jr. (1992) Immunological and conformation characterization of a phosphorylated immunodominant epitope on the paired helical filaments found in Alzheimer's disease. *Biochem Biophys Res Commun* 187:783-790.
- Lauffenburger DA, Horwitz AF (1996) Cell migration: a physically integrated molecular process. *Cell* 84:359-369.
- Lawson LJ, Perry VH, Dri P, Gordon S (1990) Heterogeneity in the distribution and morphology of microglia in the normal adult mouse brain. *Neuroscience* 39:151-170.
- Le Foll C, Dunn-Meynell A, Musatov S, Magnan C, Levin BE (2013) FAT/CD36: A major regulator of neuronal fatty acid sensing and energy homeostasis in rats and mice. *Diabetes*.

- Le Foll C, Irani BG, Magnan C, Dunn-Meynell AA, Levin BE (2009) Characteristics and mechanisms of hypothalamic neuronal fatty acid sensing. *American journal of physiology Regulatory, integrative and comparative physiology* 297:R655-664.
- Leahey TM, Myers TA, Gunstad J, Glickman E, Spitznagel MB, Alexander T, Juvancic-Heltzel J (2007) Abeta40 is associated with cognitive function, body fat and physical fitness in healthy older adults. *Nutr Neurosci* 10:205-209.
- LeBlanc AC, Chen HY, Autilio-Gambetti L, Gambetti P (1991) Differential APP gene expression in rat cerebral cortex, meninges, and primary astroglial, microglial and neuronal cultures. *FEBS Lett* 292:171-178.
- Lee KJ, Moussa CE, Lee Y, Sung Y, Howell BW, Turner RS, Pak DT, Hoe HS (2010) Beta amyloid-independent role of amyloid precursor protein in generation and maintenance of dendritic spines. *Neuroscience* 169:344-356.
- Lee YH, Martin JM, Maple RL, Tharp WG, Pratley RE (2009a) Plasma amyloid-beta peptide levels correlate with adipocyte amyloid precursor protein gene expression in obese individuals. *Neuroendocrinology* 90:383-390.
- Lee YH, Martin JM, Maple RL, Tharp WG, Pratley RE (2009b) Plasma amyloid-beta peptide levels correlate with adipocyte amyloid precursor protein gene expression in obese individuals. *Neuroendocrinology* 90:383-390.
- Lee YH, Pratley RE (2007) Abdominal obesity and cardiovascular disease risk: the emerging role of the adipocyte. *J Cardiopulm Rehabil Prev* 27:2-10.
- Lee YH, Tharp WG, Maple RL, Nair S, Permana PA, Pratley RE (2008a) Amyloid precursor protein expression is upregulated in adipocytes in obesity. *Obesity (Silver Spring, Md)* 16:1493-1500.
- Lee YH, Tharp WG, Maple RL, Nair S, Permana PA, Pratley RE (2008b) Amyloid precursor protein expression is upregulated in adipocytes in obesity. *Obesity (Silver Spring)* 16:1493-1500.
- Lee YS (2009) The role of genes in the current obesity epidemic. *Ann Acad Med Singapore* 38:45-43.
- Levin-Allerhand JA, Lominska CE, Smith JD (2002) Increased amyloid- levels in APPSWE transgenic mice treated chronically with a physiological high-fat high-cholesterol diet. *J Nutr Health Aging* 6:315-319.

- Levy-Lahad E, Wasco W, Poorkaj P, Romano DM, Oshima J, Pettingell WH, Yu CE, Jondro PD, Schmidt SD, Wang K (1995) Candidate gene for the chromosome 1 familial Alzheimer's disease locus. *Science* (New York, NY) 269:973-977.
- Ley K, Laudanna C, Cybulsky MI, Nourshargh S (2007) Getting to the site of inflammation: the leukocyte adhesion cascade updated. *Nature reviews Immunology* 7:678-689.
- Li M, Shang DS, Zhao WD, Tian L, Li B, Fang WG, Zhu L, Man SM, Chen YH (2009) Amyloid beta interaction with receptor for advanced glycation end products up-regulates brain endothelial CCR5 expression and promotes T cells crossing the blood-brain barrier. *J Immunol* 182:5778-5788.
- Li R, Lindholm K, Yang LB, Yue X, Citron M, Yan R, Beach T, Sue L, Sabbagh M, Cai H, Wong P, Price D, Shen Y (2004) Amyloid beta peptide load is correlated with increased beta-secretase activity in sporadic Alzheimer's disease patients. *Proceedings of the National Academy of Sciences of the United States of America* 101:3632-3637.
- Lindgren CM, Heid IM, Randall JC, Lamina C, Steinthorsdottir V, Qi L, Speliotes EK, Thorleifsson G, Willer CJ, Herrera BM, Jackson AU, Lim N, Scheet P, Soranzo N, Amin N, Aulchenko YS, Chambers JC, Drong A, Luan J, Lyon HN, Rivadeneira F, Sanna S, Timpson NJ, Zillikens MC, Zhao JH, Almgren P, Bandinelli S, Bennett AJ, Bergman RN, Bonnycastle LL, Bumpstead SJ, Chanock SJ, Cherkas L, Chines P, Coin L, Cooper C, Crawford G, Doering A, Dominiczak A, Doney AS, Ebrahim S, Elliott P, Erdos MR, Estrada K, Ferrucci L, Fischer G, Forouhi NG, Gieger C, Grallert H, Groves CJ, Grundy S, Guiducci C, Hadley D, Hamsten A, Havulinna AS, Hofman A, Holle R, Holloway JW, Illig T, Isomaa B, Jacobs LC, Jameson K, Jousilahti P, Karpe F, Kuusisto J, Laitinen J, Lathrop GM, Lawlor DA, Mangino M, McArdle WL, Meitinger T, Morken MA, Morris AP, Munroe P, Narisu N, Nordstrom A, Nordstrom P, Oostra BA, Palmer CN, Payne F, Peden JF, Prokopenko I, Renstrom F, Ruokonen A, Salomaa V, Sandhu MS, Scott LJ, Scuteri A, Silander K, Song K, Yuan X, Stringham HM, Swift AJ, Tuomi T, Uda M, Vollenweider P, Waeber G, Wallace C, Walters GB, Weedon MN, Witteman JC, Zhang C, Zhang W, Caulfield MJ, Collins FS, Davey Smith G, Day IN, Franks PW, Hattersley AT, Hu FB, Jarvelin MR, Kong A, Kooner JS, Laakso M, Lakatta E, Mooser V, Morris AD, Peltonen L, Samani NJ, Spector TD, Strachan DP, Tanaka T, Tuomilehto J, Uitterlinden AG, van Duijn CM, Wareham NJ, Hugh W, Waterworth DM, Boehnke M, Deloukas P, Groop L, Hunter DJ, Thorsteinsdottir U, Schlessinger D, Wichmann HE, Frayling TM, Abecasis GR, Hirschhorn JN, Loos RJ, Stefansson K, Mohlke KL, Barroso I, McCarthy MI (2009) Genome-wide association scan meta-analysis

identifies three Loci influencing adiposity and fat distribution. *PLoS Genet* 5:e1000508.

Loos RJ, Lindgren CM, Li S, Wheeler E, Zhao JH, Prokopenko I, Inouye M, Freathy RM, Attwood AP, Beckmann JS, Berndt SI, Jacobs KB, Chanock SJ, Hayes RB, Bergmann S, Bennett AJ, Bingham SA, Bochud M, Brown M, Cauchi S, Connell JM, Cooper C, Smith GD, Day I, Dina C, De S, Dermitzakis ET, Doney AS, Elliott KS, Elliott P, Evans DM, Sadaf Farooqi I, Froguel P, Ghorji J, Groves CJ, Gwilliam R, Hadley D, Hall AS, Hattersley AT, Hebebrand J, Heid IM, Lamina C, Gieger C, Illig T, Meitinger T, Wichmann HE, Herrera B, Hinney A, Hunt SE, Jarvelin MR, Johnson T, Jolley JD, Karpe F, Keniry A, Khaw KT, Luben RN, Mangino M, Marchini J, McArdle WL, McGinnis R, Meyre D, Munroe PB, Morris AD, Ness AR, Neville MJ, Nica AC, Ong KK, O'Rahilly S, Owen KR, Palmer CN, Papadakis K, Potter S, Pouta A, Qi L, Randall JC, Rayner NW, Ring SM, Sandhu MS, Scherag A, Sims MA, Song K, Soranzo N, Speliotes EK, Syddall HE, Teichmann SA, Timpson NJ, Tobias JH, Uda M, Vogel CI, Wallace C, Waterworth DM, Weedon MN, Willer CJ, Wraight, Yuan X, Zeggini E, Hirschhorn JN, Strachan DP, Ouwehand WH, Caulfield MJ, Samani NJ, Frayling TM, Vollenweider P, Waeber G, Mooser V, Deloukas P, McCarthy MI, Wareham NJ, Barroso I, Kraft P, Hankinson SE, Hunter DJ, Hu FB, Lyon HN, Voight BF, Ridderstrale M, Groop L, Scheet P, Sanna S, Abecasis GR, Albai G, Nagaraja R, Schlessinger D, Jackson AU, Tuomilehto J, Collins FS, Boehnke M, Mohlke KL (2008) Common variants near MC4R are associated with fat mass, weight and risk of obesity. *Nat Genet* 40:768-775.

Lorton D, Kocsis JM, King L, Madden K, Brunden KR (1996) beta-Amyloid induces increased release of interleukin-1 beta from lipopolysaccharide-activated human monocytes. *J Neuroimmunol* 67:21-29.

Lorton D, Schaller J, Lala A, De Nardin E (2000) Chemotactic-like receptors and Abeta peptide induced responses in Alzheimer's disease. *Neurobiol Aging* 21:463-473.

Lu DC, Rabizadeh S, Chandra S, Shayya RF, Ellerby LM, Ye X, Salvesen GS, Koo EH, Bredesen DE (2000) A second cytotoxic proteolytic peptide derived from amyloid beta-protein precursor. *Nat Med* 6:397-404.

Luchsinger JA (2008) Adiposity, hyperinsulinemia, diabetes and Alzheimer's disease: an epidemiological perspective. *Eur J Pharmacol* 585:119-129.

Luchsinger JA, Gustafson DR (2009a) Adiposity and Alzheimer's disease. *Curr Opin Clin Nutr Metab Care* 12:15-21.

- Luchsinger JA, Gustafson DR (2009b) Adiposity, type 2 diabetes, and Alzheimer's disease. *JAlzheimers Dis* 16:693-704.
- Luchsinger JA, Mayeux R (2007) Adiposity and Alzheimer's disease. *CurrAlzheimer Res* 4:127-134.
- Lue LF, Walker DG, Brachova L, Beach TG, Rogers J, Schmidt AM, Stern DM, Yan SD (2001) Involvement of microglial receptor for advanced glycation endproducts (RAGE) in Alzheimer's disease: identification of a cellular activation mechanism. *Exp Neurol* 171:29-45.
- Lumeng CN, Bodzin JL, Saltiel AR (2007) Obesity induces a phenotypic switch in adipose tissue macrophage polarization. *The Journal of clinical investigation* 117:175-184.
- Ma T, Zhao Y, Kwak YD, Yang Z, Thompson R, Luo Z, Xu H, Liao FF (2009) Statin's excitoprotection is mediated by sAPP and the subsequent attenuation of calpain-induced truncation events, likely via rho-ROCK signaling. *J Neurosci* 29:11226-11236.
- Mackic JB, Bading J, Ghiso J, Walker L, Wisniewski T, Frangione B, Zlokovic BV (2002) Circulating amyloid-beta peptide crosses the blood-brain barrier in aged monkeys and contributes to Alzheimer's disease lesions. *Vascul Pharmacol* 38:303-313.
- Maezawa I, Zimin PI, Wulff H, Jin LW (2010) Amyloid-beta protein oligomer at low nanomolar concentrations activates microglia and induces microglial neurotoxicity. *J Biol Chem* 286:3693-3706.
- Mantovani A, Sica A, Sozzani S, Allavena P, Vecchi A, Locati M (2004) The chemokine system in diverse forms of macrophage activation and polarization. *Trends in immunology* 25:677-686.
- Martin C, Chevrot M, Poirier H, Passilly-Degrace P, Niot I, Besnard P (2011) CD36 as a lipid sensor. *Physiology & behavior* 105:36-42.
- Matsubara Y, Kano K, Kondo D, Mugishima H, Matsumoto T (2009) Differences in adipocytokines and fatty acid composition between two adipocyte fractions of small and large cells in high-fat diet-induced obese mice. *AnnNutrMetab* 54:258-267.
- Mattson MP (1997) Cellular actions of beta-amyloid precursor protein and its soluble and fibrillogenic derivatives. *Physiological reviews* 77:1081-1132.

- Mattson MP (2009) Roles of the lipid peroxidation product 4-hydroxynonenal in obesity, the metabolic syndrome, and associated vascular and neurodegenerative disorders. *Experimental gerontology* 44:625-633.
- Mattson MP, Cheng B, Culwell AR, Esch FS, Lieberburg I, Rydel RE (1993) Evidence for excitoprotective and intraneuronal calcium-regulating roles for secreted forms of the beta-amyloid precursor protein. *Neuron* 10:243-254.
- McGeer PL, Itagaki S, Tago H, McGeer EG (1987) Reactive microglia in patients with senile dementia of the Alzheimer type are positive for the histocompatibility glycoprotein HLA-DR. *Neurosci Lett* 79:195-200.
- McGillicuddy FC, Chiquoine EH, Hinkle CC, Kim RJ, Shah R, Roche HM, Smyth EM, Reilly MP (2009) Interferon gamma attenuates insulin signaling, lipid storage, and differentiation in human adipocytes via activation of the JAK/STAT pathway. *J Biol Chem* 284:31936-31944.
- Meda L, Cassatella MA, Szendrei GI, Otvos L, Jr., Baron P, Villalba M, Ferrari D, Rossi F (1995) Activation of microglial cells by beta-amyloid protein and interferon-gamma. *Nature* 374:647-650.
- Meijer K, de Vries M, Al-Lahham S, Bruinenberg M, Weening D, Dijkstra M, Kloosterhuis N, van der Leij RJ, van der Want H, Kroesen BJ, Vonk R, Rezaee F Human primary adipocytes exhibit immune cell function: adipocytes prime inflammation independent of macrophages. *PLoS One* 6:e17154.
- Metcalf D (1985) The granulocyte-macrophage colony-stimulating factors. *Science* 229:16-22.
- Miners JS, Barua N, Kehoe PG, Gill S, Love S (2011) Abeta-degrading enzymes: potential for treatment of Alzheimer disease. *J Neuropathol Exp Neurol* 70:944-959.
- Mohamadzadeh M, Poltorak AN, Bergstressor PR, Beutler B, Takashima A (1996) Dendritic cells produce macrophage inflammatory protein-1 gamma, a new member of the CC chemokine family. *J Immunol* 156:3102-3106.
- Monning U, Sandbrink R, Banati RB, Masters CL, Beyreuther K (1994) Transforming growth factor beta mediates increase of mature transmembrane amyloid precursor protein in microglial cells. *FEBS Lett* 342:267-272.

- Monning U, Sandbrink R, Weidemann A, Banati RB, Masters CL, Beyreuther K (1995) Extracellular matrix influences the biogenesis of amyloid precursor protein in microglial cells. *J Biol Chem* 270:7104-7110.
- Moroz N, Tong M, Longato L, Xu H, de la Monte SM (2008) Limited Alzheimer-type neurodegeneration in experimental obesity and type 2 diabetes mellitus. *J Alzheimers Dis* 15:29-44.
- Multhaup G, Schlicksupp A, Hesse L, Beher D, Ruppert T, Masters CL, Beyreuther K (1996) The amyloid precursor protein of Alzheimer's disease in the reduction of copper(II) to copper(I). *Science* 271:1406-1409.
- Murray PJ, Wynn TA (2011) Protective and pathogenic functions of macrophage subsets. *Nature reviews Immunology* 11:723-737.
- Naito Y, Yoshikawa T (2005) Role of matrix metalloproteinases in inflammatory bowel disease. *Mol Aspects Med* 26:379-390.
- Nakarai H, Yamashita A, Nagayasu S, Iwashita M, Kumamoto S, Ohyama H, Hata M, Soga Y, Kushiya A, Asano T, Abiko Y, Nishimura F Adipocyte-macrophage interaction may mediate LPS-induced low-grade inflammation: potential link with metabolic complications. *Innate Immun.*
- Narindrasorasak S, Altman RA, Gonzalez-DeWhitt P, Greenberg BD, Kisilevsky R (1995) An interaction between basement membrane and Alzheimer amyloid precursor proteins suggests a role in the pathogenesis of Alzheimer's disease. *Lab Invest* 72:272-282.
- Narindrasorasak S, Lowery D, Gonzalez-DeWhitt P, Poorman RA, Greenberg B, Kisilevsky R (1991) High affinity interactions between the Alzheimer's beta-amyloid precursor proteins and the basement membrane form of heparan sulfate proteoglycan. *J Biol Chem* 266:12878-12883.
- Narindrasorasak S, Lowery DE, Altman RA, Gonzalez-DeWhitt PA, Greenberg BD, Kisilevsky R (1992) Characterization of high affinity binding between laminin and Alzheimer's disease amyloid precursor proteins. *Lab Invest* 67:643-652.
- Nassir F, Wilson B, Han X, Gross RW, Abumrad NA (2007) CD36 is important for fatty acid and cholesterol uptake by the proximal but not distal intestine. *J Biol Chem* 282:19493-19501.
- Niess JH, Adler G (2010) Enteric flora expands gut lamina propria CX3CR1+ dendritic cells supporting inflammatory immune responses under normal and inflammatory conditions. *J Immunol* 184:2026-2037.

- Nikolaev A, McLaughlin T, O'Leary DD, Tessier-Lavigne M (2009) APP binds DR6 to trigger axon pruning and neuron death via distinct caspases. *Nature* 457:981-989.
- Nylander O (2011) The impact of cyclooxygenase inhibition on duodenal motility and mucosal alkaline secretion in anaesthetized rats. *Acta Physiol (Oxf)* 201:179-192.
- O'Rourke RW, Metcalf MD, White AE, Madala A, Winters BR, Maizlin, II, Jobe BA, Roberts CT, Jr., Slifka MK, Marks DL (2009) Depot-specific differences in inflammatory mediators and a role for NK cells and IFN-gamma in inflammation in human adipose tissue. *Int J Obes (Lond)* 33:978-990.
- Ohyagi Y, Tabira T (1993) Effect of growth factors and cytokines on expression of amyloid beta protein precursor mRNAs in cultured neural cells. *Brain Res Mol Brain Res* 18:127-132.
- Osterberg J, Ljungdahl M, Haglund U (2006) Influence of cyclooxygenase inhibitors on gut immune cell distribution and apoptosis rate in experimental sepsis. *Shock* 25:147-154.
- Pallebage-Gamarallage MM, Galloway S, Johnsen R, Jian L, Dhaliwal S, Mamo JC (2009) The effect of exogenous cholesterol and lipid-modulating agents on enterocytic amyloid-beta abundance. *Br J Nutr* 101:340-347.
- Paloneva J, Manninen T, Christman G, Hovanes K, Mandelin J, Adolfsson R, Bianchin M, Bird T, Miranda R, Salmaggi A, Tranebjaerg L, Konttinen Y, Peltonen L (2002) Mutations in two genes encoding different subunits of a receptor signaling complex result in an identical disease phenotype. *Am J Hum Genet* 71:656-662.
- Pardossi-Piquard R, Petit A, Kawarai T, Sunyach C, Alves da Costa C, Vincent B, Ring S, D'Adamio L, Shen J, Muller U, St George Hyslop P, Checler F (2005) Presenilin-dependent transcriptional control of the Abeta-degrading enzyme neprilysin by intracellular domains of betaAPP and APLP. *Neuron* 46:541-554.
- Peranzoni E, Zilio S, Marigo I, Dolcetti L, Zanovello P, Mandruzzato S, Bronte V (2010) Myeloid-derived suppressor cell heterogeneity and subset definition. *Current opinion in immunology* 22:238-244.
- Perry G, Siedlak S, Mulvihill P, Kancherla M, Mijares M, Kawai M, Gambetti P, Sharma S, Maggiora L, Cornette J, et al. (1989) Immunolocalization of the amyloid precursor protein within the senile plaque. *Prog Clin Biol Res* 317:1021-1025.

- Perry VH, Gordon S (1991) Macrophages and the nervous system. *International review of cytology* 125:203-244.
- Poitou C, Coussieu C, Rouault C, Coupaye M, Canello R, Bedel JF, Gouillon M, Bouillot JL, Oppert JM, Basdevant A, Clement K (2006) Serum amyloid A: a marker of adiposity-induced low-grade inflammation but not of metabolic status. *Obesity (Silver Spring)* 14:309-318.
- Ponte P, Gonzalez-DeWhitt P, Schilling J, Miller J, Hsu D, Greenberg B, Davis K, Wallace W, Lieberburg I, Fuller F (1988) A new A4 amyloid mRNA contains a domain homologous to serine proteinase inhibitors. *Nature* 331:525-527.
- Poussin C, Hall D, Minehira K, Galzin AM, Tarussio D, Thorens B (2008) Different transcriptional control of metabolism and extracellular matrix in visceral and subcutaneous fat of obese and rimonabant treated mice. *PloS one* 3:e3385.
- Priller C, Bauer T, Mitteregger G, Krebs B, Kretzschmar HA, Herms J (2006) Synapse formation and function is modulated by the amyloid precursor protein. *J Neurosci* 26:7212-7221.
- Profenno LA, Faraone SV (2008) Diabetes and overweight associate with non-APOE4 genotype in an Alzheimer's disease population. *Am J Med Genet B Neuropsychiatr Genet* 147B:822-829.
- Profenno LA, Porsteinsson AP, Faraone SV (2010) Meta-analysis of Alzheimer's disease risk with obesity, diabetes, and related disorders. *Biol Psychiatry* 67:505-512.
- Puig KL, Combs CK (2012) Expression and function of APP and its metabolites outside the central nervous system. *Experimental gerontology*.
- Puig KL, Swigost AJ, Zhou X, Sens MA, Combs CK (2012) Amyloid precursor protein expression modulates intestine immune phenotype. *Journal of neuroimmune pharmacology : the official journal of the Society on NeuroImmune Pharmacology* 7:215-230.
- Quast T, Wehner S, Kirfel G, Jaeger K, De Luca M, Herzog V (2003) sAPP as a regulator of dendrite motility and melanin release in epidermal melanocytes and melanoma cells. *FASEB J* 17:1739-1741.
- Raffaitin C, Gin H, Empana JP, Helmer C, Berr C, Tzourio C, Portet F, Dartigues JF, Alperovitch A, Barberger-Gateau P (2009) Metabolic syndrome and risk for incident Alzheimer's disease or vascular dementia: the Three-City Study. *Diabetes Care* 32:169-174.

- Ramachandrappa S, Farooqi IS (2011) Genetic approaches to understanding human obesity. *The Journal of clinical investigation* 121:2080-2086.
- Razay G, Vreugdenhil A (2005) Obesity in middle age and future risk of dementia: midlife obesity increases risk of future dementia. *BMJ* 331:455; author reply 455.
- Razay G, Vreugdenhil A, Wilcock G (2006) Obesity, abdominal obesity and Alzheimer disease. *DementGeriatrCognDisord* 22:173-176.
- Razay G, Vreugdenhil A, Wilcock G (2007) The metabolic syndrome and Alzheimer disease. *Arch Neurol* 64:93-96.
- Ricquier D (2005) Respiration uncoupling and metabolism in the control of energy expenditure. *The Proceedings of the Nutrition Society* 64:47-52.
- Roach M, Christie JA (2008) Fecal incontinence in the elderly. *Geriatrics* 63:13-22.
- Rocha VZ, Folco EJ, Sukhova G, Shimizu K, Gotsman I, Vernon AH, Libby P (2008) Interferon-gamma, a Th1 cytokine, regulates fat inflammation: a role for adaptive immunity in obesity. *Circ Res* 103:467-476.
- Rodriguez A, Catalan V, Gomez-Ambrosi J, Fruhbeck G (2007) Visceral and subcutaneous adiposity: are both potential therapeutic targets for tackling the metabolic syndrome? *Current pharmaceutical design* 13:2169-2175.
- Rogers J (2008) The inflammatory response in Alzheimer's disease. *J Periodontol* 79:1535-1543.
- Rogler G, Hausmann M, Vogl D, Aschenbrenner E, Andus T, Falk W, Andreesen R, Scholmerich J, Gross V (1998) Isolation and phenotypic characterization of colonic macrophages. *Clin Exp Immunol* 112:205-215.
- Romanowska M, Evans A, Kellock D, Bray SE, McLean K, Donandt S, Foerster J (2009) Wnt5a exhibits layer-specific expression in adult skin, is upregulated in psoriasis, and synergizes with type 1 interferon. *PLoS One* 4:e5354.
- Ross R, Despres JP (2009) Abdominal obesity, insulin resistance, and the metabolic syndrome: contribution of physical activity/exercise. *Obesity (Silver Spring)* 17 Suppl 3:S1-2.

- Rossjohn J, Cappai R, Feil SC, Henry A, McKinstry WJ, Galatis D, Hesse L, Multhaup G, Beyreuther K, Masters CL, Parker MW (1999) Crystal structure of the N-terminal, growth factor-like domain of Alzheimer amyloid precursor protein. *Nature structural biology* 6:327-331.
- Saijo K, Glass CK (2011) Microglial cell origin and phenotypes in health and disease. *Nature reviews Immunology* 11:775-787.
- Sandbrink R, Masters CL, Beyreuther K (1994) Beta A4-amyloid protein precursor mRNA isoforms without exon 15 are ubiquitously expressed in rat tissues including brain, but not in neurons. *J Biol Chem* 269:1510-1517.
- Santaolalla R, Fukata M, Abreu MT (2010) Innate immunity in the small intestine. *Curr Opin Gastroenterol* 27:125-131.
- Sasaki A, Shoji M, Harigaya Y, Kawarabayashi T, Ikeda M, Naito M, Matsubara E, Abe K, Nakazato Y (2002) Amyloid cored plaques in Tg2576 transgenic mice are characterized by giant plaques, slightly activated microglia, and the lack of paired helical filament-typed, dystrophic neurites. *Virchows Arch* 441:358-367.
- Savidge TC, Sofroniew MV, Neunlist M (2007) Starring roles for astroglia in barrier pathologies of gut and brain. *Lab Invest* 87:731-736.
- Schellenberg GD, Bird TD, Wijsman EM, Orr HT, Anderson L, Nemens E, White JA, Bonycastle L, Weber JL, Alonso ME (1992) Genetic linkage evidence for a familial Alzheimer's disease locus on chromosome 14. *Science (New York, NY)* 258:668-671.
- Schmechel DE, Goldgaber D, Burkhart DS, Gilbert JR, Gajdusek DC, Roses AD (1988) Cellular localization of messenger RNA encoding amyloid-beta-protein in normal tissue and in Alzheimer disease. *Alzheimer Dis Assoc Disord* 2:96-111.
- Schroder K, Sweet MJ, Hume DA (2006) Signal integration between IFN γ and TLR signalling pathways in macrophages. *Immunobiology* 211:511-524.
- Schulzke JD, Gitter AH, Mankertz J, Spiegel S, Seidler U, Amasheh S, Saitou M, Tsukita S, Fromm M (2005) Epithelial transport and barrier function in occludin-deficient mice. *Biochim Biophys Acta* 1669:34-42.

- Seabrook GR, Smith DW, Bowery BJ, Easter A, Reynolds T, Fitzjohn SM, Morton RA, Zheng H, Dawson GR, Sirinathsinghji DJ, Davies CH, Collingridge GL, Hill RG (1999) Mechanisms contributing to the deficits in hippocampal synaptic plasticity in mice lacking amyloid precursor protein. *Neuropharmacology* 38:349-359.
- Selassie M, Sinha AC (2011) The epidemiology and aetiology of obesity: a global challenge. *Best Pract Res Clin Anaesthesiol* 25:1-9.
- Selkoe DJ, Podlisny MB, Joachim CL, Vickers EA, Lee G, Fritz LC, Oltersdorf T (1988) Beta-amyloid precursor protein of Alzheimer disease occurs as 110- to 135-kilodalton membrane-associated proteins in neural and nonneural tissues. *Proceedings of the National Academy of Sciences of the United States of America* 85:7341-7345.
- Shankar GM, Walsh DM (2009) Alzheimer's disease: synaptic dysfunction and A β . *Mol Neurodegener* 4:48.
- Shankle WR, Landing BH, Ang SM, Chui H, Villarreal-Engelhardt G, Zarow C (1993) Studies of the enteric nervous system in Alzheimer disease and other dementias of the elderly: enteric neurons in Alzheimer disease. *Mod Pathol* 6:10-14.
- Shaul ME, Bennett G, Strissel KJ, Greenberg AS, Obin MS Dynamic, M2-like remodeling phenotypes of CD11c+ adipose tissue macrophages during high-fat diet--induced obesity in mice. *Diabetes* 59:1171-1181.
- Sherrington R, Rogaev EI, Liang Y, Rogaeva EA, Levesque G, Ikeda M, Chi H, Lin C, Li G, Holman K (1995) Cloning of a gene bearing missense mutations in early-onset familial Alzheimer's disease. *Nature* 375:754-760.
- Shi C, Pamer EG (2011) Monocyte recruitment during infection and inflammation. *Nature reviews Immunology* 11:762-774.
- Shi XZ, Lin YM, Powell DW, Sarna SK (2011) Pathophysiology of motility dysfunction in bowel obstruction: role of stretch-induced COX-2. *Am J Physiol Gastrointest Liver Physiol* 300:G99-G108.
- Siemes C, Quast T, Kummer C, Wehner S, Kirfel G, Muller U, Herzog V (2006) Keratinocytes from APP/APLP2-deficient mice are impaired in proliferation, adhesion and migration in vitro. *Experimental cell research* 312:1939-1949.

- Smith CJ, Johnson EM, Jr., Osborne P, Freeman RS, Neveu I, Brachet P (1993) NGF deprivation and neuronal degeneration trigger altered beta-amyloid precursor protein gene expression in the rat superior cervical ganglia in vivo and in vitro. *Brain Res Mol Brain Res* 17:328-334.
- Smith J, Al-Amri M, Dorairaj P, Sniderman A (2006) The adipocyte life cycle hypothesis. *Clinical science* 110:1-9.
- Smits HA, van Beelen AJ, de Vos NM, Rijmsmus A, van der Bruggen T, Verhoef J, van Muiswinkel FL, Nottet HS (2001) Activation of human macrophages by amyloid-beta is attenuated by astrocytes. *J Immunol* 166:6869-6876.
- Sola C, Garcia-Ladona FJ, Mengod G, Probst A, Frey P, Palacios JM (1993) Increased levels of the Kunitz protease inhibitor-containing beta APP mRNAs in rat brain following neurotoxic damage. *Brain Res Mol Brain Res* 17:41-52.
- Sommer G, Kralisch S, Lipfert J, Weise S, Krause K, Jessnitzer B, Lossner U, Bluher M, Stumvoll M, Fasshauer M (2009) Amyloid precursor protein expression is induced by tumor necrosis factor alpha in 3T3-L1 adipocytes. *J Cell Biochem* 108:1418-1422.
- Sondag CM, Combs CK (2004a) Amyloid precursor protein mediates proinflammatory activation of monocytic lineage cells. *The Journal of biological chemistry* 279:14456-14463.
- Sondag CM, Combs CK (2004b) Amyloid precursor protein mediates proinflammatory activation of monocytic lineage cells. *J Biol Chem* 279:14456-14463.
- Sondag CM, Combs CK (2006a) Amyloid precursor protein cross-linking stimulates beta amyloid production and pro-inflammatory cytokine release in monocytic lineage cells. *J Neurochem* 97:449-461.
- Sondag CM, Combs CK (2006b) Amyloid precursor protein cross-linking stimulates beta amyloid production and pro-inflammatory cytokine release in monocytic lineage cells. *Journal of neurochemistry* 97:449-461.
- Sondag CM, Combs CK (2010a) Adhesion of monocytes to type I collagen stimulates an APP-dependent proinflammatory signaling response and release of Abeta1-40. *Journal of neuroinflammation* 7:22.
- Sondag CM, Combs CK (2010b) Adhesion of monocytes to type I collagen stimulates an APP-dependent proinflammatory signaling response and release of Abeta1-40. *J Neuroinflammation* 7:22.

- Sondag CM, Dhawan G, Combs CK (2009) Beta amyloid oligomers and fibrils stimulate differential activation of primary microglia. *J Neuroinflammation* 6:1.
- Sonnenberg A, Tsou VT, Muller AD (1994) The "institutional colon": a frequent colonic dysmotility in psychiatric and neurologic disease. *Am J Gastroenterol* 89:62-66.
- Soscia SJ, Kirby JE, Washicosky KJ, Tucker SM, Ingelsson M, Hyman B, Burton MA, Goldstein LE, Duong S, Tanzi RE, Moir RD (2010) The Alzheimer's disease-associated amyloid beta-protein is an antimicrobial peptide. *PLoS One* 5:e9505.
- Spitzer P, Herrmann M, Klafki HW, Smirnov A, Lewczuk P, Kornhuber J, Wiltfang J, Maler JM (2010) Phagocytosis and LPS alter the maturation state of beta-amyloid precursor protein and induce different Abeta peptide release signatures in human mononuclear phagocytes. *J Neuroinflammation* 7:59.
- Stalder M, Phinney A, Probst A, Sommer B, Staufenbiel M, Jucker M (1999) Association of microglia with amyloid plaques in brains of APP23 transgenic mice. *Am J Pathol* 154:1673-1684.
- Steenwinckel V, Louahed J, Lemaire MM, Sommereyns C, Warnier G, McKenzie A, Brombacher F, Van Snick J, Renault JC (2009) IL-9 promotes IL-13-dependent paneth cell hyperplasia and up-regulation of innate immunity mediators in intestinal mucosa. *J Immunol* 182:4737-4743.
- Stoger R (2008) Epigenetics and obesity. *Pharmacogenomics* 9:1851-1860.
- Styren SD, Civin WH, Rogers J (1990) Molecular, cellular, and pathologic characterization of HLA-DR immunoreactivity in normal elderly and Alzheimer's disease brain. *Exp Neurol* 110:93-104.
- Sun X, Somada S, Shibata K, Muta H, Yamada H, Yoshihara H, Honda K, Nakamura K, Takayanagi R, Tani K, Podack ER, Yoshikai Y (2008) A critical role of CD30 ligand/CD30 in controlling inflammatory bowel diseases in mice. *Gastroenterology* 134:447-458.
- Suzuki T, Oishi M, Marshak DR, Czernik AJ, Nairn AC, Greengard P (1994) Cell cycle-dependent regulation of the phosphorylation and metabolism of the Alzheimer amyloid precursor protein. *EMBO J* 13:1114-1122.
- Takechi R, Galloway S, Pallegage-Gamarallage M, Wellington C, Johnsen R, Mamo JC (2009) Three-dimensional colocalization analysis of plasma-derived apolipoprotein B with amyloid plaques in APP/PS1 transgenic mice. *Histochem Cell Biol* 131:661-666.

- Tanaka S, Nakamura S, Ueda K, Kameyama M, Shiojiri S, Takahashi Y, Kitaguchi N, Ito H (1988) Three types of amyloid protein precursor mRNA in human brain: their differential expression in Alzheimer's disease. *Biochem Biophys Res Commun* 157:472-479.
- Tanaka S, Shiojiri S, Takahashi Y, Kitaguchi N, Ito H, Kameyama M, Kimura J, Nakamura S, Ueda K (1989) Tissue-specific expression of three types of beta-protein precursor mRNA: enhancement of protease inhibitor-harboring types in Alzheimer's disease brain. *Biochem Biophys Res Commun* 165:1406-1414.
- Thirumangalakudi L, Prakasam A, Zhang R, Bimonte-Nelson H, Sambamurti K, Kindy MS, Bhat NR (2008) High cholesterol-induced neuroinflammation and amyloid precursor protein processing correlate with loss of working memory in mice. *JNeurochem* 106:475-485.
- Thorne A, Lonqvist F, Apelman J, Hellers G, Arner P (2002) A pilot study of long-term effects of a novel obesity treatment: omentectomy in connection with adjustable gastric banding. *International journal of obesity and related metabolic disorders : journal of the International Association for the Study of Obesity* 26:193-199.
- Togo T, Akiyama H, Iseki E, Kondo H, Ikeda K, Kato M, Oda T, Tsuchiya K, Kosaka K (2002) Occurrence of T cells in the brain of Alzheimer's disease and other neurological diseases. *J Neuroimmunol* 124:83-92.
- Tomita R, Igarashi S, Fujisaki S, Koshinaga T, Kusafuka T (2010) Are there any functional differences of the enteric nervous system between jejunum and ileum in normal humans? *Hepatogastroenterology* 57:777-780.
- Town T, Tan J, Flavell RA, Mullan M (2005) T-cells in Alzheimer's disease. *Neuromolecular Med* 7:255-264.
- Uryu S, Tokuhiko S, Oda T (2003) beta-Amyloid-specific upregulation of stearoyl coenzyme A desaturase-1 in macrophages. *Biochem Biophys Res Commun* 303:302-305.
- Uza N, Nakase H, Yamamoto S, Yoshino T, Takeda Y, Ueno S, Inoue S, Mikami S, Matsuura M, Shimaoka T, Kume N, Minami M, Yonehara S, Ikeuchi H, Chiba T (2011) SR-PSOX/CXCL16 plays a critical role in the progression of colonic inflammation. *Gut* 60:1494-1505.

- van Dielen FM, van't Veer C, Schols AM, Soeters PB, Buurman WA, Greve JW (2001) Increased leptin concentrations correlate with increased concentrations of inflammatory markers in morbidly obese individuals. *International journal of obesity and related metabolic disorders : journal of the International Association for the Study of Obesity* 25:1759-1766.
- Van Ginneken C, Schafer KH, Van Dam D, Huygelen V, De Deyn PP (2010) Morphological changes in the enteric nervous system of aging and APP23 transgenic mice. *Brain Res* 1378:43-53.
- Van Ginneken C, Schafer KH, Van Dam D, Huygelen V, De Deyn PP (2011) Morphological changes in the enteric nervous system of aging and APP23 transgenic mice. *Brain Res* 1378:43-53.
- Vehmas A, Lieu J, Pardo CA, McArthur JC, Gartner S (2004) Amyloid precursor protein expression in circulating monocytes and brain macrophages from patients with HIV-associated cognitive impairment. *J Neuroimmunol* 157:99-110.
- von Boyen GB, Reinshagen M, Steinkamp M, Adler G, Kirsch J (2002) Enteric nervous plasticity and development: dependence on neurotrophic factors. *J Gastroenterol* 37:583-588.
- Waddell A, Ahrens R, Steinbrecher K, Donovan B, Rothenberg ME, Munitz A, Hogan SP (2011) Colonic eosinophilic inflammation in experimental colitis is mediated by Ly6C(high) CCR2(+) inflammatory monocyte/macrophage-derived CCL11. *J Immunol* 186:5993-6003.
- Wajchenberg BL (2000) Subcutaneous and visceral adipose tissue: their relation to the metabolic syndrome. *Endocrine reviews* 21:697-738.
- Wallet MA, Wallet SM, Guiulfo G, Sleasman JW, Goodenow MM IFN γ primes macrophages for inflammatory activation by high molecular weight hyaluronan. *Cell Immunol* 262:84-88.
- Wang J, Ho L, Qin W, Rocher AB, Seror I, Humala N, Maniar K, Dolios G, Wang R, Hof PR, Pasinetti GM (2005a) Caloric restriction attenuates beta-amyloid neuropathology in a mouse model of Alzheimer's disease. *Faseb J* 19:659-661.
- Wang P, Yang G, Mosier DR, Chang P, Zaidi T, Gong YD, Zhao NM, Dominguez B, Lee KF, Gan WB, Zheng H (2005b) Defective neuromuscular synapses in mice lacking amyloid precursor protein (APP) and APP-Like protein 2. *J Neurosci* 25:1219-1225.

- Wang YD, Yan PY (2006) Expression of matrix metalloproteinase-1 and tissue inhibitor of metalloproteinase-1 in ulcerative colitis. *World J Gastroenterol* 12:6050-6053.
- Wang Z, Wang B, Yang L, Guo Q, Aithmitti N, Songyang Z, Zheng H (2009) Presynaptic and postsynaptic interaction of the amyloid precursor protein promotes peripheral and central synaptogenesis. *J Neurosci* 29:10788-10801.
- Wegiel J, Wang KC, Imaki H, Rubenstein R, Wronska A, Osuchowski M, Lipinski WJ, Walker LC, LeVine H (2001) The role of microglial cells and astrocytes in fibrillar plaque evolution in transgenic APP(SW) mice. *Neurobiol Aging* 22:49-61.
- Weisberg SP, McCann D, Desai M, Rosenbaum M, Leibel RL, Ferrante AW, Jr (2003) Obesity is associated with macrophage accumulation in adipose tissue. *The Journal of clinical investigation* 112:1796-1808.
- Weyer SW, Klevanski M, Delekate A, Voikar V, Aydin D, Hick M, Filippov M, Drost N, Schaller KL, Saar M, Vogt MA, Gass P, Samanta A, Jaschke A, Korte M, Wolfer DP, Caldwell JH, Muller UC (2011) APP and APLP2 are essential at PNS and CNS synapses for transmission, spatial learning and LTP. *Embo J* 30:2266-2280.
- Whitmer RA (2007) The epidemiology of adiposity and dementia. *CurrAlzheimer Res* 4:117-122.
- Whitmer RA, Gunderson EP, Quesenberry CP, Jr, Zhou J, Yaffe K (2007) Body mass index in midlife and risk of Alzheimer disease and vascular dementia. *CurrAlzheimer Res* 4:103-109.
- Wiercinska-Drapalo A, Jaroszewicz J, Flisiak R, Prokopowicz D (2003) Plasma matrix metalloproteinase-1 and tissue inhibitor of metalloproteinase-1 as biomarkers of ulcerative colitis activity. *World J Gastroenterol* 9:2843-2845.
- Willoughby DA, Johnson SA, Pasinetti GM, Tocco G, Najm I, Baudry M, Finch CE (1992) Amyloid precursor protein mRNA encoding the Kunitz protease inhibitor domain is increased by kainic acid-induced seizures in rat hippocampus. *Exp Neurol* 118:332-339.
- Wolozin B, Bednar MM (2006) Interventions for heart disease and their effects on Alzheimer's disease. *Neurol Res* 28:630-636.
- Wood JG, Zinsmeister P (1991) Tyrosine phosphorylation systems in Alzheimer's disease pathology. *Neurosci Lett* 121:12-16.

- Wu SZ, Bodles AM, Porter MM, Griffin WS, Basile AS, Barger SW (2004) Induction of serine racemase expression and D-serine release from microglia by amyloid beta-peptide. *J Neuroinflammation* 1:2.
- Xiong H, McCabe L, Costello J, Anderson E, Weber G, Ikezu T (2004) Activation of NR1a/NR2B receptors by soluble factors from APP-stimulated monocyte-derived macrophages: implications for the pathogenesis of Alzheimer's disease. *Neurobiol Aging* 25:905-911.
- Xu Y, Kim HS, Joo Y, Choi Y, Chang KA, Park CH, Shin KY, Kim S, Cheon YH, Baik TK, Kim JH, Suh YH (2007) Intracellular domains of amyloid precursor-like protein 2 interact with CP2 transcription factor in the nucleus and induce glycogen synthase kinase-3beta expression. *Cell death and differentiation* 14:79-91.
- Yamada T, Sasaki H, Dohura K, Goto I, Sakaki Y (1989) Structure and expression of the alternatively-spliced forms of mRNA for the mouse homolog of Alzheimer's disease amyloid beta protein precursor. *Biochem Biophys Res Commun* 158:906-912.
- Yan SD, Stern D, Kane MD, Kuo YM, Lampert HC, Roher AE (1998) RAGE-Abeta interactions in the pathophysiology of Alzheimer's disease. *Restor Neurol Neurosci* 12:167-173.
- Yang G, Gong YD, Gong K, Jiang WL, Kwon E, Wang P, Zheng H, Zhang XF, Gan WB, Zhao NM (2005) Reduced synaptic vesicle density and active zone size in mice lacking amyloid precursor protein (APP) and APP-like protein 2. *Neurosci Lett* 384:66-71.
- Yang LB, Lindholm K, Yan R, Citron M, Xia W, Yang XL, Beach T, Sue L, Wong P, Price D, Li R, Shen Y (2003) Elevated beta-secretase expression and enzymatic activity detected in sporadic Alzheimer disease. *Nat Med* 9:3-4.
- Yates SL, Burgess LH, Kocsis-Angle J, Antal JM, Dority MD, Embury PB, Piotrkowski AM, Brunden KR (2000) Amyloid beta and amylin fibrils induce increases in proinflammatory cytokine and chemokine production by THP-1 cells and murine microglia. *J Neurochem* 74:1017-1025.
- Yazawa H, Yu ZX, Takeda, Le Y, Gong W, Ferrans VJ, Oppenheim JJ, Li CC, Wang JM (2001) Beta amyloid peptide (Abeta42) is internalized via the G-protein-coupled receptor FPRL1 and forms fibrillar aggregates in macrophages. *Faseb J* 15:2454-2462.
- Yi CX, Tschop MH (2012) Brain-gut-adipose-tissue communication pathways at a glance. *Dis Model Mech* 5:583-587.

- Yin B, Hu X, Wang J, Liang H, Li X, Niu N, Li B, Jiang X, Li Z (2011) Blocking TNF-alpha by combination of TNF-alpha- and TNFR-binding cyclic peptide ameliorates the severity of TNBS-induced colitis in rats. *Eur J Pharmacol* 656:119-124.
- Yoshimura T, Leonard EJ (1992) Human monocyte chemoattractant protein-1: structure and function. *Cytokines* 4:131-152.
- Zhang H, Ma Q, Zhang YW, Xu H (2012) Proteolytic processing of Alzheimer's beta-amyloid precursor protein. *J Neurochem* 120 Suppl 1:9-21.
- Zheng H, Koo EH (2011) Biology and pathophysiology of the amyloid precursor protein. *Mol Neurodegener* 6:27.